METHODS OF IMPROVING COMBUSTION BY ELECTRICAL MEANS

By

John Clifford Hilliard, B.Sc. M.R.I.C. C.Chem.

A Thesis submitted for the Degree of

Doctor of Philosophy

Department of Chemical
Engineering and Chemical Technology
Imperial College of Science and Technology
London SW7

November 1979

ABSTRACT

Methods of interacting electrical energy with various combustion systems that exhibit both diffusion and chemical kinetically controlled heat release rates were considered from the point of view of overcoming the mutual exclusiveness of economy and emissions for such systems.

The thesis covers situations involving the application of low electrical powers, which fall into two regimes determined by the v-i characteristic, and are broadly classified under 'Electric Fields' (high voltage) and 'Electric Arcs or Plasmas' (low voltage).

Consideration was given to each of the three possible interaction stages,

i) Mixture preparation stage

ii) Conversion from reactants to products

iii) Product discharge stage

for either the high or low voltage interaction.

Experimental and theoretical results for electrostatic carburation and atomisation of fuels are presented and the practical significance discussed with respect to the unique qualities of alcohols.

The principle of combustion control through the production of non-Maxwell-Boltzmann distribution of species is presented with reference to nitrogen, hydrogen and oxygen atoms, the merits of photochemical and plasma modes of generating these distributions is presented, with emphasis on the key role played by H-atoms in controlling heat release rates. The importance of excited states in such systems is also considered.

A highly efficient novel plasma generator that enables the production of atoms and radicals from virtually any feedstock (with no noble gas additives) resulted from this work, and the design parameters are presented.

Spectroscopic studies using the novel generator provided evidence to support the theories proposed and also demonstrated the potential for electronic state selectivity in the device.

The practical significance of this work is discussed with respect to the weakness of present day energy conversion systems.

It is much easier to recognise error than to find truth, error is superficial and may be corrected; truth lies hidden in the depths.

Goethe, Spruche in Prosa

Nescit vox missa reverti

CONTENTS

ACKNOWLEDGEMENTS

The author would like to thank Professor F. J. Weinberg for all his help and advice throughout the duration of this work and for the introduction to the fascinating area of electrical aspects of combustion. Dr. A.R. Jones is particularly thanked for stimulating conversations especially during the work described in Chapter 6, at which time it is appropriate to acknowledge the ingenuity of my colleague Tony Chan in the final construction of the plasma generator described in Chapter 6.

The author is especially grateful to Professor A.G. Gaydon F.R.S., who made available spectroscopic equipment and offered much guidance in the early phases of the study, and to Professor Derek Bradley for his constructive comments on the original manuscript.

Messrs. D. Downs, R.W. Wheeler, J.G.G. Hempson, R.D. Cuthbertson and M. Thompson, of Ricardo and Company Consulting Engineers are thanked for their interest in the work and for making available equipment and research facilities where necessary, as well as constructing some of the prototype plasma generators and plugs that were used in the work contained in Chapter 4.

The technical skills of Messrs. C. Smith and K. Grose of the glass workshop were warmly appreciated at every phase of the experimental work.

Finally I would like to thank my wife who managed to endure sufficiently well to type the manuscript, her patience was an inspiration.

During the period October 1974 to October 1977 the author was supported on an SRC-Ricardo Industrial Studentship Award.

PICTURE CREDITS

The photographs contained in this thesis as Figures 4.2 and 6.5 were taken by Leonard Moulder A.R.P.S., his photographic assistance was greatly appreciated and the author learned much from him. All other photographic figures were taken by the author, who would like to thank the Imperial War Museum, London, for permission to photograph Bertelli's black pottery head of Mussolini shown as Figure 6.1.

LIST OF FIGURES

LIST OF TABLES

SYMBOLS AND NOMENCLATURE

Most material is defined within the thesis at the time of introduction, however some terms are defined here for the convenience of the reader.

HC - Hydrocarbon

FID - Flame Ionisation Detector

KLCR - Knock Limited Compression Ratio

HUCR - Highest Useful Compression Ratio

AFR - Air/Fuel Ratio

MBT - Minimum Advance best Torque (spark timing)

WOT - Wide Open Throttle

CARB - California Air Resources Board

BSFC - Brake Specific Fuel Consumption
(Brake power developed/unit mass flow rate fuel)

ISFC - Indicated Specific Fuel Consumption
(Indicated power developed/unit mass flow rate fuel)

T_i - initial temperature

T_f - final temperature

f - reactedness $\left(\frac{T - T_i}{T_f - T_i}\right)$

Arrhenius form of rate constant = $A\,T^n \exp(-\Delta E/RT)$

where A = pre-exponential factor

n = linearising index (when ln k vs 1/T is not linear)

ΔE = activation energy

R = Gas constant

Numbers in parenthesis denote material cited from the Reference section listed alphabetically.

Names in parenthesis denote material cited from the Bibliography section with authors listed alphabetically.

CHAPTER 1

INTRODUCTION

Before discussing the main aims and results of the work described in this thesis it is necessary to explain why one would ever contemplate using a highly ordered energy form such as electricity with any form of combustion. In that regard it is relevant to consider the thesis title which includes the word 'improving'.

As the 1980s are approached the reality of diminished sources of readily available fossil fuels and the increasing pressures of environmentalists have resulted in an apparent mutual exclusiveness between the constraints of economy and emissions. Improving therefore means trying to improve the efficiency with which energy conversion from thermal to mechanical takes place, while reducing the emission of pollutants that occur during that conversion process.

For convenience it is useful to think of practical engine combustion as occurring in two possible extremes, exhibiting mainly either diffusion, or chemical kinetic control and characterised largely by their rates of heat release (which for practical prime movers will also correlate with the power developed) and therefore is governed by the rate determining process in the heat release sequence. This is true whether or not the combustion occurs continuously or intermittently, and is of fundamental importance with respect to which of the three possible electrical interaction stages in the heat release sequence electrical interaction takes place, and in what form. The three stages are:-

i) Mixture preparation

ii) Conversion from reactants to products

iii) Product discharge

Considering reciprocating piston engines for example the main heat

release in a Diesel engine has a very high degree of diffusion control (although the ignition delay period in these engines, before the main heat release, tends to exhibit a significant component of chemical kinetic control depending on the physical and chemical properties of the fuel).

The Otto engine combustion however, exhibits a greater degree of chemical kinetic control in the main heat release. It is extremely unlikely that any practical situation exhibits uniquely one extreme, and an interelated combination exists. However the distinction is very useful in that, having identified what appears to be the rate controlling process, it is possible to investigate how it may be modified with the appropriate electrical interaction, and consider what interelated effects may result.

The same is true of, for example, fuel additives.
It has already been stated that the ignition delay period in a Diesel engine has a high degree of chemical kinetic control, so that additives modifying the chemical reactivity of the fuel would be expected to act as 'cetane modifiers'. If a reduction in the ignition delay occurred then this would also modify the main, highly diffusion controlled, heat release rate, because it would have started earlier at conditions of higher turbulence and compression temperature. The result is that the diffusion controlled heat release, pollutant formation and destruction processes have also been modified as a secondary effect.

The necessity to try and obtain a degree of control over practical combustion processes, in order to try and approach the apparent mutual exclusiveness of economy and emissions, is readily seen by inspection of Figures 1.1, 1.2 and 1.3 which cover practical Otto and Diesel engines. Dealing with Figure 1.1 it is possible to see how in the period 1973 to 1975, when the emission standards dealt mainly with carbon monoxide and hydrocarbon emissions, (the time axis pollutant

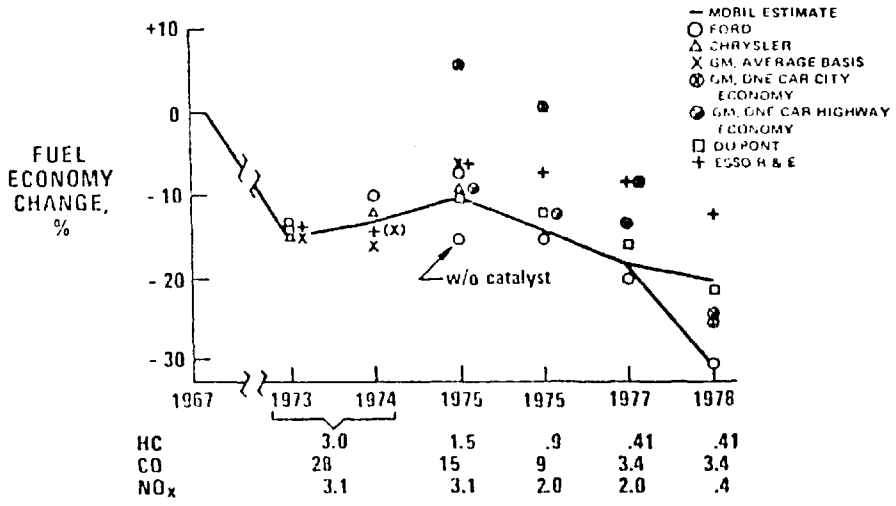

Figure 1.1 - The effect of emission standards on fuel economy. (reproduced with permission of Drs. Clewell and Koehl of reference 90)

figures are in grams/mile) there was an improvement in economy. However increasingly severe nitric oxide (and NO_x) standards have led to an increasingly worsening economy, even while vehicles have been getting lighter and smaller.

It is therefore possible, for both extremes of combustion, to classify the main pollutants into two broad categories:-

i) Emissions generated through incomplete combustion (HC, CO, Soot etc. - generally associated with inefficiency).

ii) Emissions generated through high temperatures (NO_x - generally associated with efficiency).

Inspection of Figures 1.2 and 1.3, shows for practical Diesel and Otto engine operation, the intimate link between good economy and high NO levels. This exists even though the extremes of burning

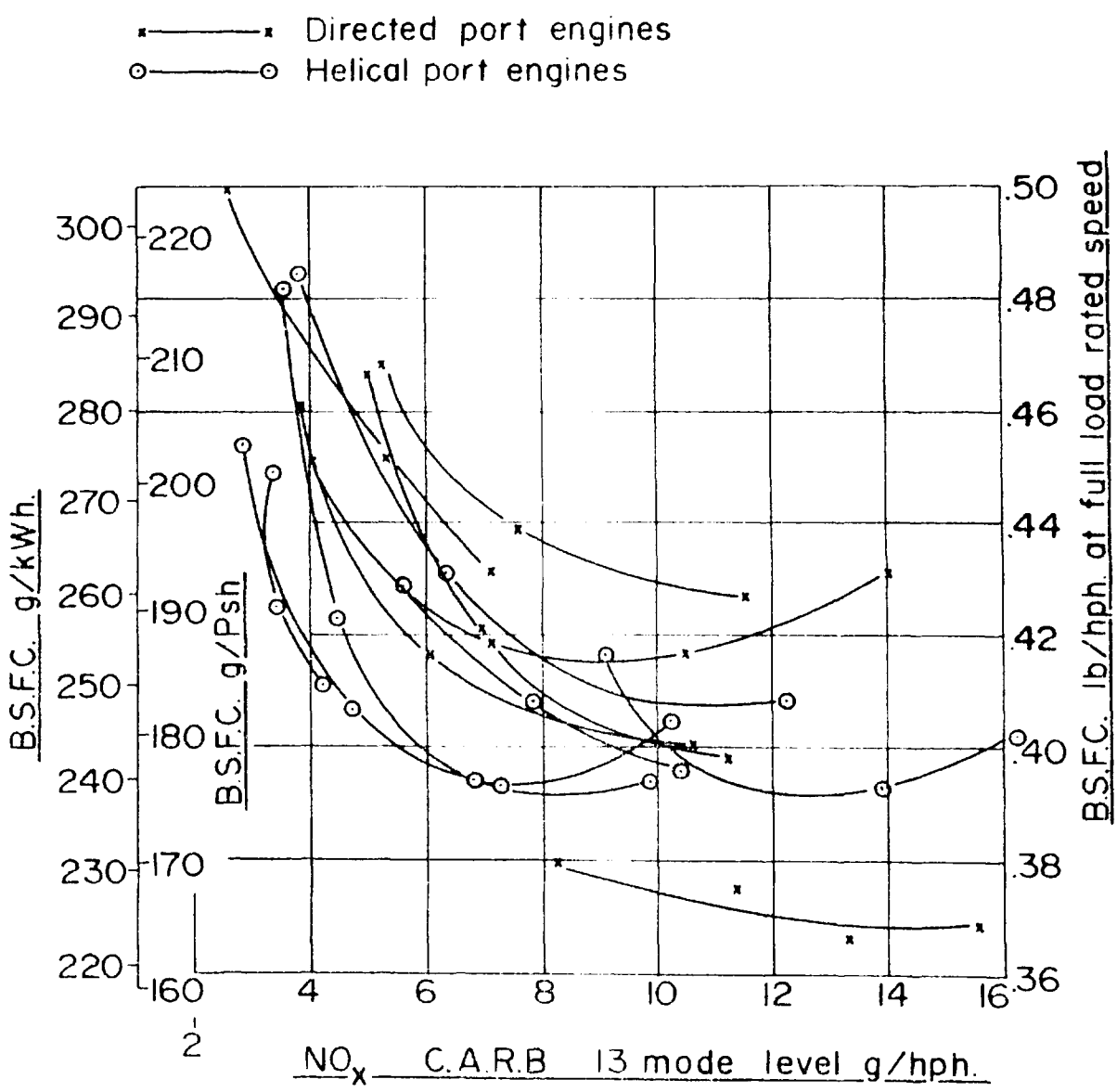

Figure 1.2 - The effect of NO reduction, by injection timing retard, on the brake thermal efficiency of Diesel engines. (data kindly provided by M.J. Wright - Ricardo Consulting Engineers.)

in both engine types are radically different as stated previously.

The brake specific fuel consumption is derived from application of the First Law of Thermodynamics as a rate equation in the conver-

sion of heat into work by the engine and is defined in the Nomenclature. It is obviously inversely proportional to the thermal efficiency of the engine and a useful comparative unit.

At this time the Diesel and Otto engines serve to highlight the two extremes of burning and the differences between them mean that emission control methods for the main emissions are very different. This is highly significant because it affects the mode in which one may introduce electrical energy, where conventional control fails. The fundamental difference lies in the mode of power control for each type. The Diesel engine is quality controlled (ie. the AFR is the power control variable) while the Otto situation is quantity controlled (ie. the AFR is only variable within certain fixed AFR values, at the present time, as seen in Figure 1.3, and the mass flow rate of charge, controlled by a throttle, sets the mode of power control).

This distinction is important because it determines what may be done at all three stages of the burning sequence. For example in the quality mode of power control the exhaust gas always contains substantial (from 10% to 20% oxygen) in the exhaust gas, whereas for a quantity mode of power control, operating at approximately stoichiometric, the exhaust will contain much less than 1% oxygen. The chemical environments of catalysts present in the exhaust gases of these two extremes are very different in that the former is always oxidising while the later is not.

This feature, as will be seen later, (Chapter 4) means that a depollution procedure involving simultaneous reduction (of NO_x) and oxidation (of CO and HC), only possible in a carefully controlled oxygen environment is not possible in the quality control situation and therefore limits methods of depollution that are possible in the product discharge stage. This is in contrast to the successful method in the

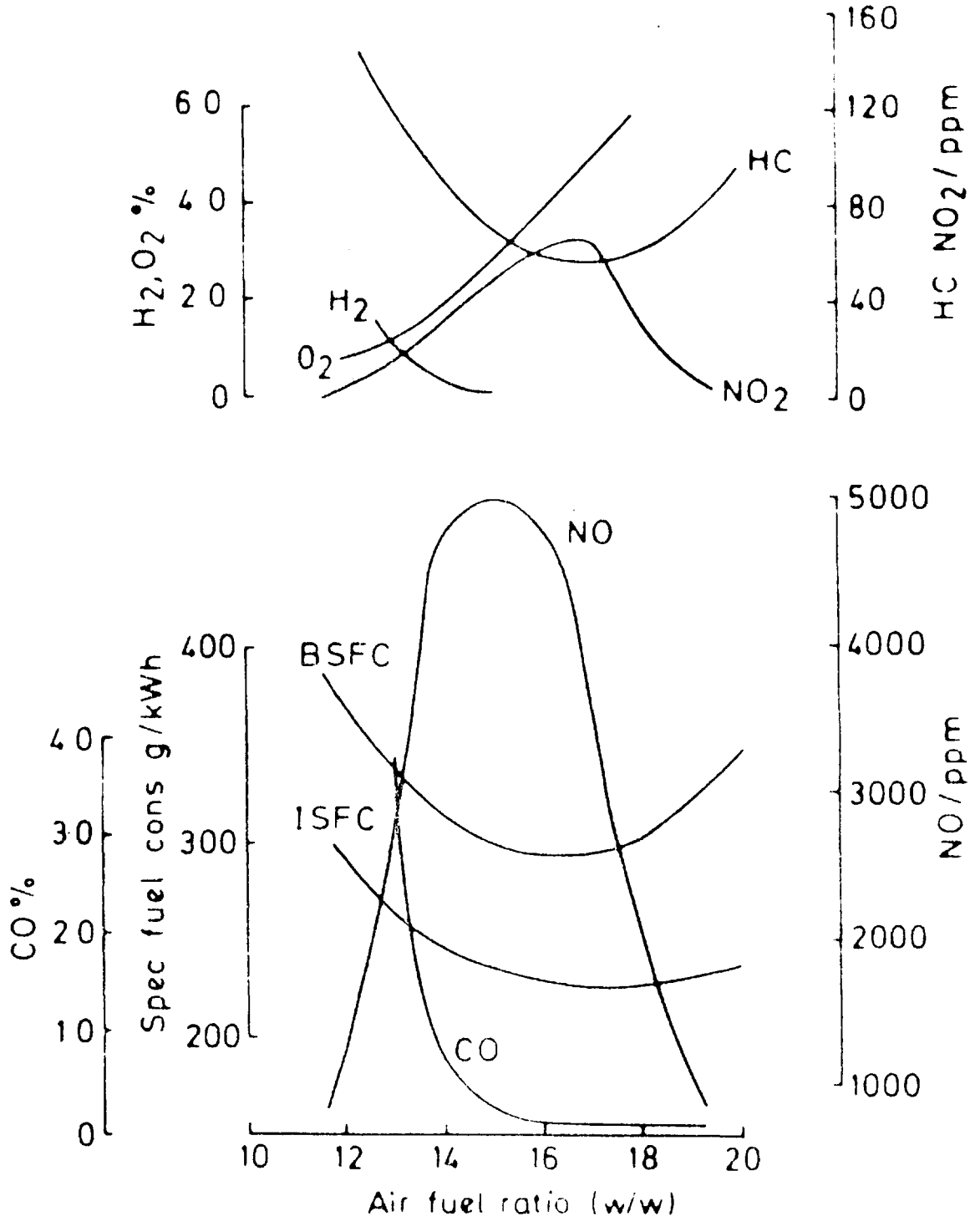

Figure 1.3 Emissions and fuel consumption curves versus air/fuel ratio for an E6 engine

(data from work conducted as part of a study described in refs. 205 and 206. Single cylinder spark ignited (MBT) gasoline fuelled engine at WOT, compression ratio 8.5:1)

quantity controlled mode involving a 3 way catalyst, Zirconia sensor, microprocessor-AFR control loop.

It would be the ideal solution to be able to control the combustion itself so that no elaborate depollution procedures, that tend to operate engines away from optimum efficiency to meet emission requirements, need be conceived. Increasingly severe standards of some emissions, notably NO_x and particulates for Diesel engines, are extremely difficult to meet, and conventional attempts at meeting these standards often result in such a worsening of fuel economy that any competitive edge such engines may have had is rapidly eroded.

The essential problems of emissions for both the Otto and Diesel engine cases are extensively reported in the Literature. (For example for Otto engine combustion see refs. 200, 202, 268, 350, 351, 352 and for Diesel engine combustion see refs. 65, 95, 322, 426, 437, 457, 467. For a general engine reappraisal ref. 231 and economy interactions see refs. 90, 321, 462)

The work described in this thesis was an attempt to see whether various low power electrical interaction techniques could be used to obtain improvements (as defined previously) with only modest investments of electrical power. Because of the steepness of the BSFC curves with operation away from optimum economy conditions, it was anticipated that the appropriate electrical interaction may result in a significant overall energy saving.

The rate of heat release is known to be linked not only to the power developed by the engine (Obert) but also to the pollutants emitted in a spark ignited engine (422) so that methods of controlling rates of heat release, as well as rates of reaction generally, were very important in this study.

The problems associated with diffusion controlled combustion

have been extensively reported (refs. 446, 451, 452) and the main problem identified as resulting from the fact that the reactants are initially separated, with the stoichiometric contour forming a barrier. Pyrolysis products form on the fuel rich side of the barrier, and high temperature oxidation products form on the other, oxidant side. A cool mass, for example air or a solid body, then serves to quench both these endothermic types of compounds to be discharged as pollutants.

Because the main pollutants associated with diffusion controlled combustion ie. NO and soot are endothermic with respect to conversion to N_2, O_2, H_2O and CO_2, at exhaust temperatures, the basic need for control of the overall rate of formation/destruction before quenching occurs is critical under circumstances where a catalyst is not operative. (By catalyst is implied a heterogeneous mainly transition metal entity; if one used the definition of a catalyst as being a material that increases the rate of attainment of equilibrium (ie. $^{dG}/_{dT} = 0$) then species generated by plasma jets, as shown latter, could be regarded as catalysts.)

The normal structure of diffusion flames, with fuel diffusing into air, results in the continuum emission from soot particles generated from pyrolysed fuel approaching the stoichiometric contour. It is interesting to note, in passing, that in recently published work (438) with a reverse situation, that of diffusion flames with air diffusing into excess fuel, such soot continuum emission is absent and the flames emit quantised radiation normally associated with lean of stoichiometric premixed flames.

With diffusion flames control of the temperature at the stoichiometric contour (and hence rate of NO formation) is not possible and almost the maximum temperature possible for the particular fuel/

air combination exists to maximise the emission of NO.

The solution to this problem possible by premixing, with resulting control of the final flame temperature, was recognised (444, 445) and extensive work undertaken with excess enthalpy combustion involving massive heat recirculation without dilution, as reported in refs. 179, 180, 236, 279, 280, 281, 448, 450. The resultant increase in control of rate of reaction and resultant flame stabilisation under excess enthalpy conditions resulted in the ability to burn at methane air concentrations of close to 1%, well below the conventional lean 'limit of flammability', while the 'final thermal dam' temperature, of approximately 1400K, led to immeasurable NO emissions.

The significance of heating with and without simultaneous dilution with hot combustion products, and electrical methods of controlling or modifying reaction rates in situations where peak temperatures are low, is discussed in more detail in Chapter 3. It was recognised (183, 447, 448) that injection of radicals/atoms that were generated in plasma jets could modify rates of reactions in flames in a manner that could not be attributed to a purely bulk thermal heating effect, and therefore provided the starting point for the plasma electrical interaction work described in this thesis.

It was not the intention of this study to devote any effort towards non-regulated emissions, especially those that may be located on particulate material (439), or formed by cross reactions of emissions (341) and possibly mutagenic in the Ames test (13). The working philosophy was that control of the particulate and NO_x emission at the combustion stage, if possible, would therefore solve these problems also.

CHAPTER 2

AIMS AND OBJECTIVES

In order to keep this work within the framework of practical viability, small electrical interaction powers invested would need to show substantial potential gains in fuel economy and emission reduction. Most of the applications reported in this thesis involve DC power, defined as the direct product of applied voltage and current drawn. The two possible low power situations are therefore:-

i) A high applied voltage, typically 500V to 30kV, and low current consumption, typically μA to mA. This type is described as an electric field interaction.

ii) A low applied voltage, typically 16 to 100V, and high current consumption, typically 5 to 30 Amps. This type is described as an electric arc plasma interaction.

Interactions under i) are found mainly in Chapter 5, while interactions under ii) are found mainly in Chapters 4, 6 and 7.

The objectives of the work were to investigate the possible ways low power electrical interactions could overcome the apparent problem of the mutual exclusiveness of economy and emissions. This involved fully identifying the most appropriate interaction stage, as described in Chapter 1, and matching it with the most appropriate electrical interaction described above.

In the case of plasma injection, the requirement for the production of the appropriate atoms and excited states at each of the interaction stages is particularly important. To this end spectroscopic studies were undertaken, as reported in Chapter 7, and a novel plasma generator designed that, following the success of the preliminary ex-

periments described in Chapter 4, would be suitable for studies relating to the spectroscopic work, as well as being in a form more attractive to practical situations. The generator design is described in Chapter 6.

CHAPTER 3

THEORY AND METHODS OF CONTROLLING REACTION AND HEAT RELEASE RATES

INTRODUCTION

This Chapter deals mainly with 'chemical' ways in which chemical reaction and heat release rates may be modified and controlled. This in no way implies that transport processes are not important. In fact they are the controlling processes that determine (in all but unimolecular decompositions) the ability of reactants to approach close enough to form a transition state before reacting to products with energy deposition into the available rotational, vibrational, translational and electronic degrees of freedom of the products that subsequently form the working fluid in the energy conversion system.

In any reacting process made up of a sequence of steps it is naturally the slowest step that controls the fastest time in which the whole process may occur. Very few, if any, reacting systems are under completely chemical kinetic control but are reacting within the framework of differing scales of turbulence length that reduce in size, approaching molecular dimensions, as the system becomes better stirred and more 'homogeneous'.

When considering heat release rates within a turbulent combustion environment it is common to define turbulence scales within the system for computation. Generally an ensemble of turbulent eddies defines the maximum length scale, and within the ensemble the individual eddies have dimensions of the order of the Taylor microscale, λ, (Kay and Nedderman; Bird, Stewart and Lightfoot), this dimension is proportional to the inverse square root of the turbulence Reynolds number for an isotropic flow system and sets the dimension for con-

sideration of the time interval (τ) in which the main heat release takes place within the eddy, by propagation of a flame front across the characteristic length, λ, at the laminar burning velocity, Su of the mixture, (ie. $\tau = \lambda/Su$).

The dimension of the 'vortex-tubes' that separate the burning eddies are within a smaller characteristic length scale that is defined by two independent properties of the turbulent system, the turbulence energy (k) and frequency of motion (f) (Launder and Spalding) and define the Kolmogorov scale ($=(k)^{1/2}/f$) considered for turbulence energy dissipation, and propagation of ignition sites (203) within the eddies.

It was not the intention of the work described in this Chapter to fully explore the effect of turbulence on heat release rates. As far as practical systems are concerned the prime importance of this for Otto engines led to the development of the famous Ricardo 'Turbulent L Head' in the 1920s (197) and turbulence does not modify the fundamental chemistry of, for example, two stage ignition (459), only the interval between events. The increased turbulence from the Comet pre-chamber also led to the development of the high speed Diesel engine (Ricardo and Hempson). Very interesting studies relating to spark ignition and propagation as functions of turbulence have been reported (55) suggesting optimum turbulence levels for lean mixtures, of importance especially in relation to novel ideas for ignition from projected spark kernels.

Transport processes and chemistry will always be interlinked; however when the system comes under a higher degree of chemical kinetic control (as in lean-burn situations) the importance of chemical rate limitations is worthy of study with a view to control of the heat release rate by electrical interaction.

Laboratory attempts to reduce the controlling effects of transport processes by reducing the characteristic turbulence length scales

to levels where the systems approach more closely kinetically limited reaction rates are in the 'well stirred reactor' (283) (often operated fuel lean (262, 263)) and 'jet stirred reactors' that have been used to obtain kinetic information for example on NO_x formation in relation to O-atoms (288, 289). The very high arc rotation rates (10^5/min) reported in ref. 183 lead to consideration of that system as a form of well stirred reactor. Early experimental work in that study showed behaviour of the material added to the arc reactants that was dependent on rotation rate at low values, becoming assymptotic at the conditions reported in ref. 183, for high rotation rates.

Under situations with a high, or significant degree of chemical kinetic control, the rate of the processes may be influenced by interactions that change the number density of various critical species in the rate determining reactions. The maximum number density of these critical species will be determined by the local thermodynamics and rate of loss upon generation of the species within the system, in the region of generation. The remaining part of this Chapter deals with identifying what these critical species are, and the best way for generation and subsequent reaction control.

HEAT ADDITION WITH PRODUCT DILUTION

The most frequently used way to increase rates of reaction is to arrange for pre-heating of the reactants; however not all reactions increase in rate upon heating. Many hydrocarbon oxidations can show negative temperature coefficient regions, as do some atom recombination reactions and termolecular oxidation. This was recognised at the beginning of this century (Hinshelwood). Other reactions, mainly atom-molecule, exhibit a zero activation energy which leads to no temperature dependence. So bulk thermal heating in these systems, to increase reaction rates, is of little use.

However in reactions that have high activation energies with respect to conversion to products, such as hydrocarbon combustion (the reason these fuels are available on Earth now for present day use) then pre-heating serves to increase the rate of conversion. The conventional method of heating involves dilution of the reactants with hot combustion products by aerodynamically induced recirculation zones or bluff bodies in the flow (Beér and Chigier) this therefore leads to simultaneous dilution of the reactants by the products.

Consideration of a closed volume (for example a spherical eddy of diameter λ) in which such heat release takes place, automatically has associated with it, a maximum in the heat release rate vs. reactedness curve as seen in Figure 3.1. This is due to the nature of the Arrhenius dependence of the reaction rate, $\dot{w}$, on both the reactant concentrations and temperature for large values of ΔE_g. As reaction proceeds within the closed volume, the temperature term in the argument of the exponent dominates for low values of f and rises sharply as seen. As f tends to 1, the reactant concentration (due to dilution) tends to zero. The direct product of these two reactedness dependent terms then leads to a natural maximum limit on the rate of heat release for such a system, located towards the end of the heat release profile as shown.

Quantitative data of this sort for ethylene/air flames with the abscissa as temperature rather than reactedness are found in refs. 275 and 276. The fact that this limit on heat release rate exists with simultaneous dilution, sets a maximum limit attainable on the combustion intensity (defined as $\dot{w}\Delta H/V$, where V is the combustion volume of, for example, the eddy previously mentioned, or the volume of a practical combustor). To bypass this constraint requires heating without corresponding dilution.

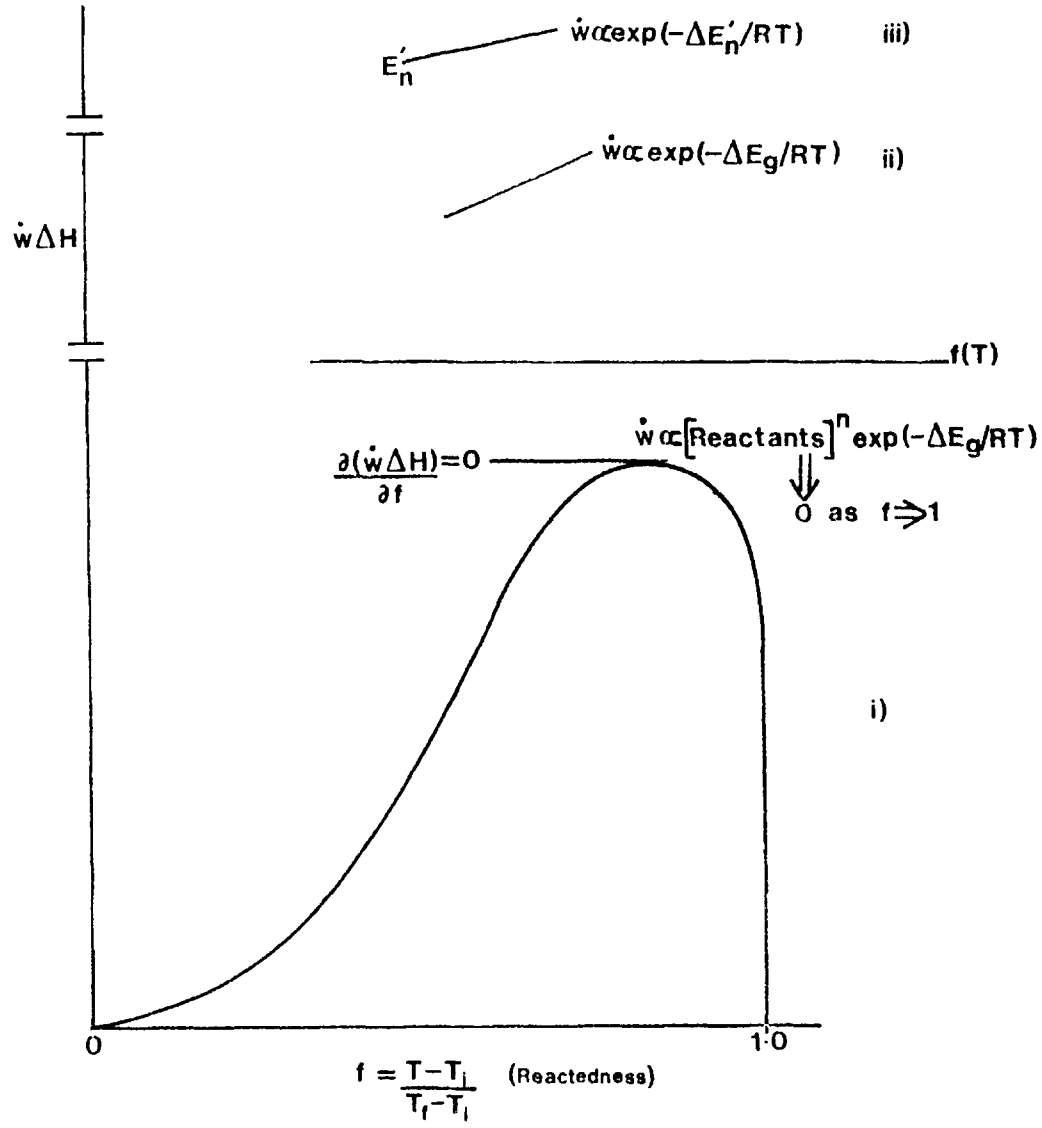

Figure 3.1 – Schematic of various ways in which rates of heat release may be modified. i) Recirculation of hot combustion products with simultaneous dilution, ii) Heating without dilution of reactants, iii) Addition of species important in the rate determining stage either in-situ photochemically or from a plasma generator.

HEAT ADDITION WITHOUT PRODUCT DILUTION

The ability to bypass the heat release maxima constraint by separating the terms of $\dot{w}$ to arrange for heating without dilution was recognised (444) and led to work on excess enthalpy burner systems of refs. 179, 279, 280 and 281, using a counter-current heat exchanger to provide a barrier preventing dilution and diffusion

but allowing enthalpy transfer. This arrangement then leads to the situation where the enthalpy of the reactants before combustion is increased over that present by virtue of their chemical composition (chemical potential) with respect to conversion to products (ie. enthalpy of combustion).

The barrier to diffusion is important because when combustion products may diffuse into reactants, as for example across a flame front, although the reactants are pre-heated, dilution with products lowers the chemical potential to offset the increased enthalpy due to heating. This happening with water vapour diffusion was suggested in original criticisms of the excess enthalpy concept (Spalding). Provided no dilution occurs, and pre-reaction is minimal (see Appendix 3) then an excess enthalpy condition exists.

In such systems, as for example the 'Swiss-Roll' burners of ref. 279, it was possible to demonstrate that the idea of a 'lean limit of flammability' as a practical constraint on combustion did not, of necessity, exist. Stable combustion was sustained at temperatures below which the emission of NO becomes significant. (A plot of d [NO] /dt against temperature is negligible up to, but rises sharply at 1800 K in a homogeneous extended Zel'dovich kinetic scheme. These units operated at close to 1400 K for methane and propane fuels).

Although such systems are of undoubted importance, they are non specific, in that when the heat is transfered from the products to the reactants all available degrees of freedom available to the reactants at the pre-heat temperature are populated. This situation, while increasing the overall global rate of formation of products, means that modes of energy absorption have been populated by pre-heat that are necessarily redundant in the main heat release sequence. For lean mixtures this is particularly significant, for example a 2% methane air system contains a mole ratio of fuel to nitrogen of 1:40. Population of rotational, vibrational and translational degrees of freedom of nitro-

gen then serves to deplete the ability to pump available energy into the principal reactants, namely fuel and oxidant. The improvements come with specificity of generation of key species from the principal reactants.

PHOTOCHEMICAL METHODS

If the rate controlling process is that of dissociation of one of the reactants, or production of species from reaction of one of the dissociated entities, then a photochemical method is obviously one of the most selective ways in which to interact for control. For example, a mixture of H_2 and Cl_2 reacts slowly at room temperature at a rate, limited by the thermal dissociation of Cl_2 at room temperature. A flash from an Hg lamp causes dissociation of Cl_2 to produce Cl atoms which perpetuate a chain reaction with generation of H-atoms. The summation of quantum yields, instead of being unity as expected from the Stark-Einstein Law (Cundall and Gilbert) then has a value of 10^6. In the absence of oxygen that competes for the H-atoms generated, the rate is nearly infinite (Hinshelwood; Laidler), with explosions often observed and in principle possible after the absorption of only one photon. (For the sake of completeness mention should be made of the hydrocarbon/chlorine system with acetylene, where the presence of even minute amounts of oxygen induces explosion even at temperatures as low as -78°C (390)).

A further feature of a photochemical method is the ability to choose the electronic state of the dissociated species produced. Such species have potentially profound effects in combustion as will be described later. The selective abilities of photochemically induced reactions depends on the radiation source. Heating of an element of gas for ignition purposes by infra-red radiation (from a CO_2 laser or a plasma source) that is focused into a combustible mixture, constitutes

a less specific mode of excitation, that is basically heating. The fact that the ignition source is situated away from walls would have advantages with respect to wall quenching and propagation, but would not be the kind of specific excitation that was sought after in this study.

For selective dissociation of the species considered of importance in hydrocarbon combustion (CH bonds, N_2, O_2 and H_2) the high dissociation energies to ground state atoms of H_2 (4.48 eV), O_2 (5.12 eV) and N_2 (9.76 eV) means that the radiation source must have a photon energy at least in excess of these levels and, in the absence of a sensitiser, the molecule must have absorption bands overlapping this radiation. A bond energy of 500 kJ $mole^{-1}$ (5.18 eV/molecule) requires a minimum photon energy supplied by radiation at a wavelength of 239.3 nm and for all the species of interest the irradiation wavelengths are into the vacuum ultraviolet.

A possible biphotonic scheme to help solve that difficulty is shown in Figure 3.2, and naturally depends on the potential energy curves of the irradiated molecules. It is interesting to note, in passing, that such a repulsive triplet surface ($^3\Sigma_u^+$) exists for molecular hydrogen into ground state atoms. (Emission from the $^3\Sigma_g^+$ to this repulsive surface giving rise to the dissociative continuum used as the uv source in the hydrogen lamp).

Photochemical methods of generating species by vacuum ultraviolet sources have been attempted in photochemical augmentation experiments involving direct generation of oxygen atoms.

O-ATOMS

The most comprehensive study of the effects of O-atoms, generated photochemically, in augmenting combustion is reported in refs. 83 and 84. In these experiments radiation, from a commercial pulsed vacuum uv source, generated O-atoms by photolytic fission of O_2 at

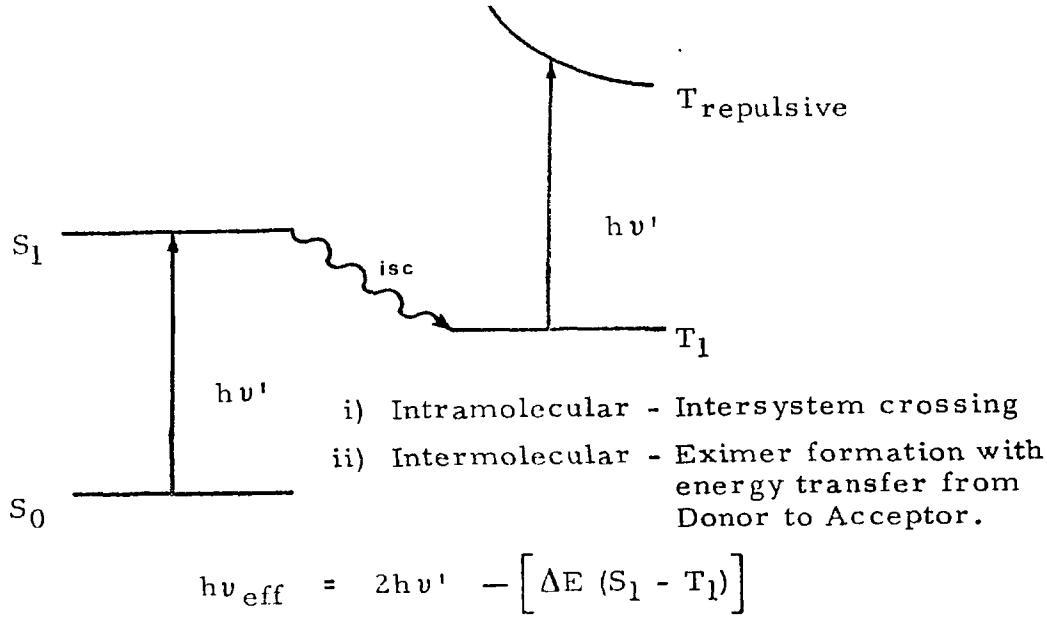

Figure 3.2 - A hypothetical Jablonski diagram of a photochemical scheme involving two modes of energy transfer leading to dissociation following biphotonic absorption.

---

wavelengths below 245 nm. Augmentation, (as determined by a lowering of ignition temperature) was seen for all wavelengths once a critical number density, greater than 10^6 atoms cm^{-3}, was established. With irradiation at wavelengths below 180 nm it was possible to establish low temperature ignition, and combustion initiation, once a critical number density of 10^{14} atoms cm^{-3} was established. The significant advantage of minimal increase in minimum ignition energy for photochemical initiation of lean combustion mixtures was demonstrated, and compared with that of spark ignition, which rises very sharply with excess air.

The most interesting aspect, from the point of view of the present study, was the reported wavelength dependence effects in the combustion experiments. Figure 3.3 shows some potential energy curves for O_2. The Hertzberg absorption is from 195 to 245 nm and leads to dissociation to the ground state, ^3P, O-atoms while the

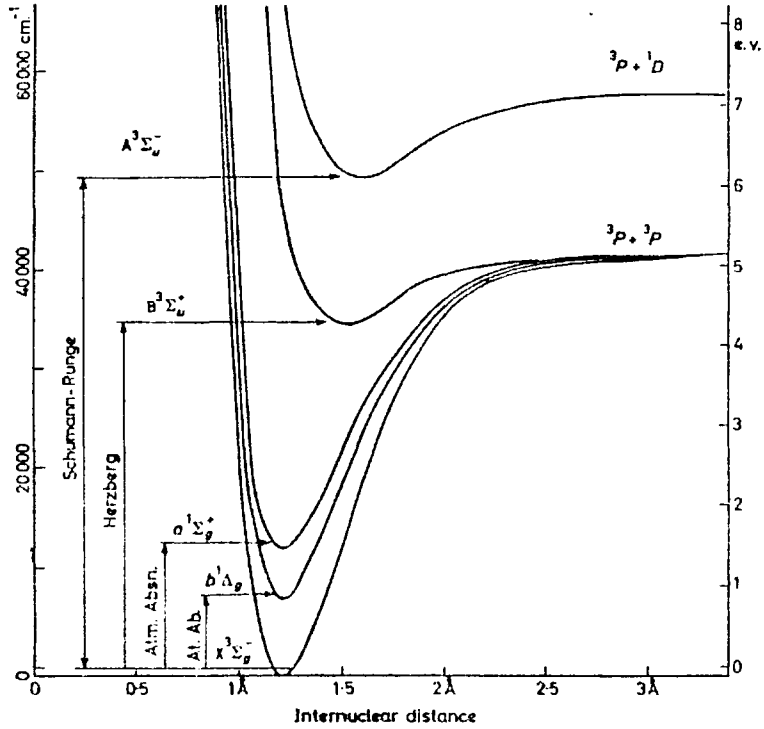

Figure 3.3 - Potential energy curves for oxygen (From Gaydon 1968).

Schumann-Runge (176 to 195 nm) and Schumann Continuum (129 to 176 nm) lead to production of the singlet ^1D atom.

The possible importance of the reactivity of these atomic states (and singlet molecular oxygen $^1\Sigma g$) were considered in ref. 83. It would appear that ^1D O-atoms are more important in ignition, while ^3P O-atoms are effective in flame propagation. This differential atomic reactivity of these species with hydrocarbons is well known (214, Wolfrum) and ground state atoms undergo preferential abstraction reactions, ie.

$$O(^3P) + RH \longrightarrow R + OH \qquad 1$$

with an activation barrier, while the excited singlet atoms undergo insertion without an activation barrier

$$O(^1D) + RH \longrightarrow ROH \qquad 2$$

Such differential reactivity as a function of electronic state may be highly significant in electrical interaction experiments using the plasma generator described in Chapter 6. The types of peroxy intermediates that would be anticipated to form, subsequently to reactions 1 and 2, have always been strongly associated with cool flame and two stage ignition phenomena (73, 120, 121, 286, 372; Lewis and von Elbe).

The importance of O-atoms in chain branching reactions such as

$$O + H_2 \longrightarrow OH + H \qquad 3$$

is well known and leads to production of hydrogen atoms. Another reaction of O-atoms of potential importance in combustion is the generation of translationally 'hot' H-atoms via reactions of the sort.

$$O + OH \longrightarrow O_2 + H \qquad 4$$

In these reactions the exothermicity is channeled into the translational degree of freedom of the H-atom rather than vibrational excitation of O_2. For reaction 4, it has been estimated that 87% of the exothermicity is partitioned into translational energy (128). The number of vibrational degrees of freedom of the secondary product molecule are of significance in determining the % partitioned in this way. O_2 has only one degree of vibrational freedom, while CO_2 has four. Consequently in reaction 5 below,

$$OH + CO \longrightarrow CO_2 + H \qquad 5$$

less than 55% of the exothermicity went into H-atom translational energy (128). The role of such atoms in combustion reactions is of particular significance here, because it represents specific excitation into a species that reacts at a temperature considerably in excess of the equilibrium temperature of the species within the bulk of the system

and may be viewed as a method of specific heating of a key species, the H-atom, without appreciable energy partition to the bulk ensemble of the remaining 'passive' molecules of the system. Further reactions of hot H-atoms may be found in ref. 328.

Hot H-atoms are not rapidly quenched (128) and reactions that lead to their formation will be significant in rate controlling processes involving H-atoms. If the H-atom generated by, for example reaction 4, subsequently reacts, the 'temperature' of, and possibly the rate of, the subsequent reaction will be determined by the energy partition to the H-atom in the hot atom generating reaction. The importance of such a process is not just hypothetical but of fundamental significance in the following chain branching reaction.

$$H + O_2 \longrightarrow OH + O \ (\Delta E = 62 \text{ kJ/mole}) \qquad 6$$

Because of the very high activation energy of this reaction, it is particularly sensitive to quenching. The possibility of selectively 'heating' such a reaction by generation of hot H-atoms via reactions such as 4 or 5 or directly via photochemical or plasma production in a lean burn situation is a possible way to reduce the quenched emission of hydrocarbons. It is the basic objective of the photochemical or plasma method described later to try to pump selectively and efficiently such key reactions. Fundamental studies on quenching, near surfaces using mass spectroscopic sampling, have shown how readily reaction 6 is quenched with resulting reduced rates of consumption of the principle reactants (394).

While the work of refs. 83 and 84 concentrated on direct generation of O-atoms, and their importance in combustion is not questioned, further research led to the conclusion that they may not be the most appropriate key species to generate for an electrical interaction.

H-ATOMS

Burning velocity measurements are one of the most important in combustion, and have been extensively studied (ref. 14 gives a review for laminar flames; refs. 1 and 15 for turbulent combustion) and control the heat release rate.

Early attempts were made to try to correlate burning velocity with various parameters of the different fuel/air systems, such as reaction zone thickness and final flame temperature (Gaydon and Wolfhard). However it was the early theories of burning velocity developed at Princeton (415, 416, 417) that were the first to consider the importance of 'active particles' in the form of hydrogen atoms as the controlling factor in burning velocity, not just because of their inherent reactivity but because of super-equilibrium concentrations (that exceeded those expected from consideration of the pre-heat temperatures) that were present ahead of the reaction zone generated by back diffusion of H-atoms from the post reaction zone gases.

The first paper in this study (416) found close correlation between calculated H-atom equilibrium concentrations at the flame temperature and the measured burning velocity. There was no correlation with O-atoms, and only slight correlation with hydroxyl radicals. In the paper they conclude "For, if the extent to which free radicals in the flame can be utilised in the combustion process depends upon diffusion - and it is logical to make such a supposition - the effect of hydrogen atoms, because of their high rates of diffusion, will overshadow that of any of the other radicals".

The basic theory is of an equilibrium hydrogen atom concentration generated at the flame temperature at the termination of the reaction zone, and these atoms then diffusing into the pre-reaction zone and controlling the burning velocity (415). Apart from the direct correlation mentioned, this concept led to the derivation of the well accepted

square root law for burning velocity and accounted for the effect of pressure on Su (417).

Subsequent work to investigate the correlation when extended to a variety of systems (31) led to the data shown in Figure 3.4, and shows the direct correlation between Su and [H]. Further studies that investigated the effects of mixture strength (339) while showing correlation with [H] did not conclude that it was the single determining factor in establishing the final burning velocity.

Further evidence to support the theories of refs. 415, 416 and 417 comes from very modern studies using molecular beam and mass spectroscopic sampling. The action of halogenated hydrocarbons as inhibitors, that lower the burning velocity, is well established (and discussed in more detail later). References 42, 43 and 271 describe an extensive series of studies to examine the effect such inhibitors have (0.3% CF_3Br was used) on the species present in the combustion of a methane/air flame.

A representative result from this study is shown as Figure 3.5. It is very clear that the two species concentrations that are lowered are CH_3 and H, with [O] and OH unchanged. Figures 3.4 and 3.5 lead to the clear deduction that increasing the H-atom concentration close to the pre-reaction zone increases reaction rates, while lowering it, by introducing species that compete for H-atoms, has an inhibiting effect on the main heat release reactions.

In principle it then appears that the H-atom concentration could be used, almost at will, to control the burning velocity of a given mixture. The maximum post reaction zone concentration of H-atoms that determines the concentration gradient driving the diffusion into the pre-reaction zone is determined by the adiabatic flame temperature, and the equilibrium H-atom concentration at that temperature. As the mixture becomes leaner this value of temperature falls with a corre-

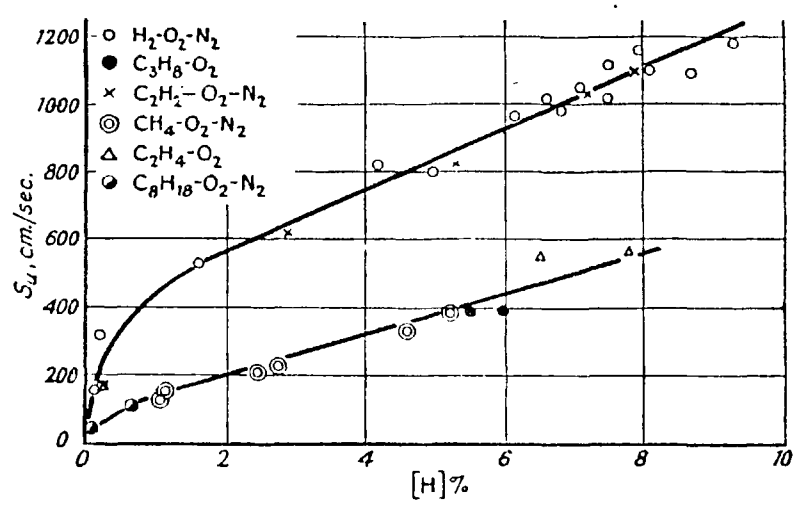

Figure 3.4 - Burning velocity vs. equilibrium concentration of H-atoms. (From Gaydon and Wolfhard).

---

sponding reduction in equilibrium concentration of H-atoms. The equilibrium dissociation of hydrogen as a function of temperature is shown in Figure 3.6, starting at a temperatures above the adiabatic flame temperatures associated with the systems of Figure 3.4. The % H_2 dissociated rises very rapidly as a function of temperature.

If it were possible to generate a [H] that was not dependent on the limitations of the thermodynamics associated with flame temperatures by generating the species in equilibrium at much higher temperatures either photochemically or via a plasma so that once formed, they diffused into the pre-reaction zone, then, according to the data as shown in Figure 3.4, the burning velocity would be under the control of the thermodynamics of the externally controlled system and burning velocity of the mixture would then cease to be a function of the properties of fuel/air mixture. This has an immediate consequence with respect to power control and emissions for practical systems.

While diffusion of H-atoms is of significant importance, diffusion alone does not guarantee reaction. A further feature that has to be considered is the type of reactions the H-atoms once generated,

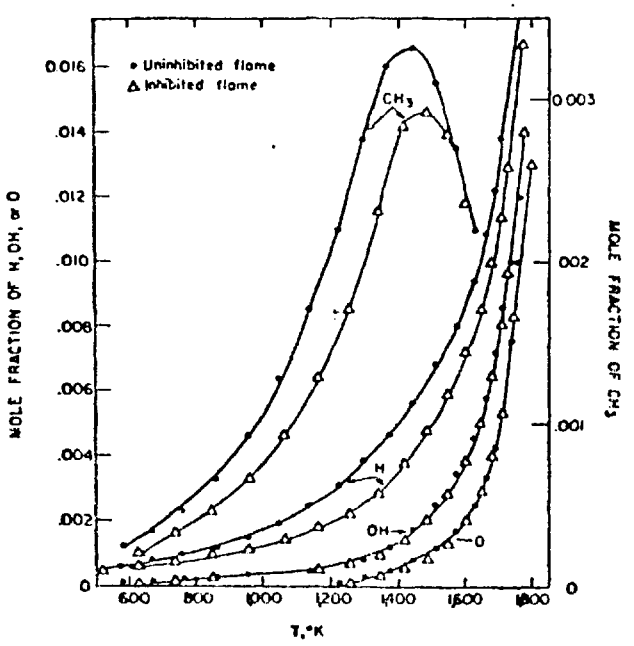

Figure 3.5 - A comparison of the mole fractions of H, CH_3, OH and O in an inhibited and uninhibited flame (From ref. 43).

---

are controlling. Chain branching of reaction 6 has been considered, however the data of Figure 3.5 for methane shows clearly the interelation between CH_3 and H-atom mole fractions for methane combustion inhibition.

Models of hydrogen-oxygen diffusion flames based on four reactions (87) and sixteen reactions (244, 304) have described the interelated chemical and fluid mechanic processes. However for methane and ethane oxidation as many as seventy-five reactions are considered necessary (454) for the chemical processes alone.

The global activation energy for methane fuel oxidation used in ref. 280 was 268 kJ mol^{-1}, and the value for the activation energy used in ref. 454 for $CH_4 + M \rightarrow CH_3 + H + M$ was 370 kJ mol^{-1}. Reactions that lead to production of methyl radicals will increase the rate of subsequent oxidation to products. Reaction 1 showed H-atom abstraction

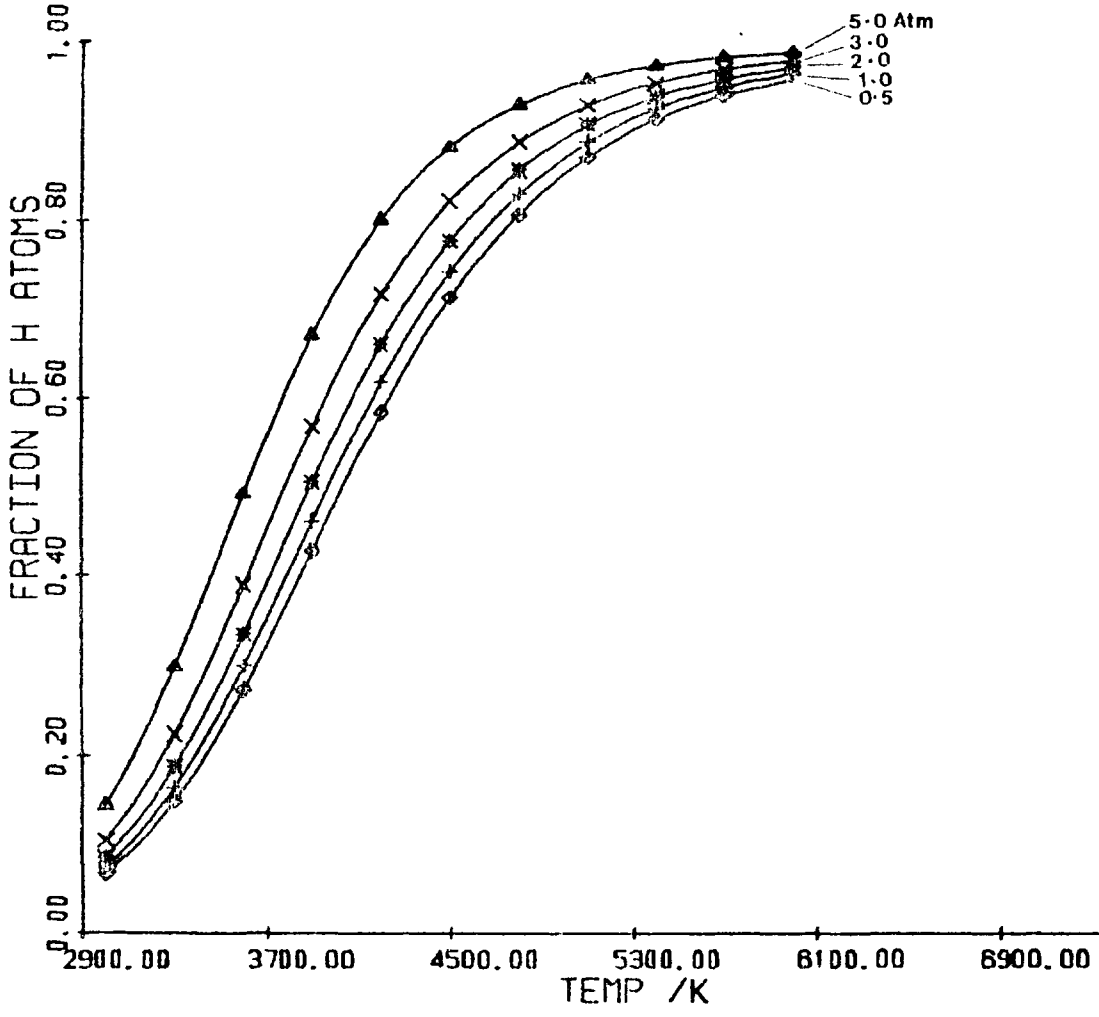

Figure 3.6 - Equilibrium fractional dissociation of hydrogen into ground state atoms as a function of temperature and pressure. (Data from Janaf).

---

by oxygen atoms possible once these species have been generated. The CH bond strength (saturated hydrocarbon molecule) is approximately 414 kJ mol^{-1} and that of H_2 436 kJ mol^{-1}, ie. effectively thermoneutral, so that atom abstraction by H-atoms does not have a high activation energy, eg.

$$CH_4 + H \longrightarrow CH_3 + H_2 \qquad 7$$

has a value of ΔE calculated at 56 kJ mol^{-1} and observed 54 kJ mol^{-1} (Laidler). In some kinetic schemes a value as low as 37 kJ mol^{-1} has been used (69). A recent review of the data gave a best estimate at 50 kJ mol^{-1} (454). The low activation energy of reaction 7 is in con-

trast to the pyrolytic formation reaction of methyl radicals from methane, with activation energy estimates nearly an order of magnitude larger (69, 195, 454) and closer to the global value. Subsequent oxidation reactions of CH_3 involving OH or O-atoms either have zero activation energies or very small values.

It appears that one of the most important rate controlling reactions in the oxidation of hydrocarbons is the H-atom abstraction of the type seen in reaction 7, and the close link with [H], flame inhibition, and $[CH_3]$ has been shown in Figure 3.5. This, combined with the data of Figure 3.4 as well as the high diffusion coefficient and importance of hot atoms, within the context of selective excitation, indicated clearly that these species were the most appropriate for burning rate control, via an electrical interaction. If the choice of H-atom source is appropriate, then the possibility exists that the hot atoms may be generated at the dissociation stage rather than by subsequent exothermic reactions (very appropriate under possible excess air quenching conditions) and further enhance the reactivity in H-atom reactions that have high activation energies. The mode of generation, apart from controlling the possible H-atom reactivity by translational excitation, may also enhance the transport processes over and above that associated with the diffusion driving force of the concentration gradient. These features will be of prime importance in practical situations with high degrees of diffusion control.

N-ATOMS

The evidence for the potential importance of these in increasing burning rates came from the study of ref.183. In that study a magnetically rotated argon arc was used to stabilise methane/air flames, and the effects of additives to the argon in increasing limiting flow rates studied. Although the rotation rates were high (10^5/min) a 'perfectly stirred' situation was not observed, as evidenced from downstream sampling. Variation in the additives used, N_2, air, fuel/air and H_2O were seen at low rotation rates, however at the max-

imum values used, Ar/N_2 was always the most effective in stabilising the flame and increasing the limiting flow rate before 'blow off'.

Some data from this study are shown as Figure 3.7. The most profound result is the demonstration shown in (b) that the effect is not one of bulk thermal heating. If it were, then based on global kinetics for the system (283) at a 10%, electrical power/total power component, an increase in limiting flow rate of nearly a factor of two would be expected. Investing the same electrical power component, not into heating, but selectively, into argon with nitrogen dissociation leads to a sevenfold increase.

The activity of nitrogen in ref. 183 was explained on the basis of production of oxygen atoms generated via

$$N + O_2 \longrightarrow NO + O \qquad 8$$

Due to the relatively long lifetime of N-atoms, the conclusion arrived at by the authors from the study is that it is best to generate species electrically with a large dissociation energy that react subsequently to produce atoms/radicals important in flame propagation.

This statement is very significant because the large dissociation energy naturally increases the power requirement of the electrical interaction. Such an electrical system being used in a practical context with argon, that was essential for stability, and generating nitric oxide was obviously not tenable. However, the work did clearly demonstrate the principle of reaction rate control through the generation of a super-equilibrium atom distribution in the main reacting volume.

In this work, reaction 8 was considered unlikely to be the principal reaction for flame stabilisation. Depending on the main system temperature, N-atoms are likely to destroy nitric oxide rather than generate it (this is discussed in full detail in Chapter 4) while other reactions involving N-atoms with hydrocarbons had shown the produc-

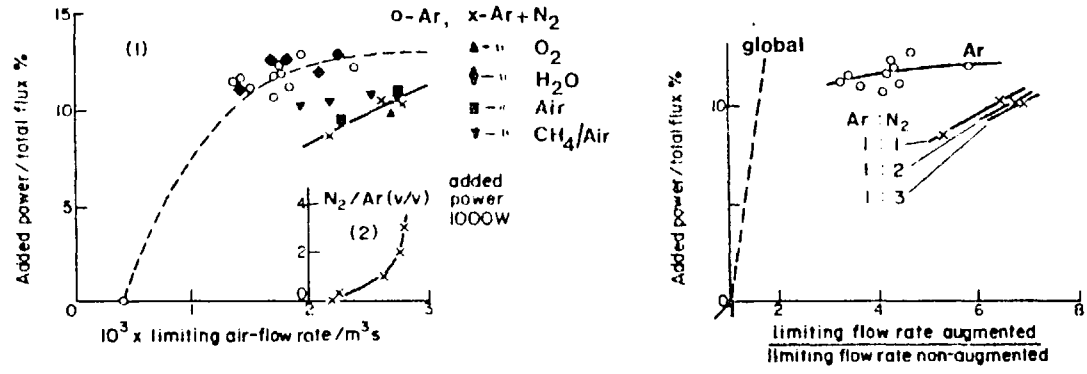

Figure 3.7 - Limiting flow rates in electrical augmentation of combustion. (From ref. 183).

---

tion of HCN/CN and the involvement of H-atoms in 'active' nitrogen/hydrocarbon systems (370, 371).

The production of the endothermic compounds HCN and C_2H_2 from hydrocarbon/nitrogen plasma reactions was considered nearly twenty years ago (273, 274), these types of reaction, mainly in the absence of oxygen, show how readily hydrocarbons produce HCN and C_2H_2 in a variety of situations with 'active' nitrogen (63, 152, 207, 249). The reaction mechanism of N-atoms with CH fragments to produce HCN, with the exothermicity channelled into vibration-rotation excitation, has been the basis of the 337 μm chemical laser (86, 155, 345) and the mechanism proposed in ref. 345 shows how the exothermicity increases from $\Delta H = 41.8$, 402, 937 kJ mol^{-1} as the N-atoms react with CH_3, CH_2, CH fragments respectively.

The work of ref. 96 considers quenching of species produced in the plasma reaction of CH_4 and N_2, but specifically in the presence of oxygen which is naturally present in combustion reactions. The work indicated that even though CH_4/O_2 ratios were low HCN was present. With the mole ratio CH_4/O_2 at 6, HCN was the product species present in maximum concentration ($\approx$29%).

In the work of ref. 96 no measurements were made of NO emission. Consideration of the appropriate kinetic data for $N/CH_n/O$ systems available (Baulch, Drysdale, Horne and Lloyd; Janaf) leads to the clear picture that even in the presence of oxygen, reaction of plasma generated N-atoms with hydrocarbon fragments leads to production of HCN, and reaction of N-atoms to produce NO and O is not the key reaction. HCN will be subsequently oxidised to NO but the controlling reaction appears to be of the form

$$\begin{array}{l} CH_n + N \longrightarrow HCN + H \\ \qquad\qquad\quad \downarrow \\ \qquad\qquad\quad NO \end{array} \qquad 9$$

Experimental evidence to support this is presented in Chapter 7. The details of the mechanism of HCN oxidation is not clear. HCN is a significant species in combustion studies because of the link to 'prompt NO' formed via faster reactions than those of the Zel'dovich scheme (476) and prior to the post flame thermal NO formation region. HCN has been observed in flames and is the most likely prompt NO generating species (190) although oxidation to NO is considered likely to be via NH_i species (135, 136) first. Reference 192 does not consider these species as necessary intermediates, and 'NH_i' can be used to reduce NO in exhaust gases (171, 285, 314) in the appropriate environment. Reference 145 suggests the presence of fuel bound nitrogen (a route to HCN) may consume NO rather than generate it when the N-atom number density is significant.

The mechanism of production of HCN has been suggested (190, 191) to be via the methylene radical,

$$CH_2 + N_2 \longrightarrow HCN + H \qquad 10$$

this reaction with CH is spin forbidden with N_2, so in the plasma situa-

tion with N-atoms dissociated in the plasma the production of HCN is even more probable.

A clear working hypothesis emerged from these investigations as to the importance of the H-atom in all forms of controlling heat release rates. The H-atoms could be generated either directly or by the intermediate reaction with CH fragments to generate CN species and H-atoms from N-atoms injected from a plasma source.

The fact that the N-atoms were seen as effective in the work of ref. 183 appears to be due to subsequent reactions in regions where the lifetime of N-atoms enables generation of H-atoms, where they would not exist due to consumption via rapid prior reaction. Naturally the extent of mixing of the system is fundamentally important. In looking for change in a 'well stirred' but not 'perfectly stirred' (as was ref. 183) the lifetime of the N-atom showed an advantage over other species, although this activity is suggested as being via the H-atom generated subsequently by the N-atom/CH fragment reactions. When looking for changes in a system with a higher degree of diffusion control, the H-atom generated directly will show advantages over that of any other species that may generate H-atoms subsequently, due to the high diffusivity and reactivity of this entity in the key reactions previously described.

At this stage of the study, many of these ideas were speculative and subsequent experiments reported in Chapters 4 and 7 were to verify these hypotheses.

ARGON

Before the plasma generator described in Chapter 6 was constructed all the experiments both previously, and reported in Chapter 4, required the use of argon gas. In the early stages of the study it was clear that argon was not an 'inert' carrier gas and flames were

stabilised with argon plasma systems. Although Chapter 6 shows it is possible to operate practical plasmas without the necessity of argon, for the sake of completeness some of the work appropriate to argon reactions will be considered.

Apart from a hot gaseous medium in which additives may dissociate, argon may ionise. The first ionisation potential is 15.76 eV while that of O_2 is 12.01 eV and CH_4 is 12.6 eV. NO^+ is the most readily formed ion in the post flame gases (see Chapter 5) with an ionisation potential of 9.26 eV and a possible excimer ion is $[ArNO]^+$. The ability of Ar^+ generated in the arc extracting, on collision, an electron from either O_2 or CH_4 was considered. The exothermicity of such a process would then be the difference in ionisation potential of Ar^+ and its excimer partner. For example if all this energy went into vibrational exciation of CH_4^+, the energy deposited in this way would be 305 kJ mol^{-1}, a value approaching the CH bond strength.

In the studies reported in ref. 228 the observed results showed such a non-translational degradation of arc energy in the inner regions of the post arc gases. A further non-translational degree of freedom available to the argon feedstock could be a reaction of the kind where Ar^+ interacts with a metastable state of equal or slightly greater ionisation potential (the Penning effect). This is a highly efficient ionisation process for small ΔIPs, that could also give rise to the results of ref. 228.

Interaction of Ar metastables with N_2 (369, 382) and repulsive potentials of O-atoms with noble gases (149) as well as a review of chemi-ionisation in the gas phase (148) were investigated; but such reactions of importance in argon plasma interactions are purely speculative, and in view of the developments in plasma generator design, not of great importance for practical plasma situations.

OZONE

A possible electrical interaction considered was to generate ozone through a silent electric discharge, and use this molecule to store labile O-atoms that, according to the work of refs. 83 and 84 are important in ignition and augmentation. It is well known that under thermal action or red light photolysis of O_3, the O-atom produced is in the ground state ^3P (Laidler), however decomposition by ultraviolet light ($\lambda < 200$ nm) leads to the production of $O(^1D)$ (the main candidate for low temperature ignition (83)) with at least two excited states of molecular oxygen involved in the overall photolysis scheme (Wayne).

A possible hybrid of 'ozone O-atom storage' followed by either photolysis or thermal decomposition of O_3 to O_2 and $O(^3P)$, according to ref. 83 would lead to a reduction in ignition temperature, while to generate the $O(^1D)$ would require vacuum uv irradiation, as in the case of O_2 photolysis to this state, but could potentially lead directly to ignition.

A simple ozone generator powered by a 6 volt trembler coil was built and produced 2% O_3 in air (by iodide assay). Very crude preliminary studies in modifying the blow off of a bunsen type flame showed no detectable change. No interpretation of such a situation is wise without experiments to monitor the ozone concentration approaching the flame front (ie. by absorption spectroscopy) because of the very facile decomposition of O_3 by O_2 ($^1\Delta g$). Because the energy separation of O_2 ($^1\Delta g$) from the ground state O_2 ($^3\Sigma g$) is only 0.98 eV (see Figure 3.3) in a Boltzman distribution of states, at pre-heat temperatures, % levels of this state may exist in the oxidant, some considable distance from the flame front. It has been considered as the most abundant metastable in atmospheric studies (12).

The reaction

$$O_3 + O_2 (^1\Delta g) \longrightarrow 2O_2 + O(^3P) \qquad 11$$

is particularly efficient at quenching O_3, due to the fact that the endothermicity is close to the value of the activation energy (143) but more importantly, for quenching, the pre-exponential frequency factor is close to the collision frequency (Mulcahy). Reactions of O_3 with H-atoms have been studied (36, 337) and lead to efficient chemiluminescent formation of OH* (313). However it is unlikely, that as such, O_3 could remove H-atoms and not modify burning velocity at all, especially when consideration is given to the sensitivity of Su to H-atom concentration. Further experiments to elucidate the exact behaviour of O_3 on burning velocity are worthy of further study, due to the potential as an O-atom source, with the proven role of the latter in photochemical augmentation of combustion.

The importance of O_3 in the context of electrical methods of improving combustion is not certain at the main heat release stage, it may be an appropriate interaction at the interface of main heat release and product discharge. In many circumstances the total heat release is quenched at the CO stage. In the oxidation of CO, the reaction

$$CO + OH \longrightarrow CO_2 + H \qquad 12$$

is considered as the fastest reaction leading to CO_2 (122, 456). However studies on the formation of ozone and interaction with CO have been made (146, 368) and are a potential electrical interaction worth further study for combustion. Research into large scale production of ozone have been made (182) with a view to NO_x emission control via NO oxidation and hydrolysis. The effects of ozone on heat release rates are not as clear as other entities considered here due to problems of quenching and the absence of in-situ optical concentration measurement

of O_3 approaching the flame front.

PEROXIDES

The presence of peroxides in the reactions associated with cool flames, pre-ignition and knock has long been known (73, 120, 121, 459; Lewis and von Elbe) and in subsequent reactions to produce excited formaldehyde (127, 385, 425). This association has led to numerous fuel additives based on peroxides as cetane number improvers for Diesel fuels (217, 220, 237, 293, 332, 347, 348, 366, 373, 432). A number of reviews on the effects of peroxides in hydrocarbon oxidations (162, 317, 318) consider the importance in low temperature oxidation reactions, and extensive studies were made during the 1930s for rocket fuels (365).

Consideration in this study was given to the possibility of photochemically induced decomposition in a manner similar to ozone, and some work specifically relating to photochemical decomposition of peroxides in combustion was recently published (10). However with all the information leading one to conclude that peroxides may modify burning velocity and cetane numbers of Diesel fuels, recent studies on both laboratory flames (312) and practical Diesel engines (204) showed them to have no major effect, other than that explainable in terms of their fuel value alone.

With such a large amount of data available to support the activity of peroxides as possible additives to influence reaction rates in combustion, electrical methods to utilise this activity were sought. No such interaction was attempted in this study, although the combination of a peroxide in an alcohol fuel combined with the kind of electrical interaction described in Chapter 5, would be worthy of further study for combustion improvement in an ignition delay context, for Diesel operation of alcohol fuels.

With more reliable thermal data available and high purity preparation of elegant peroxides (16) consideration of theories of peroxide structure and activity in combustion (35) should lead to more effective use of such additives.

INHIBITORS

These species in combustion were of fundamental importance in this study within the framework of reaction rate control, and it became apparent early in this study that these species activity was linked closely to their effect on the H-atom concentration.

The most extensively used inhibitors are halogenated hydrocarbons (42, 101, 116, 117, 284) and consideration has been given to electron attachment to the halogen atom prior to decomposition as the primary mechanism of inhibition (102, 306). Theoretical (400) and experimental (312) studies suggest that this is not a key factor. The confusing effect of some halogenated additives is the ability to act as inhibitors and catalysts of ignition (284). However in the latest review to date (116), the primary function of RX additives is reaction to the halogen acid HX, removing H-atoms. This may equilibrate later in the post flame situation leading to generation of H_2 and H-atoms as has been observed in ref. 42. This property is a function of the halogen X, where the inhibiting action generally follows the reverse sequence of the electron affinity of X (ie. Cl at 3.61 eV is the worst inhibitor).

Other compounds are effective inhibitors apart from halogens, such as metals (433). The unpaired electron of nitric oxide leads to its well known activity as a radical scavenger (403, 404) and can lead to chemiluminescent reaction with H-atoms to form HNO (423). This reaction was considered for measurement of H-atom production, however vacuum ultraviolet methods applied directly to a hydrogen arc,

to determine the number density, have been reported (33).

PLASMA METHODS

From the surveys of previous work, the species that needed to be generated for controlling heat release in flames clearly emerged as the H-atom.

A number of methods have been reported for generating such species based on heated wires or microwave sources (Laidler, Mulcahy, McTaggart and Venugopalan), however for the initial studies, addition of H_2 to argon plasmas proved to be the most readily available method. (Figure 6.20e shows the afterglow of an H-atom plasma expanding into atmospheric pressure from a total H_2 feedstock. N-atoms were generated initially by addition of N_2 to an argon plasma. One early form of such a system is seen in Figure 4.2a. Figures 6.20b and 6.20d show expansion and recombination of N-atoms from a total nitrogen feedstock plasma. The removal of the argon constraint was made possible by the development of the plasma generator reported in Chapter 6).

A plasma method to generate H-atoms could be based on plasma production by laser pulses focused on the appropriate target material. Such a technique has been considered for studies on minimum ignition energies initially without targets (453).

In the extremely elegant experiments of ref. 255, the authors show the importance of the pulse duration (energy deposition) and target material constitution in modifying the generation and subsequent propagation of the 'spherical' flame front resulting from the plasma generated by a Q switched ruby laser.

The studies of ref. 255 showed clearly, for short pulse durations (20 ns half widths), the constitution of the target material was not important because, provided ignition was established, the expanding

flame front propagated independently of the plasma constitution, which in the absence of further energy absorption from the laser to sustain it, decayed away while the flame kernel expanded. However for long durations (about 1 ms) energy is absorbed continuously into the plasma to sustain the growth of the plasma 'sphere', (the source is never a point; the plasma propagates along the laser beam from the focus (453)). The boundary of the plasma, if travelling at a greater rate than that of the flame kernel, may overtake it, and at that point in time the constitution of the plasma becomes important in the further propagation of the then turbulent combustion front.

In the experiments of ref. 255 sodium chloride was used as an inhibitor, and the plasma boundary, when overtaking the expanding flame kernel, subsequently was prevented from further growth by the chloride inhibitor, and combustion ceased. These experiments were considered particularly important in this study because of the possibility that the target material may be an interstitial metal hydride commonly used as a 'hydrogen metal sponge' that could possibly lead to transition to a detonation, which is the natural progression in consideration of increasing the rate of travel of a chemical conversion wave in this section devoted to methods of controlling reaction rates. Transitions in conversion wave velocities of 0.1 to 10 m s^{-1} for deflagration to 3000 m s^{-1} in detonations are characterised by the preheating (with negligible dilution) of the reactants by a shock wave prior to chemical transformation. The possibility of hot H-atoms, generated by a laser pulse on an interstitial metal hydride, generating species that may overtake the resultant main conversion wave could present an interesting possibility for ignition, and subsequent propagation, from an intermittent ignition source.

While H-atoms were considered as the species for controlling

heat release rates, the principle of chemical reaction control through generation of non-Maxwell-Boltzmann distributions of species applies generally to any system where the rate of transformation is under kinetic control through the limiting concentration of key species. All the plasma injection experiments may be described by a schematic diagram as seen in Figure 3.8.

In the reacting volume B, a transformation is to be established that has associated with it a Gibbs free energy ΔG, and a corresponding equilibrium constant, K ($\Delta G = -RT \ln K$) that will determine the maximum extent of possible reaction in the B region. The value of ΔG ($= \Delta H - T\Delta S$) is a function of the equilibrium temperature, exothermicity and entropy change for the conversion.

If ΔG is -ve, then given an infinite amount of time conversion will occur, however in a practical situation the residence time within the B volume may be limited, and transformation occuring at a rate determined by key species whose concentration is a direct function of the equilibrium temperature of the B region. Raising the temperature within the B region will increase the concentration of these species (as a function of $\exp(^{\Delta E}/RT)$ but may lower the value of ΔG for the overall transformation (if ΔS is +ve) and therefore the maximum extent of conversion, while at the same time causing possible loss of the key species in other reacting channels.

The A region defines a further region at thermal equilibrium at a temperature considerably in excess of the B region, where the key species for the B region transformation are ideally completely dissociated.

Having been identified as the key species, injection into the B region then causes the transformation to occur at a rate associated with a concentration of these species corresponding to a temperature very much greater than that associated with the Maxwell-Boltzmann

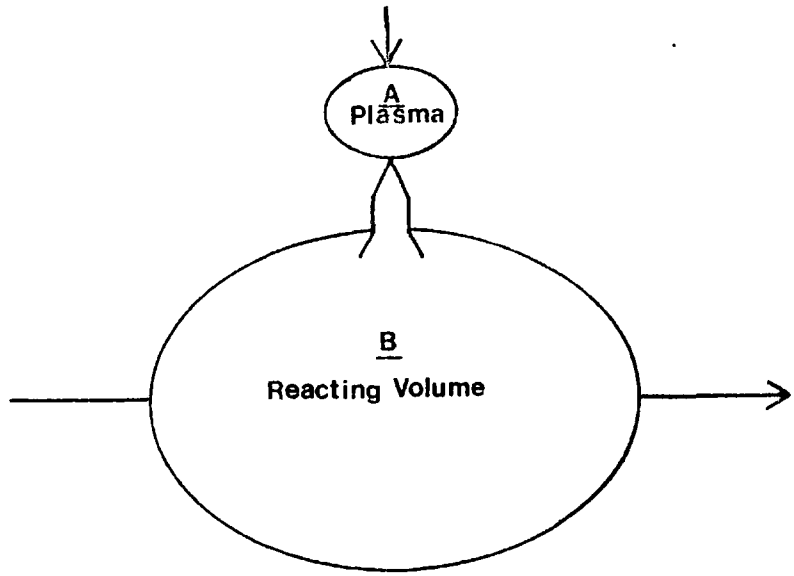

Figure 3.8 - Schematic of the arrangement for reaction rate control via injection of appropriate plasma generated molecular fragments.

distribution of the 'passive' components of the B volume system.

A 'temperature' of the B region could be defined, based on the instantaneous number density of these species at the instant they enter the B region. Practically however, if these species are key ones, then their concentration would be in steady state due to their rapid disappearance and their presence would be monitored by the increase in production rate of the stable products (or reactant loss) at the equilibrium B temperature, within the B volume.

This generalised condition exists for many pollutants in exhausts from combustion systems, as well as for the main heat release reactions. The principle may be applied to a number of reacting systems where, for example in a chemical laser, the power output may be limited by the formation rate of specific atoms within the cavity, which here corresponds to the B region.

This process then corresponds to selective 'heating' of the key reaction alone, and is therefore the most efficient way of controlling the

subsequent reaction rate. The line representing this method, with a specific $\Delta E_n'$ is line iii) of Figure 3.1.

Nitric oxide, soot and carbon monoxide are three such pollutants that are endothermic at exhaust temperatures. Chapter 4 describes plasma methods based on this principle for depollution and increasing heat release rates.

CHAPTER 4

PRELIMINARY PLASMA JET DEVELOPMENTS

INTRODUCTION

The object of this Chapter is to report some of the experiments and calculations that resulted from the considerations of Chapter 3, relating to the species N, H, O and OH generated under varying degrees of control, with ionic species from the plasma jet.

Consideration of Figures 1.2 and 1.3 shows clearly the interelation of economy and specifically NO emission. The inherently low oxygen concentration of quantity power-control mode systems of, for example Figure 1.3, enables NO_x control at the product discharge stage catalytically, under circumstances where no control is attempted at the heat release stage.

However in the quality power-control mode, NO is always present in excess oxygen and may not be reduced with a transition metal catalyst. This situation provided the ideal opportunity to demonstrate experimentally the principles shown in Chapter 3.

NITRIC OXIDE REMOVAL BY N-ATOMS

The importance of N-atoms in the flame stabilisation experiments of ref. 183, and the suggestion that they subsequently generated NO, was an obvious starting point for a study directed towards improving combustion.

Although plasma sources have been used to generate NO synthetically since the Birkelande-Eyde process of 1909, they are still researched today in the context of NO manufacture (28). This section is to demonstrate the principle of selective removal of NO by N-atoms in an exhaust environment where other methods are not successful. Because this method occurs at the product discharge stage it could potentially free all combustion constraints for such systems.

The equilibrium reaction relating to the formation of NO in post flame gases is

$$1/2N_2 + 1/2O_2 \rightleftharpoons NO$$

The equilibrium constant for this reaction increases with temperature and in partial pressures may be expressed as

$$K_p = \frac{pNO}{pN_2^{1/2}\ pO_2^{1/2}}$$

The values of K_p, and the mole % of NO as functions of temperature are shown in Table 4.1 for NO formation in air

TABLE 4.1

T/K	K_p	mole % NO
1000	8.93×10^{-4}	0.036
2000	3.84×10^{-2}	1.53
3000	1.65×10^{-1}	6.09
4000	3.54×10^{-1}	11.8

NO levels predicted by equilibrium considerations at flame temperatures are therefore very much higher than observed experimentally, while measured levels at exhaust temperatures are higher than would be expected thermodynamically at exhaust temperatures. Both the rate of formation of NO at flame temperatures, and its subsequent destruction at exhaust temperatures are therefore rate constrained.

The simplest kinetic scheme considered for the formation of NO is due to Zel'dovich (476), and may be extended to include the OH radical. The sequences are

$$O + N_2 \xrightarrow{k_1} NO + N \qquad 1$$

$$N + O_2 \xrightarrow{k_2} NO + O \qquad 2$$

$$N + OH \xrightarrow{k_3} NO + H \qquad 3$$

ΔE for reaction 3 is small and not very temperature sensitive. While reaction 1, due to the high dissociation energy of N_2, is the rate determining step. Using reactions 1 and 2, then

$$\frac{d[NO]}{dt} = k_1[N_2][O] + k_2[N][O_2] \qquad 4$$

Assuming a steady state approximation for N-atoms (ie. $d[N]/dt = 0$) then

$$\frac{d[N]}{dt} = k_1[O][N_2] - k_2[N][O_2] \qquad 5$$

$$\therefore \frac{d[NO]}{dt} = 2k_1[N_2][O] \qquad 6$$

to a first approximation equation 6 may be integrated with τ as the mean residence time in the hot post flame gases to yield

$$[NO] = 2k_1[N_2][O]\tau \qquad 7$$

This simple expression shows clearly the fundamentally important parameters in NO formation of temperature (in k_1), $[O]$ (for the observed $[NO]$ peaking at values of λ just lean of stoichiometric (Figure 1.3)), and residence time, (which results in the inverse relationship between CO and NO concentrations observed). The key species that constrains the attainment of NO equilibrium at flame temperatures is the O-atom. (It is possible to express equation 7 as $2k_1K_wK_o[H_2][N_2][O_2]\tau/[H_2O]$, using established equilibria between H_2, O_2, O, H_2O).

The atom that constrains the destruction of NO at the exhaust stage is however the N-atom. If one considers the two following reactions that may compete for N-atoms

$$N + O_2 \xrightarrow{k_8} NO + O \qquad 8$$

$$N + NO \xrightarrow{k_9} N_2 + O \qquad 9$$

Neglecting the reverse reactions and other competing channels for N-atoms, including the slow third body recombination, then

$$\frac{-d[NO]}{dt} = [N]\left\{k_9[NO] - k_8[O_2]\right\} \qquad 10$$

Therefore when $k_9[NO] > k_8[O_2]$, NO may be destroyed at a rate dependent on the N-atom concentration. The strong dependence of N_2 dissociation with temperature may be seen in Figure 6.9. Increasing the system exhaust temperature has a negligible influence on the equilibrium N-atom concentration, but increases ΔG for destruction, and since $\Delta G = -RT \text{ Ln } K_p$ this increases the value of K_p, as seen in Table 4.1.

The Arrhenius forms of k_8 and k_9 are, respectively, 6.43×10^9 T exp(-6250/RT) and 3×10^{13} exp(-334/RT). These rate constants have been plotted as a function of temperature in Figure 4.1a. The very low activation energy of reaction 9 makes it virtually insensitive to temperature, while k_8 exhibits a much stronger temperature dependence. The concentration of oxygen may be as much as 3 orders of magnitude greater than that of nitric oxide in a practical exhaust. However, as the temperature of the exhaust gas is reduced, so the term $k_8[O_2]/k_9$, representing the lowest NO level attainable on injection of N-atoms approaches zero. Figure 4.1b shows this to be possible even in the presence of air.

Therefore the generation and injection of N-atoms into an exhaust gas could, by selective low temperature pumping of reaction 9, lead to zero NO even in an oxidising environment of excess air, where catalytic reduction fails due to the oxidising atmosphere.

Experimental - The experiments to demonstrate this principle were very simple. A fast flowing synthetic exhaust gas of $N_2/O_2/H_2O/$ NO flowed at 4.2 l s^{-1}. The exhaust NO was originally analysed using a Shaw fuel cell (383) with an oxidiser tube, and later repeated with a

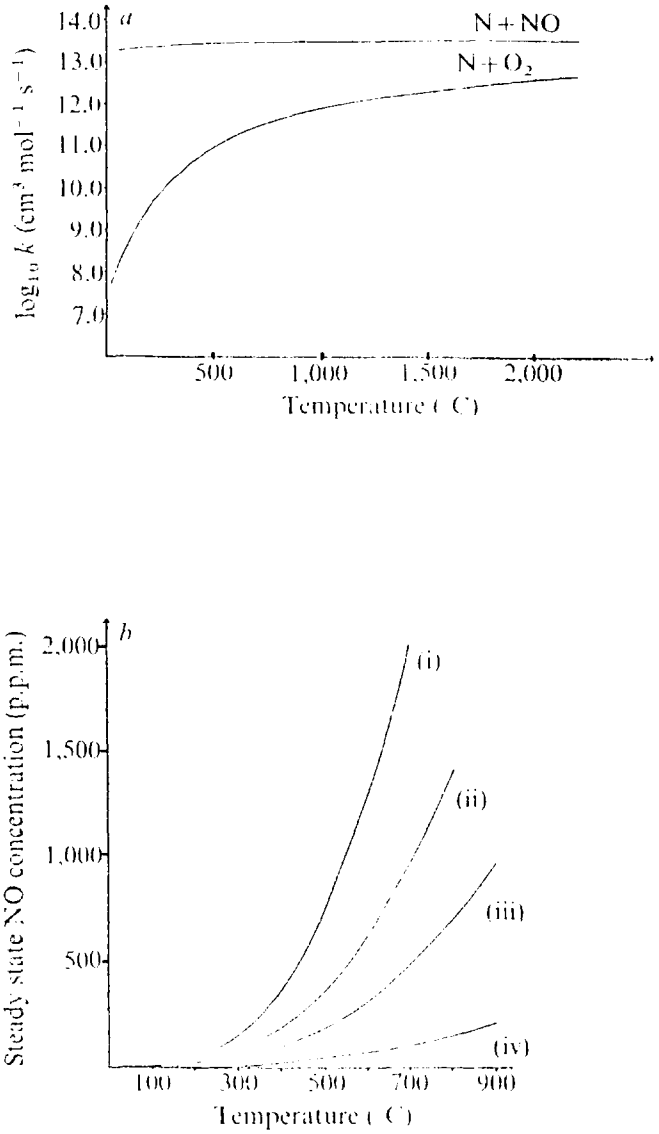

Figure 4·1 – Comparison of rates of reaction 1 and 2. a, Temperature dependences of rate constants; b, minimum nitric oxide concentration attainable for O_2 (i) 21%, air (leanest limit), for example, an unthrottled engine at low load; (ii) 10%, unthrottled engine at high load; (iii) 5%, throttled engine, low load, high air/fuel ratio; (iv) 1%, throttled engine, idle or high load.

chemiluminescent analyser in later experiments. The appearance of the control experiment was that as seen in Figure 4.2g, with an argon plasma injected. The NO present was 3000 ppm. Addition of 10% N_2 to the plasma gas resulted in an immediate reduction to 80 ppm NO in the exhaust flow, resulting in a change in luminosity as seen in Figure 4.2h. This demonstrated clearly that, even at atmospheric pressure, N-atom recombination was slow compared with the removal of NO that exhibits second order kinetics and could be used to reduce NO in the presence of oxygen.

It was possible under some conditions with an argon plasma to generate NO, through reaction 3, when H_2O dissociated at the plasma interface. Addition of N_2 to the plasma stream caused sufficient cooling of the arc, at the exhaust interface, that this NO was immediately reduced. However the reaction $N + OH \rightarrow NO + H$ has a very low activation energy and when OH is present could perturb NO removal if attention is not paid to this reaction.

Conclusion - The demonstration at this stage was far from a practical method. Consideration would need to be given to methods of generating N-atoms without argon, as well as to the total powers required, competing reactions and mixing patterns. These aspects are considered in subsequent sections of the thesis. Selective reduction of NO in an oxidising environment has obvious potential for releasing the combustion constraints of for example exhaust gas recirculation (EGR) or injection retard on NO emissions, which are closely linked to, and increase soot emissions for Diesel engines. The work of Chapter 3 introduced the importance of the electronic states of the species involved in selective reactivity. Different electronic states react very differently in bimolecular reactions, and it is not necessarily the highest excited state that is the most reactive.

The importance of the state of molecular oxygen in the exhaust is of concern in the N-atom injection experiments. The importance of the $O_2(^1\Delta g)$ state was mentioned as a quencher of O_3, where, because the

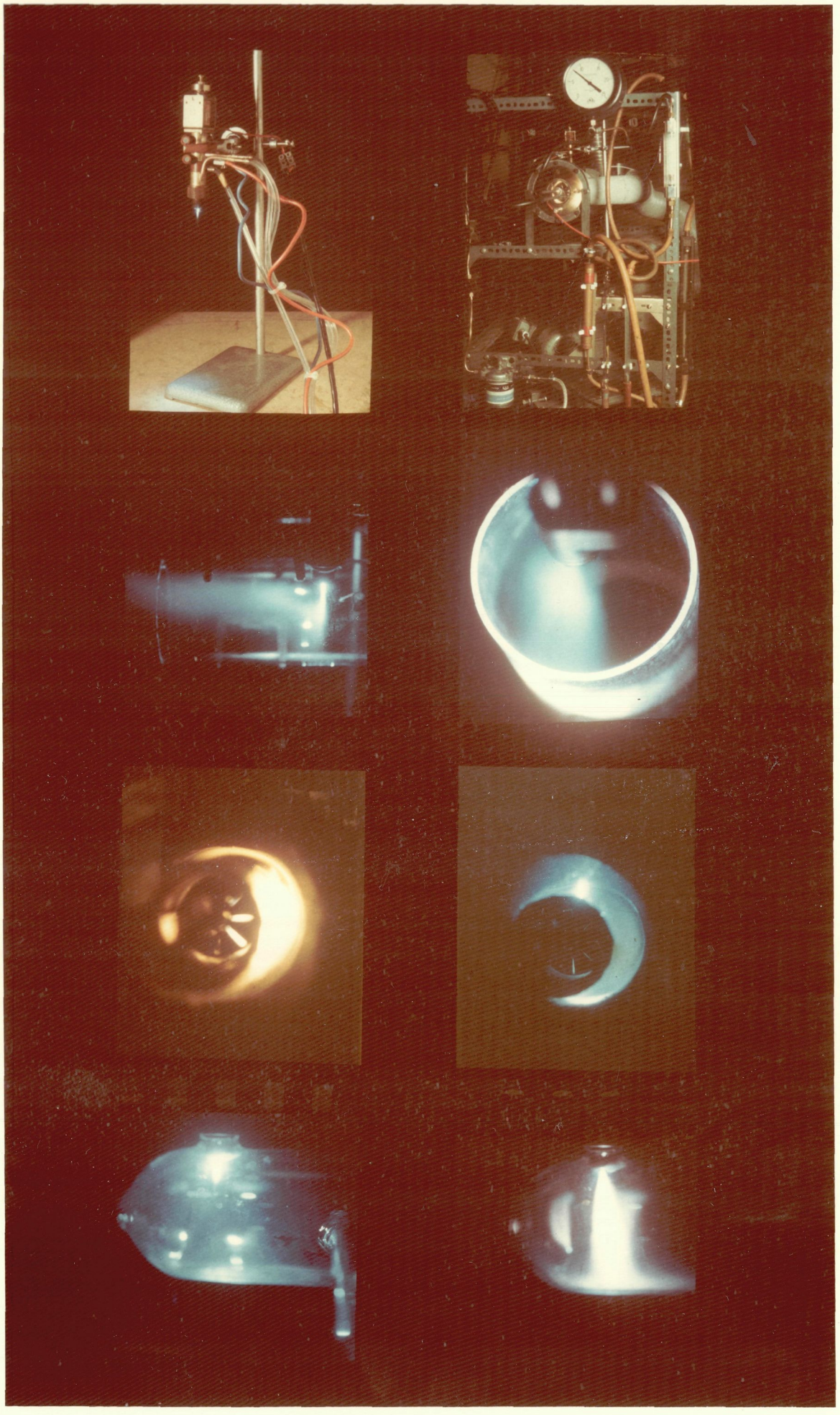

Figure 4.2

energy separation from O_2 ($^3\Sigma\bar{g}$) is only 0.98 eV, population at pre-heat temperatures is appreciable.

This situation is of concern for N-atom injection, even with lower levels of O_2 ($^1\Delta g$) present at exhaust temperatures, because of the different kinetic parameters for the reactions involved. The 'intrinsic' reactivity of a particular system is seen in the pre-exponential factor 'A' in the Arrhenius expression (as mentioned in the O_2 ($^1\Delta g$)/O_3 system quenching of Chapter 3). O_2 ($^3\Sigma\bar{g}$) with an A factor of $\approx 8 \times 10^9$ (l mol^{-1} s^{-1}) is 'inherently' more reactive than O_2 ($^1\Delta g$) with an A factor of $\approx 2 \times 10^6$ (Wayne). However the exothermicity of reaction with O_2 ($^1\Delta g$) is not only higher (134 + 92 kJ mol^{-1}) due to the 0.98 eV excess energy in O_2; this excess energy contributes to the activation energy, so that its value is approximately zero. As a consequence, the reaction with N-atoms and O_2 ($^1\Delta g$) is faster, even at exhaust temperatures, than with O_2 ($^3\Sigma\bar{g}$).

The A factor in the N-atom/NO reaction is close to collision limited and the activation energy is very small (1.4 kJ mol^{-1}). The arguments for the potential of NO removal to less than 0.1 ppm levels (as seen in Chapter 6 for example) by N-atom injection will only be possible in an oxygen environment, of for example a Diesel exhaust, when provision is made for quenching of any O_2 ($^1\Delta g$) present, prior to injection. Without such provision the results obtained on N-atom injection will lead to anomalous conclusions indicating reduced ability of NO removal (even production) and, under conditions of removal, anomalously low efficiencies, with resulting over estimates of powers required.

An obvious candidate for collision limited quenching of O_2 ($^1\Delta g$) is O_3, as mentioned in Chapter 3. Since production of this entity falls within electrical methods of interaction for control, and O_2 quenching

leads to O-atom production, a system that includes a multi-purpose hybrid is worth mentioning by way of a 'thought experiment', where an ozone injection stage is used to quench O_2 ($^1\Delta g$) and produce O-atoms for soot oxidation prior to NO removal. (The review section of Chapter 5 shows the importance of O_2 partial pressure in surface removal of soot, implying, activated chemisorption of O-atoms as rate determining. O-atoms reacting with N-atoms producing NO is a slow third order process and could be neglected).

Although N-atom injection into exhaust gases of a vehicle has been reported (449), this was under a low oxygen condition of an Otto exhaust. For Diesel application a concentration of O_2 ($^1\Delta g$) in the exhaust gas higher than the expected Boltzmann distribution, is likely to exist from formation at combustion chamber temperatures.

Consideration of the fact that, at exhaust temperatures, the activation energy for the O_2 ($^1\Delta g$)/N-atom reaction is zero means that only when provision is made for removal of this species in the exhaust gas could the ground state arguments presented at the beginning of this chapter apply, and NO be removed efficiently at exhaust temperatures. The electrical method for ensuring this with ozone could lead to some interesting potential for soot oxidation.

FLAME STABILISATION BY PLASMA GENERATED ATOMS

The demonstration that N-atoms were species able to remove NO under atmospheric conditions gave a greater practical significance to the work of ref. 183, and flame holding experiments were repeated under conditions where the basic types of plasma jet (seen in Figures 4.2a and 4.6) were used. These jets are characterised by the fact that they have no magnetic rotation, a pointed anode, and argon is used as a stabilising gas.

Experimental - The flame tube used in these experiments was a commercially available unit manufactured by Ricardo and Company Ltd. and sold by Cussons Ltd. of Manchester as a "laboratory demonstration gas generator" for turbine expansion. The only modification to this standard unit was that it was fitted with a "Sonicore"* ultrasonic twin fluid atomiser and fitted with a perspex end window for optical access. Figures 4.2b and 4.5 show this unit, but a fuller explanation of the apparatus and experiments associated with the flame-tube follows in this chapter and Chapter 5.

For the flame stabilisation experiments, the atomiser was removed from the flame tube and used as a 'burner' with premixed propane/air fuel. A flame was established and a stability loop plotted of mixture strength versus linear flow velocity at the point when the flame lifted off the nozzle and extinquished.

The gas flow to the plasma plug was kept constant (120 ml s^{-1} at 20°C, 1 Atm) in these experiments, but with no electrical power consumption in the absence of augmentation. The experiments were repeated with 400 Watts power consumption at the plasma plug, with argon alone as a feedstock, and 10% N_2/Ar.

Results - The results have been plotted in Figure 4.3. The ordinate corresponds to the potential chemical power available from the propane fuel flow rate (based on a lower calorific value of propane as -2.2 MJ mol^{-1}). In this way the quotient electrical power/chemical (or total) power is readily seen. The linear velocity values on the abscissa are based on the volumetric flow rate measured (20°C and 1 Atm) and the dimensions of the rectangular area seen in Figure 4.2d. It was not the objective to estimate linear velocity accurately, but to obtain an experimental arrangement that investigated the augmentation potential, comparatively, with different additives, under a flow condition that was not as well stirred as that of ref.183 ie. with a greater

*This is a registered trade name of the manufacturers, The Sonic Development Corporation of Yonkers, N.Y. 10705, U.S.A.

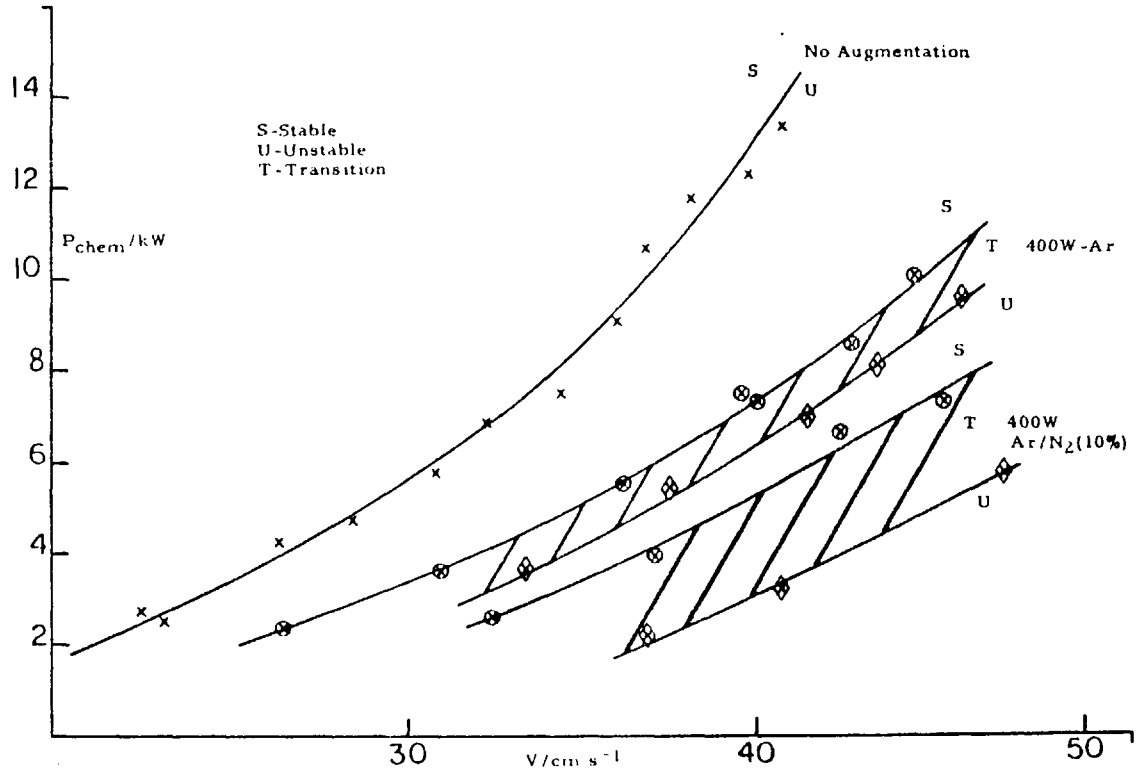

Figure 4.3 - Potential chemical power vs. linear flow velocity for the experimental situation seen in Figures 4.2 c and d.

---

degree of diffusion control and thus more representative of what is normally seen in practical systems.

Interpretation of Results - The data shown in Figure 4.3 substantiated the findings of ref. 183, in that N-atom additions were the most effective for flame holding and provided the highest return on electrical power investment, compared to argon alone.

The interpretation of this result is the same as that proposed for the system considered under N-atoms in Chapter 3, and was further evidence of the involvement of H-atoms from N/CH_n reactions as the key species in augmented situations.

For possible calculations at a later date the data was fitted to a number of empirical potential chemical power (P) vs. linear velocity (f) expressions. The best fit consistantly obtained was of the form $P = a + bf^2$ with a and b coefficients for the argon or argon/N_2 systems.

This is mentioned in order to suggest a way to correlate data from other experiments for future work. In refs. 253 and 254 involving high voltage discharges augmenting lean propane/air combustion, a loading parameter is defined as N/VP^n (253). The results indicate $n = 1.8$. It is not intended to convey the impression that this index, as close as it is to the value 2 obtained empirically in these experiments, necessarily implies a correlation, but it may be worth investigation for further studies.

Conclusion - The demonstration of the importance of the N-atom, and the suggestion that it reacts to produce H-atoms, led to the idea of trying to generate H-atoms directly in the plasma. Because this system is under a higher degree of diffusion control than that of ref. 183, data with H_2 or CH_4 (which generates 4 moles of H per mole of methane) could provide further evidence of the reactivity of the H-atom. Attempts to operate the plasma plugs of Figures 4.2a and 4.6 on Ar/H_2 and Ar/CH_4 mixtures continuously were not possible in a reproducible manner, due to difficulties of introducing these gases into the plasma plug and obtaining continuous stable operation. Both gases destabilise the arc by electron attachment (see Chapter 6) and in the case of CH_4 massive dissociative cooling, (the sum of bond energies for CH dissociation in methane is $427 + 419 + 523 + 339 = 1708$ kJ mol^{-1} for successive stripping through methyl, methylene and methine radicals), compared with 945 kJ mole for N_2. Enhanced radiative losses from carbon particles produced by pyrolysis as well as plasma anode orifice restriction by soot, did not allow any experiments with CH_4 in the plugs of Figures 4.2a and 4.6, for continuous operation.

With hydrogen addition to argon, the plasmas were stable for a few minutes only, and the red 656 nm H_α line was clearly seen with a hand held direct vision spectroscope, indicating the presence of H-atoms. Using an Ar/H_2 feedstock it was possible to stabilise linear

flow velocities up to the limit of the experimental reactant flow rate (250 cm s^{-1}) without blow off.

These experiments further substantiated the role of the H-atom as important in flame stabilisation, with the added advantage of removing the need to generate 'expensive' N-atoms, which could lead to NO via HCN. In order that accurate spectroscopic measurements could be made (as described in Chapter 7) as well as full practical advantage made of these results for improving combustion, a generator that provided these atoms in a stable reproducible manner from suitable feedstocks was required. Chapter 6 describes the development of one such atom/plasma generator. Figure 6.20e shows its continuous operation on hydrogen at atmospheric pressure and 6.20h shows operation on methane. A measure of the increased radiative transfer from a hydrocarbon feedstock due to the carbon formed by pyrolysis of the hydrocarbon in the arc, is seen in the photographs of Figures 6.20g and h which are $^1/_4$ and $^1/_{1000}$ second exposures respectively. This radiative emission is a further electrical interaction that may improve combustion within a furnace environment, at a variety of turn-down ratios - note how the flame is anchored to the generator in Figure 6.20h compared to g.

POWER REQUIREMENTS

The power requirements for a plasma interaction are of the utmost importance for a practical electrical interaction, and depend very much on the dissociation energy of the atom to be produced, and whether the operation is continuous.

Chapter 6 describes the ways in which electrical efficiency of atom generation was improved, with the novel plasma generator developed in this work. This section is included to calculate the minimum power required for NO removal by N-atoms from a system with high gas flow. Because they have the highest dissociation energy

(9.76 e V) of the diatomic species considered in this work N_2 represents a severe test on electrical interaction feasibility.

It would be the ideal situation if combustion produced no nitric oxide, or other emissions, at the heat release stage. Whether this is attainable practically depends very much on the mechanism of engine power control. If it were possible to control the power output of a conventional spark ignited engine, operating lean of stoichiometric, without the use of a throttle this idealised objective could be realised.

With no throttling, the low power operation pumping losses would be reduced, while rapid heat release would enable maximum expansion ratio to be utilised and reduce heat losses from the combustion chamber, thus increasing brake thermal efficiency. This increased efficiency would occur while nitric oxide and unburnt hydrocarbon emissions were reduced. It is clear that plasma injection is one way to assure this, and in doing so overcome the apparent mutual exclusiveness of economy and emissions.

For those practical systems that employ variation of the air to fuel ratio as a means of power control, and have highly diffusion controlled rates of heat release, the potential for emission control at the heat release stage is restricted by the nature of diffusion controlled combustion. The mechanism for prevention of emission formation at the combustion stage is less clear, and generally requires emission control at the product discharge stage. However, due to the fact that with quality power-control mode engines, there is always excess oxygen in the exhaust, the ability to reduce (in a chemical sense) the nitric oxide is inhibited due to the oxidising environment of the exhaust, as described in Chapter 1. Selective reaction pumping was the main theme of the plasma work, and the Diesel engine exhaust provides a suitable example to demonstrate selective chemical reduction in an oxidising environment.

Inspection of Figure 1.2 for Diesel engine operation shows clearly how rapidly BSFC may rise with NO reduction by injection retard. Although not shown, soot emissions are also increasing with NO reduction by injection retard. It is possible therefore, to consider for a given desired engine power output, that the power may be obtained at a minimum BSFC (b1) with an associated NO emission (NO-1) which is generally a maximum in the best economy region (it is not necessarily the maximum over all possible injection conditions since too advanced injection timing will lead to increased NO emission at increased BSFC).

If the engine is then operated at the same power output at a condition of increased BSFC (b2) to obtain a corresponding reduction in NO (NO-2) then obviously the thermal efficiency at the same power has fallen and the available energy in the fuel that was available to do work, and was used as such at b1, has been lost from the system as irreversible heat losses.

The average thermal energy stored in liquid hydrocarbon fuels on a mass basis is quite constant at ≈44 MJ/kg. On this basis the fuel wasted (b2 - b1) for an NO reduction of (NO-1 - NO-2) has meant that NO reduction obtained by injection retard has associated with it a power consumption requirement per NO molecule reduced on the basis of the fuel wastage rate. It is this figure that forms the datum on which NO reduction by N-atom injection should be judged in the electrical interaction context.

The following calculations attempt to obtain such a datum. Obviously because the ΔBSFC vs. ΔNO data is different for each engine type and operating condition, the values will vary from engine to engine and the extent of NO reduction required. Figure 1.2 shows data from a range of different engines to make the following calculations as representative as possible, as shown in Table 4.2.

TABLE 4.2

Condition	BSFC	BS NO_x
1	266	4.0
2	255	5.0
3	248	6.0
4	244	7.0
5	242	8.0

if $Q = 44\ MJ\ kg^{-1}$

then $\eta_b = \frac{1}{BSFC \times Q}$

At the power condition used, the fuel energy/unit work = $\frac{1}{\eta_b}$ = E.

If condition 5 is taken to represent the maximum economy case, then it is possible to calculate a value of ΔE/molecule of NO reduced by injection retard as seen in Table 4.3. For convenience of comparative units the final value of ΔE/molecule is given in eV/molecule, using the following:-

$$\Delta E/\text{molecule} = \frac{\Delta E}{k\ N'_A\ NO_x\ (gkWh)}$$

$$\text{with } N'_A\ (NO) = \frac{6.022 \times 10^{23}}{30} = 2.01 \times 10^{22}\ \text{molecules/g}$$

$$1\ eV/\text{molecule} = 1.6021 \times 10^{-19}\ J/\text{molecule} = k.$$

TABLE 4.3

Condition	η_b	NO_x(g/kWh)	E(kWh)	ΔE(kJ)	$\Delta E/m$(eV/molecule)
1	30.61	5.36	3.267	1040.4	60.3
2	32.00	6.70	3.125	529.2	37.0
3	32.88	8.04	3.041	226.8	13.21
4	33.34	9.38	2.999	75.0	3.78
5	33.58	10.72	2.978	0	-

For an efficiency of unity in N-atom injection removal of NO the minimum value of $\Delta E/m$ is $9.76/2 = 4.88$ eV/molecule which is much less than the fuel energy cost for NO removal by injection retard under conditions approaching those required by emission regulations. As emission regulations become more stringent the potential for a saving on an energy basis by N-atom injection increases significantly. Consideration of the increase in particulate emission with injection retard further enhances the practicality of this system.

These calculations are intended to demonstrate that once a Diesel engine is operated away from its maximum economy condition, to meet emission requirements, the highest power electrical interaction considered in this study becomes even more attractive.

The problem of NO and soot emission may be solved, even in the Diesel combustion situation with alcohol fuels, provided the problem of ignition delay for these fuels can be solved. Chapters 3 and 5 consider ways in which this could be done, which would make this plasma electrical interaction, that clearly demonstrated the principle of selective reaction rate control using plasmas, redundant at the product discharge stage.

The minimum powers required for N-atom removal of NO can be calculated by combining the concentration of NO (W in vppm) and the exhaust flow rate (Z in ml s^{-1}) to define the number of N-atoms per second required and the resulting power in N_2 dissociation. The results of this calculation are shown in Figure 4.4.

PLASMA INJECTION FOR SOOT REMOVAL

The objective of a plasma interaction, to reduce soot emissions, is to try and increase the rate of oxidation at any stage in the soot formation sequence from saturated gaseous molecules, to the fully formed soot particles.

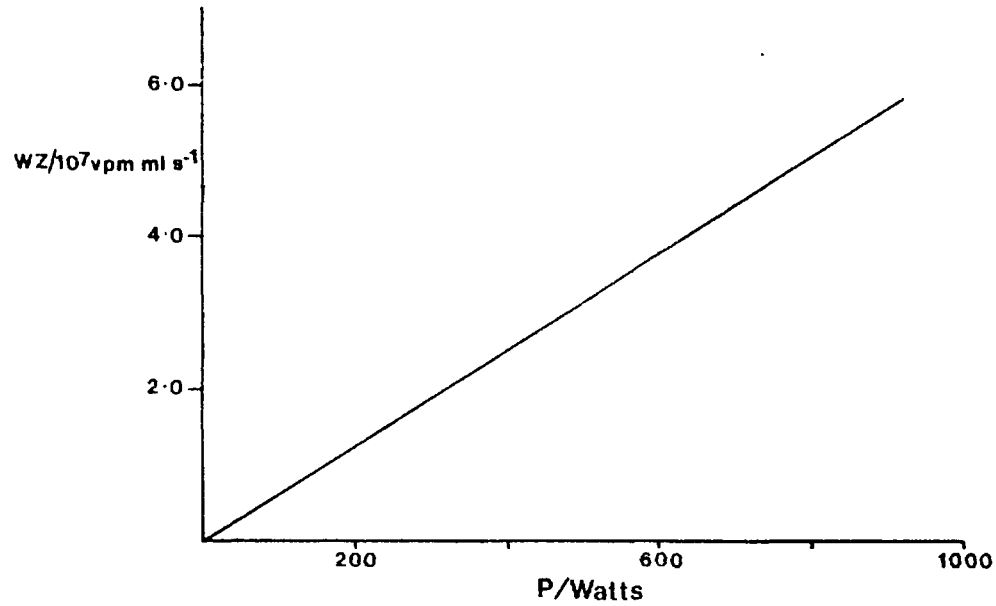

Figure 4.4 - Minimum powers required for production of ground state N(^{4}S)-atoms to reduce to zero, an initial value of WZ (NO concentration-flow parameter).

Because of the slower rate of oxidation of particles it is advantageous to interact with the soot precursors directly at the stage when rates of oxidation are still associated with gas phase kinetics. As polymerisation of gas phase hydrocarbons occurs, so the possibility exists of absorption by these species of radiation from an argon plasma (there was no emission in the visible or uv below 395 nm for the argon plasma). However such absorption could aid with decomposition, if highly oxidising species were generated.

While the plasma jets used in this work are an abundant source of electrons, known to be important in soot agglomeration (see Chapter 5), the main objective in this work was to generate O-atoms or OH radicals via the plasma interface with air or water vapour, and then to use these highly oxidising species to remove soot precursors, before the difficult phase when particles are forming.

Experimental - For these experiments the Ricardo flame tube was used, fully assembled, with the modifications shown in Figure 4.5.

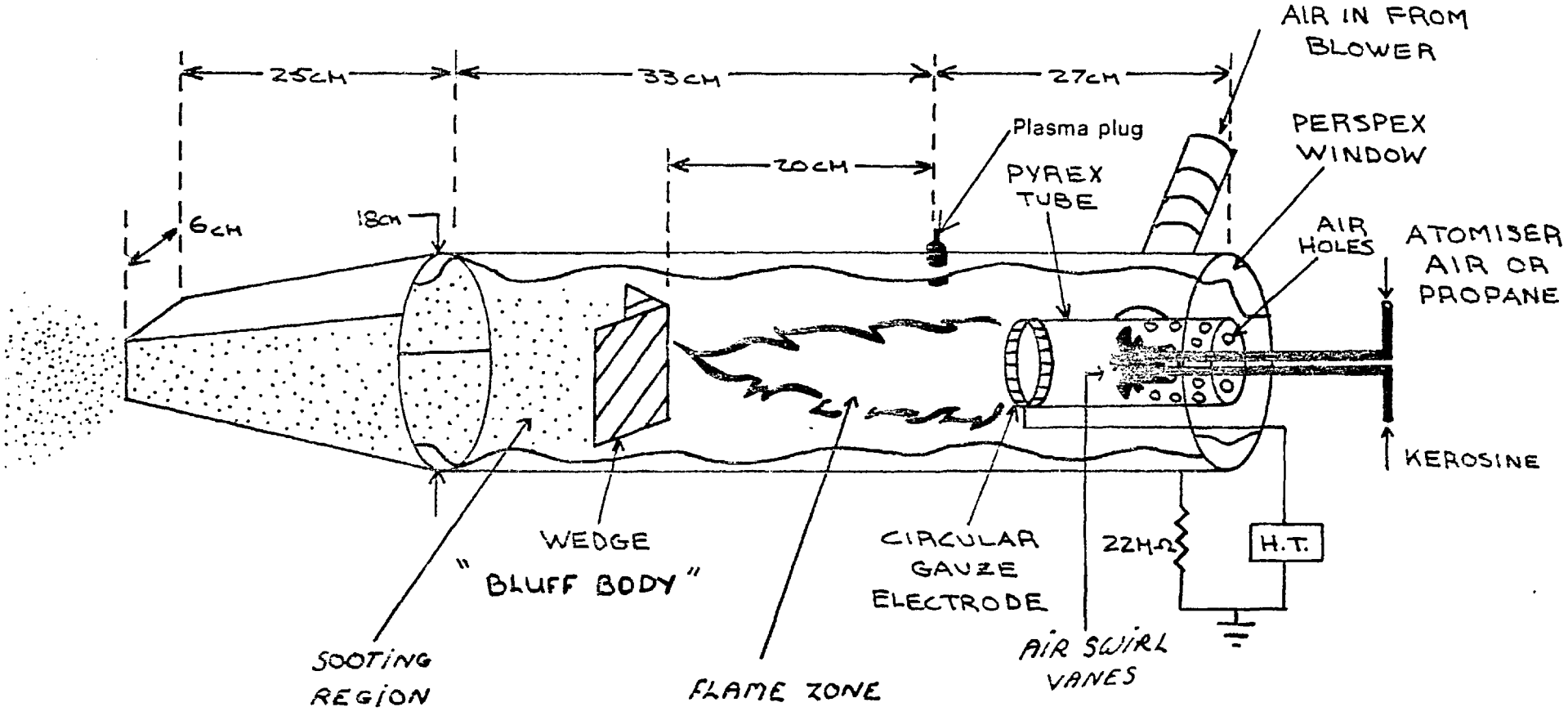

Figure 4.5 - Diagramatic of the Ricardo flame tube seen in Figures 4.2 b, e and f.

The flame tube was fitted with a Sonicore ultrasonic twin fluid atomiser. The resonator cap of the atomiser was normally driven by air. This produced a very uniform spray of kerosine droplets (when injected into ambient air, 98% of the spray had an SMD of 10 microns, measured 3 cms from the cap. This was measured using the Malvern apparatus described in ref. 290). With the aid of the swirl vanes, shown in Figure 4.5, normal operation of the flame tube gave rise to a soot free blue flame.

In order to produce a highly sooting flame, the atomiser cap was driven by propane gas instead of air. This immediately caused the flame to become luminous and generated soot. The appearance of this type of flame is illustrated in Figure 4.2e. The plasma jet seen in Figure 4.2a was installed in the flame tube (as can be seen in Figures 4.5 and 4.2b). The plasma jet used was very similar to that shown in Figure 4.6 (ie. of the early type that had a pointed tip initially and no magnetic field). The only difference was that the cathode was not rigidly mounted, so that the arc could be started by anode-cathode contact. This was before the use of Tesla coils that were used in later work for initiating the arc.

The main air flow to the flame tube could be throttled, to increase the tendency to soot further. The feedstock flow to the plasma jet (either argon or Ar/10% N_2) was kept constant at 120 ml s^{-1} (20°C, 1 Atm). Initially, before the arc was struck, the flame seen as Figure 4.2e was observed. When the plasma was initiated on argon feedstock the yellow continuum emission associated with hot soot particles was replaced by the blue radiation associated with a premixed flame. A similar observation was made with an Ar/10% N_2 feedstock to the plasma plug, as seen in Figure 4.2f, except in this case the blue flame emission had associated with it a yellow-green luminosity that spiralled down the flame tube for the duration of the plasma injection.

No experiments beyond these were attempted.

Interpretation of observations - It would be unwise to try to interpret these observations fully without more detailed studies. It was the intention in these experiments to try to generate oxidising entities of soot precursors in the form of O and OH.

The observation of the yellow-green emission with N_2 addition, as seen in Figure 4.2f, could be a very strong indication that O-atoms are being generated and responsible for the oxidation. In the absence of nitrogen in the plasma there is no chemiluminescent reaction for O-atoms to enter into, although the position of injection is in the excess air bypass stream near the walls of the flame tube and would generate O-atoms due to thermal fission at the air/plasma interface.

However when N-atoms are added to the plasma the atoms enter a region with only air present and no nitric oxide to destroy them. Using equation 10, the situation of $k_9[NO] < k_8[O_2]$ exists and NO would be generated at a rate $\propto [N]$ made in the plasma. A small proportion of the NO generated at this point may react with a fraction of the O-atoms to generate NO_2^*. The yellow-green continuum from this reaction is seen in Figure 6.20c and the spectrum shown Figure 7.3 as part of the spectra from the gas titration sequence used for the quantitative studies of Chapter 6.

The practical significance of being able to destroy soot even under conditions of diffusion controlled burning is of profound importance and worth further study.

CONCLUSIONS

These preliminary plasma jet developments in electrical methods of improving combustion demonstrated how useful specifically generated species could be to solving combustion problems. The possibility for both practical application and academic studies has been improved substantially through the developments of Chapter 6. However, these

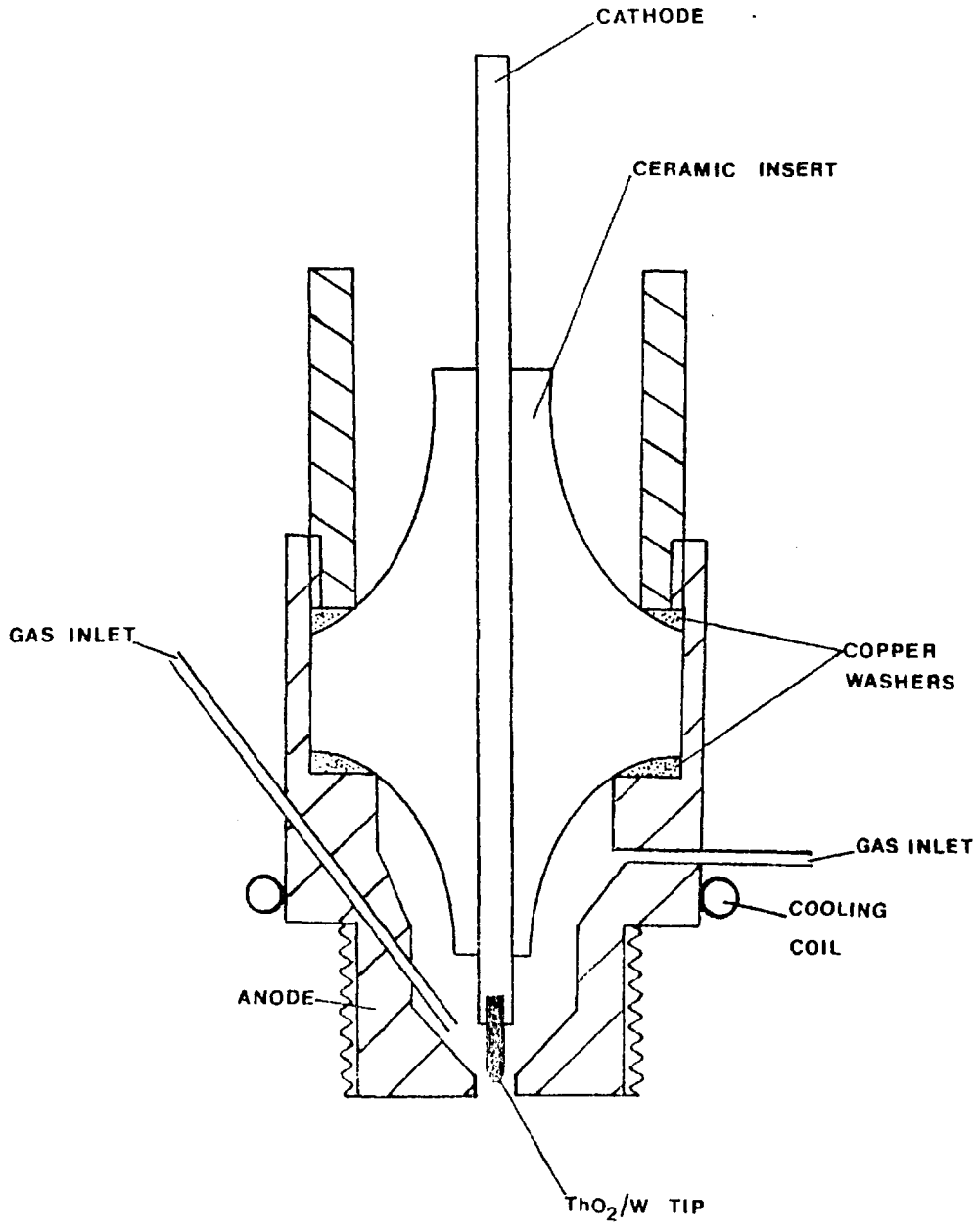

Figure 4.6 - An early form of plasma generator used in this work based on a modified sparking plug.

preliminary experiments provided the driving force for later developments.

CHAPTER 5

ELECTRIC FIELD INTERACTIONS WITH COMBUSTION

INTRODUCTION

This Chapter is divided into two sections and is directed towards DC electric field interactions at stages i) and iii) as defined in Chapter 1. That is not to say that electric fields may not be of use in stage ii). As will be seen later, in the case of droplet combustion, stage i) has a very significant effect on both stages ii) and iii).

There have been a number of studies directed towards electric field interactions with a view to modifying the burning velocity of flames that may be appropriate to stage ii). The marked effects of electric fields on flames have been reviewed by Lawton and Weinberg. The effects electric fields have on burning velocity, directly, appear to be very small (53), and any changes appear to be due to secondary effects associated with modification of transport processes of the various systems. Naturally the electrode configuration as well as the mixture strength and type of field interaction (ie. DC, AC and frequency) will determine the extent and manner in which the interaction may be coupled. For example DC and radiofrequency (6 MHz) interactions were studied and reported in the work described in reference 51. Interferometric studies showed small changes in heat transfer prior to blowoff resulting from ionic pumping modifying flow patterns. Explanations based on modification via momentum transfer of ions moving under the influence of electric fields have also found agreement with other workers (221), some with a view to commercial use (196). However, the practical applicability is dependent on the current densities available (270).

Electric fields also provide possible diagnostic techniques, such as means of measuring flame area (150) and burning velocity (39, 53, 150). However in regard to their practical effects, such as microwave

coupling with electrons as a mode of combustion enhancement (440, 441), this would require high frequency coupling for maximum effect.

Electrons have been considered as important as a first stage in combustion inhibition reactions involving electron attachment (102, 306). However the strongest evidence appears to be that of H-atom removal as being responsible for the greatest inhibiting effect. Electron attachment (and resultant dissociative recombination) as a first step in inhibition has been discounted both theoretically (400) and experimentally (312).

The ability to destroy the 'end-gas' aerodynamically has resulted in the ability to raise the knock limited compression ratio as mentioned in Appendix 2. Electric fields have also been shown to influence engine knock (40) either inducing or suppressing it. Such an interaction with the end-gas, whether physical or chemical in nature, would be desirable from the point of view of raising the effective octane number of the fuel without the need for addition of lead alkyls. This would fall within the general definition of improvement stated previously. The effect knocking combustion has in lowering the brake thermal efficiency is well known (eg. Obert, Patterson and Henein). Ideal operation of spark ignition engines, from the point of efficiency, is at a compression ratio close to the onset of knock. This has led to a number of ignition advance - knock detection systems that receive more attention later in this Chapter.

SECTION 1 - MIXTURE PREPARATION

This section deals specifically with ways in which DC electric fields may interact at the mixture preparation stage and specifically with liquid fuels to produce sprays of droplets. In order that such electrical interaction is possible these fuels need to have a finite conductivity, typically between 10^{-5} to 10^{-10} Ω^{-1} cm^{-1} (355) although charge may be sprayed onto liquids with low conductivity causing them subse-

quently to atomise. Non-conducting hydrocarbon fuels are normally made conducting by addition of an anti-static additive (234).

Although an optimum in conductivity of various hydrocarbon liquids has been reported (355) it is of course possible to spray liquid metals such as mercury and Wood's metal with conductivities significantly higher ($\approx 10^4\ \Omega^{-1}\ cm^{-1}$). On the other hand some metals in liquid form such as sodium and potassium, with nearly identical conductivities, do not produce such droplets at all, only ionic beams when stressed by an applied electric field (287, 412). This may be of significant importance with respect to the mechanism of electrostatic spraying, as well as the mode in which electric field atomisation is attempted for practical situations. This is discussed in more detail later.

Alcohol fuels however provided the ideal fuel for the work described in this section with conductivities of typically $10^{-7}\ \Omega^{-1}\ cm^{-1}$. (The value of κ measured for methanol used in this work was $2.5 \times 10^{-6}\ \Omega^{-1}\ cm^{-1}$). Alcohols have received considerable attention recently because of, in the case of ethanol, its renewable nature from fermentable material such as cassava, sugar beet or sweet sorghum. Methanol is obtainable from coal or natural gas (for reviews see refs. 160, 172, 173 and 282).

Alcohols also have some unique qualities relating to efficiency and emissions in both spark ignition and compression ignition engines, in that they raise brake efficiencies and lower most emissions over baseline hydrocarbon fuels such as iso-octane or cetane. Alcohols have problems associated with their use in practical Otto and Diesel engines however. This section deals with possible ways in which electric field interactions may solve these problems in ways that also lead to degrees of control not available by non-electrical methods. The application to either Otto or Diesel situations will be considered

separately because the modes of mixture preparation and heat release are so different.

APPLICATION TO OTTO ENGINES

The significant advantages of alcohols as fuels with inherently high octane numbers and giving rise to improved power outputs in spark ignited internal combustion engines has long been known (361, 362). More recently the concern over economy and pollution has prompted the further aspects of lead-free operation, higher thermal efficiency and faster flame speeds of alcohol and alcohol gasoline blends to be considered with respect to the potential for reduced emissions and improved economy at lean air to fuel ratio operation (7, 123, 187, 198).

However the use of alcohols as automotive fuels can present some unique difficulties associated with their atomisation and vaporisation. This is due to the oxygen atom present in the hydroxyl group (-OH) of alcohol molecules, which means they are partially oxidised (and therefore have a net calorific value lower than a normal hydrocarbon) while hydrogen bonding between these groups, see Figure 5.1, gives rise to very high boiling points, but, more importantly, very high values of latent heat of vaporisation. If one considers methanol for example and compares it with iso-octane (Table 5.1), it can be seen that the ratios of calorific value and latent heats

TABLE 5.1

Fuel	Lower Calorific value at $20^{\circ}C$/MJ kg^{-1}	ΔH_{vap} θ/kJ kg^{-1}
Iso-octane (C_8H_{18})	44.4	308
Methanol (CH_3OH)	19.9	1120

are 1:2.23 and 1:3.64 respectively, so that to vaporise (as distict from

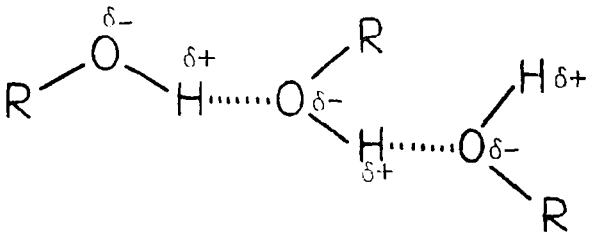

Figure 5.1 – Schematic of intermolecular hydrogen bonding (·····) between alcohol molecules in the liquid phase.

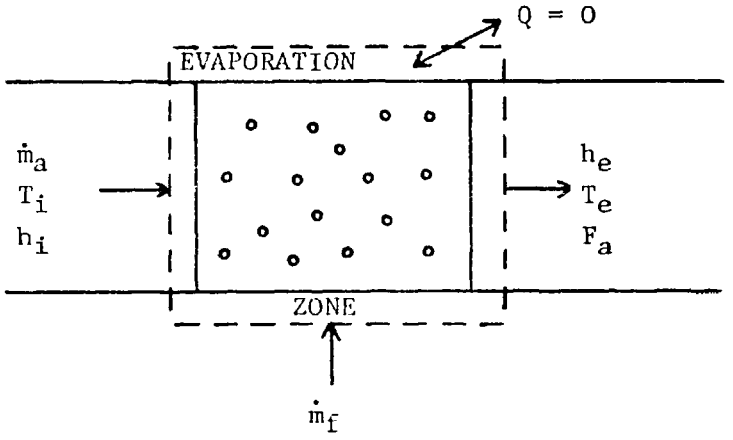

Figure 5.2 – Control Surface used for adiabatic evaporation.

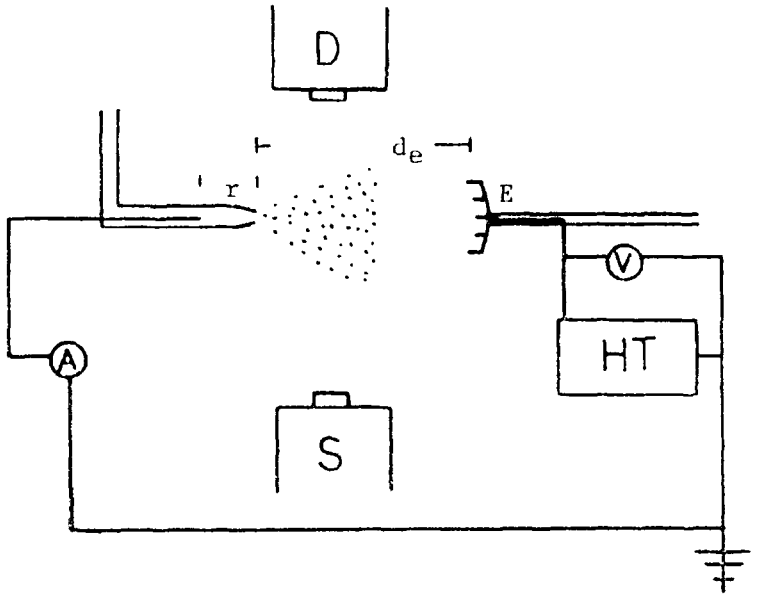

Figure 5.3 – Diagramatic of apparatus used to obtain photographs shown in Figures 5.10b to d; S and D - the Source and Detector of the size distribution analyser, r = limiting resistor column of Methanol (≃ 3 cms). d_e ≃ 10 cms. E - electrode. (ie. Corona or plate).

atomise) an equivalent energy flux of methanol would require 8.11 times as much heat flow as for iso-octane into the vaporising system.

It is also possible to see from Figure 5.1, that due to the difference in electronegativity of O and H (3.5 and 2.1 respectively) the -OH group in alcohols is electrically polarised, giving them the finite conductivity mentioned previously, and making them amenable to electrical atomisation.

The difficulties for Otto cycle applications might be solved, if it were possible to produce a spray of small droplets by electrically charging the surface of the liquid (assuming, at this stage a purely electrohydrodynamical model for disruption of liquids under applied fields, and doing work against fuel surface tension only), such that these droplets evaporated in the charge air. If this were to occur adiabatically, ie. with no heat transfer across boundaries such as inlet manifold, piston crown etc., it may be possible to achieve, by cooling contraction, a chemical energy density in the charge equal to or greater than that of iso-octane, and in part overcome the calorific value penalty of alcohol fuels. This would, in effect be like super-charging the intake, not by pressurising, but by reducing the temperature.

It had been generally assumed that increased power outputs that are experienced when running on alcohol fuels may in part be attributable to increased volumetric efficiency due to charge cooling on evaporation (47). Some Ricardo work (187), however, showed that this is not the case and methanol (and blends with petrol) may lead to worse volumetric efficiency compared to petrol. The explanation was that, due to poor carburation of methanol, the fuel lay along the inlet manifold and dribbled into the combustion chamber. Here the latent heat of vaporisation was extracted from the piston crown, displacing charge in the liquid⟶gas transition that took place, and thus lowered volumetric efficiency. The relative lowering was, as expected from this ex-

planation, engine speed dependent.

Before electrostatic spraying work was attempted, calculations relevant to this were performed to see under what conditions one might expect to see improved volumetric efficiencies for adiabatic evaporation, where it is necessary to balance volume expansion due to liquid⟶gas transition on evaporation, with volume contraction due to absorption of latent heat from the charge air.

A control volume was therefore defined as seen in Figure 5.2. For practical conditions there will always be sufficient enthalpy in the charge air for the latent heat of vaporisation to be extracted from the air (Keenan and Kaye) and not non-adiabatically by drawing the latent heat from across working surfaces with the resultant lowering in volumetric efficiency and possible 'icing-up' of carburettors and manifolds. Whether this enthalpy is available for evaporation will depend on many factors, including how the fuel is prepared with respect to atomisation. This last consideration led to the work on electrostatic carburation while the associated expansions or contractions that could modify volumetric efficiency will be considered next.

THEORETICAL

Consider the following for the constant pressure adiabatic control volume of Figure 5.2.

N	=	Number of moles of air
n	=	Number of moles of fuel evaporated
V	=	Volume
$\Delta H_{L,n}$	=	Molar latent heat of vaporisation of fuel (kJ/mole)
$\Delta H_{L,m}$	=	Latent heat of vaporisation of fuel (kJ/kg)
P	=	Pressure
R	=	Gas Constant

T_i = Initial temperature of air

T_e = Exit temperature of charge

ΔT = Temperature change in charge due to evaporation

$\bar{C}p$ = Mean specific heat of charge at constant pressure

$\dot{m}_a$, $\dot{m}_f$ = Mass flow rates of air and fuel respectively (kg/s)

h_i = Specific enthalpy of air at T_i

h_e = Specific enthalpy of charge at T_e

F_a = Actual w/w air to fuel ratio ($\dot{m}_a/\dot{m}_f$)

F_s = Stoichiometric air to fuel ratio

λ = Mixture strength (F_a/F_s)

The main condition for evaporation is:-

$$\dot{m}_a h_i \geq \dot{m}_f \Delta H_{L,m} \qquad 5.1$$

Initially, before evaporation $V_i = \frac{NRT_i}{P}$ 5.2

Finally, after evaporation $V_f = \left[\frac{(N + n)R(T_i - \Delta T)}{P}\right]$ 5.3

Enthalpy balance $n \Delta H_{L,n} = (N + n) \bar{C}p_{,n} \Delta T$ 5.4

Equation 5.3 may be expressed as:-

$$V_f = \frac{(N + n)R}{P}\left[T_i - \frac{n \Delta H_{L,n}}{(N + n) \bar{C}p_{,n}}\right] \qquad 5.5$$

$$\text{or} \quad V_f = \frac{R}{P}\left[T_i(N + n) - n \frac{\Delta H_{L,n}}{\bar{C}p_{,n}}\right] \qquad 5.6$$

Of direct interest is how V_f varies with the amount of fuel evaporated, therefore differentiating:-

$$\frac{\partial V_f}{\partial n} = \frac{R}{P}\left[T_i - \frac{\Delta H_{L,n}}{\bar{C}p_{,n}}\right] \qquad 5.7$$

Equation 5.7 gives a very interesting result and shows there are three

regimes of volume change on evaporation of the fuel under adiabatic conditions depending on the value T_i (eg. inlet manifold temperature) and the ratio $\Delta H_{L,n}/\bar{C}p,_n$. It is convenient to work in specific units and define $\beta = \Delta H_{L,m}/\bar{C}p$ as a constant having units of temperature.

if	T_i	$>$ β	.....	an expansion
	T_i	$\cong$ β	.....	no change ($\frac{\partial V_f}{\partial n} = 0$)
	T_i	$<$ β	.....	a contraction

β is not strictly a constant, but to a good first approximation may be treated as one since $\Delta H_{L,m}$ varies only slightly with temperature, while $\bar{C}p$ is more of a problem since it will vary with temperature, and the amount of fuel evaporated. (A more rigorous treatment puts $\bar{C}p$ in terms of T and n, modifying equation 5.7 accordingly.) However, if we use the fact that under combustion conditions N > n we can approximate $\bar{C}p$ to that of air at 25°C ie. $\bar{C}p \cong 1000$ J kg^{-1} K^{-1}. Table 5.2 shows the values of β for a number of fuels and for water. One then compares the values of β for different liquids with the initial values of temperature to see if the volume change is positive or negative on adiabatic evaporation. The value of β for iso-octane at $\approx$35°C is very interesting.

TABLE 5.2

Liquid	β/K
Iso-octane	308
Diethyl Ether	350
Toluene	350
Ethanol	850
Methanol	1120
Water	2260

% CHANGE IN CHARGE VOLUME

To calculate the % change in the volume of charge on evaporation, ie. V', where:-

$$V' = \frac{V_i - V_f}{V_i} \times 100 \qquad 5.8$$

we obtain V' in terms of β, which is a linear function:-

$$V' = 100 \frac{n}{N} \left[\frac{\beta}{T_i} - 1 \right] \qquad 5.9$$

V' may be plotted as a function of mole ratio fuel to air (n/N) for different values of T_i. Obviously from the way equation 5.8 is defined the gradient of this plot indicates whether a contraction (+ve gradient) or expansion (-ve gradient) occurs. From the point of view of volumetric efficiency a contraction is desirable. So far the calculations apply generally to any fuel. However considering specifically methanol (and alcohols in general) then:-

For an alcohol of general formula $C_xH_yO_z$ the stoichiometric w/w air/fuel ratio, F_s, may be calculated as:-

$$F_s = \frac{137.33M}{w} : 1 \qquad 5.10$$

where $M = x + y/4 - z/2$, $w = 12x + y + 16z$. For methanol $F_s = 6.44$ and $(n/N)_{stoic} = 0.173$.

V' has therefore been plotted as a function n/N for different likely initial temperatures as shown in Figure 5.4. As would be expected from Table 5.2, provided the inlet air temperature is below 1120 K a contraction on adiabatic evaporation of methanol is possible with resulting increased charge density and improved volumetric efficiency.

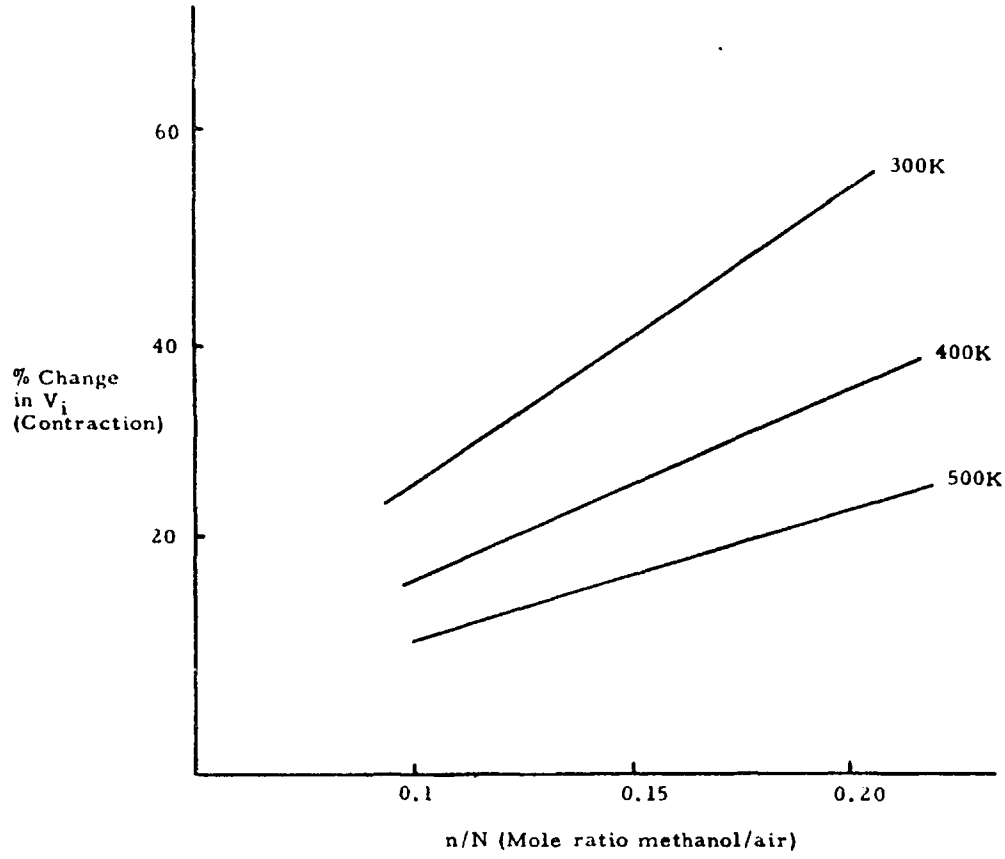

Figure 5.4 - % change in volume as a function of mole ratio for different values of T_i, less than β.

TEMPERATURE DROP ON EVAPORATION

Various detailed methods of calculating the temperature drop (ΔT) associated with the adiabatic evaporation of methanol have been attempted. The estimated values for stoichiometric methanol/air range from 122 K to 142 K (38, 172) with increasing complexity. The parameter would be important from the aspect of amount of fuel that underwent adiabatic evaporation within the control volume.

A simple method of calculating ΔT for fuels evaporating under adiabatic conditions was sought. It is written for general application to any fuel.

For combustion purposes $N > n$ therefore assume $\bar{C}p \cong 1.0$ kJ kg^{-1} K^{-1}.

On enthalpy balance $$\Delta T = \frac{\dot{m}_f \Delta H_{L,m}}{\dot{m}_a \bar{C}p} = \frac{\beta}{F_a} \qquad 5.11$$

$$\Delta T = \beta / \lambda F_s$$

Consider the three fuels shown in Table 5.3; Table 5.4 was constructed using equation 5.11.

TABLE 5.3

Fuel	β/K
Ethanol	850
Methanol	1120
15% MeOH/85% Iso-octane	430

It should not be forgotten that a decrease in temperature may still be associated with an increase in volume, subject to the conditions of β and T_i.

TABLE 5.4

	ΔT/K		
λ	MeOH	EtOH	15% MeOH/85% iso-octane
0.8	217	119	39
1.0	174	95	31
1.2	145	79	26
1.4	124	68	22
1.6	108	59	19
1.8	97	53	17
2.0	87	47	16

Table 5.4 gives some idea of the temperature drop one would expect; we see that for stoichiometric methanol/air a value of ΔT of 174 K is calculated which is within the same range as the more compli-

cated methods of calculation. Again, rigorous calculation for iso-octane gives an 18 K drop at $\lambda = 1$, (187). Using equation 5.11 and the value of F_s for octane at 15.06 gives ΔT as 20 K.

These figures provided an approximate starting point. However, for fuels that are highly hydrogen bonded, dilution in iso-octane reduces the extent of hydrogen bonding which leads to increased Reid vapour pressures for these mixtures. Table 5.4 overestimates the value of ΔT by neglecting this.

ELECTROSTATIC CARBURATION

All the calculations presented are based on thermodynamic equilibrium being established, and an assumption that the initial temperature is arbitrary. Nevertheless they indicate the best that could possibly be achieved, given sufficient time for evaporation. The atomisation and evaporation of these fuels in the fuel handling system, would not allow these steady state conditions to be realised in practice unless sophisticated controlled atomisation (tending to very small droplets) and mixing systems could be devised. It is for that reason that electrostatic methods were considered.

Electrostatic atomisation of fuels is not new (104, 427). References 478 and 479 describe the first attempts at electrostatic spraying. Before that time interactions between liquids and electric fields were associated with studies on the diversion of streams of droplets (Spherules) by electrified rods, and electrically induced agglomeration (358). The degree of control that was possible electrically over atomisation and aeration enabled the construction of a kerosine fuelled burner operating completely electrostatically (421).

The potential for electrostatic carburation of alcohol fuels is unique, in that the hydroxyl group that leads to the problems associated with lowered calorific values and high latent heats, also provides the

handle whereby these fuels may be atomised electrostatically - due to the conductivity of the functional group as described earlier, thus promising improved economy and combustion characteristics.

Most mechanical methods of atomisation (including piezoelectric) put nearly all of their energy input (typically in excess of 90% see also ref. 427) into kinetic energy of the droplets formed. For carburation this is disadvantageous for at least two reasons. Firstly, it corresponds to an energy input to the fuel which serves no useful purpose (in contrast to a Diesel injector or gas turbine fuel spray) and, secondly, any energy input of this sort gives rise to an unnecessary (however small) increase in the negative area of the indicator diagram.

For atomisation that depends on the mass flow rate of air through a venturi throat, as in the quantity mode of power control, low power requirements of the engine lead to the lowest venturi pressure drop and the worst atomisation, requiring overfuelling under these conditions with correspondingly high CO and HC emissions and reduced efficiencies. The ability to detach atomisation efficiency from air mass flow rate under such conditions would automatically result in an improvement as defined earlier.

For pressure jet atomisers the size distribution function of the fuel spray is not readily variable (Williams) and tends to be very wide (from 7 to 560 microns as seen in Tables 5.5 and 5.6 for the situations involving the Diesel injector seen in Figure 5.11). For electrostatic atomisation on the other hand there is evidence that monodisperse fuel droplets may be obtained, depending on applied field intensity and fluid flow rate (234). This was also seen in this work, but the ability to produce droplets that underwent significant evaporation (as observed by hydrocarbon analysis of the surrounding air) was strongly influenced

by the electrode configuration, and specifically by whether or not a corona discharge was present. (See for example Figures 5.10b and c). The relevance of this with respect to mechanisms of spraying and possible practical application will be discussed further, later in this section.

The failings of conventional venturi carburation, especially at low throttle openings has led to consideration of piezoelectric (62) and sonic systems (174, 311) to help solve atomisation problems. A system known as 'the Vapipe' has been suggested (185) where the fuel is vaporised using heat pipes heated via exhaust reject heat. The fuel vapour then undergoes subsequent condensation in varying amounts in the reverse of the air distillation process (30) normally associated with hydrocarbon fuels/air systems. It has been suggested that electrostatic atomisation may be explained by boiling of liquids due to Joule effects (103) in truncated Taylor cones (419) which would be the electrical analogue of the vapipe system.

Since electrostatic carburation involves no moving parts, nor does it rely on air movement directly to produce droplets, it has none of the drawbacks of conventional venturi carburation at low air flow. Electrostatic modification of carburettors has been attempted prior to this work (225) and during it (27). Some interesting schemes involving controlled discharge of charged sprays for ignition have also been proposed (407). However, to date many of the potentials of electrostatic carburation with regard to control of droplet size with subsequent control of rate of flame propagation (344) and the resultant effect on emissions (422, 429) have been overlooked. The most promising practical application would be for alcohols, as their unique combustion problems appear to be immediately amenable to an electrostatic solution.

Experimental - To demonstrate the potential for producing fuel mists of alcohols at realistic flow rates (typically 1.0 to 3.0 ml s^{-1}) the apparatus seen in Figure 5.3 was constructed. The HT supply was either a Brandenburg model 800 EHT generator (3 to 30 kV at 1 mA) or the apparatus shown schematically in Figure 5.5, which was intended to demonstrate that due to the low power requirements of electrostatic carburation, even at realistic fuel flows, the powers required are those generally associated with electronic ignition components. A number of such systems exist (eg. Refs. 147 and 158), however a 'Luminition opto-electronic system' (147) was readily available, and operated very satisfactorily with a television line EHT diode. A typical power consumption in the primary circuit was 24 Watts. The circuit shown in Figure 5.5 was not designed for efficiency, but to demonstrate that the powers required were of the same order as those readily handled with automotive ignition system components. For practical use, small solid state units would be more suitable (these may be powered by substantially smaller power supplies than lead-acid batteries, and have power consumptions much less than 24 Watts).

By way of comparison, the optimised power requirements for the piezoelectric system described in ref. 62, with the crystal operating at 60 kHz, is 24 Watts per injector, (16 W to the oscillator circuit, 8 W to the crystal) which increases with fuel flow rate at an operational pressure of 40 to 60 psi. The electrostatic spraying as seen in Figures 5.10 a to d has gravity feed of methanol at a flow more appropriate to 2 injectors.

For Figures 5.10 a to d the methanol fuel feed was earthed with a column of fuel acting as a limiting resistor to prevent spark discharge. DC fields were generated by applying either a +ve or -ve potential (in the range 20 to 30 kV) to a variety of electrode configurations.

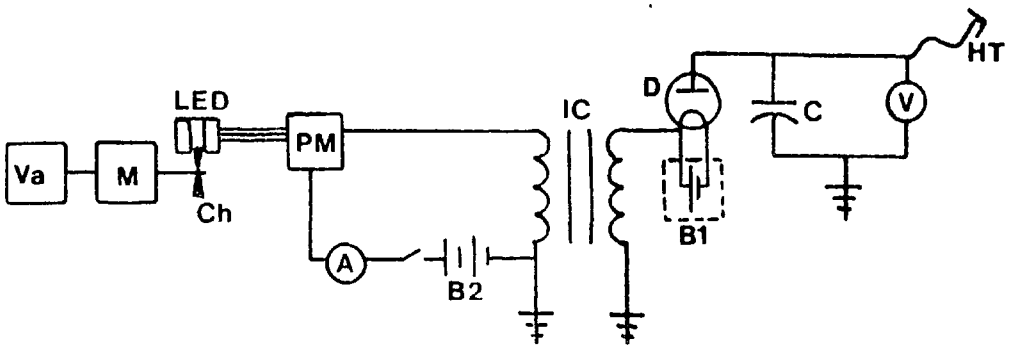

Figure 5.5 - Low power high voltage power supply based on automotive electronics parts and a television line EHT diode. Va - Variac, M - Motor, LED - Light emitting diode and receiver, Ch - Chopper, PM - Luminition ignition power module, B2 - 12 V accumulator (40 Ah), IC - Ignition coil, D - Diode (1B3GT), B1 - 1.5 V HP2 battery, C - Capacitor (50 pF at 50 kV), HT - High voltage lead.

Either a single point corona (Figure 5.10b) a multicorona source (Figure 5.10c) or a standard plate electrode (Figure 5.10d). Figure 5.10a shows the gravity free fall case.

Of definite importance for the operation of such a system on a practical engine is the size distribution function of the droplets produced, and how they may be controlled. It can be seen from the sprays of Figures 5.10 b to d that the droplets, once generated, have the same charge (with 10^6 charges/droplet reported (234)) and strongly repel each other.

Experimentally this has advantages that enable the droplets subsequent manipulation (421). However it also means droplets may attach themselves to earthed surfaces and coalesce. Movement and manipulation of charged droplets would be undesirable during carburation because to manipulate small charged droplets in this way consumes unnecessary power. A neutral spray, following the air flow into the engine, is ideal for minimum power consumption.

It was not the intention of the experimental work in this section to

design a detailed carburettor. However the ability to produce, so readily, sprays of methanol at realistic flows with size distributions of 10 to 50 microns is worth further study.

The main problem of droplet repulsion may be tackled in many ways. The way that is the least energy intensive is that involving alternately charging droplets positively and negatively. If such droplets are, for example, of identical mass but opposite charge and coalesce away from a surface without evaporation, the resulting neutral droplet has double the mass but the diameter has only increased by a factor of $\sqrt[3]{2}$ or 1.26. (The frequency with which this alternating charging should be undertaken, could be determined experimentally). Droplets carrying a net charge have been shown to be more susceptible to coalescence, than neutral droplets of the same size and impact velocity, at a neutral liquid interface (230).

Mechanism and power requirements - It is appropriate to discuss this aspect of electrostatic atomisation in relation to Diesel and Otto engine applications because the mechanism influences the power requirement and thus forms an essential part of the methodology for practical application.

There are many theories of how droplets are formed electrostatically when a liquid surface is stressed by an applied electric field, depending on liquid properties such as conductivity, viscosity, surface tension as well as the charging environment. (See, for example, refs. 25, 26, 103, 245, 326, 359, 378, 419, 420). Of these, all but ref. 103 deal with a totally electrohydrodynamic model, that is one in which the surface of the liquid acquires charge under the influence of an applied field. The disruptive forces associated with this stressing of the liquid results in the excess charge being removed from the liquid surface in a stream of charged droplets. The final charge to mass ratio (209) acquired by the resulting droplets is the result of the balance of surface

tension forces of the liquid droplet with the electrostatically induced stress as a result of the surface charge on the droplet. Rates of charging and charge dissipation are therefore important as determined by the charging environment and the transport properties of the liquid. For example thermally driven convective charge dissipation from the surfaces of droplets was demonstrated with Lycopodium dust (307).

In ref. 419 it was shown that a conducting liquid will only exist in equilibrium under the influence of an electric field when the liquid forms a cone with a semivertical angle of 49.3^{o}. (See for example, Figure 5.6). The charged droplets then emerge from the apex of the cone in a stream. Such Taylor cones were only seen in the experimental work of this section under high current flow corona discharge conditions (see Figure 5.10b) which is significant for a novel theory of electrostatic atomisation that includes Joule effects and is not totally electrohydrodynamical in nature.

Reference 103 starts with the Taylor theory (419) in balancing electrostatic and surface tension forces to form a Taylor cone with $\Theta = 49.3^{o}$. The cone is then truncated such that the minimum value of d in Figure 5.6 is the diameter of one molecular dimension of liquid. The current density that flows through this tip is sufficiently high so that even at $1\mu A$ current flow it is possible to raise some liquids to temperatures in excess of the boiling point. An expression for the temperature rise is derived that may be expressed as:-

$$\Delta T_{max} \propto \left(\frac{\sigma}{k}\right) \frac{i^2}{d^2} \qquad 5.12$$

where σ = Resistivity (κ^{-1})

k = Thermal conductivity

i = Current

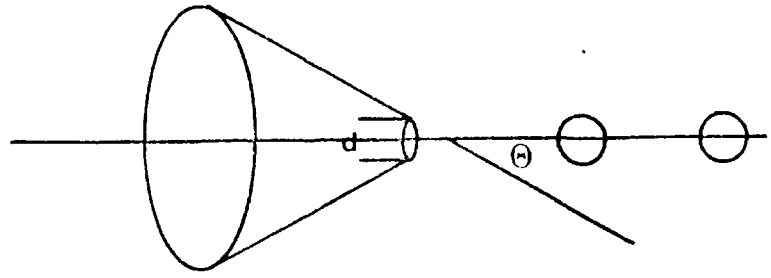

Figure 5.6 - Atomisation from Taylor cones where $\Theta = 49.3^{o}$

---

d = Molecular diameter

Basically therefore the temperature rise is determined by two transport properties; the thermal and electrical conductivities of the fluid.

For non metallic liquids with low thermal and electrical conductivities ΔT_{max} will always be above the liquid boiling points even with currents of 1 μA. Spraying then results from the cyclic sequence of cone formation, boiling with ejection of droplets; reforming of the cone starting the process again. For liquids with high thermal and electrical conductivities such as sodium and potassium, ΔT_{max} is not sufficient to raise the liquids to above their respective boiling points, with a temperature rise of barely 2 K at 1 μA. No droplets are formed, only ionic beams, as has been observed experimentally (287, 412). Liquid metals such as mercury and Wood's metal having similar electrical conductivities to Na and K but lower thermal conductivities are able to experience values of ΔT_{max} where a boiling mechanism for the droplet formation sequence is possible.

Knowledge of the detailed mechanism is important for at least two reasons for practical application:-

i) The mechanism will dictate the actual power requirements.

ii) The possibility of electrostatic discharge Joule heating of

an alcohol fuel may well be an effective way of modifying the cetane number in a Diesel application. In Diesel injection it is not desired to cool the charge air by extracting the latent heat from it (in contrast to the Otto situation). It would be advantageous to enhance the reactivity of the alcohol by aiding in both the physical processes of evaporation and the chemical processes in the ignition delay period. Flash vaporising by capacitive discharge Joule heating will be discussed in the Diesel application section.

MINIMUM POWERS REQUIRED

It is possible to calculate a minimum power requirement for electrostatic atomisation based on the fact that, independent of the droplet producing mechanism, the net result in forming the spray is work against fuel surface tension (the power then being the rate at which that work is done). If unit mass flow rate is considered, then the minimum work required to go from a condition such as Figure 5.10a, condition 1, to condition 2, such as Figures 5.10 b to d, can be calculated as follows:-

E_1, E_2 = Surface free energies in conditions 1 and 2 respectively

A_1, A_2 = Areas bounding unit mass under conditions 1 and 2 respectively

γ = Surface tension

Then $E_1 = A_1\gamma$, $E_2 = A_2\gamma$

$$\Delta E_{Elect} = (A_2 - A_1)\gamma \cong A_2\gamma \text{ since } A_2 \gg A_1$$

$$P_{min} = \frac{\gamma dA_2}{dt} = N_s a_2 \gamma = \frac{6x\gamma}{d} \qquad 5.13$$

Where N_s = number of droplets generated per second with surface mean diameter d and droplet surface area a_2 at flow rate x. With x in m^3/s and d in metres this gives power directly in Watts. γ for MeOH

was taken as 22.6 mNm^{-1}. Some results are shown in Figure 5.7.

This calculation represents an absolute minimum on a First Law basis. Obviously when charged particles move in an electric field gradient, and with ionic winds known to be present, further power is being utilised above the P_{min} level. The total power used will be of the form $P_t = P_{min} + P_{kinetic}$. However it is expected that $P_{kinetic}$ could be made small. Reference 245 is not as optimistic however, estimating that less than 1% of the total energy in electrostatic spraying goes into creating surface (ie. 99% into kinetic energy). Reference 427 suggests 30% efficiency in electrostatic surface production, compared to 0.1% for pressure jet systems.

DIESEL APPLICATIONS

This part specifically deals with aspects associated with alcohols directly injected into the combustion chamber (arguments relevant to alcohol fumigation of Diesel engines in a dual fuel approach are under the previous carburation section).

Alcohols are an ideal fuel for Diesel engine application. They have oxygen intimately bound within the molecule, which results in the absence of soot emission under diffusion controlled combustion. It also makes high in-cylinder swirl levels to improve air utilisation unnecessary. This improves brake thermal efficiency by reducing pumping losses, as well as reducing convective heat transfer losses at the cylinder wall. Combustion within an open quiescent chamber environment (highest brake efficiency conventionally) is possible with substantially reduced radiative heat transfer losses from the chamber, due to the absence of black body continuum radiation from incandescent soot particles. Combustion of alcohols is also associated with an inherently low thermal NO emission due to reduced flame temperatures of a fuel that is partially oxidised.

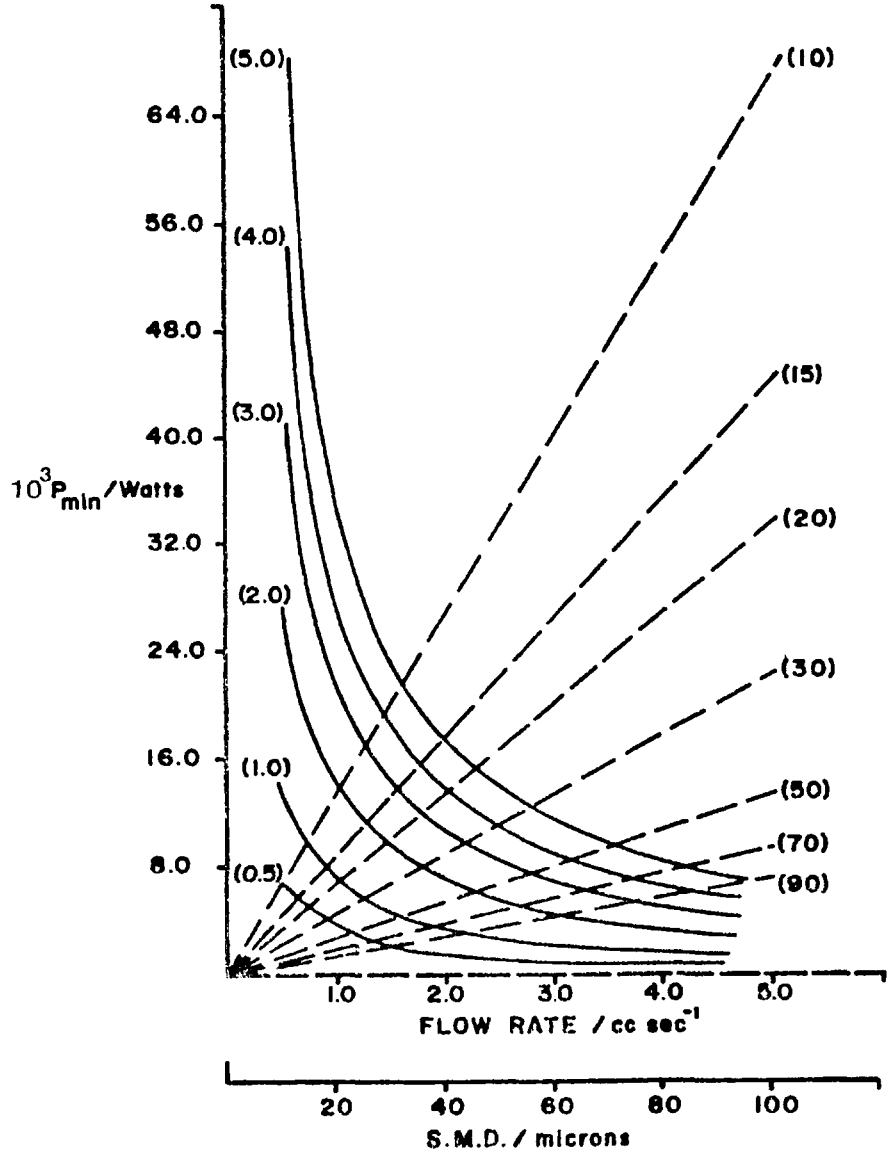

Figure 5·7 – Minimum calculated powers for electrostatic carburation as functions of i) flow rate ii) size distribution function. Numbers in parenthesis denote i) fuelling rate 0.5 → 5.0 cc/sec of Methanol ii) Surface mean diameter of droplets formed 10 → 90 microns. (as SMD ⇒ 0, power ⇒ ∞)

These potential advantages are only available in part when Diesel engines are operated in a dual fuel mode with either twin injectors or carburetted alcohols. The main source of ignition is from a high cetane number fuel. (Improvements in combustion that result, even from this approach, may be found in the Symposia proceedings of, for example, refs.161 and 411).

Difficulties with direct fuelling of alcohols in Diesel application result from the fact that the fuel has a very low cetane number (although methanol and ethanol are susceptible to surface pre-ignition at much lower than combustion temperatures).

Improvements in cetane number by the addition of known nitrate promoters (366) while aiding ignition in high concentrations (5% cyclohexyl nitrate being typical) negate the lower thermal NO emission. The effect of peroxidic additives have yet to be established clearly with alcohols. Results with peroxidic additives, on conventional Diesel fuels, as cetane number improvers has long been known (220), although recent studies indicate them as having effects explainable in terms of their fuel quality alone (204). The potential of peroxidic additives as cetane improvers of alcohols in Diesel combustion is particularly worth further study, especially if the alcohol is ethanol from biomass, where NO_x generated from nitrated additives could perturb plant metabolism.

A possible solution to both Diesel and Otto application, that superficially solves a number of problems, is alcohol reformation to CO and H_2 using exhaust reject heat. (See for example ref. 349). It is not the intention of this section to fully discount such reforming techniques, nevertheless some of the main features that are commonly overlooked by the protagonists of such systems will be cited. This may help to place electrostatic methods on firmer footing.

Reformation of methanol involves the following process:-

$$CH_3OH_{(l)} \xrightarrow[\text{catalyst}]{\Delta H(\text{exhaust eg. } 300^{o}C)} 2H_{2(g)} + CO_{(g)} \quad \Delta S^{\Theta} = {}^{268}_{\text{J/deg mole}}$$

that is conversion of one molecule of liquid fuel into three gaseous fuel molecules. While the increase in lower calorific value of the reformed fuel is often specified (approximately 4MJ kg^{-1} at $300^{o}C$) the substantial increase in entropy is overlooked entirely. Because the ability of the prime mover to do work is not simply a function of the fuel LCV, ($\Delta H'$) but determined by the availability function using Gibbs free energy (ie. $\Delta G = \Delta H' - T\Delta S$) such an increase in entropy results in a decreased ability of the reformed products to do mechanical work.

Gaseous fuels for Otto application automatically lower the engine specific power, volumetric and thermal efficiencies, also they are inherently difficult to inject into high pressure charge air for Diesel application. Hydrogen as a fuel in compression ignition engines has been carburetted in a dual fuel Diesel approach (239) and there is therefore little to be gained then by reforming. It is incorrect to think that hydrogen as a fuel in reciprocating piston engines is without problems (for an excellent review see ref. 32), Otto engines especially having very unpredictable knocking anomalies with hydrogen fuel.

Approaching the main problem of the ignition delay period of alcohol fuels in a Diesel context is particularly relevant for electrostatic solution in a single fuel approach, for the following reasons (pertaining initially to improving vaporisation before the modification of chemical processes are attempted):-

i) Once combustion is established the combustion generated ions will dictate the discharge characteristics. During the ignition

delay period these ions would not be present.

ii) The electrode arrangements are such (see for example Figures 5.8 and 5.11) that the configuration of an air dielectric capacitor is present. The fuel on emerging from the injector acts as a conducting 'track' discharging the capacitor and experiences a substantial initial discharge current. (See for example Figures 5.11 a and b with a 'capacitor' charge/discharge cycle every 2.3 seconds). If Joule heating during this period of high current flow could be demonstrated this would be particularly advantageous in that the reactivity of the fuel air system would not be reduced by a reduction in temperature of the charge air, and electrical flash vaporisation would therefore enable gas phase combustion reactions to commence. These reactions may be augmented by spark discharge from a small pocket of the combustion generated space charge and the remaining charged spray. This hybrid of spark assisted ignition in a quality-power control mode engine is the opposite concept of the so called 'Ring' process engines developed during the period 1940 to 1943 (325) for compression ignition in quantity-power control mode engines.

iii) The inner cores of fuel sprays are particularly difficult to penetrate with a practical electrode arrangement of a ring. This spray configuration exists after only a small amount of the total injection volume has taken place.

The study therefore required accurate time resolution of the injection, to investigate electrical interaction at each of the injection phases, which for convenience will be split up into three regimes. The experimental section deals with full details of the apparatus and experiments. For injection of methanol into atmospheric pressure air the spray duration (defined as the period t_d in Figure 5.9 - the interval during which fuel leaves the injector) was found to be 96 ms.

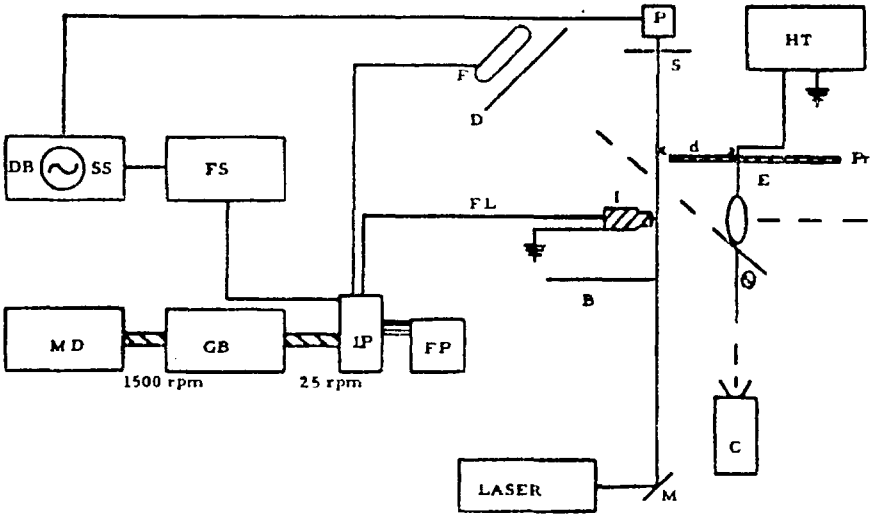

Figure 5·8 – Diagramatic of spray apparatus used to obtain pictures shown in Figures 5·11a to h; DBSS - Dual beam storage oscilloscope, FS - Flash synchroniser, MD - Motor drive (input 1500 rpm), GB - Gearbox (as torque converter to 25 rpm), IP - Injector pump, FP - Fuel pump, FL - Fuel line, I - Injector, B - Blind, M - Mirror, D - Diffuser, F - Flash tube, S - Slit, P - Photodiode, HT - High tension unit, Pr - Perspex rod, E - Ring Electrode, C - Camera, θ - Scatter angle (40°).

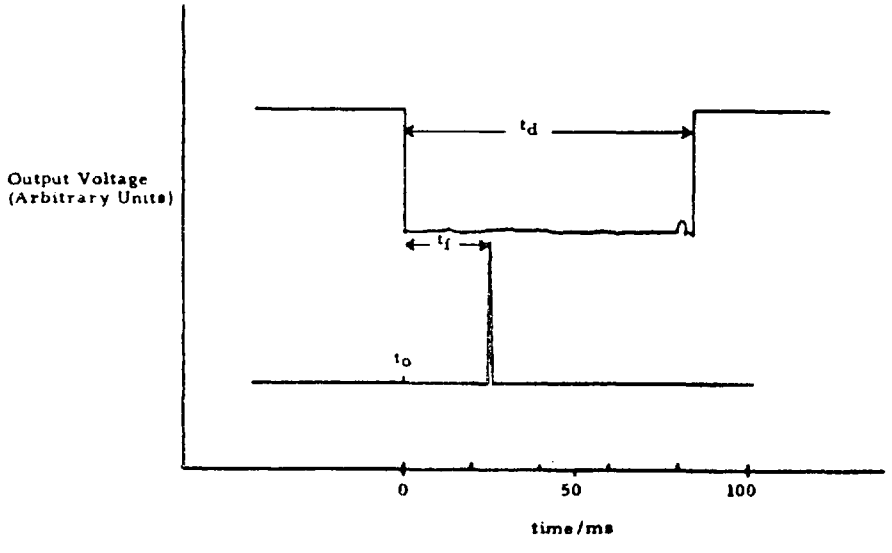

Figure 5·9 – Typical storage scope output trace, t_d = 96 ms, t_f = 5 → 109 ms for conditions shown in Figures 5·11a to h.

The phases are therefore:-

Phase 1)	0	to	10 ms	period relevant to ignition delay
Phase 2)	10 ms	to	96 ms	period relevant to main injection
Phase 3)	96 ms	to	109 ms	period relevant to after injection

Experimental - The apparatus used for the investigation of Diesel injection is seen in Figure 5.8. Details of the exact events during an injection were not required (most of phase 2 would be modified in a practical situation with flame ions present). It would have been an unnecessary complication to use high speed cine photography, instead the photographic method seen in Figure 5.8 was used. This was ideally suited to obtain information on phases 1 to 3. The instant the spray emerged from the nozzle it attenuated the laser beam, a rapid response photodiode detected this and generated t_o as shown in Figure 5.9. It was possible with a timed delay unit to freeze the spray with a flash at any point (t_f) during the spray duration t_d or beyond. The flash duration was estimated at 100 microseconds, which made this experimental method equivalent to choosing any frame from a 10,000 fps film, with better resolution and at a fraction of the cost.

Figures 5.11 a and b are representative of phase 1, Figures 5.11 c to f of phase 2 and Figures 5.11 g and h of phase 3. Details of how the distribution functions of the sprays might be modified by an electrical interaction were considered.

There are numerous droplet sizing techniques (eg. 24, 50, 118, 290, 295, 296, 354, 413, 418) involving the use of wax, impaction on magnesium oxide plates, photography and Fraunhofer diffraction of laser light. The diffraction method (413) was used because of the availability of a commercial instrument (290) loaned for a limited period of time. The only situation where sizing was attempted in the Diesel

spray was that pertaining to phase 2. The ideal situation of phase 1 results in increased evaporation and therefore it was more appropriate to look for the absence of droplets (due to evaporation) rather than the sizes of the remaining droplets. In view of the time scale of phase 1, conventional probe sampling for evaporated fuel would be inappropriately slow and fast in-situ optical probing techniques for evaporation profiles more applicable.

RESULTS

The outputs from the size distribution analyser for a phase 2 situation with no field and with -30 kV applied to the ring electrode (of Figure 5.8) are seen in Tables 5.5 and 5.6 respectively. The first three columns from left to right are droplet diameters in microns, (from a Rosin-Rammler fit), % within the size range specified and cumulative % by weight. This data was obtained from a point approximately 2 cms downstream of the electrode on the axis of symmetry of the spray (applications were limited by the value of d (Figure 5.8) to maximise field strength without spark discharge in the presence of the fuel flow for phase 2; d was generally 7 to 10 cms). The remaining results are the photographic records shown in Figure 5.11.

INTERPRETATION OF RESULTS

Phase 1 - Comparison of Figures 5.11 a and b at t_f = 5 ms show very clearly the difference in penetration and width of the spray. The extent of penetration of the fuel sprays under phase 1 shows clearly that, in the case of the applied field, it has been reduced nearly 50%.

The extent of penetration of such a spray is very strongly affected by the sizes of the initial droplets that emerge, (334) due to the momentum imparted to the charge air initially, that subsequently affects the remaining spray penetration.

Table 5.5

```
# TY
S=   +562.86 E=    +3.72% P=  +133.33% C= 3333 T= 3195 V= 3493
S=   +281.71 E=    +3.37% P=  +133.33% C= 3333 T= 3311 V= 3211
S=   +163.29 E=    +3.13% R=   +99.87% C= 3335 T= 3493 V= 3494
S=   +112.86 E=    +4.77% P=   +95.13% C= 3333 T= 3743 V= 3747
S=    +84.29 E=   +18.18% P=   +76.93% C= 3742 T= 1394 V= 1199
S=    +64.57 E=   +24.32% R=   +52.66% C= 1823 T= 1485 V= 1411
S=    +53.29 E=   +21.54% R=   +31.12% C= 3936 T= 1875 V= 1764
S=    +38.86 E=   +13.93% R=   +17.32% C= 3583 T= 2344 V= 2347
S=    +33.29 E=    +7.96% P=    +9.36% C= 3335 T= 1931 V= 2347
S=    +23.71 E=    +4.41% P=    +4.95% C= 3185 T= 1661 V= 1693
S=    +18.57 E=    +2.95% P=    +2.62% C= 3393 T= 1354 V= 1139
S=    +14.57 E=    +1.24% P=    +1.36% C= 3352 T= 1131 V= 1359
S=    +11.43 E=    +3.61% P=    +3.75% C= 3325 T= 3875 V= 3347
S=     +9.14 E=    +3.36% P=    +3.36% C= 3315 T= 3691 V= 3635
S=     +7.14 E=    +3.17% P=    +3.21% C= 3337 T= 3527 V= 3564
```

?3262

Table 5.6

```
# TY
S=   +562.86 E=    +1.39% P=   +[illegible] C= 3357 T= 3636 V= 3556
S=   +281.71 E=   +11.31% R=   +97.66% C= 3344 T= 3369 V= 3744
S=   +163.29 E=   +17.97% R=   +69.71% C= 1393 T= 1142 V= 1332
S=   +112.86 E=   +17.31% R=   +52.73% C= 3968 T= 1323 V= 1963
S=    +84.29 E=   +14.34% R=   +38.67% C= 3799 T= 1624 V= 1674
S=    +64.57 E=   +13.73% P=   +27.94% C= 3611 T= 1817 V= 1488
S=    +53.29 E=    +8.44% R=   +19.53% C= 3483 T= 1977 V= 1483
S=    +38.86 E=    +5.95% P=   +13.55% C= 3339 T= 2344 V= 1963
S=    +33.29 E=    +4.17% R=    +9.37% C= 3237 T= 2323 V= 1963
S=    +23.71 E=    +2.93% R=    +6.44% C= 3167 T= 1943 V= 1674
S=    +18.57 E=    +2.32% R=    +4.41% C= 3115 T= 1792 V= 1674
S=    +14.57 E=    +1.43% R=    +3.31% C= 3379 T= 1626 V= 2347
S=    +11.43 E=    +3.93% R=    +2.12% C= 3351 T= 1429 V= 1863
S=     +9.14 E=    +3.69% R=    +1.43% C= 3339 T= 1211 V= 3744
S=     +7.14 E=    +3.43% R=    +1.33% C= 3324 T= 3991 V= 3558
```

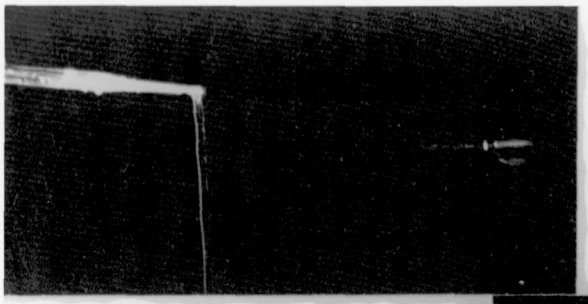

a) Free fall

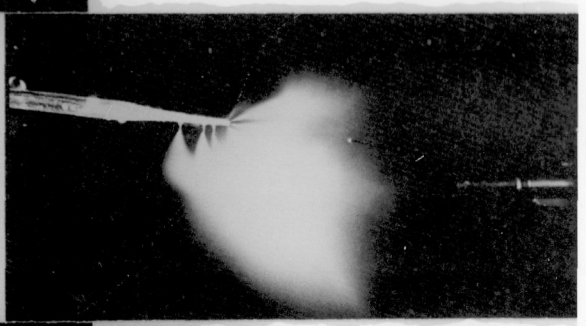

b) Single - corona electrode (-30 kV)

c) Multi - corona electrode (-30 kV)

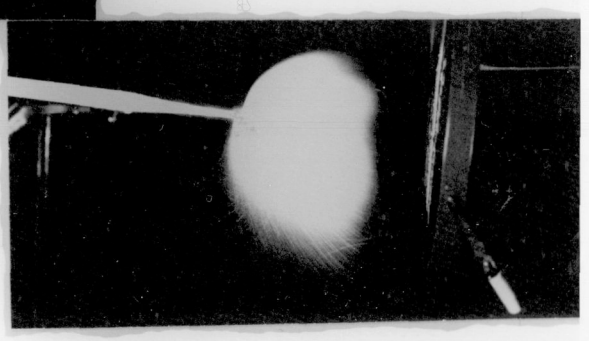

d) Plate electrode (-30 kV)

Figure 5.10 - Photographs of sequences associated with continuous operation.

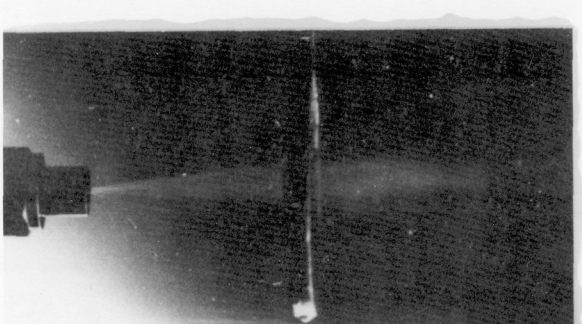

a) 5 ms - No field

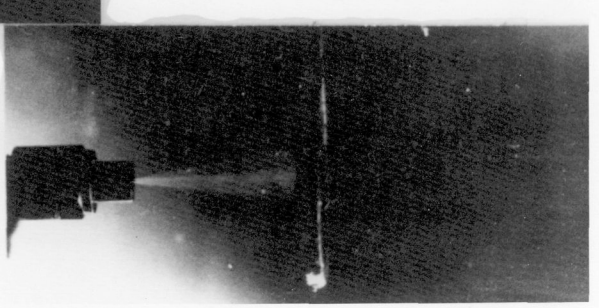

b) 5 ms - Field applied (-30 kV)

Figures 5.11 a) and b)

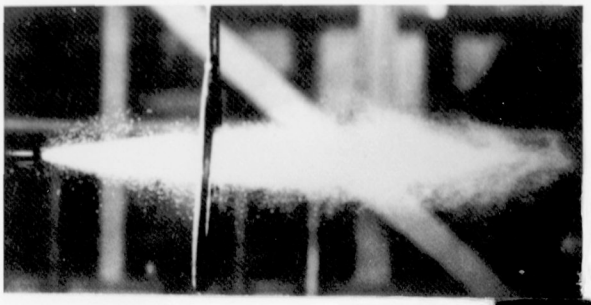

c) 46 ms - No field

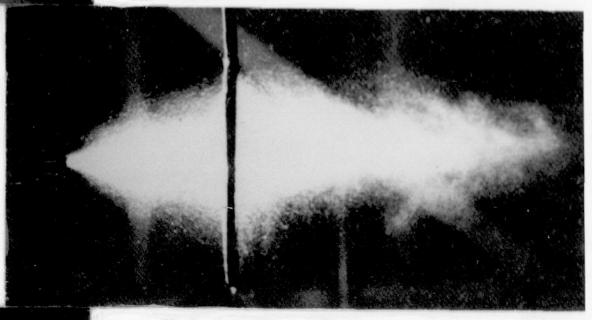

d) 46 ms - Field applied (-30 kV)

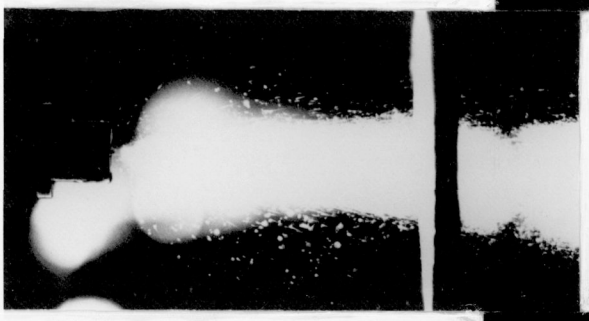

e) 46 ms - No field (Close-up shot)

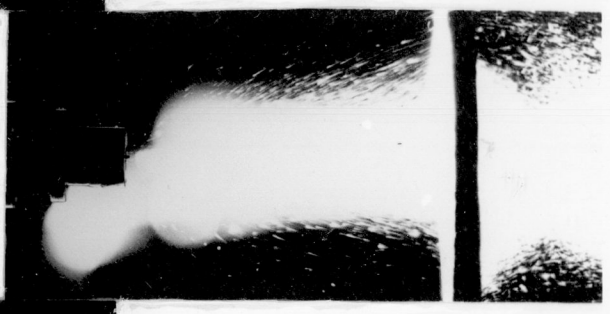

f) 46 ms - Maximum field intensity configuration at -30 kV

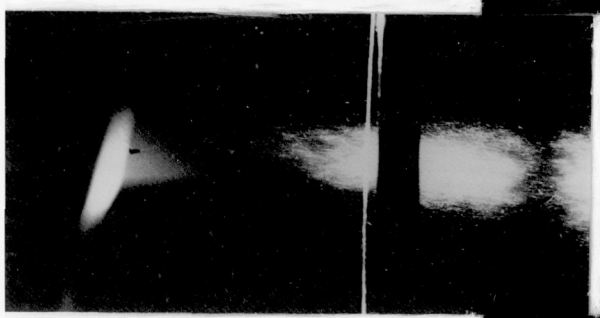

g) 109 ms - No field

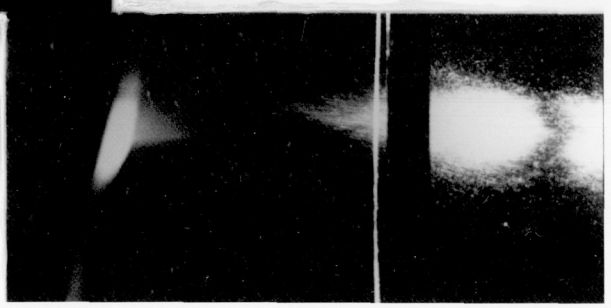

h) 109 ms - Field applied (-30 kV)

Figure 5.11 - Sequences associated with Diesel spray modification.

Qualitative interpretation of Figures 5.11 a and b indicates reduced penetration due to the complete evaporation of the initial injection droplets which is the desired property in the first stage of controlling the ignition delay of these fuels. The possibility of Joule heating at this phase seems highly likely.

Phase 2 - Comparison of Figures 5.11 c and d shows very little change in penetration. However the cone angle of the spray at the injector has been increased from approximately 20^{o} in the absence of the field to approximately 60^{o} in the presence of the field. It is also possible to see that droplets 'frozen' in space by the flash in the absence of the field are streaked in the presence of the field indicating their increased velocity (Figures 5.11 e and f show this more clearly).

The injector used in this work was a CAV single holed pintle nozzle. There are significant advantages to being able to increase the cone angle for such a single holed injector to improve air utilisation without swirl. When the mass of air is between 1 to 2 orders of magnitude greater than the mass of fuel (ie. a Diesel application) the situation where the mass of fuel is moved rather than the air (conventionally the air is swirled) would raise brake efficiencies due to reduced pumping and convective heat transfer losses).

This effect is more readily demonstrated under these laboratory conditions than is likely to be of practical use, because of the difficulties of controlling the spray charging and droplet movement in the combustion environment within the cylinder of a practical engine, once the main heat release has commenced.

Phase 3 - The spray apparatus shown in Figure 5.8 very closely modelled a practical situation, in that the injector pump (IP) was driven under high torque, due to the speed reduction of the gearbox arrangement as shown. All other apparatus were iden-

tical with a practical engine. Due to the operation of the jerk pump the pressure pulse required to lift the injector needle for the main injection travels from IP to I and is then reflected back to IP and returns to I, substantially attenuated, but often able to cause the needle to lift and inject a further quantity of fuel.

This 'after-injection' is responsible for a significant proportion of the soot emission from Diesel engines and there is a direct correlation between the mass of the 'after-injection' and the soot emission (Patterson and Henein). It was therefore within the scope of this study to see if this phase 3 period could be modified. Figures 5.11 g and h illustrate phase 3 operation. The section of spray that is separated from the end of the main spray seen in the photographs corresponds to the 'after-injection'.

Close inspection of the no field, and field applied case show, in the latter photograph, streaking due to the charged particles moving towards the ring electrode. No meaningful quantitative information could be obtained from these photographs. It was only possible to conclude that even at the end of the spray, in the absence of flame ions, the 'after-injection' was still being charged, and therefore amenable to electric field manipulation.

CONCLUSIONS

Carburation - Electrostatic carburation, specifically of alcohol fuels, looks particularly attractive. Although the voltages are high, 20 to 30 kV, the V x i power consumptions are modest (currents from 100 μA to 1 mA are likely depending on electrode configuration) at flow rates that approach practical consumptions. The powers therefore are within the same order of magnitude as for electronic ignition systems.

The detailed charging criteria to avoid droplets impacting on

manifold walls and other earthed surfaces, due to mutually repulsion of a unipolar cloud of droplets, is the first main obstacle to be overcome.

Better carburation than that available by conventional venturi systems is highly desirable at low engine load situations for any fuel and the possibility of solving the problems of cold starting, manifold freezing and lowered volumetric efficiency for alcohol fuels is unique in the case of electrostatic carburation.

For engine combustion there is considerable evidence (294, 336) that (apart from the reduction in charge density) fuel/air mixtures that are homogeneously dispersed on a molecular scale are far from optimal. Mixtures that are aerodynamically stratified into a uniform dust or mist suspension are the optimum for both flame propagation and emissions.

The effects of droplet size on burning velocity (344) and minimum ignition energies in fuel mists (29) have been reported. The wider 'flammability limits' of dust or mist suspensions is also well known (Gaydon and Wolfhard). Layered fuel/air mixtures are also known to exhibit flame propagation velocities several times the stoichiometric mixture flame speed (134). Recently it has been observed (85) that NO_x emissions from laboratory monodisperse droplet combustion show minima as a function of droplet diameter (see also Figure 5.12).

The possible degree of freedom offered by detaching the atomisation efficiency and droplet size distribution function from the inlet air mass flow rate in a throttled system is a strong potention advantage to electrostatic carburation. The further effects that varying the droplet size in fuel/air mists into the engine may have on combustion and emissions leads to consideration of electrostatic carbu-

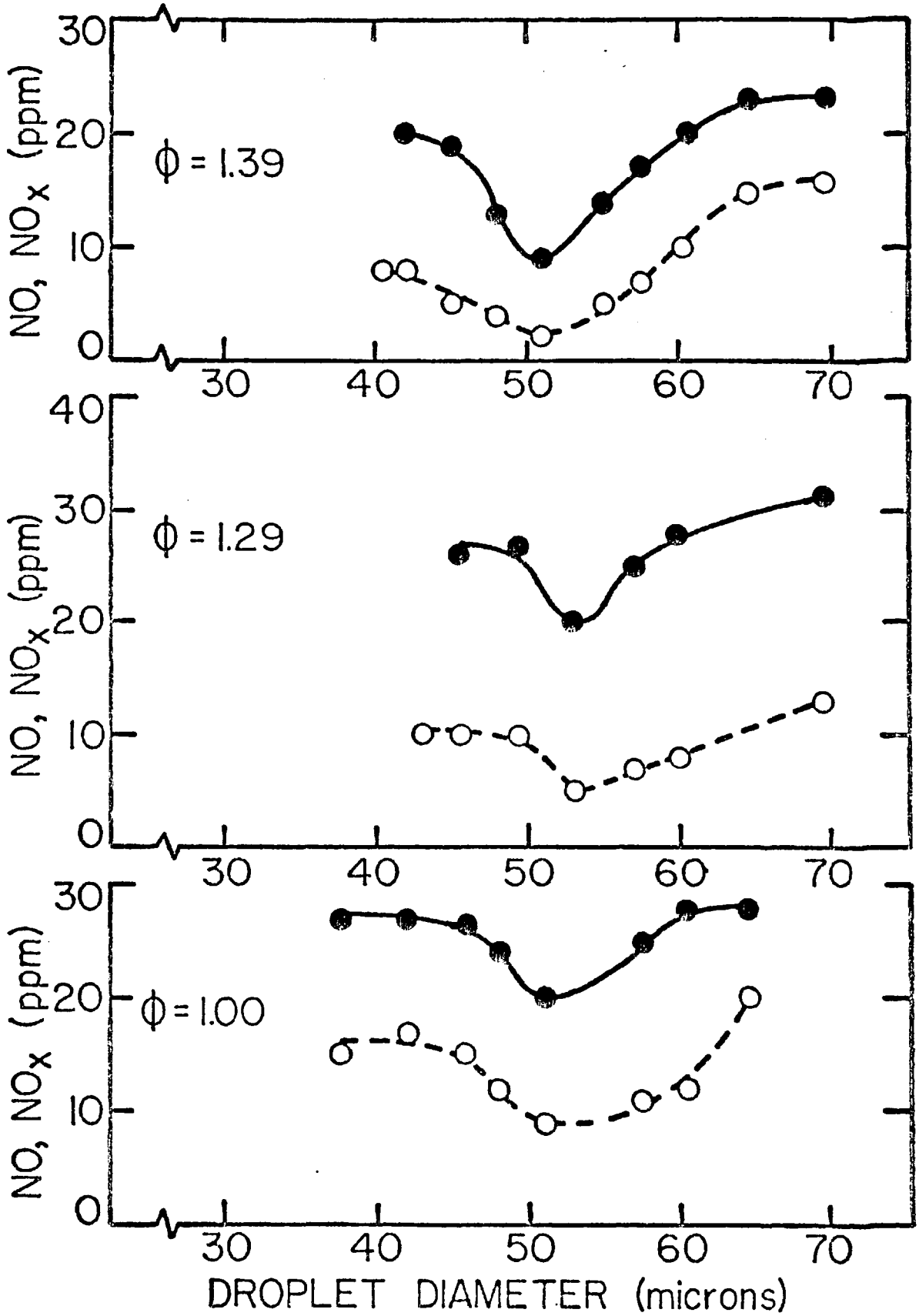

Figure 5.12 - NO_x emission as a function of droplet diameter (data from ref. 85)

ration as an engine research tool.

If specific spray characteristics are required for optimum economy and emission operation (for alcohols or conducting non oxygenated hydrocarbons) as a function of load, the input parameters to the carburettor of field strength and power consumption are readily amenable to microprocessor control. (Electronic carburettor AFR control for example already exists (18)).

The detailed electrode configurations and charging criteria are well worth further study for practical application.

Injection - Most of the injection work has been specifically directed to Diesel application. However, while the arguments of carburation apply to a non-alcohol injected dual fuel approach in a Diesel engine, so also do some of the injection arguments for injected Otto engines. Work in Japan has shown how injection flash boiling of methanol leads to improvements in engine performance in Otto engines (250, 251, 411). The fuel is heated electrically. Preparation of mists of droplets in this way then made possible unthrottled operation of a spark ignited engine operating on methanol.

The biggest problem for utilisation of alcohol fuels in Diesel engines is reliable compression ignition which is synonymous with a low cetane number. The possibility of modification of the phase 1 period in a way that allows rapid vaporisation of the fuel with the latent heat supplied by Joule heating would prevent lowering of the compression temperature. The combination of a spark augmented Diesel system may also allow a lowering of the compression ratio to a value below that normally required for compression ignition of the Diesel fuel. It may then be possible to approach a compression ratio that corresponds more closely to that required for optimum brake efficiency (see also appendix 2). This would further add to the economy and emission advantages that would be available for single fuel Diesel com-

bustion of alcohol fuels, once the reactivity in the ignition delay period has been enhanced and controlled. The combination of electrical interaction to generate a fuel vapour with non-nitrogenous cetane modifiers, specifically peroxides, is particularly worthy of further study.

As far as practical utilisation is concerned, the maximum field intensity, that is normally limited by spark breakdown, will be much higher than the atmospheric pressure preliminary laboratory experiments, and is advantageous. The Paschen law (Cobine) states that the sparking potential for breakdown is a function of the pressure(p) and gap width(d) only, so that for air with a 'pd' value of 10^3 (mm. Hg mm) at $20^{o}C$, increasing the pressure by a factor of 10 raises the sparking potential from an initial value of 7 kV ($pd = 10^3$) to 40 kV ($pd = 10^4$). The increased field intensity that is available before breakdown under high pressures should be a feature that further enhances the possibility of practical solution to the Diesel ignition problem. As in the case of the carburettor the details of the electrode configurations, specifically this time for incylinder geometries have yet to be established.

To conclude, this section has dealt mainly with electrical application to alcohol fuels primarily as a single fuel. It is possible to add alcohols to pure hydrocarbon fuels to produce for example 'Gasohol' (generally a blend of 10 to 15% by volume alcohol, balance gasoline) and countries such as Brazil, Canada, Japan, New Zealand, Sweden and the United States have carried out extensive studies with respect to production and utilisation of alcohols. 'Pure' Ethanol may be purchased at gasoline stations in Brazil and 10% Ethanol-gasohol, for example, regularly sells at stations in Nebraska and Iowa, USA. Although alcohols as fuels have been used in engines since the early part of this century (362) the concern over economy and emissions

especially in the USA has required closer evaluation (76, 124, 430) with regard particularly to aldehydes and evaporative losses.

While intuitively one might suppose that small additions of alcohols to, for example, iso-octane would result in the smallest perturbation and therefore the minimum modification in utilisation for practical situations, this is not the case. As can be seen from Figure 5.1, in the liquid phase alcohol fuels are highly hydrogen bonded, 'dilution' of the alcohols that results in gasohols lowers the extent of hydrogen bonding and the molecular clusters present in the liquid phase that give rise to the high latent heats are less likely, and the mobility of gaseous alcohol molecules is increased.

The alcohol additions therefore lead to increased evaporative losses from gasohols resulting from the increased Reid vapour pressures due to reduced H-bonding. When the individual alcohol molecule is very reactive (especially methanol) this has distinct disadvantages especially when the gaseous molecule has an affinity for plastic components such as perspex and polyurethane which may be completely dissolved by methanol/gasoline blends, when they are completely inert to either of the pure fuels separately (82, 161). Such blends also can cause enhanced blood uptake levels of methanol from both inhalation and cutaneous exposure (139). Further difficulties with alcohol blends arise due to phase separation. It is conceivable that this may be amenable to an electrical solution, in that the conducting component would respond to an applied field and may aid the dispersion of a two component fluid. This suggestion is purely speculative at this stage. Alcohols are partially oxidised, and they may undergo further oxidation, by aerobic bacterial action, to produce acids both in production and storage. Conventional carburettors contain metals that are amphoteric (eg. Al and Zn) and are rapidly eroded by these acids.

An electrostatic carburettor may be constructed from a variety of materials that need not be amphoteric.

This section has shown the potential for electrostatic methods to solve many of the real combustion problems for both intermittent and continuous mixture preparation. The power consumptions are modest at fuel flow rates approaching practical values and are worthy of further consideration for practical situations, especially with alcohol fuels.

SECTION II - PRODUCT DISCHARGE

Introduction - This section deals with electric field interactions at the product discharge stage, with emphasis on soot control and emission reduction. In Chapter 2, the modes of electrical interaction were subdivided into high and low voltage applications. However, it is convenient for this section to subdivide the high voltage (electric field) interactions into two further subsections, a first involving voltages in the region of 500 Volts (electron manipulation) and the second, voltages of 10 to 30 kV (ion manipulation).

This classification is significant because the two subsections deal with the two main charged entities that appear to be most closely linked with soot formation and destruction, namely the electron and positive ions or particles. This does not mean that negative ions are not important in soot formation and destruction, but that most of the previous work in this area has been directed towards these two entities.

The role of negative ions may be of importance for those species present in combustion which have large electron affinities, such as the halogens in inhibited flames (F = 3.45, Cl = 3.61, Br = 3.37, I = 3.0 eV; data from Gaydon and Wolfhard). However, electron attachment as a key feature in inhibition was discounted early in Section I. Nevertheless

it is interesting to note that hydrocarbon fragments have particularly high electron affinities (CH = 2.6, C_2H = 3.0, C_2 = 3.4 eV) even compared with oxidising entities (O_2 = 0.44, O = 1.47, OH = 1.83 eV). The possible role of such hydrocarbon nucleophiles in fuel polymerisation mechanisms early in soot formation, and especially with aromatic molecules does not appear to have been fully investigated, and could provide an interesting way for electrically interacting with these species with a view to soot formation rate modification. These species are certainly very important in the pure hydrocarbon plasmas seen, for example, in Figure 6.20h.

All the molecular species present in flames have very high ionisation potentials with most over 10 eV (Gaydon and Wolfhard). However nitric oxide at 9.26 eV has the lowest, because the electron that is lost in ionisation comes from an anti-bonding orbital and, in forming NO^+, the electronic configuration of the molecule is isoelectronic with N_2. This has made NO^+ the most abundant molecular ion in the post flame gases and led to the consideration of dissociative recombination, as shown below, as a means of nitric oxide control (125).

$$NO^+ + e^- \longrightarrow N + O$$

This process is exothermic and has been estimated to be at least 10^4 times faster than all formation processes (125).

However the main consideration of the electron in the work described in this section was not for dissociative recombination of positive ions, but modification of agglomeration processes.

Because of the high mobility of electrons, around 4000 $cm^2\ s^{-1}\ V^{-1}$ compared to 1 $cm^2\ s^{-1}\ V^{-1}$ for positive ions in flame gases (Gaydon and Wolfhard), charge separation is possible at substantially different

magnitudes of applied field (thermal diffusion also generates charge separation). For that reason the two subsections mentioned previously will be dealt with under the following headings:-

a) Electron Manipulation

b) Ion Manipulation

a) Electron Manipulation - Before the experimental work is described that fell under this subheading it is pertinent to outline the incentives for, and anticipated results of, such an electrical interaction.

In Chapter 1, Figure 1.2, the effect NO_x emission control has on BSFC was shown through the mechanism of injection retard in a quality-mode power control situation. A further effect that was not superimposed on that data was how the smoke emission also rises with increasing BSFC. The proposed level of 0.2 g/mile particulate emission for Diesel vehicles (363) is very difficult to meet and leads to a further constraint in the multivariate problem of NO_x vs. BSFC, that seriously affects the practical economy gains of Diesel engines.

It would be especially desirable therefore if it were possible to control the soot emission from Diesel engines either by preventing its formation or by increasing the rate of oxidation of soot particles. Efficient control of the after-injection previously described is the initial point at which to start with Diesel engines, as this gives rise to an unnecessary soot emission. However, this section describes work to investigate methods of controlling soot emissions produced inevitably through diffusion controlled combustion.

Once combustion generated soot has been produced it is not easy to oxidise due to the limited time available between production and quenching in the exhaust. Catalytic oxidation of particles by metal surfaces has not been very successful due to the fact that the

active contact area between the surface of the catalyst and the particle is so small. Increasing the residence time of soot particles in a hot oxidising environment using 'filters' can show reductions in mass emissions of up to 28% (95). However, these devices lead to increases in exhaust back pressure and consequent lowering of brake thermal efficiency and thus BSFC.

Fuel additives have been reported as a possible effective way of reducing smoke emissions from practical engines as early as 1967 (303) but have received considerably more attention recently in a practical context (95, 132, 159, 181, 258, 327). These additives have generally been salts of the alkali or alkaline earth metals of the periodic table, although first row transition metals have been used; mainly manganese (132, 159, 181) which has the widest range of oxidation states. (Methyl cyclopentadienyl manganese tricarbonyl is a hydrocarbon soluble organometallic complex of Mn that may be used. It also has anti-knock properties).

The effects of metal additives on laboratory premixed and diffusion flames has long been known (409). Gaseous additives may also modify soot, SO_3 having a very marked promoting effect on soot emissions in premixed flames (Gaydon and Wolfhard). The possibility to enhance or reduce soot emissions with metal additives has been observed in many studies depending on the manner of addition (68, 97, 141, 374). This behaviour has been explained by considering the possibilities of superimposed chemical and physical mechanisms with ionic mechanisms promoting soot emissions and chemical oxidation lowering the emission (141).

Some researchers have preferred a purely chemical mechanism (97) and others concentrated on electrical mechanisms (52, 68, 374). The attraction of an electrical mechanism is the apparent correlation

between ionisation potential of the additive and its activity. The possibility of combined chemical and physical mechanisms has been given further support in a recent study (193).

Consideration of the possible ways in which a hydrocarbon fuel may be converted from gas phase hydrocarbons to small nuclei and then fully agglomerated soot particles (see for example Figure 140.1 of ref. 64) makes it apparent that any process that modifies the rate of oxidation of soot precusors or rate of agglomeration of soot particles will automatically modify the soot emission. Complete oxidation of soot particles, in limited time before quenching occurs, is favoured by the highest surface to mass ratio of the soot particles which is synonymous with reduced agglomeration.

It was not the intention of this study to fully explore the detailed mechanisms of how these additives behaved, but to examine possible ways in which whatever electrical interaction these additives had could be utilised for combustion improvement.

The author, in a study of vehicle particulate emissions in 1974, blended a fuel additive that was based on alkaline earths (11.2% Ca, 2.4% Ba, 1.3% Sr) and added to Diesel fuel at a concentration of 0.6% by weight. The particulate emission was monitored using the experimental procedure described in ref. 95. The mass emission was then compared with fuel without the alkaline earth additive. The vehicle used for the study was a 183 in^3, IDI, light duty Diesel truck. The results are seen in Table 5.7.

TABLE 5.7

Fuel	Total particulate emission (mg)	g/mile particulate emission
i) Gas Oil	100.1	0.88
ii) Gas Oil + 0.6% Additive	130.8	1.18

It was apparent that while the particulate material in case ii) had a more grey appearance than case i), the total mass of particulate emission had increased due to the presence of alkaline earth oxides as particulate material. A flame test on the soot collected when viewed with filters showed the presence of calcium (red) and barium (green). A method of extracting the activity of these metal additives without the additives themselves being present to contribute to the particulate emission as the metal oxide or hydroxide was sought. (Although barium sulphate, with a solubility product of 10^{-40}, is not toxic this is not the case with the oxide).

The hypothesis of the electron as an important agent in modifying soot agglomeration was reported in ref. 52. The effect of ionisation potential has been mentioned, and this section of the work was firstly to try to investigate whether electrons emitted from surfaces could be used to modify soot emissions, and secondly, if this were the case, any material could then be utilised that underwent electron emission under conditions of the application of small (10^2) bias voltages.

In this context when talking of surfaces emitting electrons it is more appropriate to consider the thermionic work function. Barium has a low thermionic work function (≈ 2.1 eV) and depending on the form of carbon the work function is from 4 to 5 eV. Graphite is normally quoted as 4.34 eV (389), (free carbon atoms have a first ionisation potential of 11.265 eV) and a study of the work function of soot particles in flames (389) estimated a value of 8.5 eV. If it were possible to demonstrate the role of the electron as the principal agent, then the interesting possibility existed that soot deposited on a surface could be utilised to control the agglomeration of soot in the gas phase with subsequent control of radiative and particulate emission.

The following experiments were performed to gain an insight into this possibility.

Experimental - The experimental arrangement is shown in Figure 5.13. A rich (λ = 0.48) premixed ethylene/air flame was arranged with a quenching shield of nitrogen. The N_2 cooled exhaust gas passed through a preweighed Whatman GFA Borosilicate glass fibre filter (recommended in ref.256) that was oven dried and cooled in a dessicator. The timed soot emission was collected, kept in a dessicator containing phosphorus pentoxide dessicant, and dried to constant weight. The emission was then estimated in $\mu g\ s^{-1}$.

A set of 25 measurements of soot emission, with sampling intervals of 8 to 12 minutes, gave an emission rate of 26.4 $\mu g\ s^{-1}$, with a standard deviation of ± 6% for the unperturbed situation.

The electrical interaction involved preparing a stainless steel gauze electrode as a control and a further gauze electrode coated with barium hydroxide. The gauze electrode formed the emitter, while an earthed copper collector completed the circuit of the flame diode. The separation (d) was variable to facilitate electron removal at different locations. The V-i characteristics of these diodes are shown in Figure 5.14. As expected the lower thermionic work function of the coated gauze leads to substantially higher current flow at a given applied potential. The maximum applied potential before ionic wind perturbations became apparent on the visible flame structure was 400 volts, with d at 5.0 cms, and this determined the maximum field intensity.

The objective was to measure soot emissions with an uncoated and coated gauze as a function of applied potential.

Results - The results are shown in Figure 5.15. Although the experiments led to very reproducible soot emissions in the absence of a coating, and the minima in emission was repeated

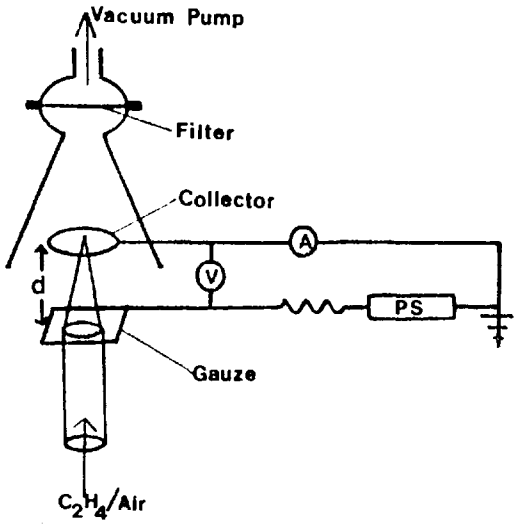

Figure 5.13 - Schematic of small field soot emission apparatus.

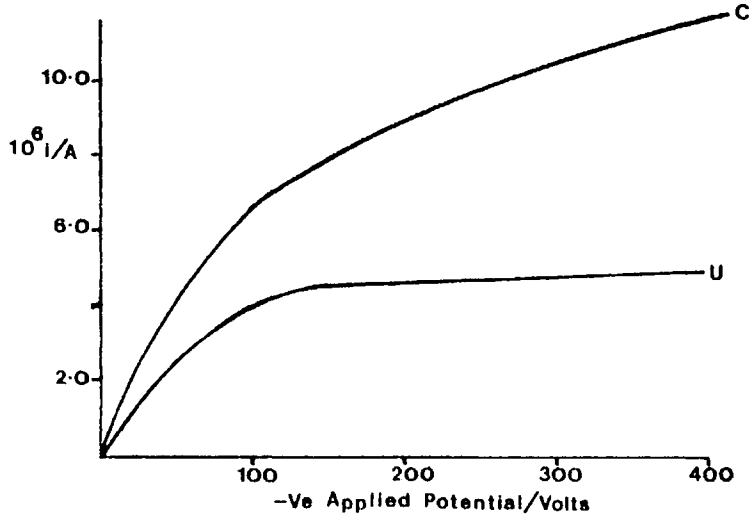

Figure 5.14 - V-i curves of uncoated (U) and barium nitrate coated (C) stainless steel gauze.

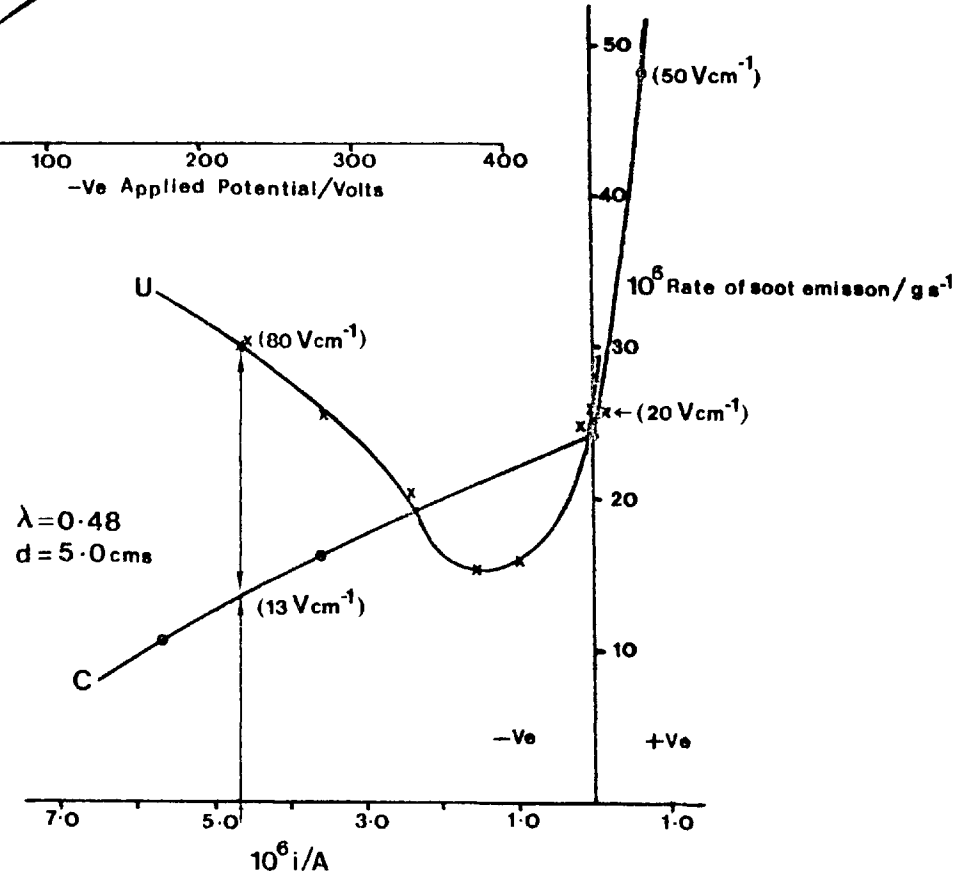

Figure 5.15 - Rate of soot emission vs. current drawn at increasing potential.

on three occasions, such repeatability was not possible with the barium coated gauze, and only the best set of data, is presented. The possibility of material becoming dislodged from the gauze and contributing to anomalous results was considered, and a mass spectrum of a soot sample was taken, to see if there was any barium in the soot.

Table 5.8 shows the spectrum. There is no peak around a mass number 154 corresponding to either the oxide or the hydroxide of barium, so it would appear that barium inclusion in the soot particles may be ruled out. Unfortunately, due to time constraints, and the success of the plasma jet experiments that were undertaken in parallel, no further work on electron injection was possible. The results of this part of the study are presented here, to provide data that may be of use in any further work directed towards "small-field" modification of soot emission from combustion.

Interpretation - Figure 5.14 shows the voltage-current characteristics of the "flame-diode" experimental arrangement shown in Figure 5.13. These V-i curves are very similar to those for barium coated and uncoated Nichrome wires held in diffusion flames, and reported in reference 52. In the work cited in reference 52, the wires were held within the stoichiometric contour, so that flame temperatures were experienced along parts of the length of the wire.

Due to the location of the coated and uncoated gauzes at the base of the flame in this work, these surfaces were at temperatures lower than those of the wires. Consequently, for a given value of V in these experiments the values of i are lower than those reported for the wires. The strong temperature dependence of thermionic emission is well known (Cobine) and may be described by the Dushman equation, 5.14.

$$j = AT^2 \exp\left(-b/T\right) \qquad 5.14$$

where j = Current density (amps/cm^2)

T = Temperature (^{o}K)

b = $\phi e/k$

k = Boltzmann constant

e = electronic charge

ϕ = Thermionic work function

A = Material constant (A $\simeq$ 60 amp/cm^2 deg^2 for most metallic surfaces)

Negative potentials applied to surfaces may lower the effective work function, due to the Schottky effect, and therefore increase j for a given value of T by the reduced effective value of ϕ. Positive potentials applied to surfaces may totally suppress electron emission from the uncoated surfaces, however, coated ones may emit positive ions as reported in the higher temperature experiments of reference 52.

Inspection of Figure 5.14 indicates that there was no appreciable electron emission from the uncoated surface. The evidence for this is the fact that a saturation current was established at an applied voltage of 150 Volts, and further increase in applied potential to 400 Volts shows no appreciable increase in current. (The upper limit of 400 Volts was set by the field intensity (80 V cm^{-1}) at which ionic wind perturbation caused a visible disturbance to the flame). The saturation level indicates that electrons were being removed as rapidly from the flame as they were generated there, with no addition as a function of increased potential from the uncoated gauze.

The experimental results of soot emission rate shown in Figure 5.15 need to be interpreted by considering an emitter (of electrons or positive ions) in the coated case, and a non-emitter in the uncoated case. Also, the effects of the applied electric field on the trajectory and number density of the positively charged species (gaseous ions and particles), as well as the electron, need to be considered for both types of surface.

The soot emission rate at $\approx 26\,\mu g\ s^{-1}$ for both the coated and uncoated gauze at zero potential, (and small positive potential (100 V) to the uncoated electrode) represents the systems 'natural' or unperturbed soot emission rate.

The abscissa of Figure 5.15 is measured current. Due to the different V-i characteristics of the coated and uncoated electrodes, it is evident that two markedly different values of field intensity are responsible for a given value of measured current. To highlight this, the field intensities for a current flow of 4.7 μAmps have been marked on Figure 5.15 for 'C' and 'U' as 13 and 80 V cm^{-1} respectively.

To attempt to explain these results requires consideration of the various charged species within the flame, and how these are influenced by the various applied potentials for the given electrode properties. It is assumed that there are two types of positively charged entity that are present within a flame of this sort. The first type are small (in comparison to particles) positively charged ions with the dimension of molecular ions (ie. $d < 10$ Å) and mobilities of the order 1 $cm^2\ s^{-1}\ V^{-1}$ (Gaydon). Such species might be $C_3H_3^+$, CHO^+ or polynuclear aromatic molecular ions. Ions of this soot have been suggested as efficient nuclei for primary particle formation (300). In the following discussion these species will be referred to as ions.

The second type of positively charged entity to be considered would more closely resemble the solid phase, rather than the gaseous phase, and have dimensions of 100 to 200 Å. These species would have lower mobilities than positive ions, typically 10^{-3} to 3×10^{-2} $cm^2\ s^{-1}\ V^{-1}$ (300). This type of entity more closely resembles the soot particles emitted from a flame, and has been shown to acquire a positive charge (unit charge per particle) in the presence of an applied field (300). Thermionic emission may also lead to such charge acquisition, due to the relatively low work function of soot quoted earlier. In the

following discussion these species will be referred to as particles.

The most abundant negatively charged species will be assumed to be the electron. It has been shown to be the predominant negative charge carrier in the high temperature zones of flames (Lawton and Weinberg). The high mobility of 4000 $cm^2\ s^{-1}\ V^{-1}$ (Gaydon) also gives it the largest diffusion coefficient of any other entity in the flame. This is in no way intended to imply that negative ions are not present, only that the explanation of these results does not, of necessity, require any other negatively charged species.

An attempt to explain the results will be made under the headings of the nature of the gauze electrode.

Uncoated electrode - At zero applied potential, the soot emission rate is identical (within experimental limits) to that of the coated electrode. With increasing negative potential (0 to 100 V) applied to the gauze the main effect is to withdraw the mobile positively charged ions to the cathode. This process results in a removal of these nuclei thus preventing soot formation by reducing the agglomeration to larger particles. At the mixture strength used ($\lambda = 0.48$) total suppression of soot formation did not occur. With increasing negative potential the larger particles were moved against the gas flow, thus increasing agglomeration of the larger particles, due to the increased residence time. The surface to mass ratio is therefore reduced and subsequent burn-up of these larger agglomerates, in the hot post flame oxidation zone, less likely. This results in an increased soot emission as was observed. The removal of ions and retention of particles are competing effects in terms of the soot emission rate, and the minimum as shown in Figure 5.15 results. With increasing applied potential, to the ionic wind limit, the soot emission rate increases.

If this explanation were correct, the feature of the minimum would be very sensitive to mixture strength and reactant flow velocity.

If λ and velocity were increased, the minimum would move to lower currents and emission rates. In the limit of complete removal of these ions, the formation of soot may be completely suppressed. Reduction of over 90% in soot emission, by applying electric fields to counter-flow diffusion flames, have already been reported (300, 342, 343).

Applying a positive potential to the uncoated gauze caused a negligible change in soot emission rate.

Coated electrode - As can be seen from Figure 5.15, applying a positive potential to the barium coated gauze gave rise to a nearly double soot emission rate over that of the zero field rate. Positive ion emission from a barium coated wire was proposed in the diffusion flame experiments reported in reference 52. In the gauze experiments the measured currents, under positive potential, were much lower due to the lower temperatures of the gauze electrode compared to the wire. (Losses from the coated gauze electrode, due to volatilisation, was ruled out in these experiments, under negative applied potential, due to the absence of a barium salt signal in the mass spectrum shown in table 5.8).

It is postulated, by way of an explanation of the increased soot emission under positive potential, that barium ions were emitted from the gauze when a positive voltage was applied. The emitted barium ions were acting as positive inorganic ion soot nuclei, and serving the same function as the organic ion nuclei that are normally present.

Applying a negative potential to the coated gauze suppresses positive ion emission, and increases the electron number density in the flame progressively. Due to the low work function of the barium coating, the field intensities to cause appreciable electron injection are well below those levels where the larger positively charged particles move against the gas flow to increase sooting. The main effect of the added, highly mobile, electrons is to neutralise the positively

charged species and reduce the number density of ionic nuclei and lower agglomeration rates. This is seen by the continuous reduction in soot emission rate with current.

Conclusion - These results lend support to the already published work concerning the importance of electrons, and small positively charged species, in the formation and emission of soot from flames. Positively charged species that provide both nuclei for agglomeration, and interact in the soot agglomeration process, may be neutralised by the addition of electrons or withdrawn by applied fields. The applied field intensities should be such that enhanced soot emission does not take place due to increased residence times of less mobile, larger, soot particles that have acquired a positive charge. It appears, as far as nucleation is concerned, that the nature of the positive ion ie. inorganic (eg. $Ba\,OH^+$) or organic is not as important in increasing soot emission as the number density of such ions.

Further quantitative studies would be worthwhile, especially ones identifying barium ion inclusion in the soot, when a positive potential is applied to coated electrodes. The competing effects of electron neutralisation and ionic nucleation may provide some insight to the "pro" and "anti" roles observed with soot formation when alkaline earths are added to flames (68, 141, 374).

b) Ion Manipulation - As stated previously no intentional attempt was made in this study to interact negative hydrocarbon molecular ions with applied fields. The emphasis described in this subsection was the manipulation of positively charged soot particles formed by combustion. The plasma developments described in Chapter 4 indicated direct interaction with the soot formation process at the precusor stage which would lead to the most 'dramatic' changes associated with an electrical interaction. Modification by particle manipulation would lead to less substantial changes in the post flame

regions, with modest powers, than those observed by particle manipulation at or before the agglomeration phase, due in part to the high drag coefficient of the particles (435). Very profound changes in soot emission by removal of growth surface in the agglomeration phase have been reported (Lawton and Weinberg).

This section could be regarded as an extension to electrostatic precipitation. Precipitation of particulate material electrostatically is extensively documented (White) both with respect to interfacial interactions (397) and powers required (398). Normally the emitted particles are charged with a corona discharge, but in the case of soot particles a substantial proportion of the particles are charged already and available for electric field manipulation with a resultant lowering of power requirement. Such systems have been extensively studied with a view to subsequent electrical control (Lawton and Weinberg, 178, 300, 342, 343, 444, 451) as well as during initial pyrolysis in the absence of oxygen (54).

Table 5.8

Atomic Mass No.	% Dist.	AMN	% Dist.
212.66	1.56	46.19	6.64
197.71	1.95	45.16	37.50
95.88	1.17	44.19	7.42
95.35	1.56	43.16	1.56
85.99	1.56	43.13	1.17
83.07	1.56	42.08	5.47
81.77	1.17	42.05	1.17
71.85	1.95	41.08	2.34
69.99	1.73	33.05	2.73
67.97	1.56	31.95	2.73
63.94	1.56	30.81	1.17
58.06	4.30	29.92	1.95
57.03	1.56	29.88	6.25
56.03	3.91	28.92	19.92
56.94	1.56	27.93	4.29
47.14	1.17	26.99	1.56

Mass Spectrum - see list of tables

Because this part of the work was directed towards the subsequent oxidation of soot particles in a hot oxidising environment, based on the assumption of their inevitable formation under diffusion controlled combustion, it was appropriate to consider the main species that may be important in oxidation of soot, as well as soot oxidation kinetics. Analytically, the problem of calculating actual powers required, which is always the fundamental question in the electrical interaction context, requires knowledge of many properties of the system that are not only chemical but also physical in nature.

Increasing the residence time of soot particles in a hot oxidising environment leads to consideration of a 'd^2' type law, that has been applied to droplets, to obtain a burn-out time (Williams). There are however, significant differences between droplet and particle combustion. The surface properties of soot are most important in determining the rate controlling processes of oxidant adsorption attachment and product desorption (Shaw). These processes make application of such an empirical law to soot combustion hazardous. The immediate surface structure of the particles adds to complication in the extraction of a rate constant for surface removal. Reference 130 suggests a modified rate constant for surface removal, $k' = k(1 + \sqrt{SD/k})$ where k is the rate constant for particles free of cracks burning under kinetic control, S is the internal surface area of the cracks, D is the diffusion coefficient along the crack. These properties of soot are not immediately available.

The movement of charged soot particles in an applied field requires an electrical body force, F, that is a function of the charge of the particle and is given by $F = E\ e\ n$ (Lawton and Weinberg). A final velocity is attained when this force is balanced by the aerodynamic drag on the particle. This is obviously related to the Reynold's number of the system, which is determined by the ratio of inertial to

viscous forces operating, and dependent on the size and trajectory of the particle with respect to the main gas flow, within the particular combustion system.

The viscous forces for small particles (uncharged) in flow are very high (Shapiro). During oxidation the particle size would be continuously decreasing (elastic collisions assumed) and the viscous component of drag continually increasing. The effects of Reynold's number on drag coefficient of charged particles has been considered for practical application (Lawton and Weinberg and references therein). These studies have separated the particle-flow systems into two regimes, a Stokes and Newton regime, depending on particle size and Reynold's number. Recalling that the Reynold's number is an expression of the ratio of inertial to viscous forces acting on the particle, it is interesting to note that (for a given charged particle within the range of practical interest) the Reynold's number was computed independent of partical size.

If the rate of oxidation of the particle is independent of its relative velocity with the oxidation gas (such a condition could exist, for example, if the rate controlling step in the oxidation were adsorption of O_2 onto the particle in excess air or desorption of CO_2 from the oxidising particle) electrical movement of the particle in the gas phase would then be an unnecessarily high electrical power requirement that then served no useful purpose. Electrical attachment to a plate, or the combustor wall, that acted to increase the residence time for reaction would be the most appropriate electrical interaction.

It is possible therefore, that, depending on the history of the particle in the hot oxidising environment, the high voltage electrical interaction may be either to recirculate particles or merely deflect and hold for oxidation. One advantage of such a system is that without any baffles in the flow, the pumping losses to the brake efficiency of the conversion system are minimal.

Soot particles in combustion range in size from 0.001 μm (233) to 1 μm (247) and there is evidence of a bimodal nature in the size distribution function in Diesel exhaust (247). The ability of the human nose to filter very small particles is not high, and an electrical interaction that reduced combustion emitted particles to a size range where potentially carcinogenic material, located on the particulate, was available to pass through nasal passages and enter the lungs, could not be regarded as an improvement. It is known that carbonaceous particulate material has adsorbed on its surface condensing hydrocarbon material that is in equilibrium with the particles (107). This material may have a potentially carcinogenic polynuclear aromatic (PNA) fraction and such compounds present that may enter the lung wall are of obvious environmental concern (363). A PNA route to soot formation has been suggested (2) and may possibly involve negatively charged molecular ions.

There is evidence that some of the metal additives previously added to fuels to lower the soot emission result in increased number density of smaller particles (193) that may potentially burn out under the appropriate oxidising conditions. Previous experiments discussed in subsection (a) showed that the total mass emission under such conditions actually increases, yet visually the exhaust appears 'less black'.

The human eye is not a very efficient estimator of light intensity under any circumstances. Particles that are small compared with the wavelength of incident light (ie. values of $x < 1$, where $x = 2\pi r/\lambda$ - Rayleigh scatterers) have symmetric scattering diagrams (233). As the particles become larger and x increases (Mie scatterers) the scattering patterns change, becoming unsymmetric with greater components of forward scatter.

The values of x for the range of particle sizes mentioned in ref. 247 are from 1.8×10^{-2} to 18.0 at 350 nm and 9.0×10^{-3} to 9.0 at 700 nm. An observer, viewing the exhaust flow at right angles

and observing light passing through the exhaust in foward scatter for a plume with a predominant number density of particles with x greater than unity, would receive a reduced intensity at the same location, if the component of forward scatter were reduced due to an increased number density of smaller particles due to the effect of the additive, even with the mass flow rate of particulate material the same. While this situation may be deceptively pleasing to the eye, experimental work shows an increased mass emission of particulate material. Later work has also shown this in Diesel exhausts (258). Earlier work on flames showed soot retention of the metals used (Mn and Fe increased soot oxidation rates by a factor of 2 to 3, but were retained in the particles (Fe as bis-π-cyclopentadienyl iron). Cobalt was ineffective in modifying oxidation (309)).

As far as the oxidation of soot to obtain a burning rate for this work is concerned, the most comprehensive study of soot oxidation up to 1962 was that of ref. 272. This worked showed a first order dependence of surface oxidation rate on oxygen partial pressure over a wide range of values. Later work, and the most definitive to date, is that of refs. 19 and 333 that endorse the empirical expression for graphite oxidation (320), applied to soot, and the main dependence of rate of surface removal on the partial pressure of oxygen.

The work of ref. 137 did not find a strong link to oxygen partial pressure, and suggested OH as the main oxidising species. However the main body of experimental evidence (19) supports a linear dependence of specific soot oxidation rate, at combustion temperatures, with oxygen partial pressure up to 1 Atm. The oxidation rate becomes assymptotic at a level of $\approx 10^{-2}$ g cm^{-2} s^{-1} at partial pressures from 1 to 100 Atm.

This behaviour isvery important since it indicates that the rate controlling process in the oxidation mechanism is activated adsorption

of oxygen, which is first order, until all the active sites are filled, becoming zero order at higher O_2 partial pressures.

The effect of surface properties in rate modification was considered in ref. 130, mentioned previously, while the differential reactivities of surface sites was considered in the early theory of ref. 44, and used in the work of ref. 320.

In combustion exhaust gases where the ve is disequilibrium of soot particles with excess air, and soot formation cannot be eliminated at source, the most advantageous solution appears to be to increase the residence time at zones of high partial pressure of oxygen. The appropriate temperature is as yet uncertain, but the highest value possible may not be optimum. Mechanisms that reduce the particle size of fuel droplets (by, for example, microexplosions of water/fuel emulsions or infra-red absorbing fuel additives) aid by reducing the resulting size of the soot particulates to be oxidised and prevent cenospheres forming in residual fuel oil combustion.

While an analytical description of the combined processes that take place by applying an electric field in this way are very complicated, the basic experimental system to study the potential for electrical manipulation, in a practical situation, requires only a single high voltage electrode, and for that reason was worthy of some initial experimentation.

Experimental - The Ricardo flame tube, as seen in Figure 4.5, was installed with a circular gauze electrode inserted into a pyrex sleeve that was drilled to enable air passage past the swirl vanes. The outer metal housing was at earth potential.

Four CdS photoresistors were placed symmetrically on the perspex observation window (seen in Figure 4.2b) to obtain an initial estimate of any change of flame radiative emission on the application of an electric field. A collimated beam from a white light source

passed at right angles to the exhaust flow, and observation of the scattered light was made with a camera at right angles to the axis of the illuminating beam.

The flame tube atomiser was a twin fluid 'Sonicore' ultrasonic atomiser, that under normal design operation for the flame tube, with air as the atomiser driver fluid, produced kerosine droplets with a spike size distribution function at 10μm (measured experimentally using the Malvern apparatus of ref. 290). Normal operation on kerosine produces a blue flame and no soot. However, to simulate some smoky practical exhausts, the air was throttled to 7 l s^{-1} (20°C, 1 Atm) and atomiser air replaced by propane, at a flow of 17 ml s^{-1} (20°C, 1 Atm). The fuel flow rate was 0.2 g s^{-1} of kerosine.

Results - Photographic records were made of the light incident on the camera resulting from scattering at right angles from the particles in the exhaust flow. Under the experimental conditions described, application of a potential of -15 kV to the gauze (the limit before spark breakdown with combustion) produced no detectable change in intensity, either at the perspex window or at the camera from particle light scattering.

Application of +15 kV however, while producing no detectable change in intensity measured at the CdS detectors, resulted in a substantial attenuation of the light reaching the camera from particles downstream of the throat.

The success of the plasma interaction experiments, that were being pursued in parallel, made unnecessary full quantitative studies of this experiment. However, the effect of throat exit velocity was crudely estimated by varying the extent of throttling. This would be potentially very important for the particle momentum and the final powers required for practical use in manipulation.

Interpretation of results - Due to the limited detailed experi-

mental work done in this area only general interpretations may be made. The fact that a -ve potential produced no detectable change indicates that movement of positively charged particles towards the gauze and negatively charged particles towards the flame tube body appeared not to modify substantially either soot formation or oxidation rates. The exact location of field lines in the presence of combustion ions in the turbulent flow field would be difficult to establish with certainty, however.

The gauze electrode when at +15 kV meant that positively charged material moved towards the combustor wall, and subsequent inspection of inside the wall surface of the flame tube showed a layer of soot there, although there was no excessive build up.

As the blower air was progressively unthrottled, so the air velocity at the throat (excess air was always present) and the particle momentum increased. The electrical interaction produced less soot reduction over that of the unperturbed situation. This is due to the combined effects of reduced soot emission in the unperturbed state, and the fact that, although the momentum of the particles had increased, the ability to generate a rate of change of momentum of the particles electrically, was still limited by the field intensity seen by the particles and set by breakdown in the presence of flame ions.

This system is worthy of further, more detailed, study. These preliminary experiments demonstrated that even under the conditions more closely related to a practical combustion condition, the soot particles show a predominant component that are positively charged due to thermionic emission and may be manipulated by an electric field. As the momentum of the particles obtained from the air flow increases, the ability to change the trajectory, electrically, is reduced, requiring higher field intensities that are limited by the location of the electrodes with respect to the flame.

CONCLUSIONS

This work has shown that electrical modification of emissions in the product discharge stage of diffusion controlled combustion is possible, and worth further work to identify the best electrode configuration for application to practical systems.

The interaction via electron manipulation appears to be mainly for modification of the agglomeration process, and may be attempted nearer the main combustion regions, and perhaps in cylinder; while that of particle manipulation needs to be in the post flame gases. Although manipulation in the agglomeration region produces removal of growth surface, this was shown for a counterflow diffusion flame, which has a high degree of control for academic studies and is not very similar to most practical conditions.

The evidence from the comprehensive studies reported, indicates oxygen to be the most important soot oxidising species. This work leads to the suggestion therefore that the best form of particle manipulation device for soot removal is of a form where the electric field is applied in a manner that does not require substantial movement of the positively charged particles against the gas flow, but where the exhaust fluid flows into a section that operates as a diffuser for decelerated flow, or to reduce the momentum of the fluid flow (perhaps at the momentum transfer stage of a turbocharger) with the particles then moved electrostatically at lower power requirement and held on a plate for oxidation by the exhaust air, which even at full loads, with maximum soot emission, operates with excess air present.

The difficulty with soot oxidation is similar to that of CO, NO and other endothermic pollutants, and even the lean-burn situation, in that, at exhaust temperatures, reaction to non pollutants such as CO_2, N_2, H_2O and O_2 is thermodynamically allowed, while at the same time being rate constrained within the exhaust and quenching time scales.

While this problem is resolvable catalytically in the quantity power-mode situation with low oxygen concentrations in the exhaust, the irony for the quality power-mode system is that nitric oxide, the species that requires chemical reduction, is present in an oxidising environment, while the species that requires oxidation is present in a form that is particularly difficult to oxidise in the limited time available in the oxidising environment.

A similar situation existed for the conditions of the Otto engine as seen for example in Figure 1.3, ie. that of NO reduction and simultaneous CO and HC oxidation. One solution to this problem has been the 3-way catalyst working in the narrow AFR window centred at 14.5. Such a solution for a Diesel engine, while in principle possible, is likely to be difficult and may be assisted by electrodeposition of soot particles.

Generally the particulate emissions from Otto engines are not as high as from Diesel engines, although older engines show particulate emissions that are a function of oil viscosity. The author as part of the earlier study at Ricardo mentioned previously, also measured vehicle particulate emissions as a function of oil viscosity. Table 5.9 shows some results, by way of comparison with the Diesel figures quoted previously. New gasoline vehicles using unleaded fuel emit less than 0.02 g/mile.

The data of Table 5.9 shows particulate material that was not mainly soot but oil mists. Within the context of electrical improvement it is interesting to finally conclude by suggesting a method that may utilise the unusual emission of soot from Otto engines for ignition advance control.

The importance of accurate control of ignition advance for economy and emissions has led to consideration of a number of possible knock detectors to provide a feedback sensor for ignition advance/

TABLE 5.9

Oil Viscosity Type	g/mile Particulate Emission
SAE 10	0.80
SAE 20	0.88
SAE 30	0.65
SAE 40	0.62
SAE 50	0.41
SAE 20/50	0.33
SAE 20/'60' synthetic oil	0.24

retard in closed loop control systems (20, 106, 261, 356, 434). Most are based on detection, via a transducer, of the characteristic dP/dt behaviour of knocking combustion either piezoelectrically or by analysis of the vibration signature from the output of a magnetostrictive accelerometer.

It was observed in early First World War spark ignited tank engines, under load, that knocking combustion resulted in emission of small amounts of soot for the duration of knock (Ricardo and Hempson). This observation was even used to support an early theory of knock (77) that suggested knocking arose from rapid combustion of H-atoms, stripped from hydrocarbon molecules, with the carbon skeletons emitted as soot.

Soot particles in Diesel exhaust impacting on surfaces are known to generate a triboelectric charge (95). However, the polarity of the charging is very load dependent. The possibility exists therefore for a novel detector of knock, based on triboelectric charging, with a sensor that need be no more complicated than an insulated metal plug. Such a detector with a high gain DC amplifier could in principle be used to provide a gated output for the onset of knock without the neces-

sity for background discrimination circuits. The possible methods for electrical interaction to improve combustion are very wide.

CHAPTER 6

DESIGN CONSTRUCTION AND PROPERTIES OF A NOVEL PLASMA GENERATOR

Following the success of the experimental work described in Chapter 4 it was necessary to take a detailed look at the problems associated with respect to the features of early plasma jet designs. The features not only detracted from their potential practical application, but prevented the ability to have stable, reproducible, continuous operation for detailed spectroscopic work that was necessary to help substantiate some of the predictions made in Chapter 3.

In the most sophisticated of the basic designs of early plasma jets involving continuous DC operation (eg. Lawton and Weinberg, or ref. 183) the electrodes consisted of a pointed thoriated tungsten cathode, and the anode was a cylindrical enclosure defining an approximate path for the anode root as the arc channel rotated under the influence of an axial magnetic field, provided by an electromagnet. The location of the cathode spot was not controlled. Electrical losses to the electrodes, which were water cooled, were of the order of 60%. In order to keep the discharges stable, addition of substantial amounts of noble monatomic gases was necessary (in the experiments of Chapter 4 using similar designs it was not possible to operate below 90% Argon). The heating of carrier gases further constituted a major loss in the electrical efficiency of a generator that was required to produce specific species.

The importance of specific atoms in combustion has already been considered. It was important therefore to define a meaningful efficiency with which to evaluate the performance of a generator operating specifically to produce various molecular fragments. The following definition was used in all the evaluation work:-

$$\eta = \frac{\text{Power absorbed in producing species i, in state j, at rate } \alpha}{\text{Voltage x current drawn}} \qquad 6.1$$

Using this definition, η is dimensionless, since species i and state j define the energy absorbed (J) (eg. Figure 6.8 for N_2) while the rate at which this process occurs gives the final units of Watts ($J\ s^{-1}$).

This definition is important since the plasma itself is unlikely to be in complete thermal equilibrium and at best a local thermal equilibrium exists within the central core of the arc channel depending on the critical electron density (45). The efficiency as defined in equation 6.1 was therefore determined experimentally for a number of operating conditions by applying a detailed steady state - steady flow thermodynamic analysis to the experimental system shown in Figures 6.16 and 6.17 which determined α, while spectroscopic studies identified i and j.

The need to carry a supply of a monatomic gas clearly detracts from any practical viability of these plasmas, and when considering the use of a highly ordered energy form such as electricity with combustion, any effect that tends to lower η must be minimised.

DESIGN

The final design of plasma generator described in this chapter was the result of considering the fundamental weaknesses of previous designs and identifying how these weak points could possibly be removed by taking into account all possible design variables such as electrode configuration, arc length, arc guidance, rotation frequency, magnetic field, operating powers and operating gaseous medium, to try and produce a design with low electrode erosion/contamination, low electrode cooling losses and no carrier gases, thus generating maximum values of η.

The most sophisticated plasma jets used in the work summarised above employed a pointed cathode (usually of thoriated tungsten, even papers devoted entirely to plasma jet design (260, 319) used a pointed

cathode) surrounded by a water-cooled anode and were provided with a circumferential solenoid. The axial component of the magnetic field produced by the latter interacts with the radial component of the current, causing the DC arc to rotate at high speed about the central cathode. This helps to heat the gas uniformly, generates swirl and turbulence and minimises anode erosion. However, it does not cause the central cathode spot to move in any organised fashion. Melting tends to occur at the pointed cathode tip and the achievement of a compromise between rapid consumption of the cathode and maintaining the cathode spot at a sufficient temperature for plentiful electron emission is made difficult, in the case of gases such as oxygen and hydrogen, by electron attachment, as well as lowering of conductivity due to dissociation of polyatomic gases, especially nitrogen. It is the consequent impairment of arc stability that has necessitated admixture of large amounts of argon or other monatomic diluents in the past. Because these gases only have translational and ionisation degrees of freedom available (with first ionisation energies of gases used in plasma applications being high eg. Ar and He are 15.759 and 24.587 eV, respectively, (Tennent)) higher temperatures are attainable with these gases present to help stabilise the arc.

That is not to say that these jets may not be run without these noble gas additives, but the powers required are far too high and efficiencies too low for practical consideration with combustion systems.

In order to understand how these difficulties were overcome in the present design it is necessary to appreciate what is required of the unit and how these requirements influenced the design. The design constraints applied with only minor modification to the main feedstocks considered ie. hydrogen, hydrocarbons or nitrogen.

Plasma jets operating on nitrogen/hydrogen gas are commonly used in spraying and cutting applications with power inputs typically 40

to 100 kW (222, 223, 224). The author was interested in low overall power inputs (typically 500 Watts) with high electrical efficiency without electrode erosion/contamination. (The selectivity defining the efficiency.)

ELECTRODE CONFIGURATION

i) Cathode - As one can see from Figures 6.2 and 6.3 the basic construction differs fundamentally from previous designs of plasma generator, in that the pointed cathode has been replaced by one that is plane ended in the proximity of the cathode spot. The geometry near the spot may be considered as the solid of rotation formed when an initially pointed cathode is tilted (such that a line bisecting the cone angle of the tip intersects the anode surface at right angles) and rotated through 360 degrees about the axis of symmetry seen in Figure 6.13.

This geometry therefore enables both the anode root and cathode spot to rotate synchronously about their respective paths under the influence of a magnetic field. The features that are required of the pointed cathode, namely adequate heat conduction away from the tip to avoid melting from positive ion bombardment heating, and a point of convergence of lines of electric field intensity are still present. At any instant during rotation of the arc about the cathode, the spot would be located on a point, the exact location of which on the active cathode surface, would be changing continuously at a rate dependent on the rotation frequency.

Figure 6.1 shows the fundamental philosophy of the cathode design, from the sculpture of Mussolini. The tip of the nose may be regarded as an early pointed cathode tip, and rotation about the axis of symmetry through the head has resulted in a solid of rotation so that to an observer walking around the sculpture the geometric property of the nose is always recognised in any position. The exact location of

the nose, as observed, is changing at a rate determined by the pace of the observer around the sculpture (the observer has no knowledge of his speed from observation of the nose tip alone).

In short, therefore, it is only the geometric property of the tip that is important for the cathode, provided sufficient electron emission may be maintained. In so far as this electron emission is determined thermally, the integrity of the tip will be assured provided the heat transfer to the tip is optimised to assure no erosion during heating for thermionic emission. Field emission from the cathode, however, would ensure that the 'essential' heating loss to the cathode was not required and thus releases a new degree of freedom into the rotation frequency, as well as further lowering cathode erosion, thus increasing efficiency.

The further design features that need to be specified are therefore the geometry of the anode, arc characteristics, operating pressure, rotation frequency, feedstock and coolant flows as well as operating powers. It is difficult to deal with each of the features individually since they are not independent properties and the values chosen were the results of experimental and numerical optimisation, the interelations will be highlighted separately.

ii) Anode - In order to keep electrical efficiency high, all forms of energy losses have to be minimised. This includes losses to carrier gases as well as cooling of electrodes and non-specific modes of excitation. The properties of both the electrodes are therefore very important, excitation within the arc is the raison d'être of the generator and species produced there must be delivered to the downstream area without recombination losses both within the generator and subsequently. Recombination on the anode surface will automatically constitute a lowering of efficiency as defined by equation 6.1 and the disso-

ciation energy deposited at the anode necessitates extra cooling to avoid erosion that recombination hot spots generate.

The optimised form of the anode as shown in Figure 6.2 is therefore convergent - divergent (flow through apertures and such arrangements having been used extensively in molecular beam work (144)) and constructed of material with a low recombination coefficient and high thermal conductivity, such as copper. The importance of the different relative abilities of surfaces in recombining, as well as reacting with atoms and radicals has long been known, and was used in early 'mirror removal' tests (335, 364) to demonstrate the reaction of metal surfaces with these entities. If radiation from the arc is required (eg. Figure 6.3) the anode material may be chosen with regard to the wavelength desired (as will be seen later, arcs of about 300 microns proved to be optimal; short arcs further aiding efficiency by keeping the arc surface area from which radiation escapes, lowering efficiency, to a minimum. Energy transfer modes involving radiative properties are significant for polyatomic plasmas (401)).

The values of r and d were determined by the operating conditions. However, the anode with a threaded construction means the same generator may be used for a variety of pressure applications by readily interchanging the anodes. (Generally for very low pressure applications, since the cathode diameter is normally 0.5 mm larger than 2r, (Figure 6.2) the cathode may also be interchanged if required.)

The exact anode dimensions depend very much on the actual application requirements, and under some conditions no water cooling is required. A range of optimised design parameters that operated very well from downstream pressures of 6 to 800 Torr are to be found with the List of Figures for Figure 6.2. Depending on the application, critical flow may be desirable both for supersonic species quenching

and for protecting the arc from downstream pressure fluctuations.

iii) Anode-Cathode Combination - The combination of the electrode geometries as seen in Figure 6.4 ensured that, for small arcs, maximum arc stretch for either of the possible displacements of the cathode spot from the required edge trajectory occurred. It was anticipated from the application of the 'Steenbeck Minimum Principle' (212) that the arc would tend to oppose any constraint that tended to increase its surface area (ie. width or length). Having the half angle, ϕ, at 45°, helps to assure that small displacements lead to the maximum stretch and are therefore opposed, the arc is thus 'guided' around the cathode edge, as can be seen from the micrograph of Figure 6.5.

In order to obtain this record of the arc movement on the cathode the unit was run for several hours at a reduced feedstock flow rate. Normal operation, since it involves negligible erosion, (less than 1/10,000 g after five hours operation combined electrode weight loss) leaves no record of arc movement. The rotation frequency was monitored inductively and a Lissajous figure established using the apparatus shown in Figures 6.16 and 6.17.

Further to this, the minimum distance between the cathode tip and the anode surface is always such that the line joining them (the arc channel itself, if assumed to behave as a small arc spoke) always intersects the anode surface at right angles. As the distance between the electrodes is tuned for specific gases this has, as a further feature, that a small but finely controlled movement of the arc to reduce its length results in the power density being raised rapidly but controllably. The result of this is to generate, in a controllable manner, higher excited states of the atoms required from the feedstock. This feature receives more attention in Chapter 7.

From Figure 6.2 one can see that the arc length = $h \sin\phi$

and that the change in arc length, Δa, with rotation of component M of the generator shown in Figure 6.13 is such that $\Delta a = \text{Sin}\phi / x$ where x = number of threads/unit length of component H.

If $\phi = 45^{\circ}$ and $x = 40$ TPI then $\Delta a = 1.25$ microns/degree of rotation. Naturally ϕ had to be optimised, the value of 45° was the best for maximum stretch, while supersonic expansion and fine tuning would favour smaller angles.

ARC CHARACTERISTICS

It was anticipated before the final electrode configuration was established that the arc length would be much less than 1 mm in length. The requirements of low power, selectivity, high efficiency, no erosion and no carrier gas make this property of the arc a key feature (apart from this being a requirement in arc guidance).

It is well known that generally a linear relationship exists between arc voltage and arc length, as seen in Figure 6.6, due to a relatively constant electric field strength in the arc column. However, as the arc length is reduced to values less than 0.4 cms the voltage falls away from 100 V to zero rapidly. (This may be seen in von Engel, Cobine or ref. 4.)

The operating voltage naturally drops with increasing current and rises with increasing gas flow rate and operating pressure (two parameters needing to be optimised also). In order to sustain arcs in the feedstocks of interest overall field intensities (defined here as operating voltage/arc gap) were anticipated from 10^2 to 10^3 V cm^{-1}, as seen in Figure 6.7, with currents in the range 5 to 30 amps depending on the behaviour of the feedstock in the arc. The current in the arc channel needs to be sufficient to maintain a stable arc without placing too high a thermal loading on the electrodes.

The shape of the arc as a function of gap width has been extensively studied and reported in ref. 4. Also reported was a now well established (Lawton and Weinberg, 5, 93, 154, 166, 167, 267, 315) empirical relationship between arc rotation frequency in a magnetic field and the current I and magnetic field B. This is shown in one form as equation 6.3. For fixed values of I and B the rotational frequency is independent of gap width for values in excess of 2.0 cms. However, as the arc length is reduced below this value, the frequency is a function of the width (4). This arc feature proved to be critical in the final design.

The final arc length that was established was approximately 300 microns for nitrogen ($\pm \approx 200$ microns for other feedstocks) producing ground state (^4S)-atoms. This length will vary depending on exact operating conditions, but it gave the required overall field intensity range at the optimum operating voltage of 50 to 70 Volts and currents of 5 to 12 amps, with values of P_1 up to five atmospheres.

At 300 microns and 50 Volts for example the overall field intensity is 1.67×10^3 V cm^{-1}. This is higher than might be expected from Figure 6.7 at 10 amps operation, due to the strong dependence of operating voltage as a function of pressure. A nitrogen arc for example at 30 Atm drawing 10 amps has an operating voltage over three times that when operating at 1 Atm (Cobine). Arcs in gases susceptible to electron attachment, particularly hydrogen, become very unstable at high pressures. At 100 Atm pressure a hydrogen plasma was stable for less than 10 ms (Cobine), for intermittent operation, with events initiated in less than this time interval, this would not be a major problem. For continuous operation the operating pressure is very important for stability.

OPERATING PRESSURE

Nitrogen is a suitable gas to demonstrate the principle of choos-

ing this parameter. The dissociation and ionisation at atmospheric pressure in arc discharges leads one to expect over 15% dissociation at 6000 K and to be complete at 8000 K (von Engel, ref.177). The dissociation energy for N_2 (to ^4S) is very high, 9.76 eV, (Figure 6.8) so it undergoes appreciable dissociation only at temperatures much in excess of the melting points of the cathode and anode (3680 and 1356 K respectively) and since the main ions in the N_2 plasma are positively charged the cathode undergoes high bombardment heating. The anode suffers severe heating from atom recombination. A further result of the large dissociation energy of nitrogen is that it may also absorb large quantities of energy into vibrational excitation before dissociation occurs. From the point of view of efficiency, as defined in equation 6.1, this constitutes a lowering (this is especially true in microwave sources). The definition shown as equation 6.1 is intentionally severe on the generator because it relates to the production of atom/radical species of importance in this work. However, if the efficiency were defined simply in terms of the increase in enthalpy of the gas passing through the generator (after equilibration of all the internal degrees of freedom at the final temperature) the definition would not be as severe.

Figure 6.9 shows the equilibrium dissociation data for N_2 (from Janaf) as a function of temperature and pressure. Increasing the pressure from 1 to 5 Atm at 6100 K lowers the fraction dissociated. A high pressure (P_1) in the upstream region of the generator (N in Figure 6.13) is very desirable for high expansion ratios, for quenching into the downstream region P, and stability. However, heat losses to the electrodes would be expected to increase with increasing pressure. The operating optimum was found to be from 2 to 5 atmospheres.

Figure 6.9 may be used to define an effective operating temperature for the unit, based on the following. The gas titration experiments,

that formed the method for determining α in equation 6.1, also enabled a fractional dissociation to be calculated. Knowing the upstream pressure then identifies an effective temperature that corresponds to the fraction dissociated. This is of value only in comparisons between operating conditions. Because the type of arc present in the generator would not be expected to be even close to equilibrium (Venugopalan Vol. I), and small changes in convective velocities of gases relative to the arc have long been known to markedly affect the temperature (405), such an effective temperature is an empirical mean value rather than a 'true' value.

ROTATION FREQUENCY

As expected, this was a key feature of the design. The 'variables' that were available to influence this were the arc current, length and magnetic field. The thermal loading on the electrodes has associated with it an optimum frequency of rotation. Thermionic emission from the thoriated cathode is a required feature for stable operation of the arc, in the absence of appreciable field emission.

The frequency was determined purely experimentally; it was anticipated that too slow a rotation frequency would result in too much heating of the respective electrodes, while too high a frequency, while reducing the time available for heating, would not enable sufficient heat dissipation between rotations.

The rotation frequency was established using the basic electrode configuration seen in Figure 6.2 while a 1500 turn electromagnet provided a variable magnetic field that was measured with a Hall Effect probe. The rotation frequency was monitored inductively with a reed coil, using a calibrated oscillator input that generated a Lissajous figure on the x - y plates of an oscilloscope. The further fine tuning of arc separation established a rotation frequency of 200 to 500 Hz as optimal with the feedstocks of interest. It was apparent from the com-

bination of arc current at 10 amps, gap at 300 microns and associated magnetic field in the region of 250 to 300 Gauss that the required frequency could be obtained with the magnetic field from an inexpensive bonded ferrite permanent magnet. By constructing the components C and G (Figure 6.13) out of mild steel, an annular magnet, with field B in the direction shown in Figure 6.2, was held in place magnetically (bonded ferrite is not easy to machine).

The magnet is sufficiently far away from the arc to remain at a temperature below its Curie point. Component G serves to focus the magnetic field along the axis of the generator in a manner that leads to a predominant component intersecting the line of the arc (as seen in Figure 6.2) at right angles to maximise the Lorentz force for rotation.

It is possible to stabilise the arc without G being constructed in a ferromagnetic support material (eg. brass and aluminium were used) however, stronger magnets were required. The final design, as shown in Figure 6.13, has the obvious feature that the anode jet of the generator may be placed in high temperature environments without damaging the magnet or diminishing its strength. (The magnet location may also be moved further back towards, for example component M. Bonded ferrite is also sufficiently non-conducting, at the operating voltage, that it could replace component J which was a perspex plate.)

Not requiring an electromagnet further enhances the overall electrical efficiency as well as enabling the whole construction of the unit to be reduced dramatically in size, as seen in Figure 6.14. (The 50 pence piece acts as a length scale and indicates the price of the magnet!.) Apart from the obvious advantages of size and electrical efficiency, the permanent magnet does not suffer from the disadvantage associated with an electromagnet in that there are no widings to be 'shorted-out' under the influence of the high voltage Tesla coil that was used to initiate the arc.

Photographic records as well as search coil monitoring of arc movements in ref. 4 showed that for the large involute arcs, that exist with lengths greater than 1.0 cms, the arc movement about the anode is far from uniform. There was a periodicity with respect to rotation, however, each rotation is characterised by the anode root 'sticking' on the anode surface and 'jumping' from one arc location to another around the circumference of the anode.

Such arc movement was not seen in the experiments reported here due to the fact that the arc length was small, and the arc was able to move uniformly along its preset trajectory, (some very high frequency electrical noise (kHz) was removed with a capacitor). Non-uniform movement would be disadvantageous for electrical efficiency because of overcooling of hot spots, at either electrode, generated by the arc 'sticking' there. The photographic history of the arc rotation refinement sequence in the experiments is shown in Figures 6.10 to 6.12.

OPERATING POWERS

The powers readily accommodated by the generator are from 250 Watts to 1500 Watts. This is determined by the required operating conditions. The generator operated for several hours with minimal electrode erosion as explained previously. An open circuit voltage across the generator of at least 220 Volts is required for Tesla coil starting. In stable operation typical values of voltage and current would be 60 Volts and 10 amps.

A standard 3 phase, 6 diode (RS261-542, 600 V, 26 A) full wave rectified power supply was built with a split 9 ohm resistive load as seen in Figure 6.17. Previous work had shown that lead-acid batteries provide a very stable power supply as well as 'smoothing capacitors' for continuous operation. It was anticipated for some of the spectroscopic work that, along with a smoothing circuit, a current regulating circuit might be required. A standard 6 transistor (2N3055) control

unit was built. However, the extraordinary current and rotation stability of the generator meant the regulating circuit was not required.

STABILITY

As mentioned previously, equilibrium within the arc may not be assumed. Graphs of Enthalpy - Temperature (T-h) data for various gaseous feedstocks particularly, hydrogen and nitrogen, are to be found in many publications, including some dealing with plasma welding or cutting (eg. 219, 222, 223, 224). The effects of ionisation and dissociation are readily apparent in lowering the equilibrium calculated temperature. Spectroscopic studies were particularly important therefore, to identify the energy levels of species produced, in order to estimate the unit efficiency.

A number of gas titration techniques exist for both H and N-atoms (see for example Mulcahy, McTaggart, Venugopalan II and Wolfrum. Reported uses of photometric assays, especially for nitrogen are also reported in refs. 34, 186, 199, 243, 257, associated with interest in studies directed towards the N_2 recombination afterglow (78, 292, 410)).

To determine the efficiency of the generator(to obtain the data for the components of equation 6.1)required the units stable operation for several hours of gas titrations to estimate the number of $N(^4S)$-atoms generated per second to determine α. Both a photometric end point and a novel method involving a highly accurate volumetric end point were used in establishing α. (A typical gas titration curve is shown in Figure 6.19.)

The photometric gas titration produces NO* with strong emission in the blue (see for example Figure 6.20a). The generator was sufficiently stable with a high enough rate of production of N-atoms (typically 10^{20} to 10^{21} s^{-1}) that all of the reported bands (Pearse and Gaydon) of the NO emission spectrum within the range 2000 to 8000 Å could be recorded photometrically in one experiment.

Figure 6.18 shows one peak from a low resolution spectrum of the NO*β system ($B^2\Pi \longrightarrow X^2\Pi$) expanded to enable the rotational fine structure to be resolved. The line of maximum intensity corresponds to the R head of the 0, 8 (v' v'') transition of the β system. For better dispersion this spectrum was obtained using a 3000 Å grating in the second order. The marked neon calibration lines (6383.0, 6402.3, 6506.5, 6532.9, 6599.0) were obtained from an identical spectrum with a neon source superimposed and recorded at the same time using the grating in the first order.

Greater details of the spectroscopic work are reported in Chapter 7. Figure 6.18 shows how stable the unit was in operation with sufficient atom flux to enable a direct photometric recording.

FEEDSTOCK FLOWS AND COOLING LOSSES

The generator can accommodate gaseous flow rates within the range 100 to 700 ml s^{-1} (measured at 20°C and 1 Atmosphere). Water cooling requirements depend on the application and details of the anode dimensions. Generally an optimum exists between expansion ratio set by the application pressures and surface recombination losses through the anode. Under the worst conditions of water cooling (lowest pressure application was 6.0 Torr) 45% of the electrical power was lost to the electrodes. Under most atmospheric pressure applications the water cooling loss was less than 20%, and with an anode orifice diameter of 2.5 mm and at 500 ml s^{-1} of N_2, it was possible to operate with no water cooling at all. In all the early experiments the units were over-cooled, not because of electrode cooling requirements, but due to initial failure of rubber O ring seals, before silicon-rubber ones were used.

EXPERIMENTAL

The basic apparatus for the thermodynamic analysis are shown

in Figures 6.16 and 6.17. The spectroscopic work that identified i and j of equation 6.1 involved installing 4 quartz windows to arms on the pyrex tube. Radiation was focused onto the entrance slit of a 0.5 m Ebert mounted, Jarrell-Ash scanning monochromator with a quartz lithium fluoride achromatic triplet lens. Radiation from the exit slits fell on an EMI 9529B photomultiplier tube, chosen because of its wide spectral response.

The signal to noise ratio was sufficiently large that no cooling of the PM tube was required. The tube power supply was a Harrison 6516A DC unit. The output was displayed on a DVM and recorded on a paper chart recorder.

For the photometric gas titration experiments a yellow/green filter and slits were fitted to the PM tube instead of a monochromator.

Because of the difficulties generally associated with efficient production of N-atoms, as well as their specific importance in combustion (especially their reactions with hydrocarbon fragments to generate H-atoms along with NO and soot removal) the experimental section will deal mainly with the N-atom titration experiments. It should be stated that the generator operates very efficiently on hydrogen and hydrocarbon feedstocks also (propane, ethylene and methane have all been used successfully). See also Figure 6.20.

All the spectra associated with the $N(^4S)$-atom titration experiments; the N_2 yellow recombination first positive afterglow, the NO β and γ systems and the NO_2 yellow/green continuum were readily obtained (along with other spectra associated with higher levels of excitation) and compared with spectra in the literature (Pearse and Gaydon, refs. 218, 382).

In order to improve the accuracy of the titration technique, and to make the apparatus suitable for estimating higher atomic states, the

exhaust gas from the apparatus was analysed with a TECO model 10A chemiluminescent NO_x analyser and a volumetric end point determined as well as a photometric one. This modified gas titration, since it involves a straight line intersection, proved to be highly accurate and reproducible, especially at high pressure applications where the photometric assay was not. All the time the N-atom generation rate exceeds the rate of flow of NO molecules into the pyrex reactor the level of NO in the tube was always less than 0.1 ppm. The experimental arrangement shown in Figures 6.16 and 6.17 enabled a range of upstream (1.5 to 5 Atm) and downstream (6 to 800 Torr) pressures to be studied as well as anode geometries.

RESULTS

If	Power consumed by arc (v x i)	=	P Watts
	Moles NO/sec flowing into reactor at end point	=	X_i
	Dissociation Energy of N_2 into $N(^4S)$	=	D_{N_2}
	Water cooling losses	=	$W(J\ s^{-1})$

then equation 6.1 reduces to:-

$$\eta = \frac{D_{N_2}\ X_i}{2\ (P - W)} \qquad 6.2$$

Table 6.1 gives a range of experimental values obtained for the generator.

D_{N_2} was taken as 949.4 kJ $mole^{-1}$

The average arc rotation frequency was 310 Hz

y = N_2 flow rates (ml s^{-1}) at 1 Atm pressure and 20°C

B = Cathode diameter = 3.0 mm

2r = Anode orifice diameter (mm)

P = Power measured in Watts

P_2 = Downstream Pressure (Torr)

E = Expansion Ratio (P_1/P_2)

In the early designs used for the original gas titration experiments rubber O rings were used. Merely as a precaution to avoid all possibility of leakage past these rings over the extended period of measurements for the gas titrations, excessive water cooling was used. This heating loss has therefore been subtracted in equation 6.2 and in the calculations shown in Table 6.1.

TABLE 6.1

P_2	E	2r	P	y	(%)
30	36	2.0	714	480	54.7
100	11	2.0	714	480	47.0
290	8.5	2.0	900	700	28.5
10	76	0.7	780	118	49.2
11	69	2.5	500	100	64.7
760	2.5	2.0	712	480	28.0
760	1.8	2.5	720	520	49.2

Experimental and theoretical relationships exist that predict arc movement properties as a function of such variables as B, i, $\dot{m}$, electrode radii and arc gap (4). For example a relationship for cathode spot velocity, U, with B in Gauss and i in amps is given as:-

$$U = 57\ B^{0.6}\ i^{0.33}\ \text{cm/s} \qquad 6.3$$

Using representative values of B and i from the experiments of 250 Gauss and 10 amps yields a value of U = 3350.0 cm/s. Measured values of optimum rotation frequency were 310 Hz, with a cathode diameter of 3.0 mm this yields an actual spot velocity in the generator of 292 cm/s.

In studies on magnetically rotated arcs that were used mainly for the purpose of bulk heating of gases (215, 216 and references therein) a theoretical relationships was derived for rotation frequency that may be expressed as:-

$$f = \frac{i \bar{B}}{2\dot{m} \pi R_1^2} \quad \text{Hz} \qquad 6.4$$

on the assumption that $R_1 >> R_0$, where R_0 = radius of cathode and R_1 = radius of cylindrical enclosure of anode, ($\dot{m}$ = mass flow rate of cold gas, and $\bar{B}$ is in Wb/m^2). Obviously for this generator that assumption does not hold and quite the reverse is true, ie. $R_0 >> R_1$ (or in the terminology of Figure 6.3ii, B >> a) modifying the derivation of equation 6.4 for this condition leads to:-

$$f = \frac{i \bar{B}}{2\dot{m} \pi B^2} \quad \text{Hz} \qquad 6.5$$

This expression includes a mass flow rate dependence. The generator described in this study has a very high gas bypass and the measured rotation frequency was found not to be a strong function of $\dot{m}$. However, taking as a representative example 1.0 g/s gives a value of f = 440 Hz.

It was not expected that either f or U would agree very closely with the measured values (in fact the agreement is really closer than expected) since in the work used to obtain equations 6.3 and 6.4 the arc gap is much greater than the electrode diameter and 'electrode effects' in the boundary layers, become more important as the arc gap is reduced, these are likely to be very important in this generator.

CONCLUSIONS

A sharp-edged cathode combined with a carefully controlled rate

of arc rotation makes it possible to design a plasma jet with a finely adjustable interelectrode spacing which operates stably over long periods of time and with a variety of gases. It requires no noble monatomic carrier gas, and works well at very high (sonic) flow velocities thereby minimising heat losses to the anode. It can act as an efficient generator of particular radicals and specific excited states and can be used with a supersonic nozzle expansion to help quench these. The compact and inexpensive construction using a bonded ferrite permanent magnet, weights only 600 grams, with the outer casing made in brass for ease of machining. This weight could easily be reduced using a lightweight insulation casing, allowing miniaturisation and making possible its use in various applications previously not available for conventional plasma torches.

Because the final rotation frequency results from the balance of the Lorentz force driving the arc, and the aerodynamic drag forces on the arc as it moves through its own wake; for large arc gaps the behaviour of the arc is therefore as an involute (4), and under these circumstances the length of the arc is not equal to the arc gap. As was stated earlier, from ref. 4, the final rotation frequency is a function of the gap width (and arc shape). In this generator, because the arc has been reduced in length, the behaviour is more like that of a spoke, in that respect it has been 'streamlined' with respect to an involute. Although the optimum frequency in the present work was about 300 Hz, there was some evidence, from the Lissajous figures, that with this type of small arc rotation frequencies very much higher than this may be achieved, (if desired for a particular application). Subject of course to the thermal properties of the electrodes, and constitution of the plasma being compatible with very high rotation rates, stable operation may be obtained.

The plasma constitution is very important with respect to the tuning and operational stability of the generator. In noble gas plasma, and those containing nitrogen, the predominant ions are positively charged (Venugopalan) and require lower longitudinal fields than those species susceptible to producing negative ions such as oxygen, hydrogen and hydrocarbons. Thermionic emission aided by bombardment of heavy positive ions helps to sustain the cathode. The nature of the plasma will also modify the positive ion space charge in the cathode voltage drop region which is the determining region for field emission. The exponential dependence of thermionic emission with temperature leads to appreciable currents only at temperatures close to the melting point temperature of the cathode and makes field emission highly desirable to keep erosion levels low. Increased field emission may also remove a constraint on the rotation frequency.

The very low levels of erosion and high stability (especially with nitrogen; N_2 has generally been the most difficult plasma to maintain (Chapter 4)) shown by this generator is strong evidence that field emission as a component of arc stabilisation is present.

The possibility of field emission stabilisation was anticipated as a possible design feature. However, overall field intensities used in the generator of 10^2 to 10^3 V cm^{-1} were three orders of magnitude too low to anticipate a significant field emission (Cobine). However, it is the cathode drop region that determines the effective field intensity at the cathode tip and this region is very much smaller than the length of the arc gap and could lead to values closer to 10^6 V cm^{-1}. Using nitrogen, and conditions similar to those of the experiments described here, the voltage drop region was estimated at 6×10^{-5} cm (Cobine). The presence of thorium and the sharp edged cathode would further aid a possible field emission stabilisation component by giving rise to a

local increase in positive ion space charge, further increasing the effective field strength. Such possibilities are worth investigating, along with ways in which the anode may also act to stabilise the arc (additions of radioactive material for example) so that it may operate in a role other than species quenching.

The small size of the arc in the plasma generation region makes conventional solid probe techniques difficult (see Bibliography and refs. 58, 60, 88, 89, 395). Extraction of the radiation as seen in Figure 6.3 may be of use for in-situ studies on excitation processes.

A general review of possible uses of low temperature plasmas based on previous designs is in the Literature (269). Uses for carburising of metal components with hydrocarbons are also reported (164, 165), this design differs fundamentally from all previous designs of plasma generator and makes it of use both in academic and practical studies.

Arc heaters have been used previously in academic studies (41, 475). Devices have also been reported specifically for generating small ions (37, 460), and numerous patents exist for various processes involving continuous discharges (for example ref. 470) and have been reported at Symposia (for example refs. 241, 360, 399, 470, 472, 473). The common electrode materials are normally copper and tungsten. However, in the very early Wood's tube Aluminium electrodes were used (466).

Difficulties with electrode contamination and erosion has favoured the use of various 'electrodeless' discharge arrangements which are inductively coupled to the plasma. Either an 'E-Type' or an 'H-Type'. The E-Type include microwave discharges where excitation comes from a high frequency microwave source, eg. 2.45 GHz (113, 133) acting as a diathermy unit with a cavity normally tuned into resonance. The H-Type uses a solenoid at RF frequencies (eg. 35 MHz ref. 360)

where the plasma is maintained by Joule heating resulting from its behaviour as the short circuited secondary winding of a transformer, with the RF lead acting as the primary. Such discharges have been used in combustion studies (232).

Generally microwave units are used in academic studies involving atom generation (for reviews see 194, 226, 384) with atoms generated from subsequent reactions often the principal ones for study (241). Both types of discharge have very high gas bypass and the electrical efficiency of atom production is low. Both are extremely sensitive to the nature of the surface of the containing vessel.

For nitrogen atom production such types have very high amounts of energy partition into bulk thermal heating, although it is possible to improve N-atom production by the inclusion of a sensitiser, notably SF_6 (474). While there is some evidence of various different electronic states being produced in 2.45 GHz sources with oxygen (ie. $^1\Delta g$ ref.113) it is unlikely that, due to the difference in the mode of excitation, that the tunability present in the generator described in this chapter (ie. to go, at will, from the condition that leads to the emission seen in Figure 6.20a, to that seen in Figure 6.20d) would be found with microwave sources.

As a final conclusion, the generator shown diagramatically in Figure 6.13 has solved all the problems generally associated with arc discharges, as well as having characteristics that make it superior to inductive systems generally used hitherto because of electrode contamination problems. The result is a design of generator that is superior for a number of practical as well as academic applications.

Initial experiments indicated that the power supply shown in Figure 6.17 may be replaced by batteries, with a reduced ballast resistive load. However, a separate capacitive discharge circuit in combination with the Tesla coil would be required for initiating the arc.

Having demonstrated the efficiency of the generator, improvements in the efficiency of the power supply, to avoid dissipating an equivalent amount of power in the ballast load, would be an obvious next step for practical application.

Another feature for practical application is the powers required for pumping feedstock gases. With an arc of only 300 microns in length, rotating at 300 Hz, it is evident that most of the gaseous feedstock to the plasma generator actually bypasses the arc. For the applications considered with this device (ie. selective production of species, rather than bulk thermal heating of all the feedstock) this is advantageous for increased electrical efficiency, as described by equation 6.1. However, for practical application, consideration needs to be given to the total power requirement, which would include the power required to pump gases to the generator.

The reason a high gas bypass of the arc improves the species generation efficiency, is that when the species are generated by close contact with the conducting channel, they are admixed with a vast excess of undissociated gas, and the probability of atom-atom recombination by collision, prior to the desired reaction, is significantly reduced. This has effectively increased their mean free path and hence lifetime with respect to recombination losses. For a single component diatomic feedstock, an atom-molecule collision will result in no loss of atoms.

To calculate what percentage of the feedstock comes into contact with the conducting channel requires some assumptions. Firstly an arc thickness has to be assumed, and then the assumption that the gas expansion on approaching the arc, causing an overflow of the conducting channel, does not occur to any significant extent. Lawton and Weinberg state that the general condition for a gas flowing at linear velocity, v, to experience the passage of the discharge at least once,

is given by $w > 2\pi v/d$ where w = the angular velocity and d = the 'effective' arc channel thickness. This condition is not met by this generator, and it is evident that less than 1% of the gas flow would come into 'contact' with the arc with an assumed thickness as large as 1 mm.

The percentage dissociation of nitrogen measured in these experiments was between 1 to 5% of the total feedstock flow rate. This is higher than might be expected with such a high gas bypass. The reason for that is only speculative at this stage, but may be due to 'up-pumping' of vibrationally excited molecules passing through the convergent-divergent nozzle of the generator, thus leading to dissociation on expansion. This type of process is considered in ref. 80, and will be strongly influenced by the operating pressures.

Calculation of the total gas pumping power to a generator of this sort, may be estimated as follows:-

$$\text{Pumping Power} = \dot{W} = \dot{m}\Delta H_{act} = \bar{C}p(\Delta T)_{act} \qquad 6.6$$

The pumping will be done by a compressor with an isentropic efficiency defined as follows:-

$$\eta_c = \frac{(\Delta H)_s}{\Delta H_{act}} \qquad 6.7$$

$$\dot{W} = \frac{\dot{m}(\Delta H)_s}{\eta_c} = \frac{\dot{m}\ \bar{C}p\ (\Delta T)_s}{\eta_c} \qquad 6.8$$

Using as an example Nitrogen gas, initially at 1 atm and 300 K, delivered to the generator at 5 atm. For adiabatic, isentropic compression:-

$$T_2 = 300(5)^{0.4/1.4} = 482.8\ K \qquad 6.9$$

$$\therefore (\Delta T)_s = 183\ K$$

To a first approximation $\bar{C}p = 1.0$ kJ kg^{-1} K^{-1}. Using a representative flow of $N_2 = 1.0$ g s^{-1} then $\dot{W} = 183/\eta_c$ Watts.

A representative figure for η_c would be 0.75 to 0.8 (Rogers and Mayhew), so that pumping powers of 250 W per unit could be anticipated. This value is nearly half that of the electrical power dissipated by the arc.

From these calculations it is evident that the pumping powers will not be insignificant. This will not necessarily preclude the use of these units for practical application and this will be determined by what overall gains may be expected.

It would not be unrealistic to imagine, for example, a CH_4 plasma generator firing a large natural gas two stroke pumping engine. There, the high pressure CH_4 feedstock is already available at the engine. Such engines have severe difficulties meeting emission standards (461) and a fast, lean-burn solution would be very advantageous.

There have been developments in non-cryogenic separation schemes (see also Appendix 1), which would provide high pressure O_2 as well as N_2 gas streams. The positive effects of O_2 enrichment in Diesel engine operation have not been fully explored, and a hybrid of an O_2 enrichment and N_2 plasma could provide a hybrid for low soot and NO_x emissions. Naturally, the pumping powers will always need to be considered in the total energy calculations, but they may not necessarily rule out practical use. This will depend on consideration of all the potential gains that the plasma generator could make available.

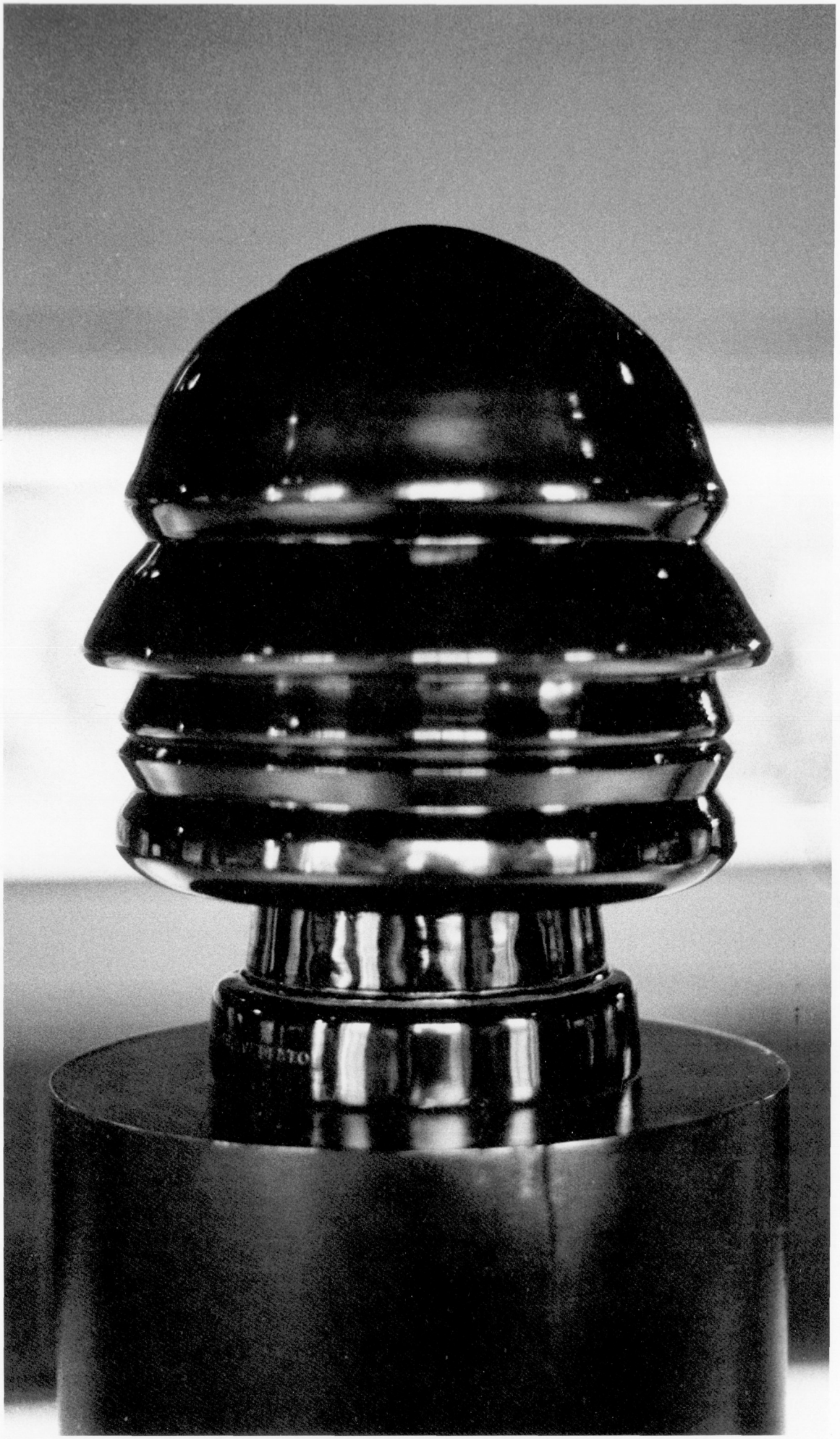

Figure 6.1 - Bertelli's Mussolini

Figure 6.2 - Fine detail of cathode-anode arrangement

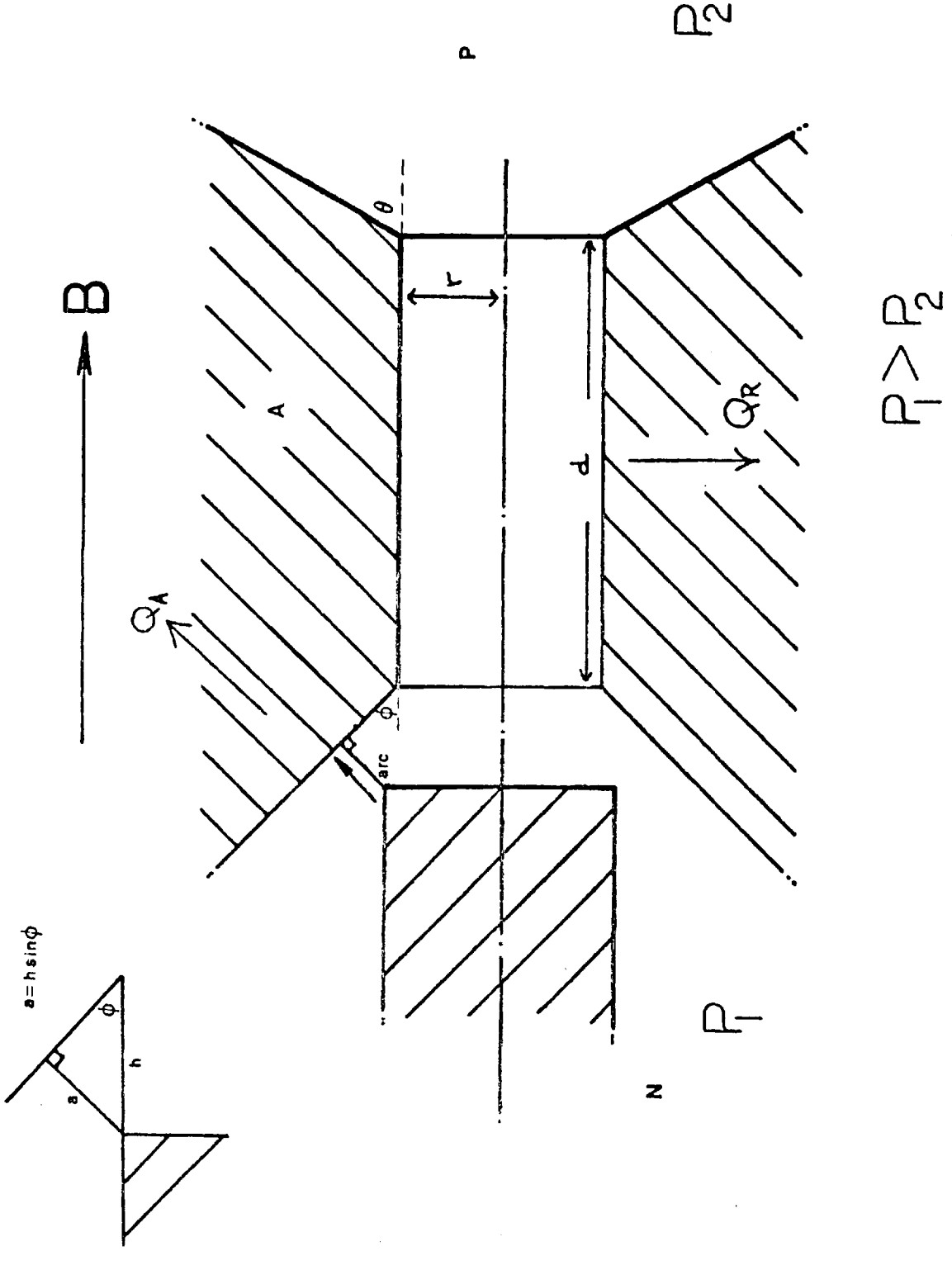

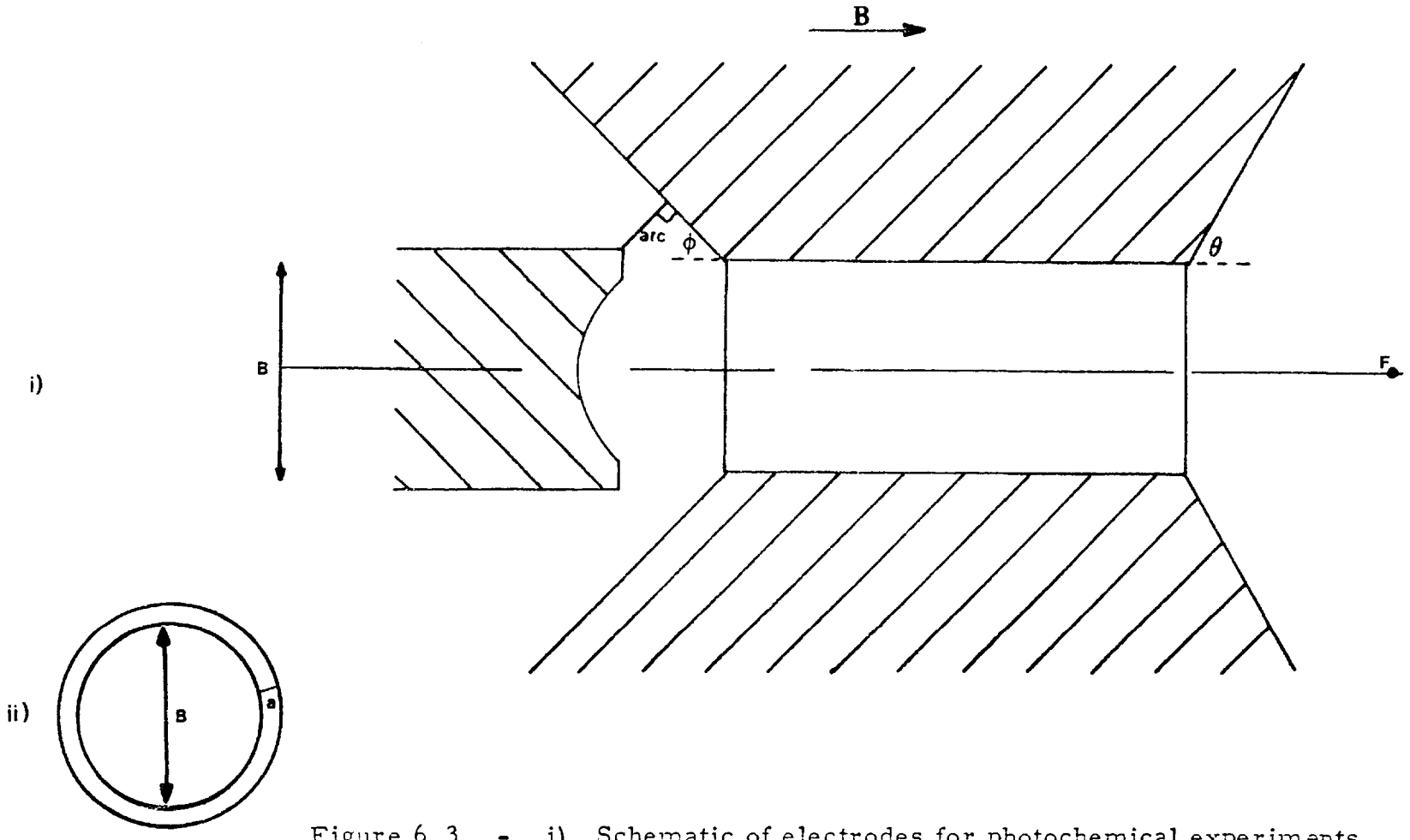

Figure 6.3 - i) Schematic of electrodes for photochemical experiments
ii) Cross section of electrodes indicating anode root and cathode spot trajectories.

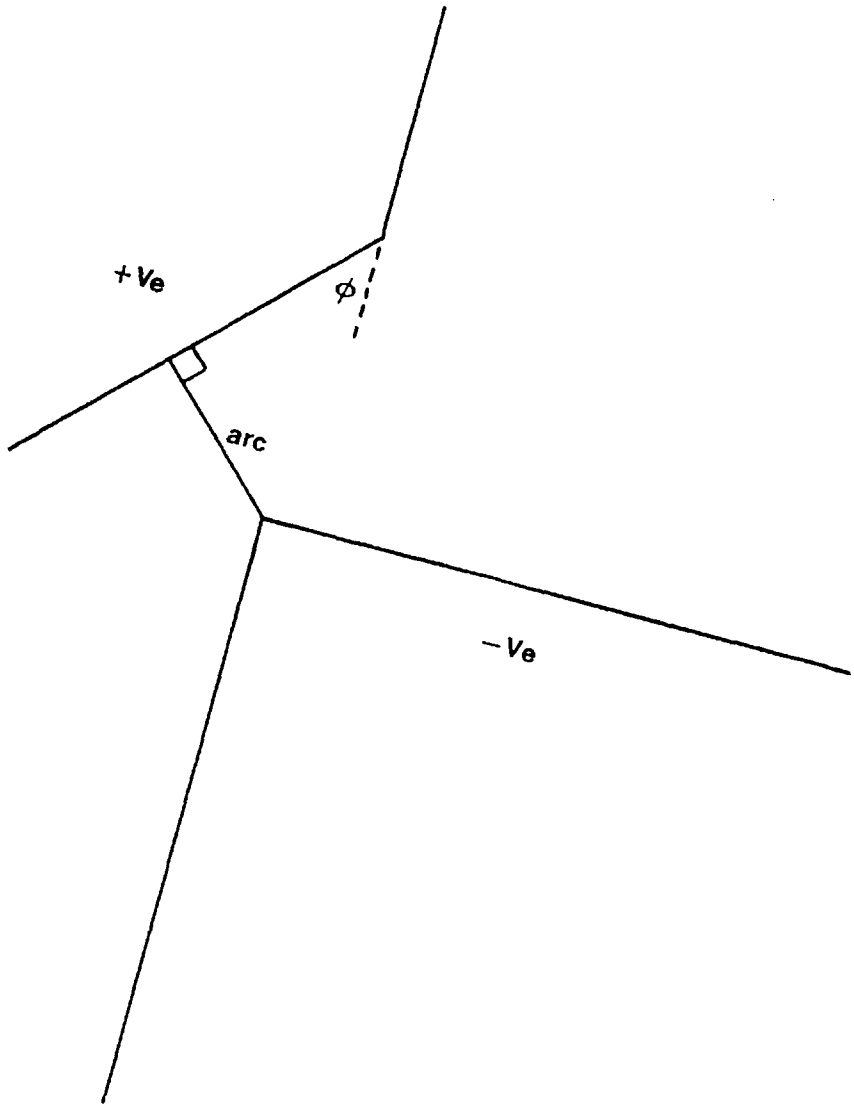

Figure 6.4 - Schematic of maximum arc stretch that occurs with deviation from preset trajectory, a result of the combined electrode geometry.

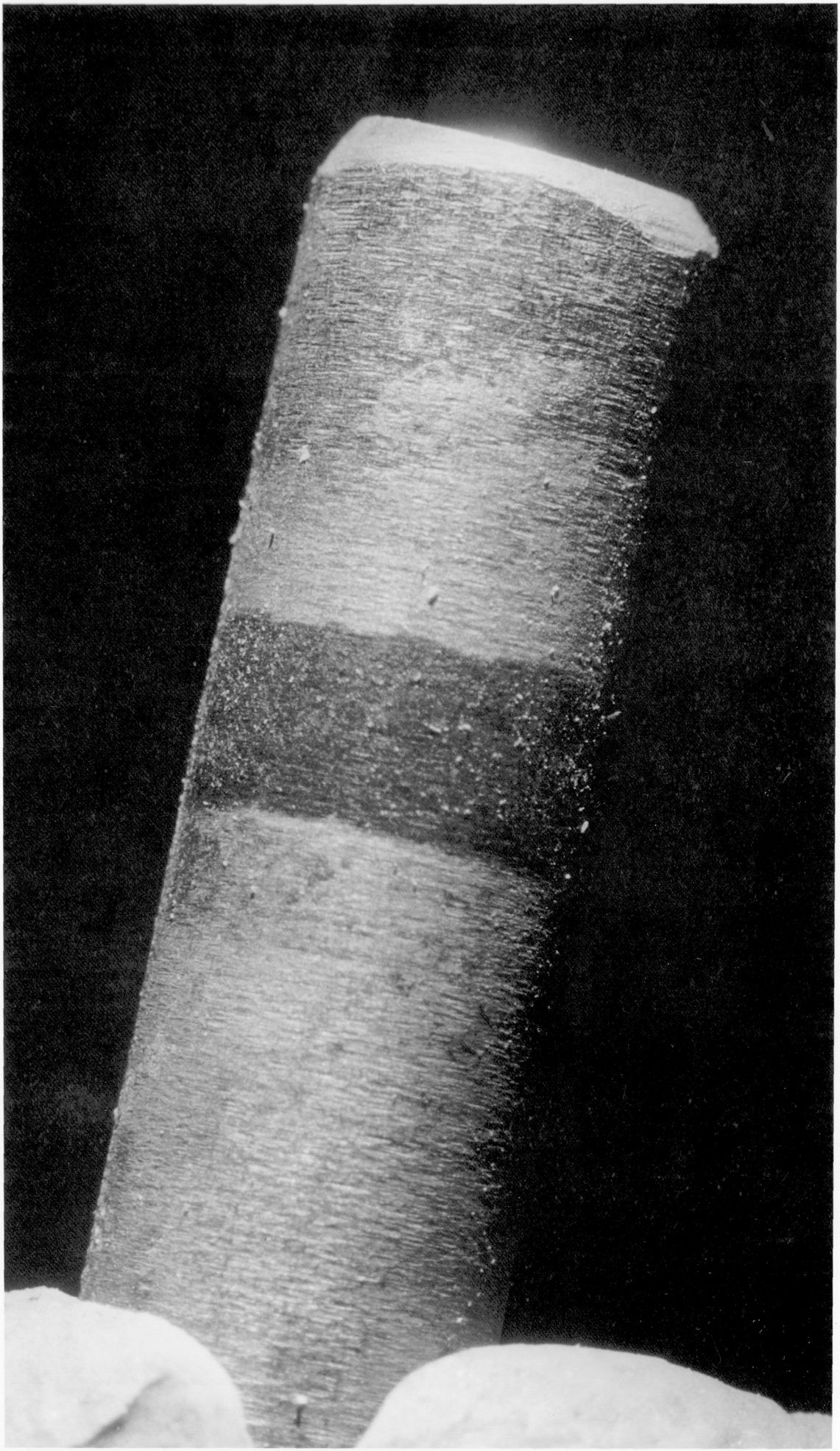

Figure 6.5 - Cathode micrograph

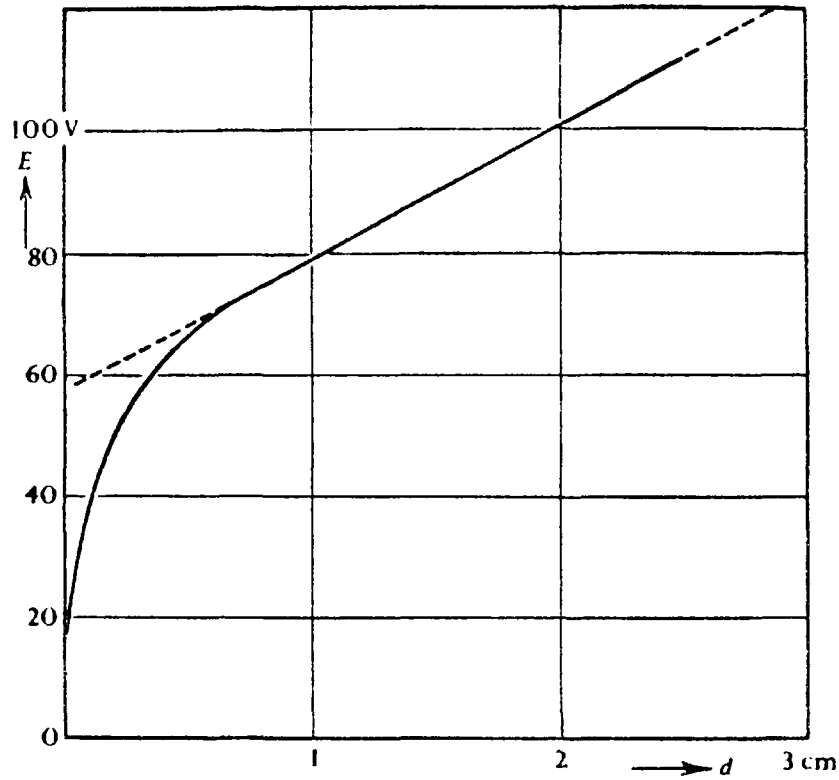

Figure 6.6 - Arc voltage as a function of separation (from von Engel, p261)

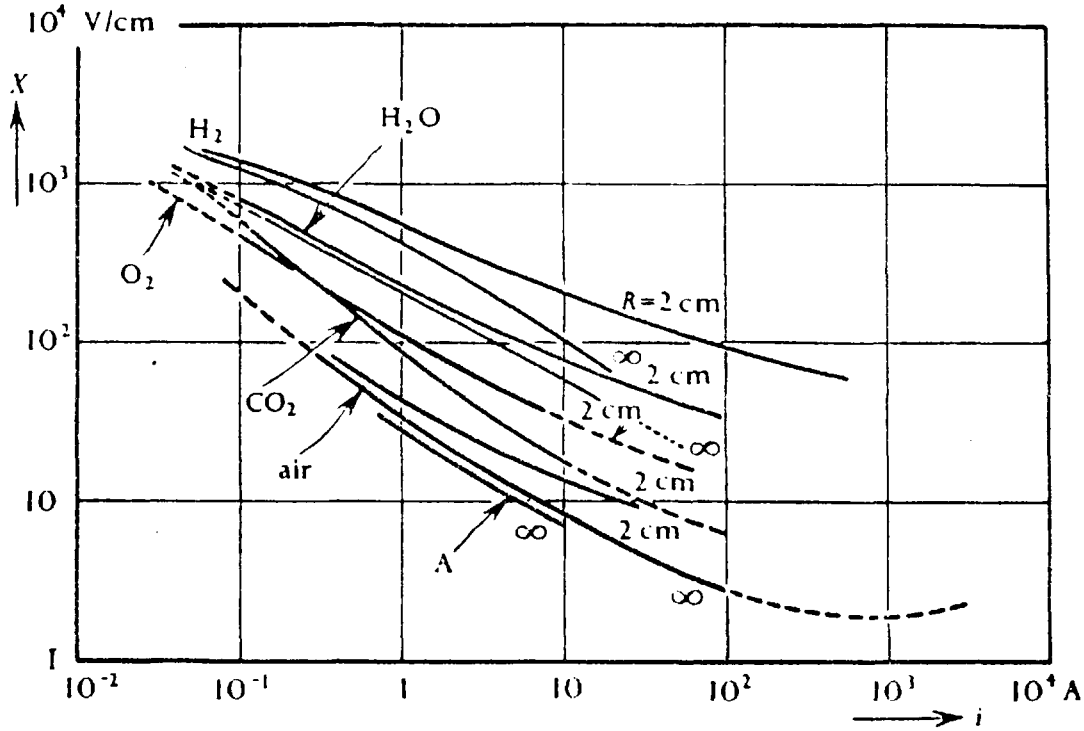

Figure 6.7 - Longitudinal component of electric field as a function of current at 1 Atmosphere for different gases. (from von Engel, p262)

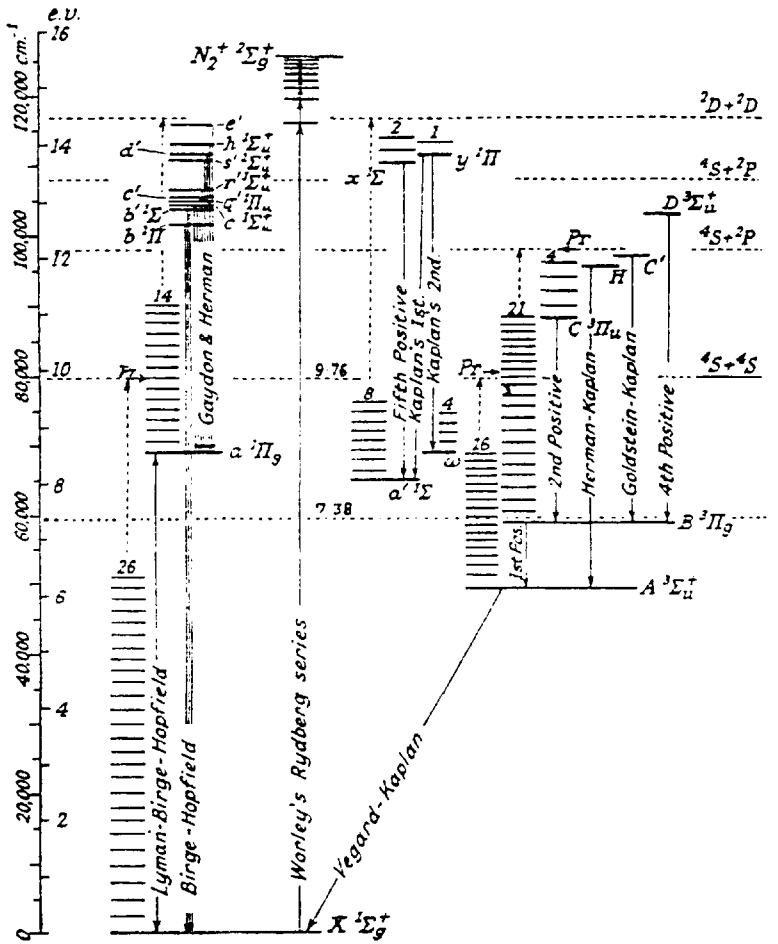

Figure 6.8 - Energy level diagram for Nitrogen (from Gaydon, 1968, p188)

Figure 6.9 - Equilibrium fractional dissociation of nitrogen into ground state (^4S) atoms as a function of temperature and pressure.

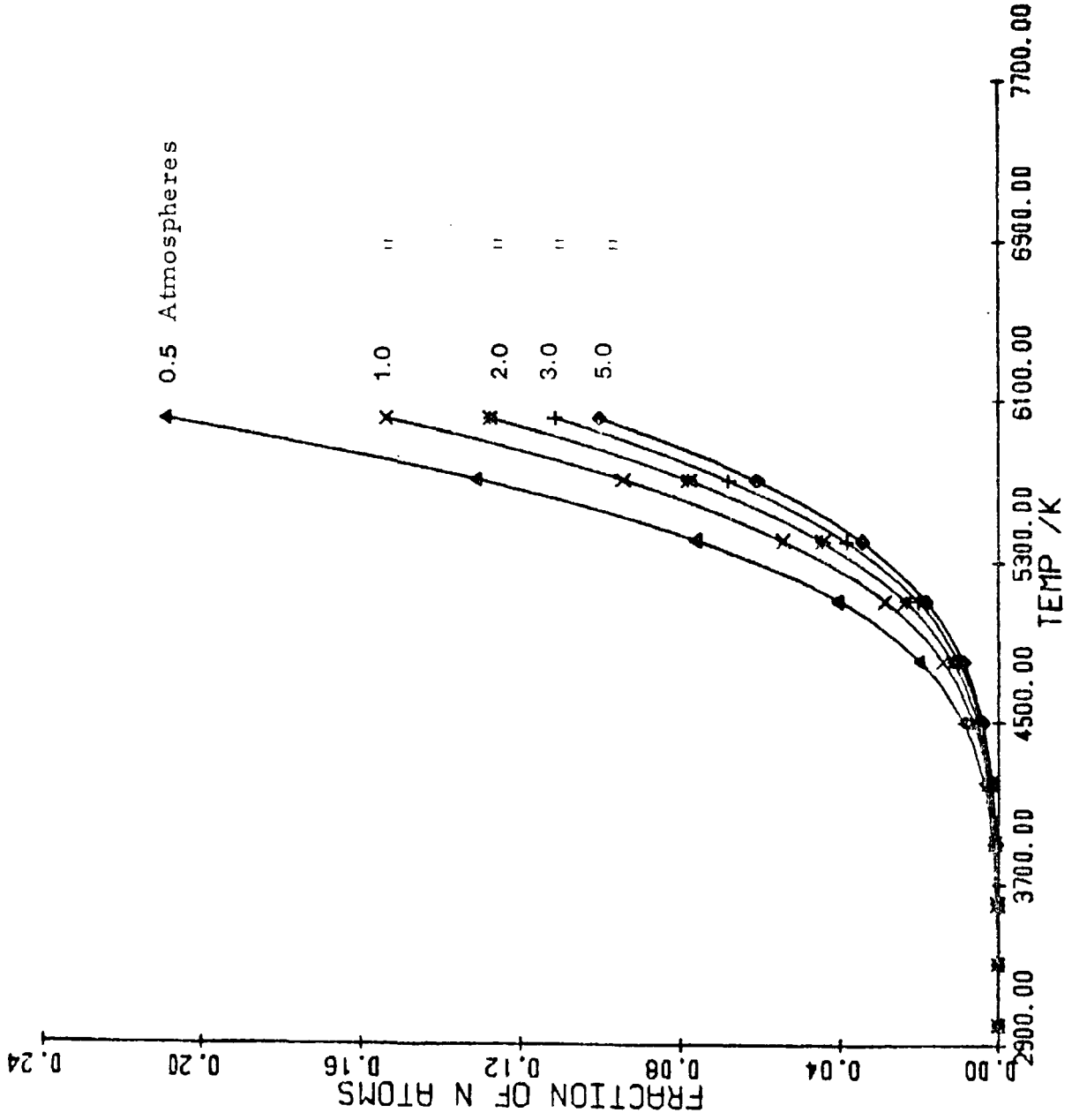

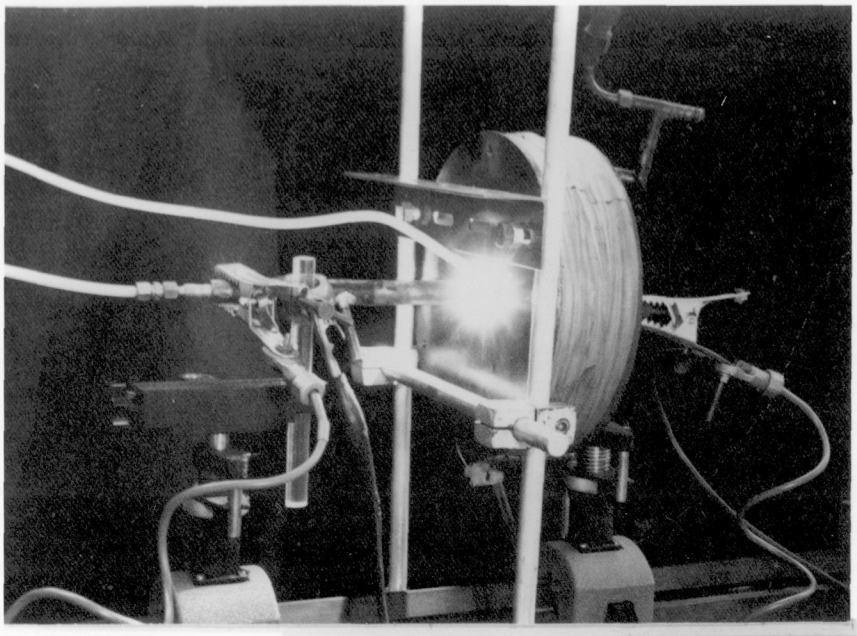

Figure 6.10

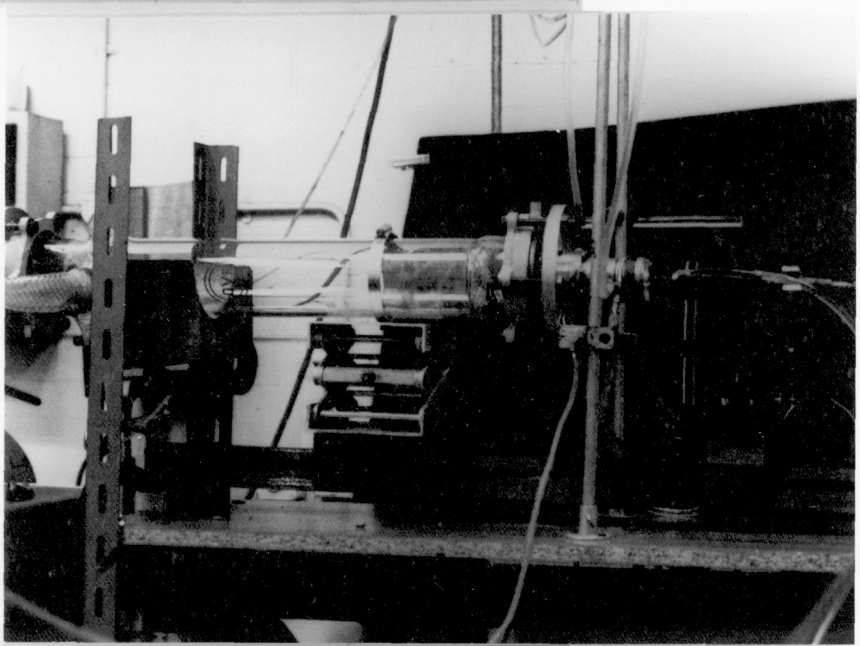

Figure 6.11

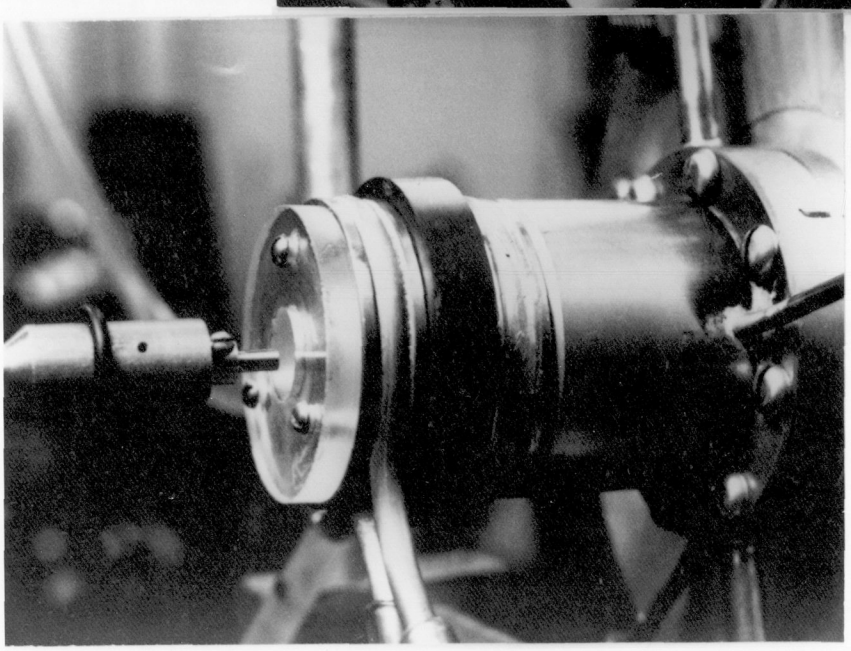

Figure 6.12

Figures 6.10-6.12 - Sequences in rotation rate refinement (see also list of figures)

Figure 6.13 - Schematic of the final construction

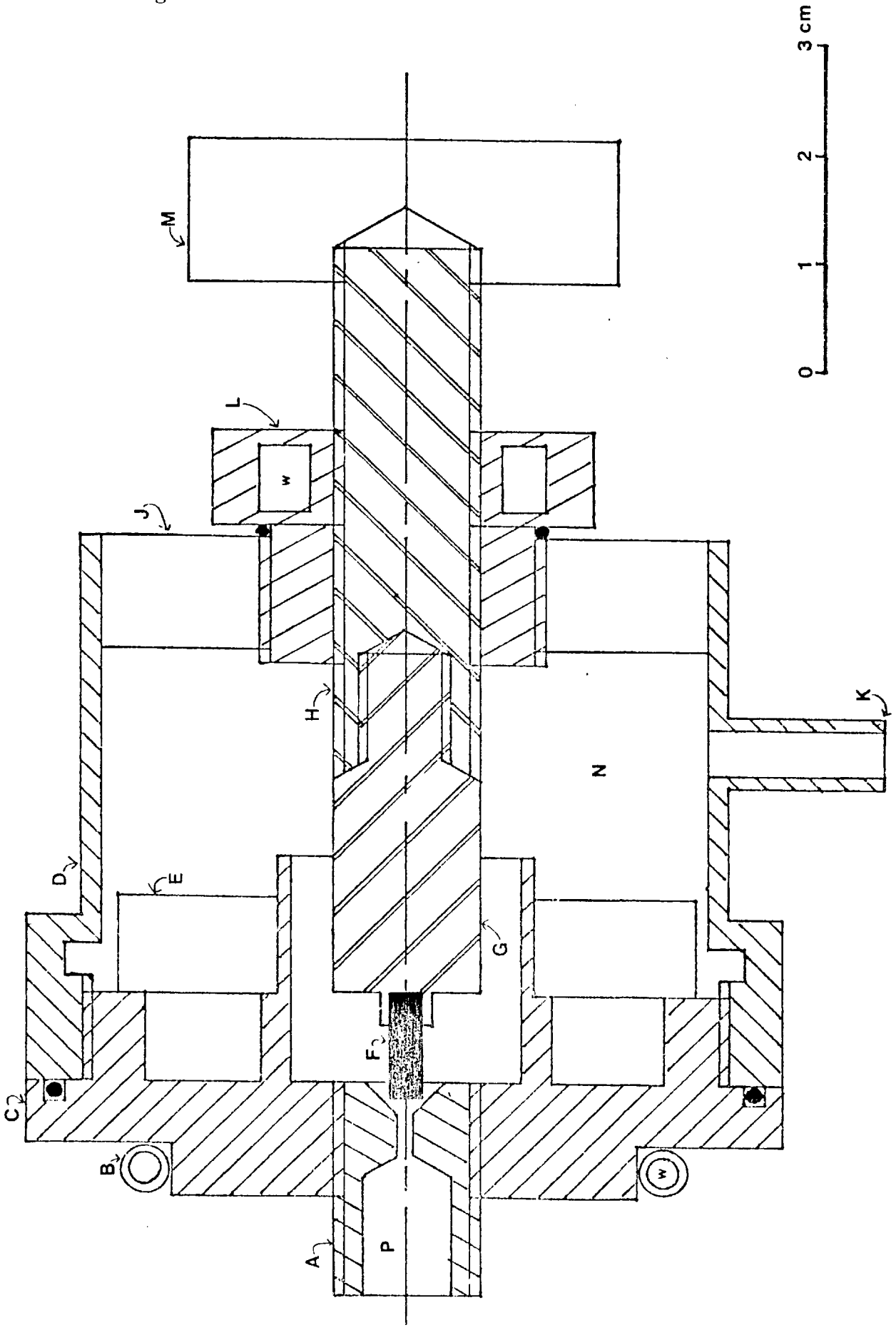

Figure 6.14

Figure 6.15

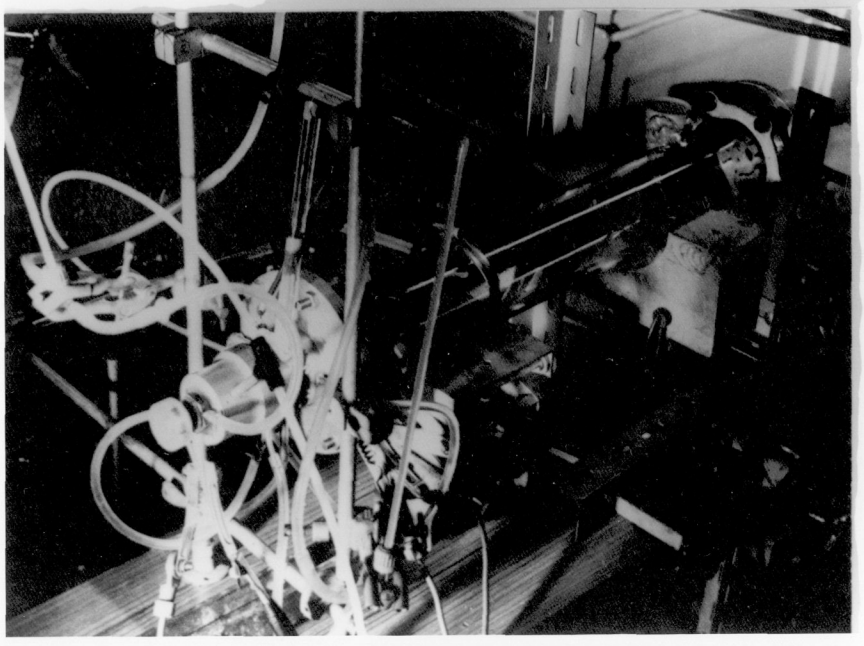

Figure 6.16

Figures 6.14-6.16 - See list of figures

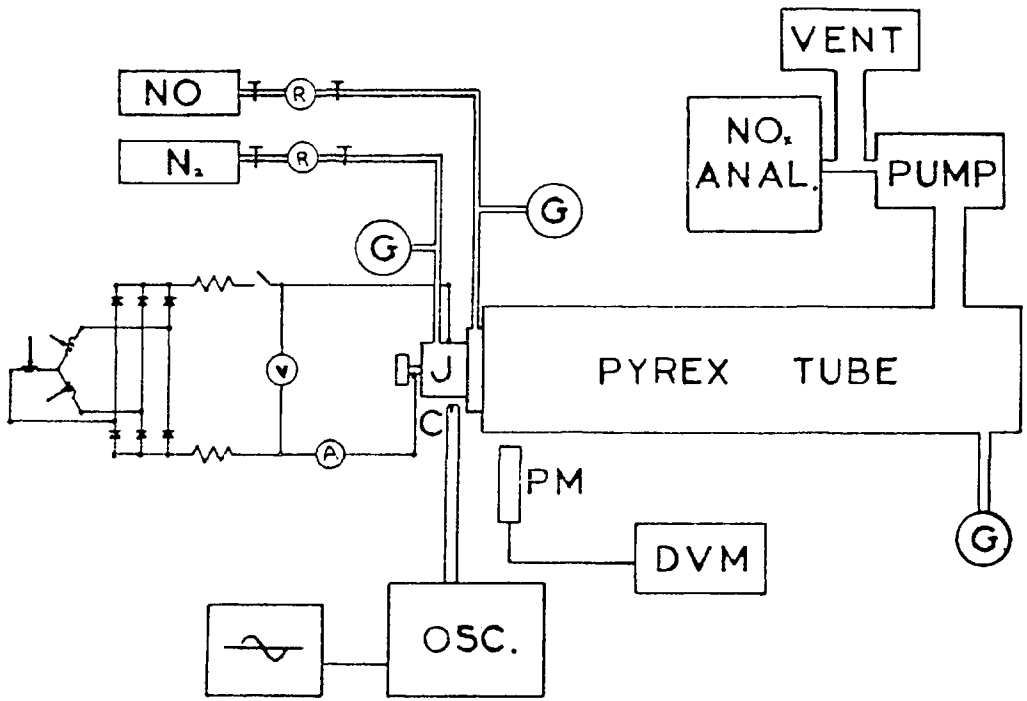

Figure 6.17 - Schematic of the steady state steady flow evaluation apparatus seen in Figure 6.16

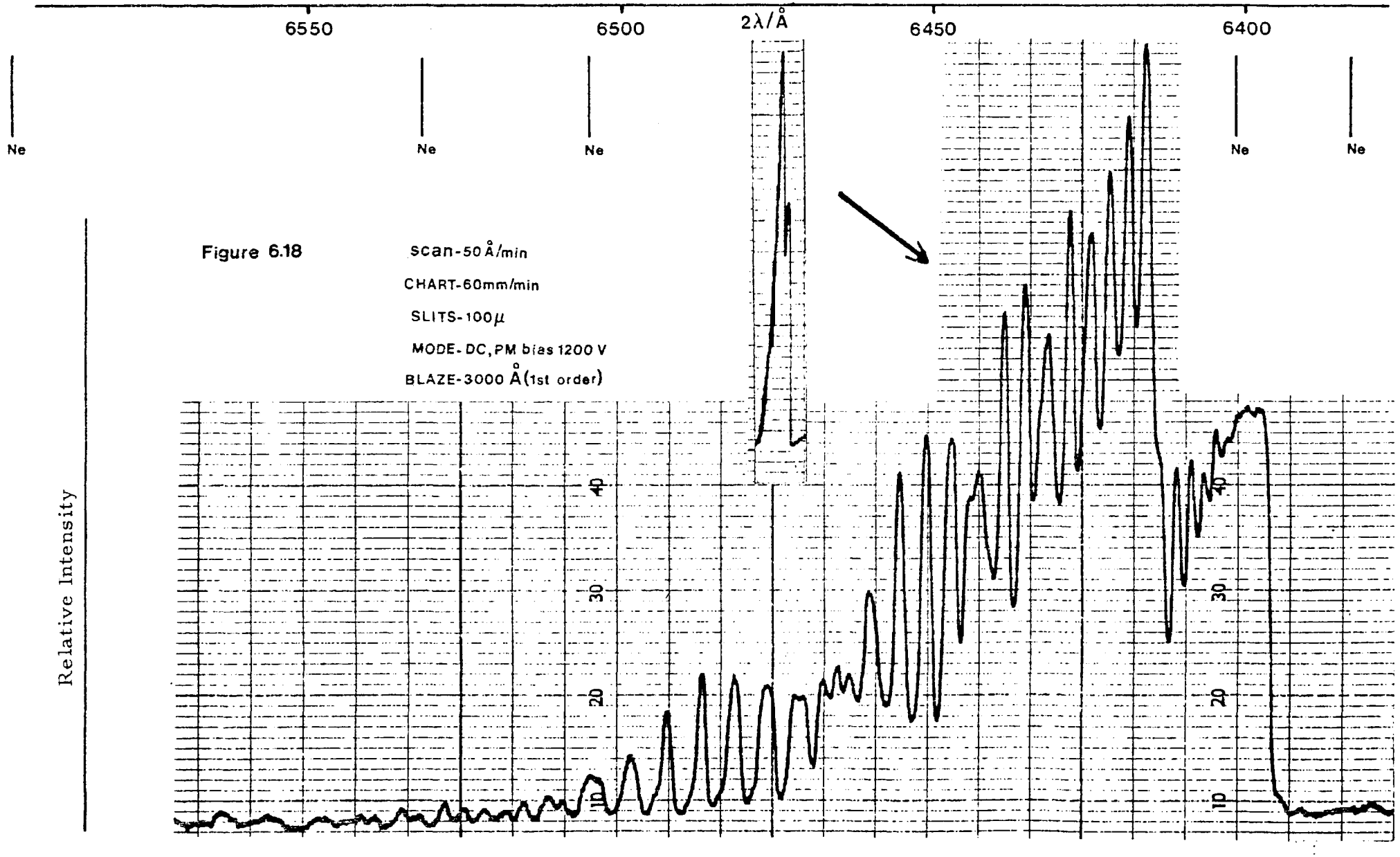
6550
6500
2λ/Å
6450
6400
Ne
Ne
Ne
Ne
Ne
scan-50 Å/min
CHART-60mm/min
SLITS-100μ
MODE-DC, PM bias 1200 V
BLAZE-3000 Å(1st order)
Relative Intensity
40
30
20
10

Figure 6.18

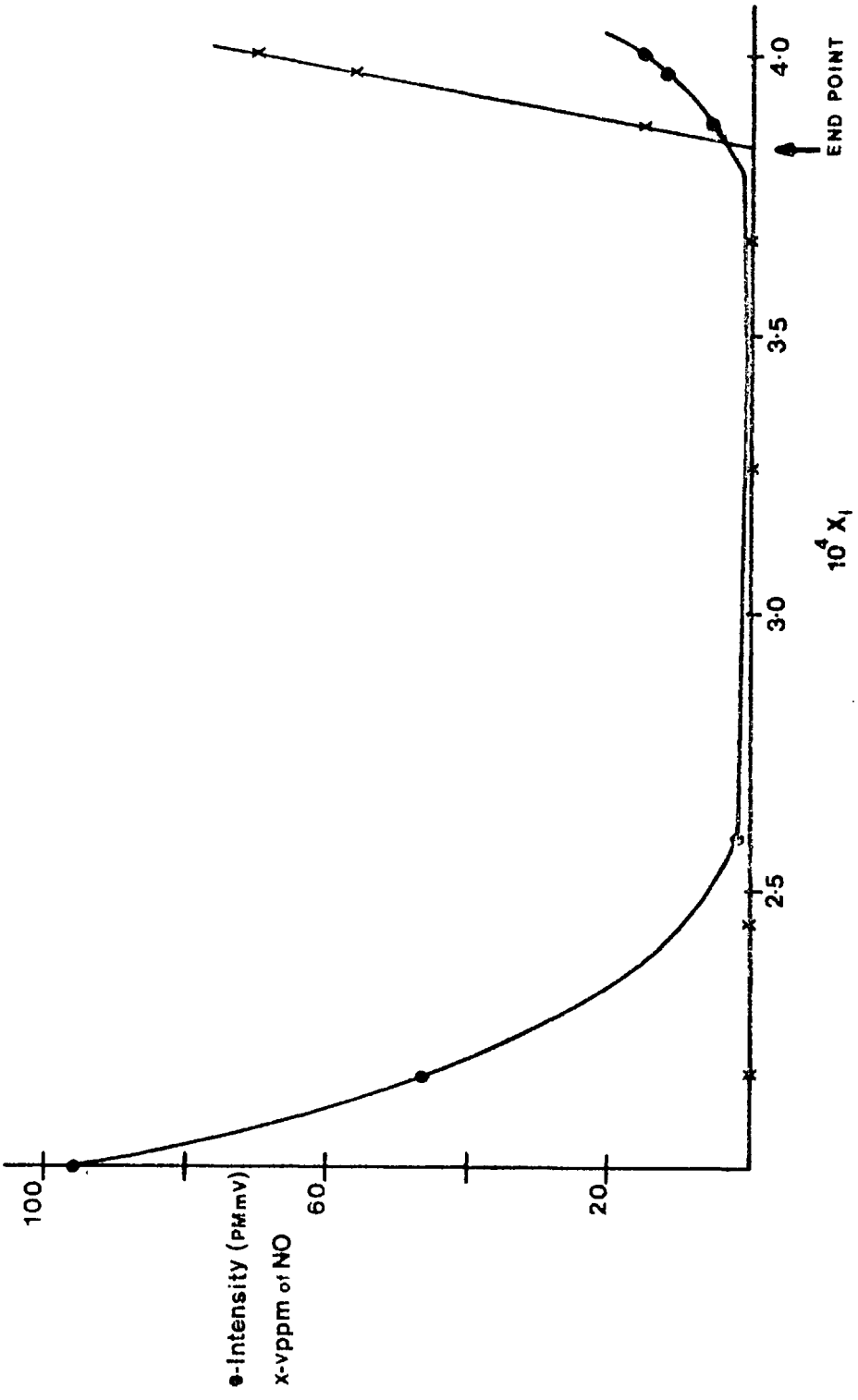

Figure 6.19 - A typical combined photometric and volumetric gas titration diagram

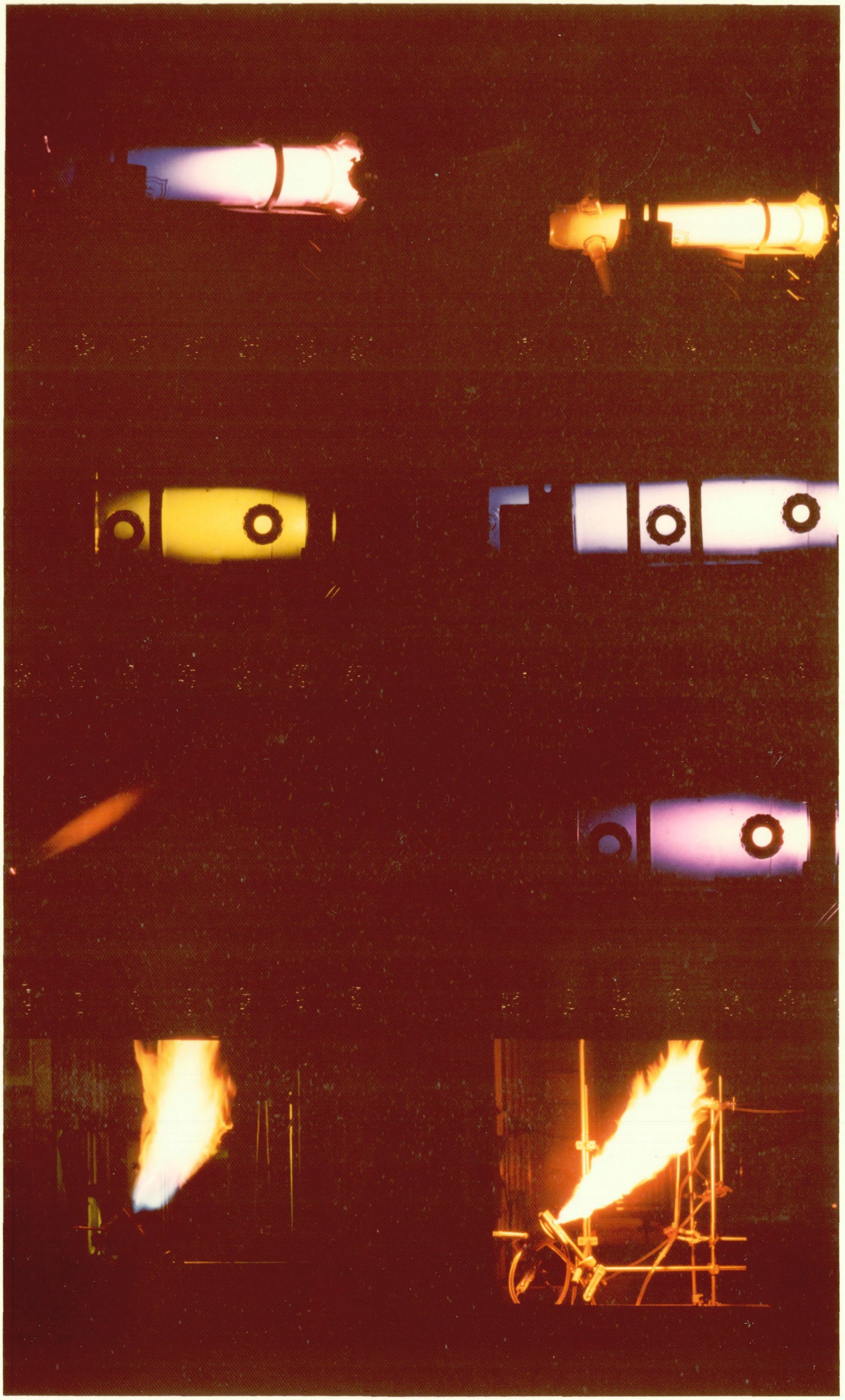

Figure 6.20

CHAPTER 7

SPECTROSCOPIC STUDIES

INTRODUCTION

This Chapter describes experiments and results that formed a part of, and supplement to, some of the arguments of previous Chapters. The ease with which emission spectra could be obtained with the plasma generator, for the conditions shown in Figure 6.20, facilitated detailed quantitative analysis. For example, the spectrum shown as Figure 6.18 readily yields the rotational constant for NO and the complete spectrum enables accurate calculation of the anharmonicity constant. This data was obtained directly (ie. without the use of a spectrum plate and microdensitometer) in a matter of minutes.

The main aim of the spectroscopic work described in this Chapter was to show experimentally the link between N-atoms and H-atoms in the electrical augmentation work. Other spectroscopic information is readily available with the total experimental system shown in Figure 7.1. The relevant spectra will be presented, with each species section dealing with individual parts that are either directly relevant to this thesis or of possible use to further work in this area.

EXPERIMENTAL

The basic apparatus is shown in Figure 7.1. It is an extension of that described in the experimental section of Chapter 6 and shown as Figure 6.17.

Calibrations for the spectra shown in this Chapter were obtained by using calibrated argon, helium, mercury or neon sources. Images of the sources were superimposed on the entrance slits of the monochromator, simultaneously with the radiation from the reacting system under study, at the time of recording, for highest accuracy of calibration. Wavelength data for these sources were obtained from the

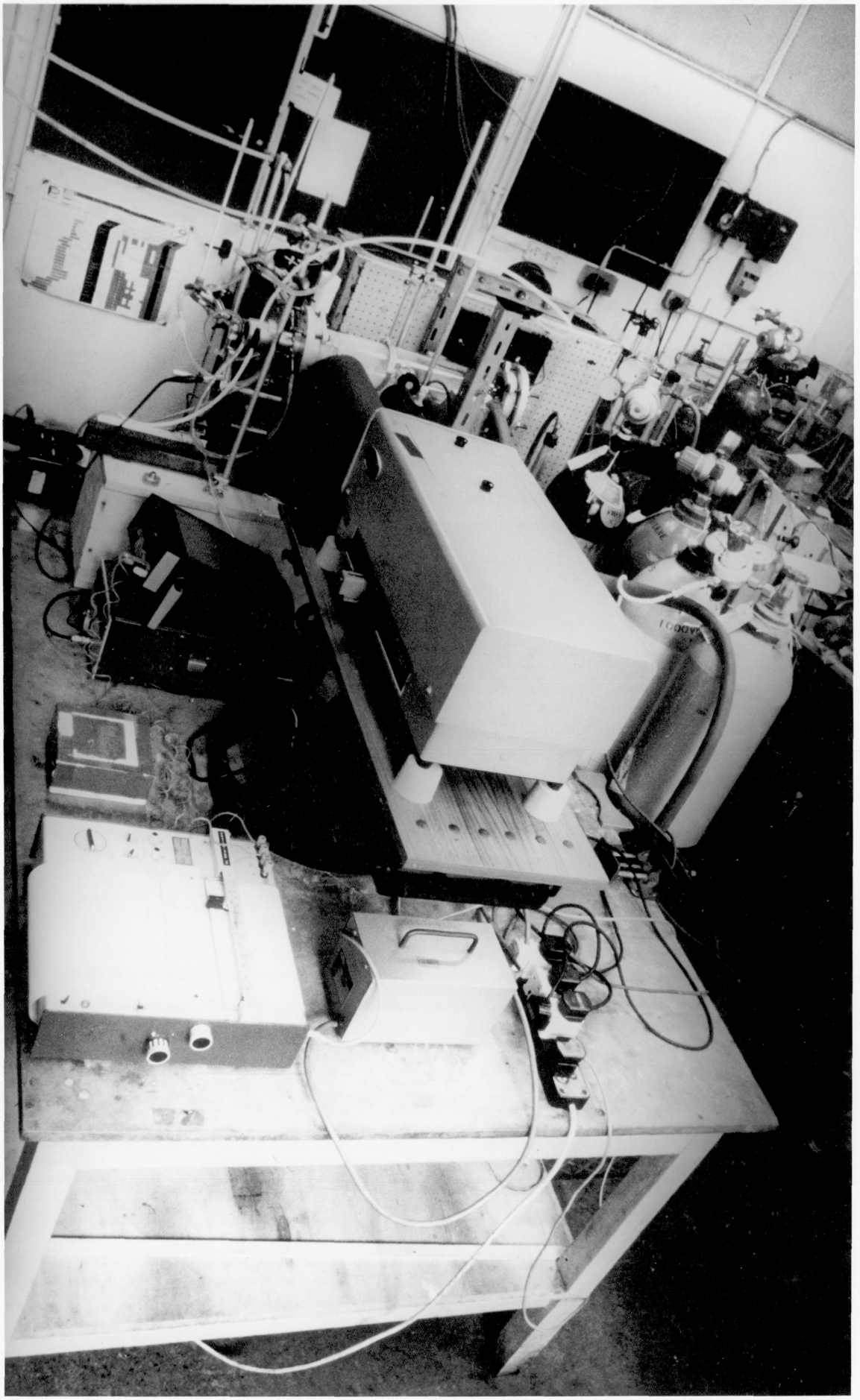

Figure 7.1 - Plasma spectroscopy apparatus

manufacturers ('Pen-Ray' lamps - Ultra-Violet Products Inc., and Ealing Beck Company) and from published sources, such as refs. 11, 49, 99 and 151.

NITROGEN

The yellow first positive nitrogen afterglow may be seen in Figure 6.20b. This afterglow has been studied extensively in investigations involving the recombination of atoms generated in electrical discharges. It is fully characterised (Pearse and Gaydon, 78, 382, 471, 472, 473). First and second positive emissions have been recorded in NH_3/F_2 flames (81).

The yellow first positive afterglow results from the recombination of ground state (^4S)N-atoms along the $A^3\Sigma_u^+$ surface (see Figure 7.2), with a proportion undergoing intersystem crossing into high vibration levels of the $B^3\Pi_g$ state. It is the transition $B^3\Pi \rightarrow A^3\Sigma$ that gives rise to the yellow emission. Direct transition from the A state to the ground state gives rise to the radiation of the Vegard-Kaplan band ($A^3\Sigma \rightarrow X^1\Sigma_g^+$), which due to the change in multiplicity (forbidden) is weak and rarely seen, although some bands are present in Figure 7.4.

In Chapter 6 the possibility of state selectivity with the plasma generator was introduced, and this attention to the details of the spectrum is to show that the principal emission recorded in that spectrum arose from recombination of ground state atoms.

In a detailed study of the recombination afterglow of nitrogen (78), it was stated that general agreement had been reached among spectroscopists that the characteristic yellow afterglow was associated with recombination of ground state (^4S)N-atoms. On progressive addition of nitric oxide in these experiments, the yellow afterglow (Figure 6.20b) was replaced by a blue emission (Figure 6.20a) and finally

by a yellow/green emission (Figure 6.20c). In between the conditions shown in Figures 6.20a and c there was a point at which there was no emission of light at all from the experiment.

The sequence of colour changes forms the basis of the established photometric gas titration technique that was employed for the N-atom generation rate calculations described in Chapter 6. The transition from colourless to yellow green is sharp, and therefore acts as an indicator, thus establishing the end point for the N-atom formation rate determination shown in Figure 6.19. As stated previously,a yellow filter was placed over the PM tube for the titration experiments.

The blue emission is associated with NO* (one peak of which has been shown as Figure 6.18) and Figure 7.3 shows the yellow/green NO_2* continuum formed by reaction of NO with O. The NO_2* spectrum is included because of its possible significance for the observations made on soot removal described in Chapter 4. The importance of O_2 chemisorption and OH oxidation of soot however, make the role of O-atoms less clear. Further work is required in this area.

The NO_2* produced by reaction of NO and O is one reaction that could occur with O-atoms in a combustion environment. This reaction has been used to estimate temperatures in a spark ignition engine (431). The reactions of O-atoms are well documented (79, 92) and studies of direct reaction with hydrocarbons are also reported (316).

O-atoms could be produced from a plasma directly, or as seen here, indirectly from a subsequent reaction. These processes may be significant in ignition (the role in photochemical ignition was mentioned in Chapter 3) and soot oxidation. O-atoms could also be linked to the visible emission reported in the plasma/flame-tube experiments of Chapter 4.

The reaction of $N(^4S)$ with NO is often used as a source of O-atoms for subsequent reactions (241, 242) (along with $H + NO_2$, for

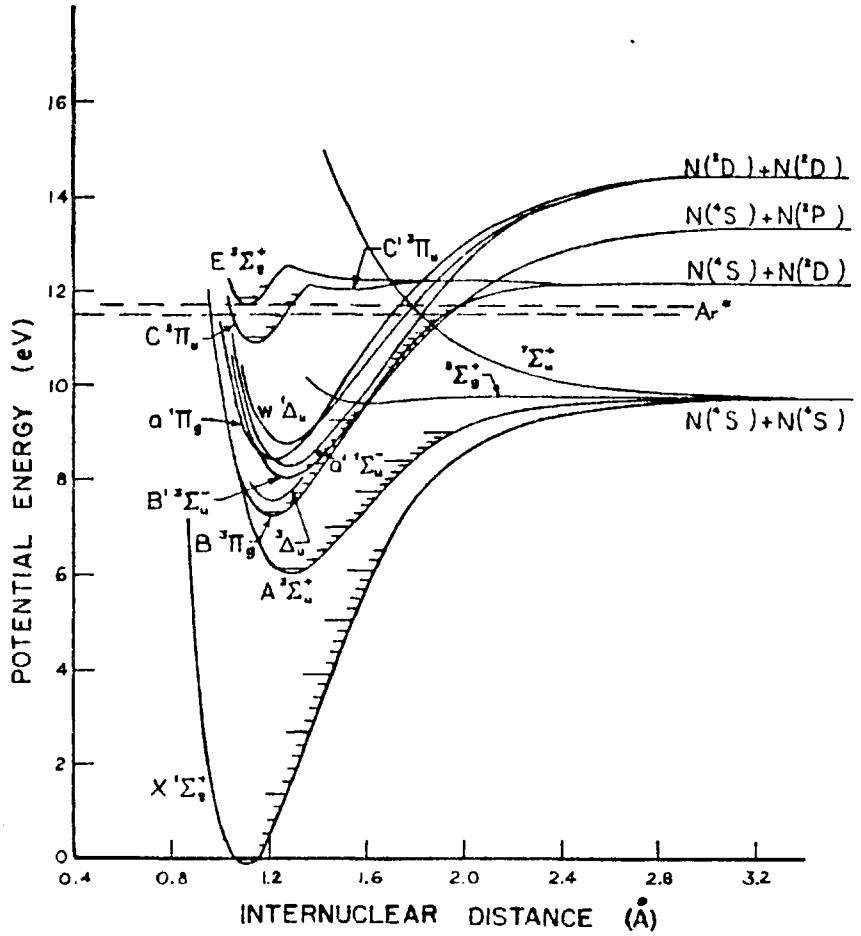

Figure 7.2 - Potential energy curves for nitrogen (from ref. 382).

O + HC reactions for, example see ref. 213). According to the previous Chapters, direct reaction between CH fragments and N-atoms to generate HCN and H-atoms was anticipated with subsequent oxidation of HCN to NO_x. Hydrogen cyanide will be considered next.

HYDROGEN CYANIDE

To demonstrate the preferential formation of hydrogen cyanide and H-atoms even in the presence of combustion air, the pure NO inlet, that had been used for the gas titration experiments, was replaced with an air stream saturated with chloroform from an isothermal bath. The air flow was from 1.7 to 7.2 ml s^{-1}. In the absence of the hydrocarbon NO_x levels were less than 5 ppm.

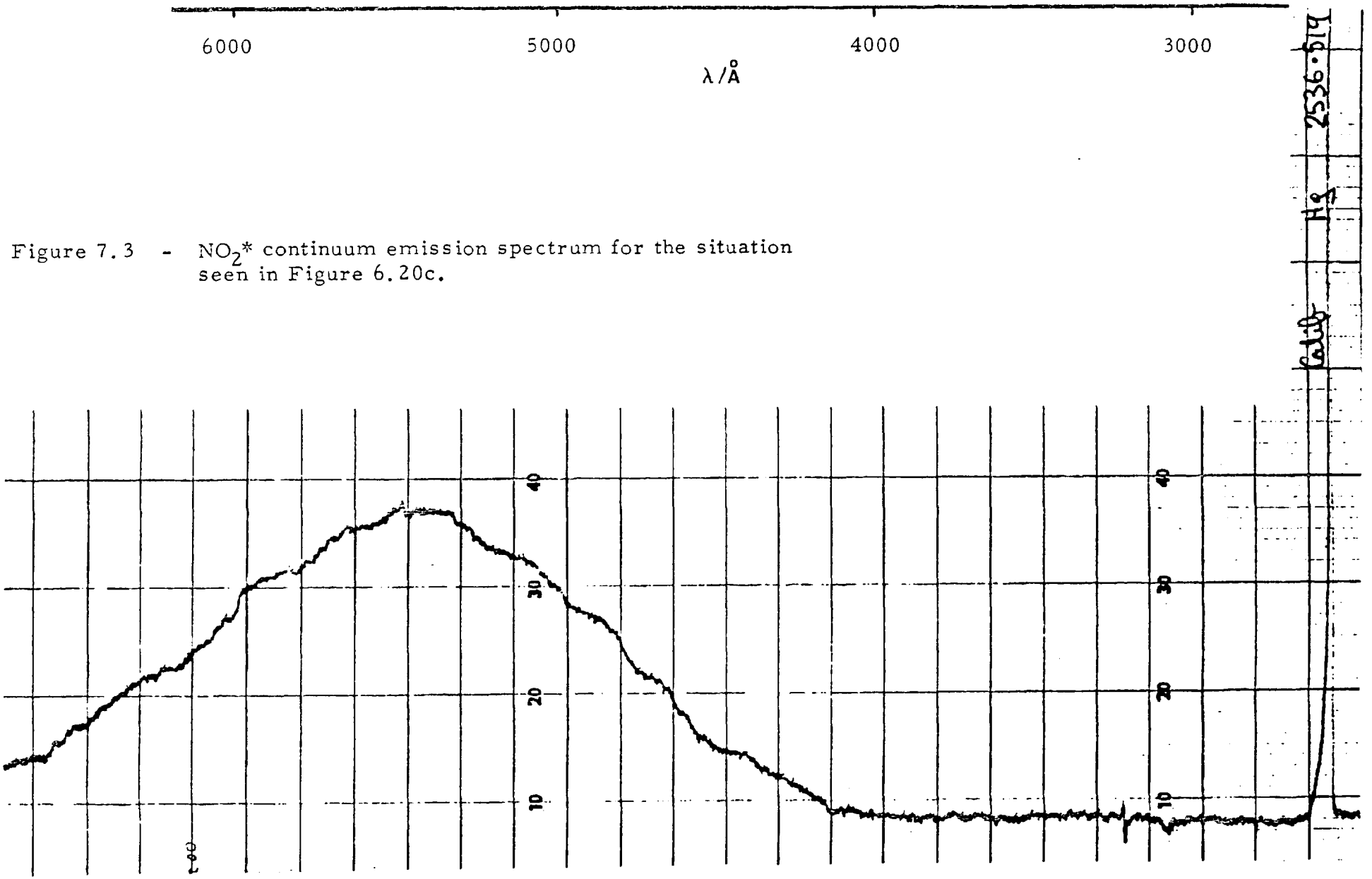

Figure 7.3 - NO_2* continuum emission spectrum for the situation seen in Figure 6.20c.

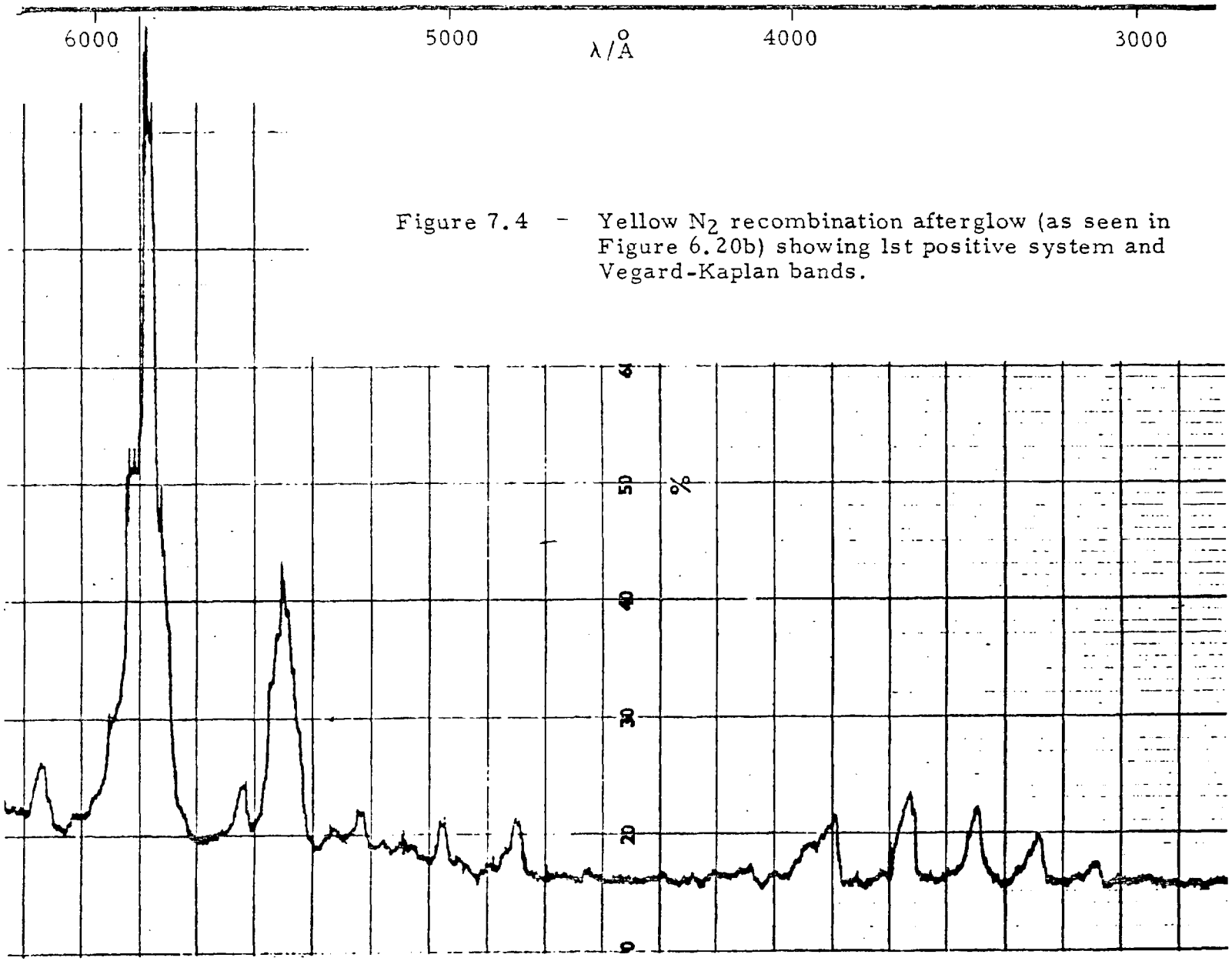

Figure 7.4 – Yellow N_2 recombination afterglow (as seen in Figure 6.20b) showing 1st positive system and Vegard-Kaplan bands.

On the introduction of increasing amounts of air saturated with $CHCl_3$ the spectra changed, as shown by the sequence Figure 7.4 to Figure 7.7. It is evident that the spectra collapse to the single intense CN line of the violet system (the 0, 0 transition is at 3883 Å; Pearse and Gaydon) and the hydrocarbon is responsible for consumption of the $N(^4S)$-atoms generated in the plasma.

The exhaust gases from the reaction were analysed for NO_x continuously (with known air dilution in the chemiluminescent analyser, with the Shaw cell (383) in parallel). Samples were also taken for analysis of hydrogen cyanide, according to the ion selective method of ref. 408 (Dr. Stinton kindly analysed the samples that formed the data for the abscissa of Figure 7.8).

The results shown in Figure 7.8 show clearly the direct correlation between the NO_x emission and the residual HCN concentration. The main feature of this result is to show that, in the presence of a hydrocarbon/N-atom/O_2 reacting medium, hydrogen cyanide is produced (and oxidised to NO_x) in preference to NO removal by N-atoms. The NO removal reaction is very fast (Chapter 4), but the route to HCN is obviously faster.

Nearly identical spectra were obtained with methane, propane, ethylene and CH_2Cl_2. Therefore, it appears that N-atom attack on the hydrocarbon in HC/air/N-atom reacting systems is a possible first and fast raction.

This does not prove that H-atoms would be generated subsequently. However, production of H-atoms from plasma generated HCN has been reported (63).

To explain the mechanism of augmentation of combustion does not require only consideration of attack by N-atoms on the oxidant to produce O-atoms (Previously considered in Chapter 3). Interaction with hydrocarbons directly may not be ruled out, and with the mounting

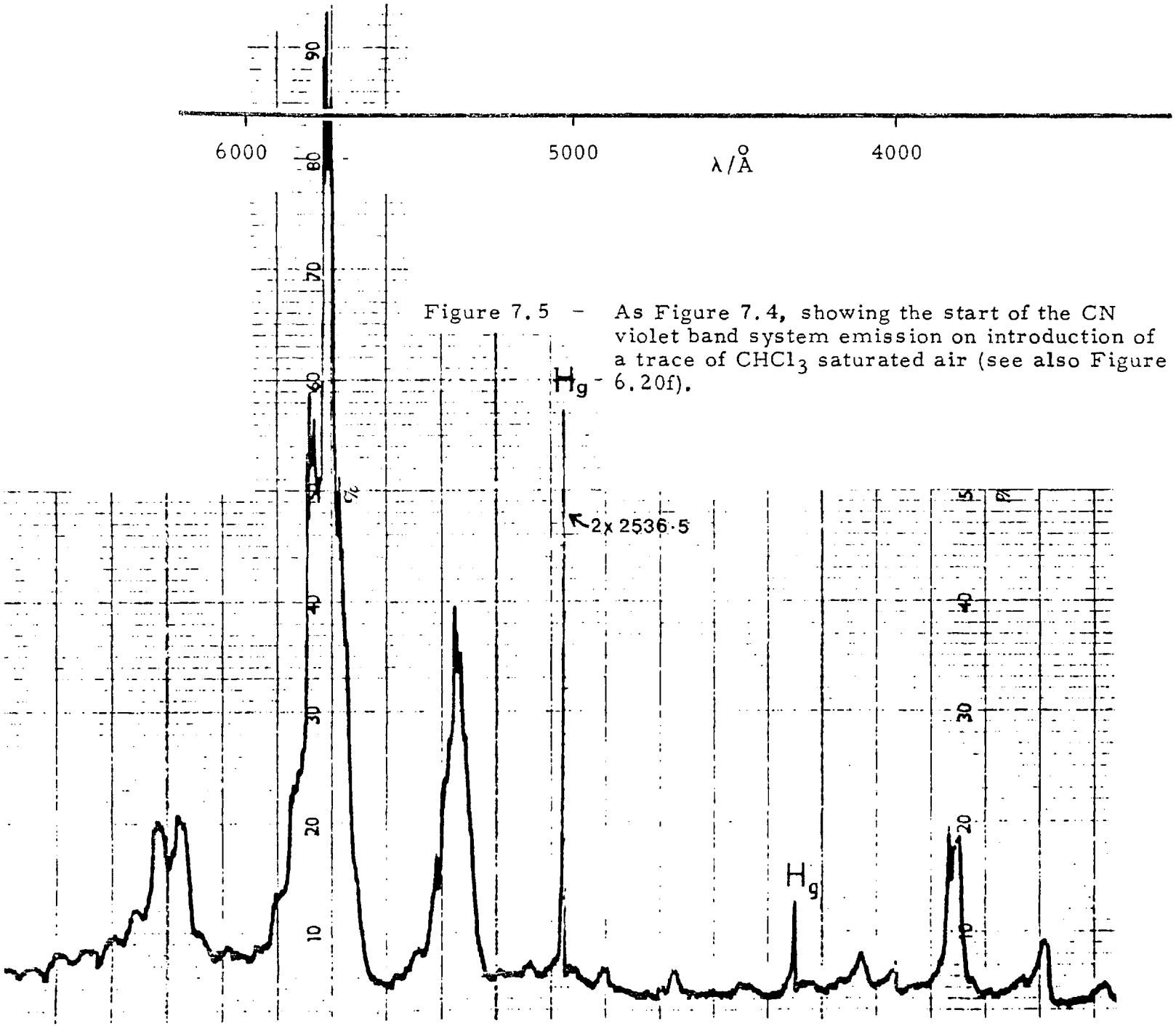

Figure 7.5 – As Figure 7.4, showing the start of the CN violet band system emission on introduction of a trace of $CHCl_3$ saturated air (see also Figure 6.20f).

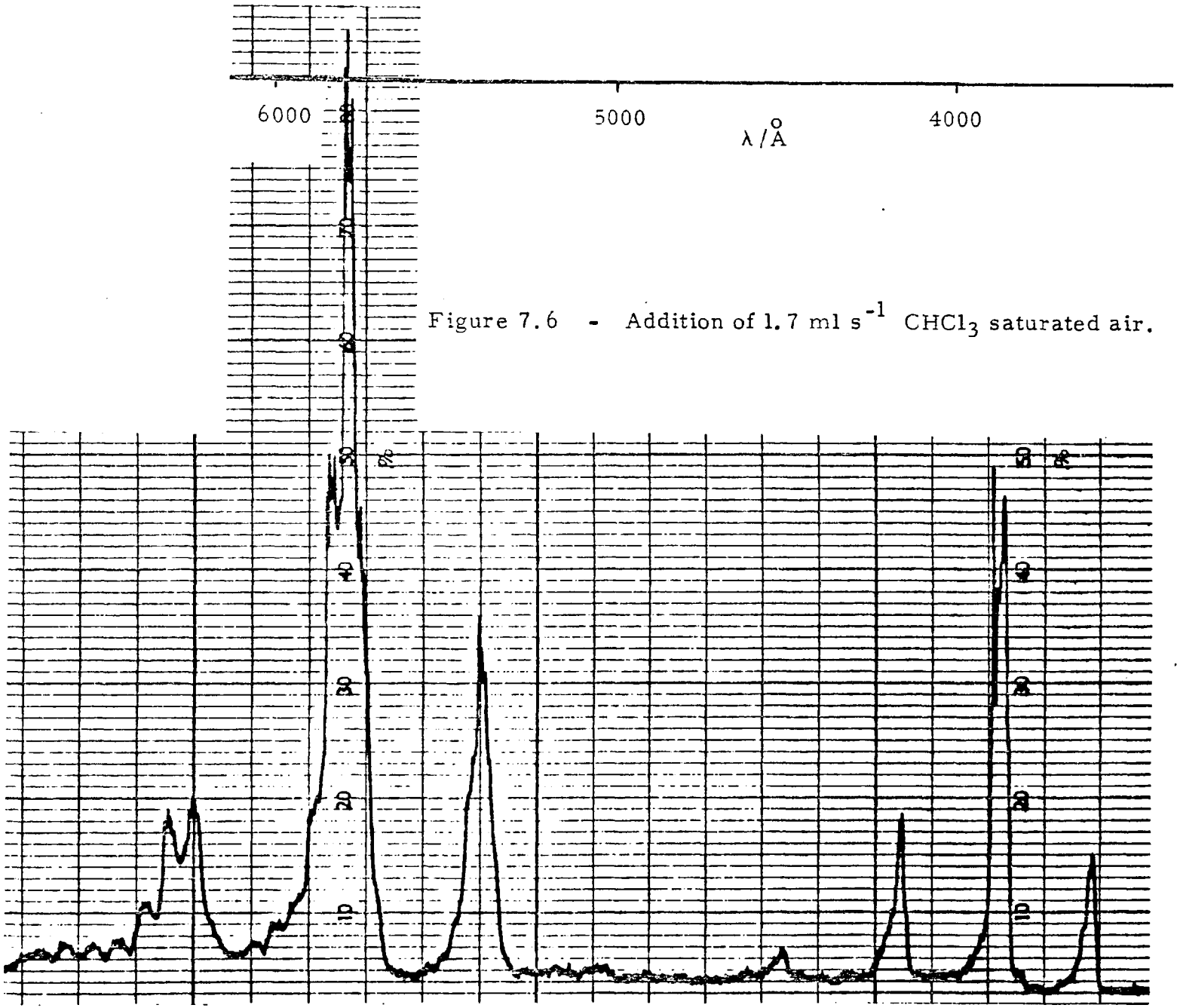

Figure 7.6 - Addition of 1.7 ml s^{-1} $CHCl_3$ saturated air.

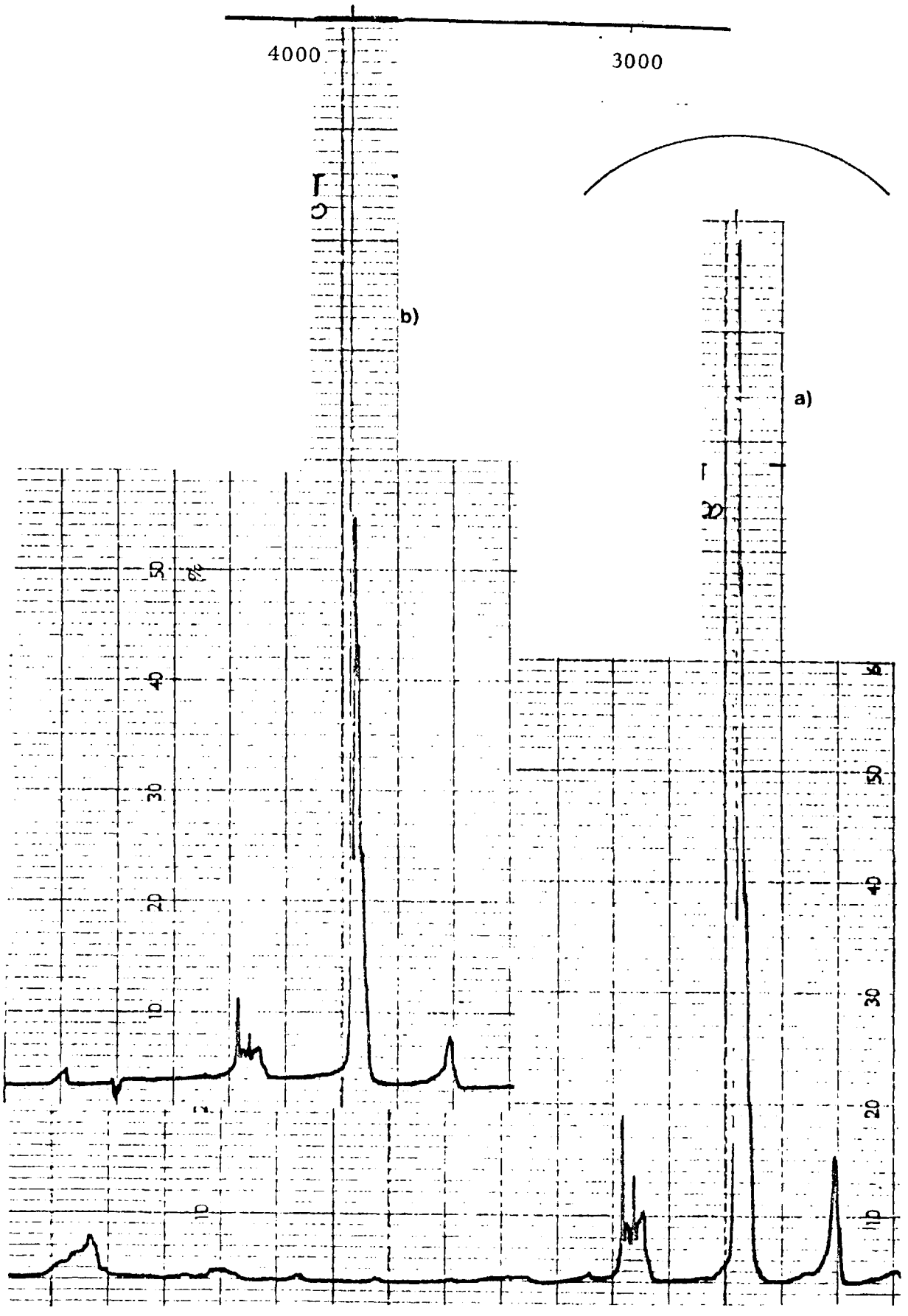

Figure 7.7 - a) 3.0 ml s^{-1} $CHCl_3$/air.
b) 6.2 ml s^{-1} $CHCl_3$/air.

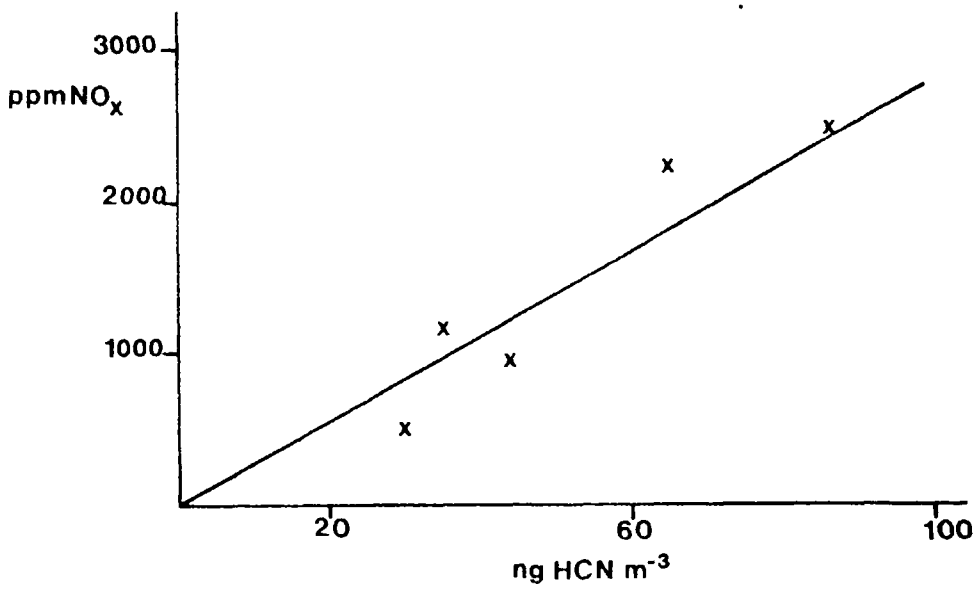

Figure 7.8 - Data demonstrating correlation between HCN and NO_x concentration in the reaction of plasma generated $N(^4S)$ with CH from $CHCl_3$.

---

evidence for the importance of H-atoms, such an explanation is worthy of more detailed study.

A recent study on N-atom reactions with ketene shows similar spectra (67) and CN* emission.

HYDROGEN

The plasma generator described in Chapter 6 operated very well on a H_2 feedstock (Figure 6.20e). No experiments were possible with direct reaction of H-atoms from this generator with hydrocarbons, and this is an obvious area for further research. A number of possible H-atom generators have been proposed, and that of ref. 75 appears to be highly efficient. Before any comparison could be made with the generator of Chapter 6, the thermodynamic evaluation that was done for nitrogen to obtain η in equation 6.1, would need to be done for H-atoms. A number of techniques exist for H-atom titration (75, 91, 105, 423), and if NO_2 is used ref. 375 provides useful kinetic data for the NO_2/H_2 system, and ref. 338 for N/NO_2 (also 114, 175).

ARGON

An emission spectrum of an early plasma jet (Figure 4.6) operating on argon was taken. The spectrum showed line emission down to 394.9 nm and evidence of OH below that. There is emission in the vacuum uv from argon arcs (6, 402). No attempt was made to record the vacuum uv emission in this study, or use it directly, although it was considered as a source of O-atoms for photochemical ignition.

STATE SELECTIVITY

Figure 7.9 shows the emission spectrum associated with the violet recombination seen in Figure 6.20d. It was possible with the plasma generator of Chapter 6 to move at will from the condition shown in Figure 6.20b to that of 6.20d by raising the 'power density' of the arc, and by variations of length, gas flow and power consumption. The violet recombination afterglow underwent the same colour changes in the gas titration experiments with NO. Quenching of the emission with molecular hydrogen was very readily demonstrated, at mass flow rates of H_2 below that expected to lead to total consumption of all the N-atoms produced.

Comparison of the emission spectra of Figures 7.4 and 7.9 for an N_2 feedstock show that distinctly different transitions are taking place. Those of Figure 7.4 arise from $N(^4S)$, as previously described, while the second positive emission arises from the presence of $N(^2P)$ (see also refs. 78 and 423). The detailed analysis of the spectrum without further experiments cannot rule out the presence of $N(^2D)$. Further studies of the spectra under higher resolution will enable clearer assignment of the atomic states produced to be made.

TEMPERATURE MEASUREMENTS

No temperature measurements were made in these experiments. This section is included to assist any further studies in this area,

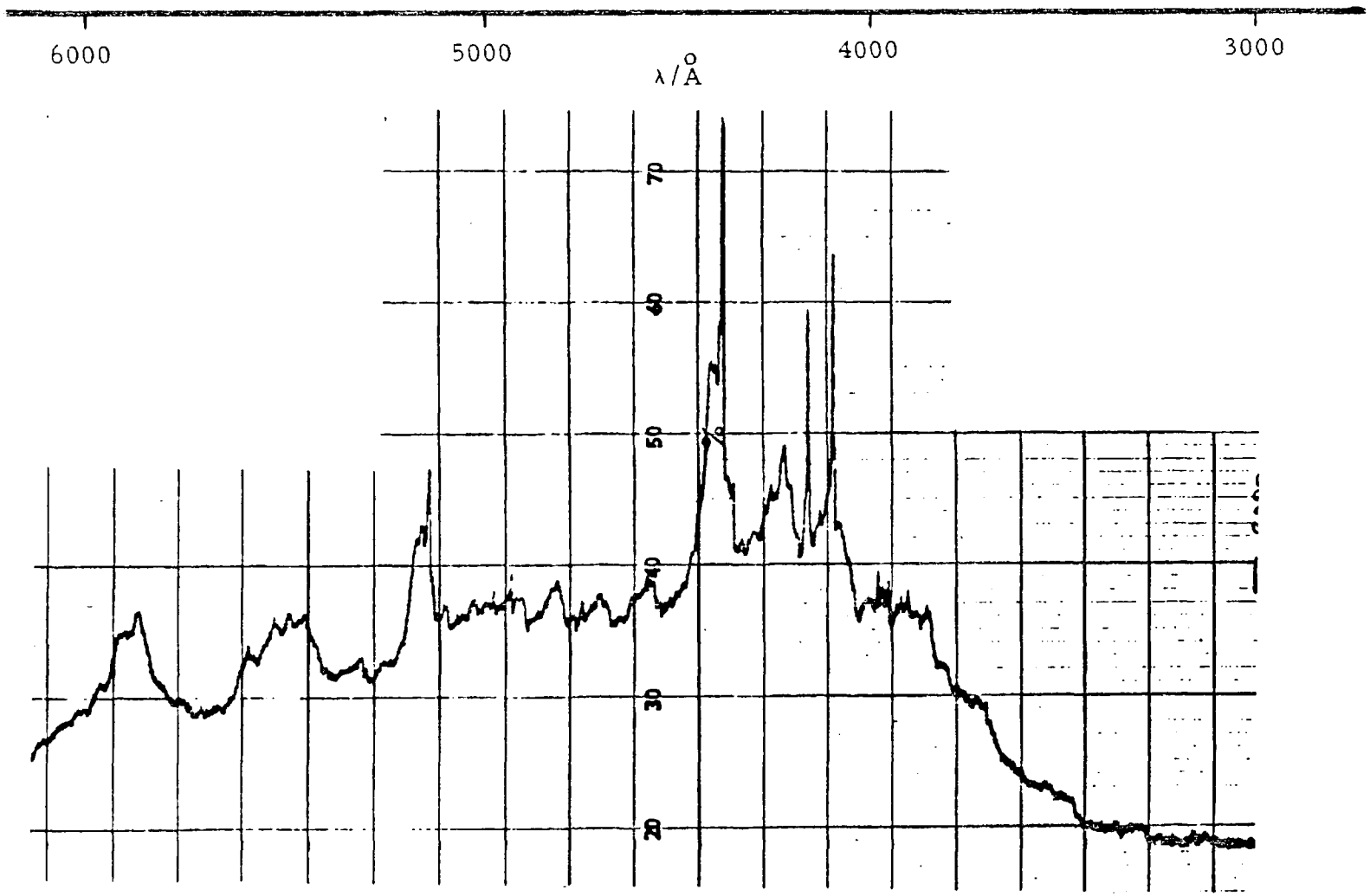

Figure 7.9 - Emission spectrum of violet N-atom afterglow, as seen in Figure 6.20d.

where temperature measurements are required. It is possible to obtain a number of estimates of temperature both within the plasma itself (71, 264, 265, 266) and from reactions in the downstream region. The photomultiplier tube used (EMI 9529B), whilst having a low quantum efficiency (≈6%) had a nearly constant efficiency from 500 nm to 250 nm so that relative intensity measurements between these limits would be comparative and relatively linear, as shown by Figure 7.10.

Although estimates of temperature could in principle have been made from experimental data obtained, no such measurements are presented. It is well known that electron temperatures in flames exceed those of the bulk of the gas (61) and values of this temperature may result from energy transfer from chemiluminescent emitting species notably OH* (59), and rotational temperatures of OH with atomic flames, as high as 8000 K are reported (157). Temperature measurements based on such species would have deviated from the main theme of the thesis and are not included.

CONCLUSIONS

This spectroscopic work has demonstrated the potential for the plasma generator in combustion studies generally, and for providing some explanations as to the modes of chemical reactions resulting from plasma electrical interactions.

There have been some very successful calculations for dissociation of H_2 and N_2 in non-equilibrium plasmas (80) and these, with combined in-situ arc spectroscopy, as well as extensions to the experiments described in this thesis, may provide further information on dissociation efficiencies.

Some of the less easily explained observations, especially on the roles of infra-red and uv radiation, on ignition and soot removal, will require further study. Unless there is photon energy pooling,

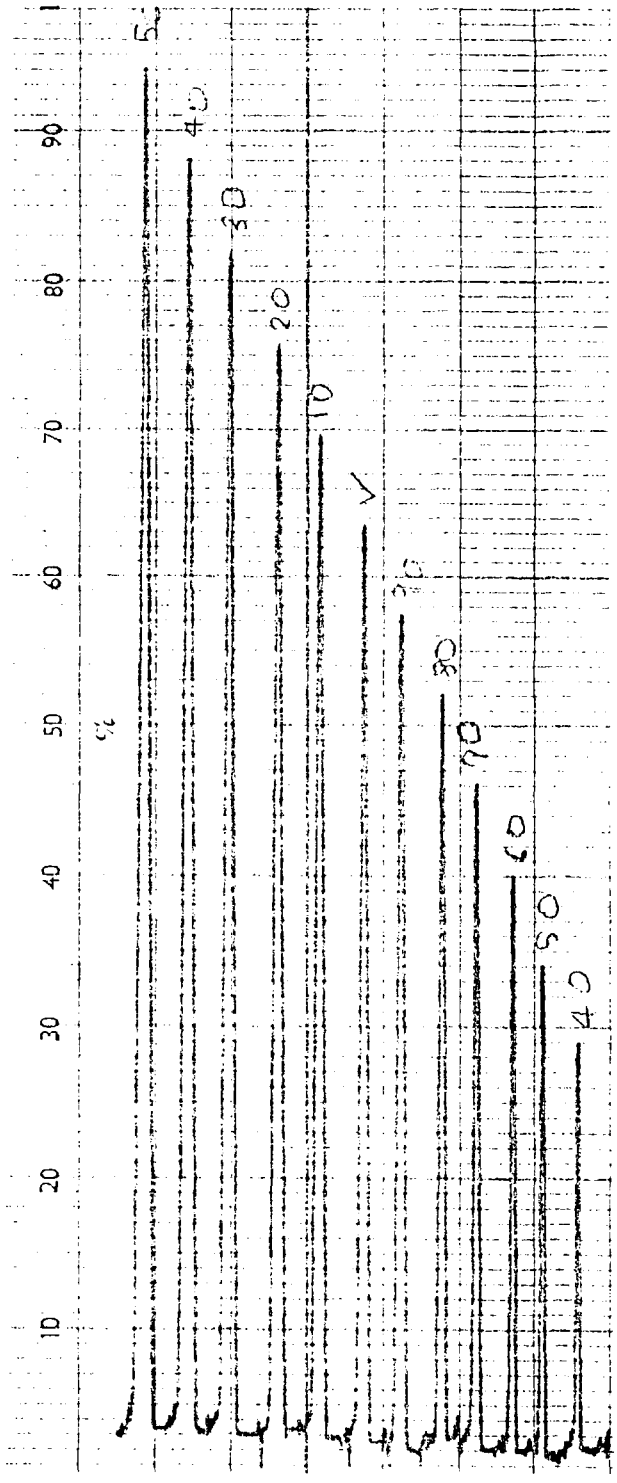

Figure 7.10 - Intensity response of photomultiplier output on increasing monochromator entrance slit width.

long range photochemical effects from dissociation are unlikely because of the wavelengths involved. However, subsequent chemiluminescent reactions, such as the one generating the extremely intense CN emission shown in this Chapter are worthy of further study.

In the presence of a hydrocarbon in the plasma the high resolution emission in the infra-red, using the apparatus of ref.176, could provide information on long range heating of reactants by infra-red radiation. This is a less specific mode of excitation and weakens the strength of the electrical interaction methods.

The area in this study that is least explained, is that of soot removal by both Ar and Ar/N_2 plasmas. It is possible to speculate about possible schemes, and the possibility of reacting in the early phases of soot formation (shown for example in refs.64 and 409) with 'O' or OH generated, possibly photochemically, is an area that should be investigated spectroscopically and theoretically. Water vapour in contact at the interface of the Ar or Ar/N_2 plasma will dissociate and produce OH. Polynuclear aromatic molecules have been suggested as soot precursors, and reaction of OH with them, as an oxidative scheme inhibiting soot formation, may be possible. Relative rate constants for OH with various hydrocarbons, including aromatic molecules have recently been published (278).

CHAPTER 8

CONCLUSIONS

This study has separated the two extremes of burning according to the mode of power control. For both types of practical quality and quantity power-control mode systems, the practical reality is that economy and emissions are mutually exclusive, at the present time.

In systems that have strong degrees of diffusion control in the main heat release the problem is not readily resolved, at the product discharge stage, due to the presence of a species (NO) that needs to be reduced, being present in an oxidising environment of excess air. This occurs simultaneously with a species requiring oxidation (soot), that is not readily oxidised in the limited time available before quenching, even in the excess oxygen atmosphere.

The problem may be solved by the use of high electrical powers in the form of N-atom plasmas, and potentially the energy used per molecule of NO reduced by this method is less than that of injection retard. However, N-atom injection constitutes the highest energy electrical interaction, and could only be considered practically viable when emission constraints on NO and soot cannot be met by conventional methods.

The difficulty associated with diffusion controlled combustion can be overcome with alcohol fuels, due to the oxygen present in the fuel. These fuels produce no soot under diffusion controlled combustion, and have cooler combustion characteristics. However, for Diesel application of such fuels, high voltage electrical interaction to modify the ignition delay period, could potentially solve all the combustion generated problems for a Diesel engine.

The Otto engine however is one engine where the potential for solving all the problems of combustion generated emissions and econo-

my may be solved in a unique way electrically, both at the mixture preparation stage, and the stage of conversion from reactants to products.

To appreciate how this may be done requires a review of the basic problems, work that has been attempted to solve them, and why the kinds of electrical interaction lead to improvements over and above that obtained by conventional methods.

LEAN BURN

The attempts at lean burn combustion have been directed towards operating at mixture strengths much weaker than 20:1 AFR. However, as can be seen from Figure 1.3, while NO levels fall to low values, with increasingly weaker mixtures, BSFC rises, as do hydrocarbon emissions (and sometimes carbon monoxide), and the NO_2 component of NO_x increases.

Attempts to improve lean burn combustion by producing homogeneous mixtures on a molecular scale do not provide the solution, and only highlight the problem of turbulence at the ignition phase and main heat release phase. Low levels of turbulence are preferable until the establishment of a propagating flame front, when increased compression turbulence is desirable (74). This concept of optimum turbulence at different phases in the heat release has been demonstrated experimentally (55) and methods of projecting the spark kernel away from quenching regions have been considered, mainly with laboratory studies (56, 184). In various torch chamber concepts a late firing torch has been considered to generate this late turbulence, to increase power, and reduce the loss in efficiency associated with increased burn times of lean mixtures (3).

It was recognised that as mixtures became leaner, so the ignition sources would, of necessity, have to change (17, 72, 379, 436). However, it is not only ignition that limits lean operation, but also

the rate of flame propagation. This has been considered in reference 352. These results have led to confusing aspects about limiting features of flame chemistry and turbulence in lean burn situations. However, it is becoming clear that as far as spark ignited systems are concerned homogeneous mixtures are not optimal (294, 352) and some form of aerodynamically stratified charge is appropriate. The potential for these in controlling heat release rates, and the resultant effects on emissions (351, 422, 429) makes research in that area of prime importance for electrostatic carburation for production of uniformly dispersed aerosols, independent of air mass flow rate.

Ignition generated turbulence from ignition sources specifically designed for that purpose (386) or resulting from various forms of prechamber torch ignition have been identified as being able to assist in increased rates of burn of lean mixtures. It is hard to separate such systems from plasma jet systems so they will be considered next.

PLASMA JET IGNITION

There are many varieties of high energy ignition and plasma jet ignitor systems in the literature that have received attention recently (21, 22, 23, 46, 109, 211, 329, 330, 424). However, only in the case of ref. 211 was any specific attempt made to generate H-atoms directly, which according to this work would be the most effective in augmenting lean combustion. The work of ref. 211 showed clearly how lean mixtures could readily burn when ignited by H-atoms from a discharge into H_2 or CH_4.

Although described as plasma jet ignitors they are basically high energy spark systems, which because of the nature of the spark discharge circuit makes them very difficult to characterise.

It is common, for example ref. 379, to talk about the total spark duration and total current, whereas in reality the discharge process

is characterised by different processes occuring in different time scales within the spark. The two basic components of a coil spark discharge have long been known and studied with respect to ignition, and with a view to controlling the discharge characteristics as early as 1933 (142). The initial high energy 'capacitive' component results from the discharge of the self capacitance of the high tension circuit. It is the high current part of the discharge, with peak current as high as 200 amps and duration 1 to 10 ns (291) that has the greatest influence on ignition. Depending on the components of the system the duration may be increased to 100 ns with peak currents of 20 amps (376, 377). Photographic records resulting from the comprehensive work described in refs. 9 and 291 show production and propagation of three strong shock waves within the first 10 ns. Consequently, duration and total energy alone do not totally define even the very short initial component.

The second component of the discharge is the low energy 'inductive' component that results from oscillation in the primary circuit continually transfering energy to the secondary. The duration is longer typically 50 μs and low currents of the order of 1 amp. The effects of these two components on ignition characteristics have been investigated (406, 463) especially with respect to minimum ignition energy.

The high current flow is characterised by an arc, while the low current is characterised by a glow discharge. One significance of the plasma generator described in Chapter 6 is that it has taken the characteristics of the initial component of a spark discharge and allowed it to be operated continuously. The experimental evidence (291, 406) suggests that it is the initial component that controls the subsequent ignition.

Reference 291 chooses to further subdivide the initial component

into a 'breakdown' phase before arc type discharges. In this transient region it is suggested that energy transfer to the plasma is greatest due to reduced radiative and heat transfer losses to the electrodes (367) before an arc forms. The design of the plasma generator of Chapter 6 has considerably reduced these two causes of major energy loss.

Of significant importance in any form of spark discharge is how the energy is transfered from being stored electrically in the external circuit to the reactants. The gases around the spark itself are therefore extremely important because the increased spark energy may be wasted heating gases that may either generate pollution or absorb most of the spark energy into modes that are redundant in the establishment of the flame kernel. Nitrogen gas should therefore not be present close to the spark, for the ability to absorb up to 9.76 eV before dissociation is a major sink. Once dissociated, it may react to produce HCN and subsequently NO from the fuel component or directly to NO when the conditions described in Chapter 4 are met. The desirability of keeping air from the spark to reduce NO emissions was recognised some time ago (436).

This present study has explained the role of the N-atom in increasing reaction rates as via production of H-atoms. Direct discharge in the absence of nitrogen into either hydrogen or a hydrocarbon is therefore the most promising initial method for ignition to produce H-atoms as has been demonstrated (211).

The superimposed roles of chemical reactivity and mobility of the H-atom has been demonstrated and the evidence for its key role in specific combustion reactions shown. Further spark ignition studies should therefore utilise this fact to try to lower combustion chamber turbulence, not increase it, by using the high diffusivity of

H-atoms and imparting to them high translational energy at the time of generation.

High turbulence levels that are associated with, and required for, lean burn operation reduce the combustion interval thus lowering the time for heat transfer losses from the cylinder and raise efficiency and power. However, turbulence results in increased convective and pumping losses. The controlled discharge to produce H-atoms could lead to this turbulence as unnecessary.

It has long been known that slow running gasoline engines with low turbulence have a high tendency to knock, and that increased turbulence destroys the 'end-gas'. This has led to the design of a special 'fireball' chamber that has enabled operation at compression ratios nearer the optimum levels for best BSFC (94, 140, 297, 298, 299) ie. 12 to 15 and normally not available for Otto engines. The knock limited compression ratio rises with lean operation, and multipoint ignition from an H-atom plasma could potentially simulate the same 'fireball' operation without charge turbulence.

HIGH CHEMICAL ACTIVITY OF INCOMPLETE COMBUSTION PRODUCTS

The high reactivity of incomplete combustion products has been reported in a number of papers from work done in Russia. The LAG process (100, 168, 169, 170) was based on chain propagating theories of Semenov. A recent appraisal (100) considers the flame propagation to be dominated by diffusion of radicals. It seems that the key species is the H-atom for the reasons outlined in this study.

The concentrations of CO and H_2 in combustion gases rise sharply as mixtures become richer (Figure 1.3), with $[H_2] \simeq 1.3\ [CO]$ generally observed. The presence of hydrogen in recirculated exhaust gases used as a means of NO_x control, could, with an extended ignition source, improve flame propagation by generating H-atoms leading

to increased efficiency. Evidence for this is already documented in ref. 8. In recent two-stroke gasoline engine studies to improve scavenging of exhaust gases (323) it was observed that the activity of the exhaust gas was such that under some operating conditions multipoint ignition was established in the fresh charge without the need for a spark, and resulted in reduced HC emissions and lowered BSFC.

STRATIFIED CHARGE COMBUSTION

Stratified charge combustion is not new, and a Ricardo patent in 1915 was the first to lay down the basic design (459) for such a system. Its advantages are the possibility of low NO_x levels, and the potential for power control without a throttle - the main efficiency loss in the quantity mode of power control. A variety of systems have been considered (see for example refs. 3, 126, 131, 188, 259, 391, 428, 455, 464, 465, 469) with ref. 465 covering the much sought after ideal of open chamber and unthrottled operation. The most successful is the throttled Honda CVCC 3-valve system with a rich prechamber. The problem even with this very successful (non catalyst) system is the production of quench hydrocarbons. Reference 469 describes a further advance in design for this system involving a 'Branched Conduit' that joins the chambers of this new system (BCCVCC!).

The main incentive for stratified charge combustion has always been to operate with reduced throttling for power control. Secondary improved efficiency features that result from this are, an increased knock limited compression ratio, lower dissociation losses, lower fuel sensitivity and a higher ratio of specific heats of the working fluid.

The CVCC system has a prechamber that leads to higher chamber surface to volume ratios, and therefore potentially greater heat losses, thus lowering efficiency. Also, increased turbulence and pumping losses, resulting from gas passage through the connecting

throat, while increasing rates of burn and reducing heat loss intervals, lead to increased convective heat transfer and pumping losses. These will always be high with this type of chamber. Hydrocarbon emissions from the CVCC system will necessitate the use of an oxidation catalyst for more stringent emission requirements.

The present trend has been to move away from stratified charge configurations and aim for very fast lean burn in open chambers. The leading example of this, at the present time, is the Nissan NAPS-Z system, with two sparking plugs.

The potential for an H-atom plasma jet, as a novel form of stratified charge concept, seems clear. One advantage would be that the high mobility of the H-atoms generated would allow rapid heat release in an open chamber geometry that was initially quiescent. This would reduce the pumping and heat transfer losses associated with gas movement. For plasma ignition, the prechamber would also be absent thus lowering the overall surface/volume ratio. Rapid heat release in a lean mixture with H-atom multipoint ignition would alleviate any knock constraints.

The exact degree of mixedness of the main charge is uncertain. There is evidence, at least for internal combustion engines, that a charge that is not totally homogeneous is advantageous for economy and emissions (294). An aerodynamically stratified suspension of rich pockets in air has been shown to burn very rapidly (294). This arrangement more closely resembles a dust suspension, where 'flammability limits' are known to be wide, and may be used for increased flame propagation rates in imxtures that are overall very lean. The electrostatic carburettor may be a device that could assist the formation of an aerodynamically stratified charge.

Reference 469 describes improvements in reductions of HC and NO_x with the 'BC' addition to the CVCC. However, in the film records

shown as Figure 3 in that paper, combustion with the 'BC' shows the ejection of a "red flame" "not observed in combustion without branched conduits". A reduction of 20% in HC with the BC system is observed. In all the experiments involving H-atom generation in this study the red Hα line at 656 nm was always seen (see for example Figure 6.20e). The possibility of the 'BC' system resulting in the production of hot H-atoms, by the kind of reactions described in Chapter 3, and pumping (amongst others) the main quench reaction, as described, while purely speculative at this stage, is certainly an area worthy of further study. However, if substantiated, the complexity of the combustion chambers could be reduced, with heat release rate (and therefore pollutant emission) controlled at the plasma and carburation stages via the external circuit characteristics of the plasma discharge and its composition, and the size distribution function of the droplets of the charge in the electrostatic carburettor.

IGNITION BY RADIATION

Attempting to cause ignition by radiation has been described in Chapter 3 with respect to vacuum uv absorption of O_2, and focused lasers onto targets, specifically interstitial metal hydrides. Infra-red radiation has been used to ignite practical engines to characterise ignition away from quenching surfaces (110, 111, 112). These studies used a TEA CO_2 laser radiation at 10.6μm. The plasma generator described in Chapter 6 could be used in such a form, especially with a feedstock of pyrolysing hydrocarbon (as seen in Figure 6.20h). However as such this is excitation through infra-red absorption and lacks the specificity of uv irradiation. The importance of uv radiation on spark discharge potentials in minimum ignition studies has been reported (406) and with respect to radiative decay in hydrogen (229); hydrocarbons can raise the sparking voltage (210) but little of the uv

radiation from sparks appears to have been used directly for inten tional ignition.

One problem with spark ignition not experienced with pulsed laser sources (for example Figure 4 of ref. 110) is the difficulty of reproducing spark characteristics from cycle to cycle. This makes for a major difficulty with cyclic variations and characterising the lean misfire limit (387) and flame propagation times (310).

Infra-red laser ignition sources (as with any infra-red radiation source focused into a combustible mixture containing air and fuel) have been observed to generate more NO_x. This problem may be overcome with H-atoms generated in the absence of air.

APPLICATIONS OF ELECTRICAL DISCHARGES IN COMBUSTION SYSTEMS

This section title is the same as a conference where some of the potentials for electrical interaction were discussed (see for example ref. 458). Electrical interaction with flames is not new and apart from the work already described in previous chapters many practical applications have been considered (98, 240, 269, 324, 458). However, much of the specificity which is possible to solve practical problems has been completely overlooked, and the necessity to use argon in many applications prior to this work lowered the practical viability. This specificity is desirable firstly because it makes for more efficient use of the power in the electrical interaction and secondly specificity leads to selective control once the limiting stage in the process has been identified.

Some concern has been expressed as to the ability to initiate arc/hydrocarbon combinations (138) however this has never presented any problem in previous studies (227) and with the new design described in Chapter 6, no problem of initiation was ever experienced.

The increasing demands of emission constraints has meant that

more and more valuable transition metal catalysts, many with rare earth additives to improve cold start performance, are to be spread over the junk yards of the western world. One potential to reduce the rare earth content of the catalyst if considered necessary (and sensible use of the appropriate electrical interaction has demonstrated that such catalysts are unnecessary) is atom recombination on the surface of the catalyst to generate a hot spot to 'light-up' a low grade metal catalyst (eg. Cu/Cr) and remove Ruthenium or Rhodium for more appropriate catalysis in the pharmaceutical industry. The plasma generator described in Chapter 6 has a variety of possible non-specific utilisations, direct reforming of alcohols for example for cold starting, even carburising metal components (164, 165). However, it is the specificity that was the main objective of this study. This specificity leads to potential for laser systems briefly mentioned in Chapter 3 and seen in the spectra of Chapter 7, but discussion of these systems is beyond the scope of this thesis.

HYDROGEN ADDITION

Hydrogen addition to the air intakes of Otto engines has been the subject of two recent publications (238, 357) to aid lean burn operation. This is not a new concept and data for hydrogen addition in this way is presented in ref. 32 from the work done in the 1920s (362). The benefits of hydrogen addition in increasing burn rate and therefore power and efficiency are fully expected from consideration of Chapter 3. However, the maximum effect possible is limited by thermodynamics at the flame temperature. Generation of H-atoms in a plasma, as can be seen from Figure 3.6, not only produces higher concentrations, but very high translational energies may be imparted to these species aiding in overcoming activation barriers for key quenching reactions and further driving the transport processes to ensure rapid mixing in the main chamber.

OVERALL EFFICIENCY

The potential for practical application in combustion systems will be limited by all forms of power requirement. Removing the necessity for argon was obviously the first major hurdle. Laboratory experiments with argon/methane mixtures has shown the possibility of better specific power utilisation at high flow rates (248) and the powers required for gas flows to the generator need to be considered in an overall efficiency analysis.

Chapter 6 has mainly considered the power requirements of the plasma generator, and its electrical efficiency in isolation and under steady state conditions. For practical use it would be necessary to consider the unit in a total energy analysis scheme as well as the unit's ability to handle transient situations and variable turn-down ratios. There have been significant advances in many technological areas appropriate to the total energy analysis, and this section is intended to cite various work that would be relevant in subsequent development of the research.

A state of the art appraisal of power metering may be found in ref. 302. The required control circuit would be taylored to the particular application, power metering would probably be a second order effect in the overall efficiency. Of much greater significance, in the case of gaseous feedstocks, is the electrical/chemical energy utilised for gas purification and pumping to the appropriate upstream pressure dictated by the unit and the application.

For stationary natural gas fired pumping engines these calculations would not be as critical when the appropriate feedstocks, for example methane, are already available at high pressure. For other applications, where the plasma feedstock is to come from either the fuel, air or cooling water to form a self contained unit, along with the prime mover, these calculations would be critical.

The power required for purification and compression will be a function of the required purity, maximum pressure, required flow rate and compressor efficiency. The final overall system efficiency is a function of the direct product of the individual component efficiencies (plasma generator, compressor, purifier etc.). For steady state operation, at high flow rates, the pumping powers will be significant and could possibly be greater than that of the generator itself. For conditions such as intermittent ignition plasmas high pressures would be required but the volumetric flow rate would be low.

In the case of hydrogen feedstocks it is relatively easy to envisage low grade exhaust heat driving interstitial metal hydrides (32) or for small flow rates, electrolysis of water with the hydrogen readily separated by effusion or thin sheet diffusion. (Helium is separated from natural gas by diffusion through thin sheets of pyrex glass and silicone rubber is extremely permeable to H_2 (66)). For larger flows controlled pyrolysis of liquid fuels to produce H_2 and gaseous hydrocarbons, especially methane, is appropriate.

Figure 6.20h shows the plasma generator operating on a methane feedstock. Figure 6.20g is for the same feedstock with no power to the plasma generator. Rapid expansion of the hydrocarbon through the anode causes air entrainment, so lift-off can be seen from the generator in Figure 6.20g. Two things may be observed by comparison of these Figures. Firstly, the flame is anchored to the generator in Figure 6.20h and secondly, there is enhanced radiative emission from the flame in combination with the plasma.

The plasma generator, in its present form, could be used as a burner to handle a high turndown ratio (ratio of maximum to minimum load or throughput) and to control the emissivity of the flame in a furnace application. There is evidence that suggests that carbon produced in hydrocarbon arcs occurs by a different mechanism to that producing

the other main pyrolysis products of methane, namely H_2 and C_2H_2. These products, along with H-atoms generated, may enhance the flame stabilisation and facilite the increased throughput. One volume of methane produces 4 volumes of H-atoms in comparison to 2 from hydrogen. The red H-atom afterglow shown in Figure 6.20e, for a pure H_2 feedstock, is probably obscurred here, due to the continuum emission from carbon.

The situation for a nitrogen feedstock is more serious. Although present in air at 79% the physical similarity with oxygen has meant that separation has normally had to be achieved commercially by distilation of liquid air. Combustion itself is a process that converts a diatomic oxide (O_2) into two triatomic ones (H_2O and CO_2). In principle, extraction of these two components from the exhaust gas of a stoichiometric mixture is easy with either cooling and/or a molecular sieve, leaving a gas that would be essentially nitrogen. However,consideration of the material in Chapters 1 and 4 has shown that one of the main potentials for an N_2 feedstock is under those conditions which run with excess air and have precluded the use of reduction or 3 way catalysts in the past. Since these exhaust gases will always have high O_2 concentrations such a scheme is therefore less attractive unless the system comes under high load thus reducing the oxygen concentration in the exhaust; this of course has the problem normally associated with reduced O_2 - that of increased soot emissions.

If the exhaust gas were considered as having undergone the first phase of deoxygenation during combustion followed by a second stage that involved, for example, membrane separation then such particulate material would of necessity have to be removed from the feedstock before passage to the membrane. There are a variety of possible schemes to remove such particulate material other than direct filtering, electrostatic precipitation (White) or using spiral soot oxidation (Figure 9

of ref. 95 are two examples). Naturally, any such process adds to the cost and power requirement of the overall system.

The energy intensity of air liquefaction as a means of separating oxygen and nitrogen from air has led a number of companies, notably General Electric (66, 252) and Bendix Corporation (156) to consider various non-cryogenic separation techniques based on membranes or molecular sieves (see Figure 8.1). The main incentive for these has been the need for oxygen enrichment of air for medical and combustion purposes. An oxygen enriched stream naturally means a corresponding oxygen depleted, or nitrogen enriched one (see also Appendix 1). P. J. Gardner (156) working in this area kindly showed the author results of research work covering gas flows up to 10 CFM with pumping powers up to 3.5 HP depending on enrichment and product flow. He also showed results with nitrogen streams of purities in excess of 98%. (Because this work was of a proprietary nature full details were not available.)

Since that time there have been developments in reversible oxygen coordination compounds based on Magnanese (II) salts (331) that mimic the function of the blood pigment haem in the respiratory process. These compounds are therefore able to reversibly extract oxygen from air, leaving a stream of high purity nitrogen, and oxygen that may be deposited, instead of to myoglobin in the biological system, into the combustion air.

Obviously, from the feedstock flow aspect of the power consumption of plasma generators in the total power analysis, this component is going to be strongly linked to the feedstock. Particular application, purity, flow rates and pressures, as well as available technology will all influence practical applicability. It is evident that, at least as far as low power separation of nitrogen from air is concerned, the technology is moving very rapidly.

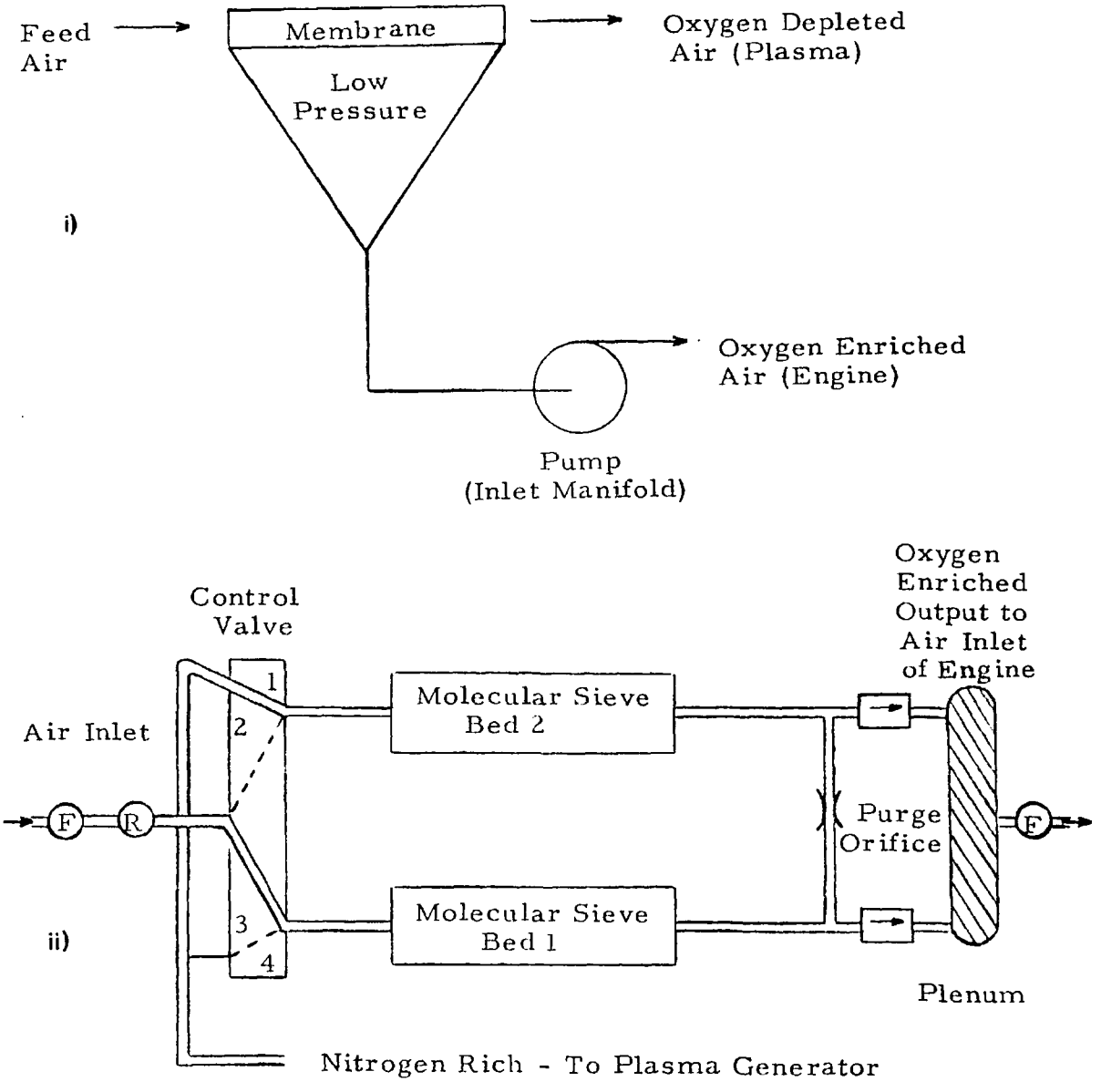

Figure 8.1 - Two schemes for non-cryogenic separation of O_2/N_2 from air i) A General Electric method (from ref. 66) ii) A Bendix method (from ref. 156).

The use of ammonia (or NH_i) as an agent to remove NO has been considered both theoretically (171) and for practical use (285, 314). It should be stated that production of ammonia (Haber process) is very energy intensive, using high temperature (880°C) and pressures (1000 Atm) as well as catalysts. The high powers required for nitrogen plasma production are due to the high dissociation energy (9.76 eV) of the N_2 molecule. Until Nature's method of nitrogen fixation may be duplicated on a sufficient scale any method of production of ammonia from hydrogen and nitrogen will always require operating conditions of high temperatures and pressures.

Injection of ammonia into exhausts may give rise to undesirable amino compounds as well as, with high sulphur fuels, ammonium sulphate aerosols. Although ammonia contains both N and H-atoms in a neutral molecule, inclusion at the combustion stage to generate species that may remove NO and enhance flame propagation could be considered. However, one would hope that under conditions where the H-atoms were required the NO concentration would be sufficiently low not to require the energy intensive N-atom.

For large scale combustion applications, where the potential of ammonia has been demonstrated, the possibility exists that, if hydrogen were obtained from one source as previously outlined and nitrogen from air, the plasma generator could serve as a reactor to synthesise NH_3 in-situ from these feedstocks at a rate determined by the combustion condition.

DIESEL VERSUS OTTO

Considerable attention has been focused on comparisons highlighting some of the advantages of both engine types. In the absence of emission constraints (that are very difficult to resolve with the inherent problems of diffusion controlled heat release, in the absence of an al-

cohol) Diesel systems have a higher brake thermal efficiency (153, 340, 380). Generally, due to the diffusion controlled heat release, the specific powers are less for Diesel engines, but modes of boosting are possible (308). The reduced thermal efficiency that prechambers generate is explainable thermodynamically (442) and yet such prechambers are the design many 'novel' Otto stratified charge engines are heading towards. The lower cost of Otto engine fuelling systems and engine manufacture, the inherently better mode of heat release and the demonstration of removal of a limiting compression ratio (Appendix 2) and the ability to use renewable alcohol fuels readily, warrants further study to utilise low power electrical interactions in the form of H-atom plasma power control of the rate of burn. Potentially, electrostatic carburation could generate an aerodynamically stratified charge in a quiescent open chamber, unthrottled system. The initial phases to justify such an effort have been shown in this study.

Further work in this area could include theoretical studies involving use of established theories of ignition and propagation (301, 396, 477) with codes that predict cycle efficiency and emissions (201) and reactor performance (289, 346) to investigate the perturbation by a pulse of hot H-atoms on heat release, with its economy and resultant emission repercussions.

An immediate possible practical application of the plasma generator resulting from this work is in solving the emission and economy problems of large natural gas fired pumping engines (461), where all the basic feedstocks and requirements are present already.

Although some energy analysis calculations are critical of the economy of arc plasma combinations (57) that is because the considerations for these calculations have been on general aspects of heating overlooking the possibility of specificity, with respect to species generated, not readily available by any other methods. Before this

specificity may be utilised the problem needs to be defined and the limiting species identified. For practical engine situations that is aided by fully characterising the combustion plasma as well (353).

It has been the primary objective of this study to try to control the combustion at the heat release stage to avoid elaborate cleaning up procedures afterwards, that involve larger power requirements. Novel burner systems from previous studies have been described (452) and a further electrical method of improving combustion is via electrofluidised beds (115).

This thesis study highlights the following three electrical methods as worthy of further practical consideration. They appear to be the lowest power interactions that maximise positive effects on economy and emissions.

i) Electrostatic carburation of alcohol fuels.

ii) Electrostatic modification of Diesel ignition delay intervals with alcohol fuels.

iii) H-atom plasma injection for heat release rate control in a quiescent aerodynamically stratified charge.

All aspects of electrical interaction are worthy of further experimental and theoretical studies for practical application.

APPENDIX 1 - Calculations relevant to nitrogen purification and extraction from air.

Consider the O_2/N_2 separation process (eg. Figure 8.2) to be represented schematically as follows:-

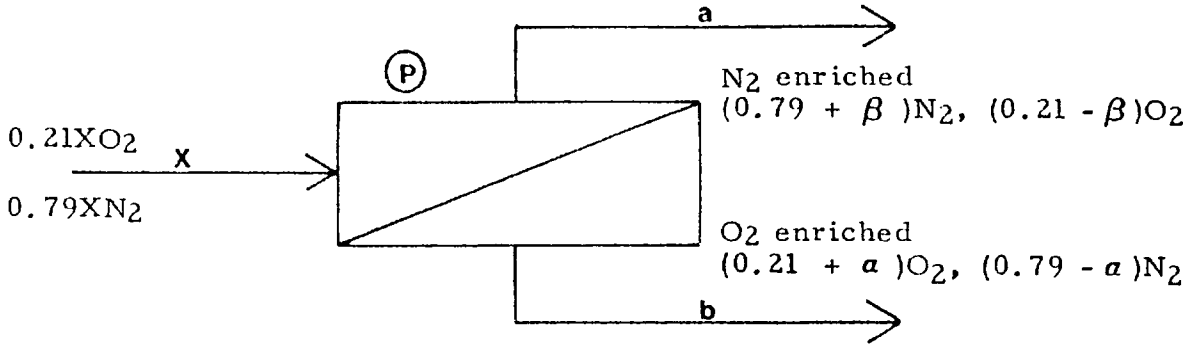

Let X = input flow rate of air

a = output flow rate of N_2 enriched gas

b = output flow rate of O_2 enriched gas

β = enrichment coefficient of N_2

α = enrichment coefficient of O_2

B = % O_2 on b side

A = % N_2 on a side

P = operating pressure

Data supplied is mainly in terms of O_2 concentration on the O_2 enriched side ie. $B = 0.21 + \alpha$ $(A = 0.79 + \beta)$

Conservation Considerations

Conservation of air $X = a + b$ 1

Conservation of N_2 $0.79X = (0.79 + \beta)\,a + (0.79 - \alpha)\,b$ 2

Conservation of O_2 $0.21X = (0.21 + \alpha)\,b + (0.21 - \beta)\,a$ 3

Reality Conditions

Always $\alpha \leq 0.79$ $\beta \leq 0.21$

$(0.21 + \alpha)\,b \leq 0.21X$ $(0.79 + \beta)\,a \leq 0.79X$

$Bb \leq 0.21X$ $Aa \leq 0.79X$

$$\eta_b = \frac{Bb}{0.21X} \leq 1 \qquad \eta_a = \frac{Aa}{0.79X} \leq 1$$

For nitrogen plasma feedstock values of A are required for different values of a and b. Most of the data available (66, 156, 252) has been given for the b side. Therefore, rearranging 3 in terms of:-

$$0.21X = Bb + 0.21a - a\beta$$

$$\text{Gives } \beta = \frac{Bb + 0.21a - 0.21X}{a}$$

Minimum pumping power requires knowledge of total volumetric flow (X) for required purity at desired stream flow rate (a) and requires knowledge of separation efficiency at the operating pressure of the separator.

APPENDIX 2 - Efficiency of idealised Diesel cycle in the limit as cut-off ratio tends to unity, and its significance.

The idealised Diesel and Otto cycles differ in that the former adds heat at constant pressure, while the latter at constant volume.

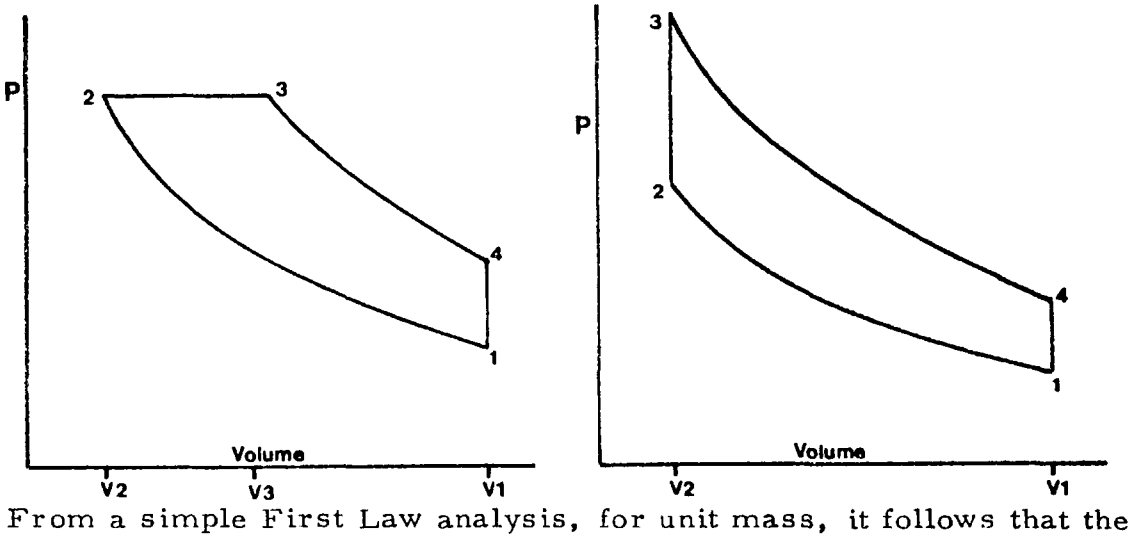

From a simple First Law analysis, for unit mass, it follows that the efficiencies of each are:-

$$\eta_{Diesel} = 1 - \frac{1}{r_v^{(\gamma - 1)}} \left\{ \frac{r_c^{\gamma} - 1}{\gamma (r_c - 1)} \right\} \qquad 1$$

$$\eta_{Otto} = 1 - \left\{ \frac{1}{r_v^{(\gamma - 1)}} \right\} \qquad 2$$

where $r_v = v_1/v_2$ (compression ratio)

$r_c = v_3/v_2$ (cut-off ratio)

It is apparent that for the Otto case the efficiency is only a function of two cycle properties, the compression ratio and the ratio of specific heats ($\gamma = C_p/C_v$) of the working fluid. The Diesel cycle efficiency, however, is linked to the amount of heat added ie. r_c. As r_c increases, η decreases. Obviously when $r_c = 1$ the expression for the Diesel efficiency becomes badly defined. It is interesting therefore to see what happens to the efficiency as $r_c \Rightarrow 1$.

Since r_c is only present in the bracketed part of equation 1

$$\text{let} \quad \left\{\frac{r_c^{\gamma} - 1}{\gamma(r_c - 1)}\right\} = \Delta \qquad \text{and examine } \Delta \text{ as } r_c \Rightarrow 1$$

$$\equiv \text{let} \quad r_c = 1 + \delta \qquad \text{and examine } r_c \text{ as } \delta \Rightarrow 0$$

$$\Delta = \frac{(1 + \delta)^{\gamma} - 1}{\gamma(r_c - 1)} \quad \text{as} \quad \delta \Rightarrow 0, = \frac{1 + \gamma\delta - 1}{\gamma(r_c - 1)} = \frac{\gamma\delta}{\gamma(r_c - 1)} = 1$$

$$\therefore \text{ as } r_c \Rightarrow 1, \quad \eta_{\text{Diesel}} \Rightarrow 1 - \left\{\frac{1}{r_v^{(\gamma - 1)}}\right\} = \eta_{\text{Otto}}$$

One can see therefore that as the limit of no heat addition is approached the Diesel cycle efficiency tends to that of the Otto, ie. the more efficient cycle. The effect of the cut-off ratio is to lower the effective compression ratio.

While it is true that in practical engines there is the possibility of the Diesel engine operating at higher compression ratio, the optimum value of around 12.5 to 14.5, before increasing frictional losses lower the brake efficiency (189, 305) is only available in direct injection Diesel engines. Indirect injection engines are as far to the right of the optimum in the graph of brake efficiency vs. compression ratio as early Otto engines are to the left.

Recent combustion chamber design innovations that have raised the knock limited compression ratio to those nearer the optimum values have been reported (297, 298, 299) with corresponding brake specific efficiencies exceeding those of Diesel engines.

Naturally the pumping losses of throttled engines exceed those with quality power control and comparison based on emissions or cost of the prime mover is not the purpose of this appendix.

The ratio of specific heats is the final variable in equations 1 and 2. Simple kinetic theory leads one to expect values of γ for mono, di and triatomic gases of 5/3, 7/5 and 9/7 respectively. Apart from ad-

vantages of reduced heat transfer coefficient there are advantages to using a monatomic gas (ie. helium for closed cycle units) to obtain gains in efficiency (the Joule cycle efficiency = $1 - \left\{\left(\frac{1}{r}\right)^{(\gamma - 1)/\gamma}\right\}$, r = pressure ratio, P_2/P_1). The ideal Joule cycle efficiency has simi-variables to that of the Otto cycle, and closed cycle Brayton units using helium ($\gamma = 1.67$) have been built. However, for open cycle systems such gases are impractical.

Because air is essentially a diatomic gas while combustion products contain triatomics, it is advantagous to operate lean of stoichiometric to increase the value of γ for the working fluid. Further advantages are: lower dissociation losses in the working fluid that serve to lower the effective compression ratio, reduced heat losses from the combustion chamber and the ability to raise the KLCR which increases as AFR is increased.

The potential that plasma jet ignition offers for controlled rates of heat release in very lean mixtures would further aid the brake efficiency by dealing with the major loss associated with quantity power control via the throttle.

It is more realistic, because constant pressure or constant volume heat addition is purely imaginary, to consider any heat addition being made up of a constant volume followed by constant pressure component. For the sake of completeness of this appendix the efficiency of such a cycle (the mixed or dual) is included here as:-

$$\eta_{mixed} = 1 - \frac{1}{r_v^{(\gamma - 1)}} \left\{ \frac{r_c^{\gamma} r_p - 1}{(r_p - 1) + \gamma r_p (r_c - 1)} \right\} \qquad 3$$

r_p in equation 3 is therefore P_3/P_2 with all the cycle stages numbered in the format of compression being state $1 \longrightarrow 2$.

APPENDIX 3 - Calculations relevant to excess enthalpy combustion.

The importance of an excess enthalpy concept in combustion waves as a hypothesis in correlation of ignition energies was suggested in the 1930s (Lewis and von Elbe). Recently the excess enthalpy concept has been applied to various burner geometries with a view to increasing heat release rates in lean mixtures without corresponding dilution with exhaust products. The basic successful design used in the work of refs. 279, 280 and 281 is shown in Diagram 1, and data that demonstrated the ability to burn below the conventional 'limit of flammability' is shown in Diagram 2.

Some interesting thermodynamic calculations have been attempted (180) and analytical studies of combustion in such heat exchangers made (236). Experimentally, the work on 'Swiss Roll' burners showed a minimum final combustion temperature for methane at around 1400 K. It was, experimentally independent of flow velocity over the ranges used, and approximately similar in value for the two hydrocarbon fuels used. The values quoted are CH_4 = 1403 K, C_3H_8 = 1295 K.

It was relevant to the electrical methods work, to ensure that the interaction power is kept as low as possible, to investigate what the system can possibly achieve without any electrical interaction. The excess enthalpy work, already published, has shown what can be done when reactants are preheated without dilution with exhaust products. Dilution had previously been a limiting factor in the control of heat release rates. Equilibrium thermodynamics at combustion temperatures and rate constrained heat release rates are the two main limiting factors that may be resolved with a plasma interaction. The possibility of an excess enthalpy interaction with a plasma jet led to the work of this appendix. An attempt was made to determine if the

minimum value of the thermal dam temperature, observed experimentally, was a 'fundamental constant' for the system, or may be explained by consideration of the geometry and flow characteristics of the burner, and characteristics of the fuel air mixture.

The following simple model was developed along a 'characteristic time' approach as a first approximation. The basic model concept is shown schematically in Diagram 3 for the Swiss Roll configuration. Considering the temperature profile of Diagram 3 then:-

τ_1 = induction time at temperature T_1

τ_2 = induction time at temperature T_2

τ_{cc} = residence time of element in the combustion volume V_{cc}.

The object was to try to calculate the minimum height of the thermal dam, that corresponds to the value of the temperature T_2, based on the form of the temperature profile that was observed experimentally and shown in Diagram 3.

Initially two basic assumptions were made, in the format of the model presented here:-

i) Diffusion effects are neglected - The basis for this is the assumption of very high turbulence levels in V_{cc}. For example even though the burning velocity of a limit mixture of methane/air is 0.05 m s^{-1} it was observed that in these burners, even at 1/5 of the limit methane concentration, stable combustion was obtained with flow velocities estimated at 2 to 6 m s^{-1} (281).

ii) Instantaneous flame kinetics - The basis for this, is the assumption that the induction period is much greater than the interval in which the main heat release takes place, so, the total heat release interval is equal to the induction period.

Based on these assumptions two conditions are therefore required for a stable situation as shown in Diagram 3.

Condition 1 $\tau_1 \gg \tau_2$ - This is required in order that a ther-

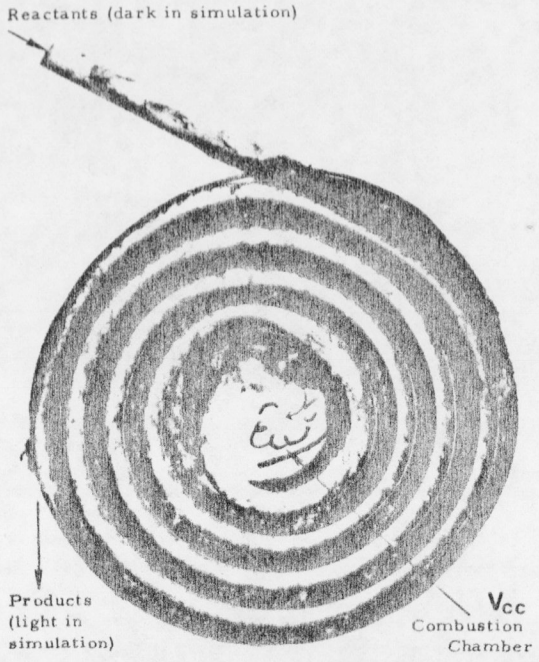

Diagram 1

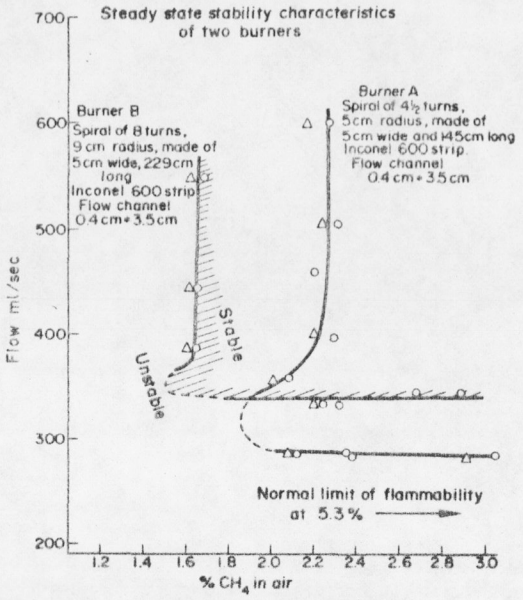

Diagram 2

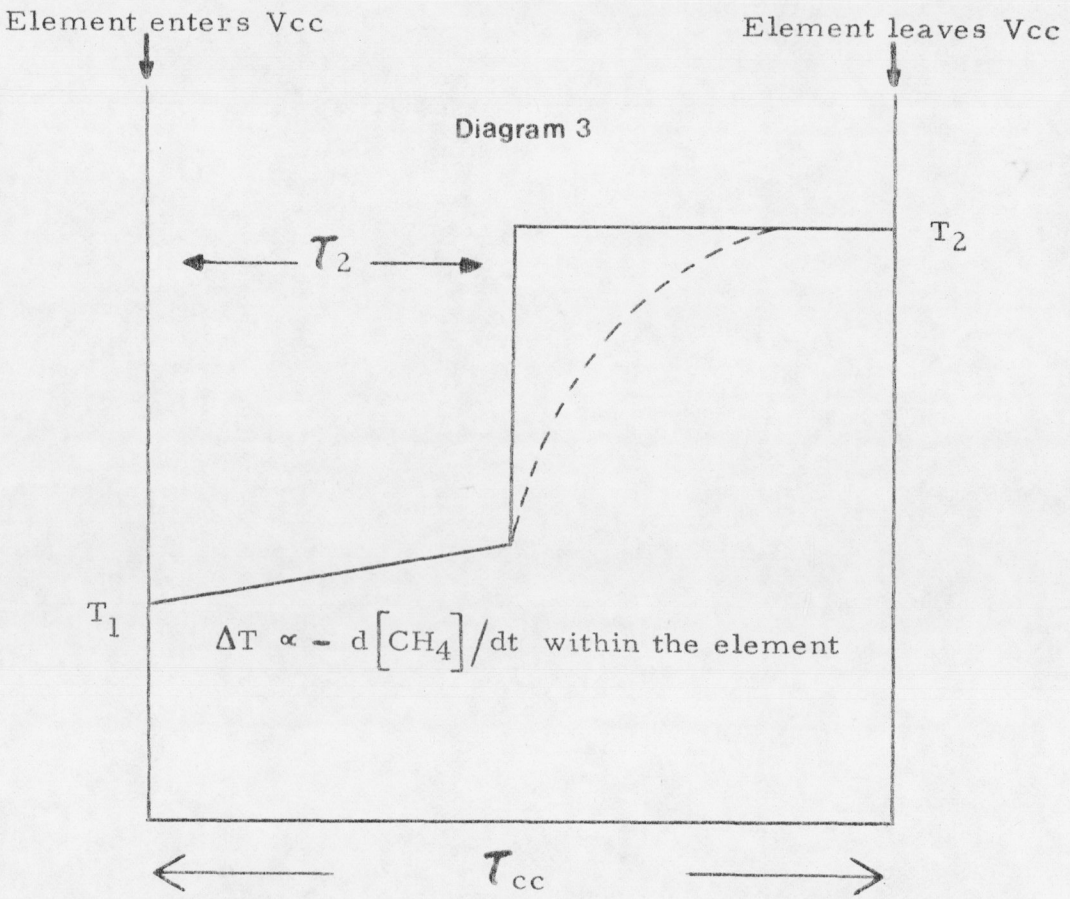

Condition ② $T_2 \leqslant T_{cc}$ with instantaneous flame kinetics minimum

T_2 such that $T_2 = T_{cc}$

mal dam may be established. The activity of the reacting system is therefore important in the form of $\partial\left(\exp(^{\Delta E}/RT)\right)/\partial T$. The importance of activation energies in this context is described in ref. 443. Data relevant to this expression is presented later.

Condition 2 T_2 $T_{2\,min}$ must ensure that $\left.\begin{matrix}\tau_2 \leq \tau_{cc} \\ \tau_2 = \tau_{cc}\end{matrix}\right\}$ is when - This is required so that combustion takes place within the volume V_{cc}. This condition combines chemical reactivity and flow rate properties of the system.

Induction data for various fuels could then, in principle, calculate the value of T_2. The appropriate data for H_2, C_2H_4, C_3H_8 and CH_4 was obtained from the literature (48, 69, 70, 119, 129, 163, 195, 277, 381, 392, 393, 414, 454), mainly from shock tube studies, where the induction period is defined as the interval between heating of the gas by the reflected shock wave and the onset of rapid chemical reaction (seen by a photodetector etc.).

As in all experiments where an interval (or rate constant) is measured as a function of temperature, an Arrhenius type plot (to linearise the data and obtain 'parameters', and extrapolate to different experimental conditions) of log (τ) as a function of inverse temperature for various systems was presented. This leads to an empirical expression as follows:-

$$\tau = \frac{A \exp(^{\Delta E}/RT)}{[\text{oxidant}]^a \; [\text{fuel}]^b \; [\text{inert}]^c}$$

where τ = induction time (secs)

$[\;]$ = molar concentration (moles ml^{-1})

A = apparent pre-exponential factor ($s/mole\ ml^{-1})^{a+b+c}$)

E = apparent activation energy (cal $mole^{-1}$)

R = gas constant (cal $mole^{-1}\ K^{-1}$)

T = temperature (K)

a, b, c = correlation index

For the CH_4/O_2/inert system, an unweighted best fit from the available data yielded:-

$$\tau = \frac{5.85E\text{-}17 \ \exp(45940/RT)}{[O_2]^{1.37} \ [CH_4]^{-0.17}}$$

Two unknowns at this stage were the pressure to be used (which has an effect mainly on the reactant concentrations) and the value of V_{cc}. If all the combustion took place in the chamber then V_{cc} had a maximum value of 20 cc. The value for this was initially estimated at 10 cc, and it is the weakest point in the present treatment. Methods to solve this problem will be shown. The flow rate of reactants, f, was taken as 0.3 to 1.1 l s^{-1} (279); $\tau_{cc} = V_{cc}/f$. The temperature and pressure rise effects in the burner were assumed to compensate in the reactant concentrations.

The concentrations of methane considered were from 2 to 5% in air. Not unexpectedly the most important factor affecting τ in the parametric study was the value of T. In regard to condition 1, Diagram 4 shows the behaviour of log τ vs. temperature, for the fuels used in the experimental work of, for example, ref. 279 where the fuels used were methane and propane, and it can be seen quite clearly that condition 1 ($\tau_1 \gg \tau_2$) is satisfied. This is not true for hydrogen or ethylene.

While it may be possible to generate a thermal dam for H_2 and C_2H_4 under appropriate conditions, Diagram 4 suggests that these conditions are not the same as those for CH_4 or C_3H_8. It was observed experimentally by one of the authors of ref. 279 (SAL) that H_2 would not burn stably in the type of burner shown in Diagram 1. The explanation was that, due to filamentary burning resulting from the differential diffusion coefficient of fuel (H_2) and oxidant, a stable flame

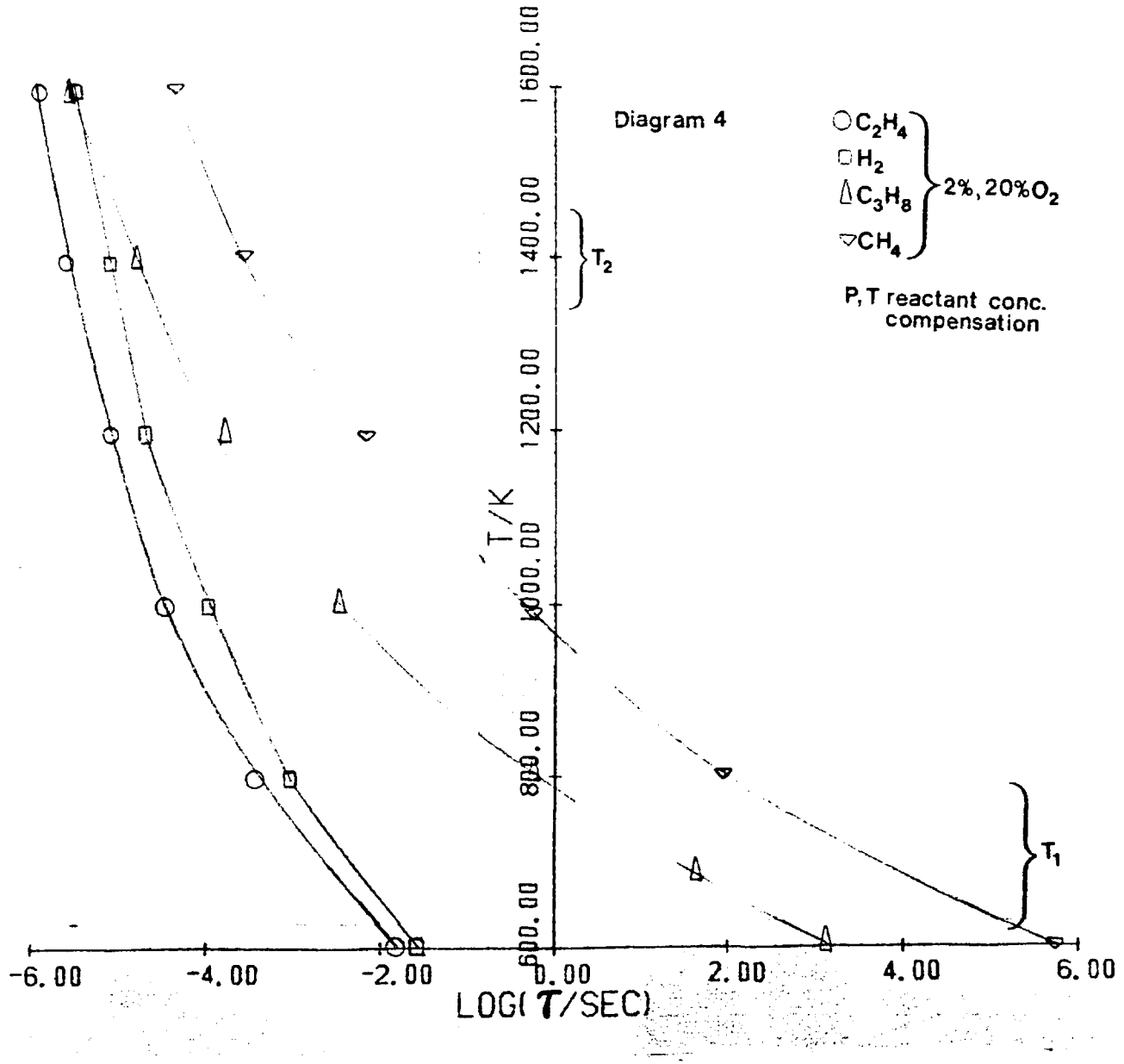
Diagram 4
C_2H_4
H_2
C_3H_8
CH_4
2%, 20%O_2
P, T reactant conc. compensation
T_2
T_1
T/K
1600.00
1400.00
1200.00
1000.00
800.00
600.00
-6.00
-4.00
-2.00
0.00
2.00
4.00
6.00
LOG(τ/SEC)

front was not maintained within the combustion chamber. Lean limit methane/air flames however, also exhibit the characteristic of discontinuous flame fronts (Gaydon and Wolfhard) and the possibility of the combustion of such mixtures being aided in 'Swiss Roll' burners by small quantities of H_2 present, generated within the combustion chamber, to augment the lean limit combustion of methane may be possible. Diagram 4 however indicates clearly that ethylene (that does not have the large differential diffusion coefficient with respect to oxidant) would not sustain stable combustion in the type of burner shown in Diagram 1, with the same temperature profiles obtained for C_3H_8 and CH_4.

So far the basic assumption of the value of V_{cc} has not been used in this section, an estimate of τ_{cc} is required to calculate $T_{2\,min}$.

For 2% CH_4 using $V_{cc} = 10_{cc}$, and the experimental flows of ref. 279, the following results were obtained:-

$f/l\,s^{-1}$	0.3	0.5	0.7	0.9	1.1
τ_{cc}/s	3.33E-2	2.0E-2	1.43E-2	1.11E-2	9.09E-3

The empirical induction delay equation was solved for the condition $\tau_{cc} = \tau_2$ to obtain T_2. The results are shown in Diagram 5 below. It can be seen that the value is close to that observed experi-

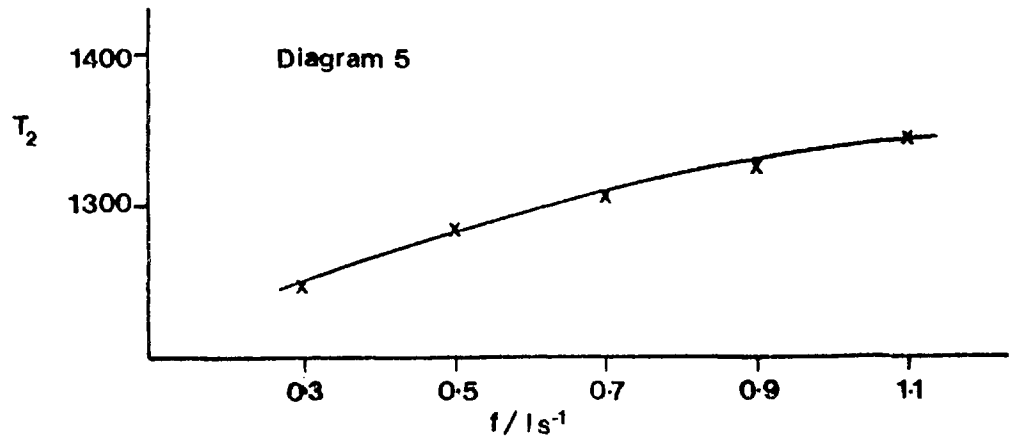

mentally for methane, with a low flow rate dependence that appears to level off towards 1400 K. Similar calculations for C_3H_8 suggest a lower dam temperature, nearer 1200 K.

The calculations shown here are by no means exhaustive, and merely attempt to indicate the potential, in design of such burners, of comparing residence times with ignition delay times at various locations along the spiral. This comparison may be done for various fuels, mixture strengths and temperature profiles within the burner.

The two basic conditions for stability described in this appendix may be met by any mechanism that either modifies the residence time, or the induction time. One mechanism for this, for example, would be to reduce the cross sectional area, and thus the residence time, of an element of gaseous reactants along the spiral pre-heat path to the combustion chamber. This could be done in combination with, or instead of, external programming of the pre-heat temperature profile.

The calculations have indicated that, with the burner size, geometry, flow rates and feedstocks used in the work of ref 279, the stability conditions specified in this appendix were met. It is not suggested that H_2 and C_2H_4 fuels could not be burnt under excess enthalpy conditions, only that the geometry and temperature profiles would need to be different to that of CH_4 and C_3H_8, to meet the general stability conditions 1 and 2.

One feature of these calculations has been the calculation of a minimum thermal dam temperature that was close to that observed experimentally, for both CH_4 and C_3H_8. The calculation of this temperature has been based on a realistic estimate of V_{cc} but the exact value for V_{cc} is never known with certainty. This is a weakness in the present treatment and consideration was given to ways in which this could be solved. Two possible methods are:-

i) Determine V_{cc} experimentally - An estimate of V_{cc} could

be made optically, or via a saturation current measurement (150).

ii) Eliminate V_{cc} from the theory - This is possible, at least in principle, by the use of gaseous additives known to modify the induction period. NO_2 is particularly effective for the CH_4/O_2 system, with reductions in τ of 1/2 to 1/3 possible (108). The calculations should be expressed in a form that establishes a lowering of the value of T_2 (eg. Diagram 5) as a function of the reduction in induction period, with increasing concentration of NO_2 in the reactants. Assuming that V_{cc} is not modified by the addition of NO_2, V_{cc} then cancels out in the expression for ΔT_2. Experimentally this value may be determined and compared with the calculated value. With NO_2 present the thermocouples should be coated, and all intrinsic errors (246) minimised. This experiment, particularly, would lend support to the model presented here and is worth further study.

Calculation of the induction time from first principles is possible from knowledge of the basic kinetic equations for methane oxidation (454), and turbulence properties of the system that relate to ignition delay and combustion intervals (203). This is also worth further work particularly with respect to tayloring reaction profiles within excess enthalpy burners.

REFERENCES

1. ABDEL-GAYED R.G., BRADLEY D. and McMAHON M., 17th Symposium (International) on Combustion, Leeds, (1978).

2. ABRAHAMSON J., Nature, 266, 323 (1977).

3. ADAMS T.G., SAE. 780631.

4. ADAMS V.W., Her Majesty's Stationery Office, CP743, (1964).

5. ADAMS V.W., LORD W.T., GUILE A.E. and NAYLOR K. A., Proc. IEE., 114, 1556 (1967).

6. ADCOCK B.D. and PLUMTREE W.E., J. Quant. Spectrosc. Radiat. Transfer, 4, 29 (1964).

7. ADELMAN H.G., ANDREWS D.G. and DEVOTO R.S., SAE. 720693.

8. AIMAN W.R., Combustion Science and Technology, 15, 129 (1977).

9. ALBRECHT H., BLOSS W.H., HERDEN W., MALY R., SAGGAU B. and WAGNER E., SAE. 770853.

10. ALCOCK W.G. and MILE B., Combustion and Flame, 24, 125 (1975).

11. ALDER J.F. and MERMET J.M., Spectrochim Acta, 28B, 421 (1973).

12. ALI A.W., KUMMLER R.H., GILMORE F.R. and McGOWAN J.W., Naval Research Laboratory Memorandum Report 3920, February 1979.

13. AMES B.N., McCANN J. and YAMASAKI E., Mutation Research, 31, 347 (1975).

14. ANDREWS G.E. and BRADLEY D., Combustion and Flame, 18, 133 (1972).

15. ANDREWS G.E., BRADLEY D. and LWAKABAMBA S.B., Combustion and Flame, 24, 285 (1975).

16. ANON, Laporte Industries Limited, Report GC16.

17. ANON, SAE. Automotive Engineering, 78, 95 (1976).

18. AONO S., HOSAKA A. and INOUE M., SAE. 790743.

19. APPLETON J.P., Description of work carried out under NSF., Grant GK-33933, Mechanical Engineering Department, MIT., Cambridge, USA.

20. ARRIGONI V., CALVI G.F. GAETANI B. and GIAVAZZI F., SAE. 780153.

21. ASIK J.R., PIATKOWSKI P., FOUCHER M.J. and RADO W.G., SAE. 770355.

22. ASIK J.R., PIATKOWSKI P., FOUCHER M.J. and RADO W.G., Based on SAE paper 770355, Published by Automotive Engineering, p40, May 1977.

23. ASSOCIATED ENGINEERING DEVELOPMENTS, Advance Information Bulletin, PL304, April 1974.

24. AUSTEN A.E.W., C.A.V. Limited, Report No. C.29008, (1948).

25. BAILEY A.G., Sci. Progress, 61, 555 (1974).

26. BAILEY A.G. and BORZABADI E., Proceedings of the 3rd International Congress on Static Electricity, pla-lf, Grenoble, (1977).

27. BAILEY A.G. and CETRONIO A., J. Phys. D:Appl. Phys., 11, L23 (1978).

28. BAJOREK R., 3rd International Symposium on Plasma Chem., Limoges, (1977).

29. BALLAL D.R. and LEFEBVRE A.H., Private Communication, Professor Lefebvre, May 1978.

30. BARBER E.M. and MacPHERSON J.H. Jr., SAE. Quarterly Transactions, 4, 15 (1950).

31. BARTHOLOME E., Naturwissenschaften, 36, 171 (1949).

32. BEARD C.A., Ricardo Consulting Engineers, DP 20933, February 1976.

33. BEHRINGER K., Applied Physics, 20, 19 (1979).

34. BENNETT J.E. and BLACKMORE D.R., Chem. Commun., 1521, (1968).

35. BENSON S.W., J. Am. Chem. Soc., 87, 972 (1965).

36. BENSON S.W., Editor, International Journal of Chemical Kinetics Symposium No.1, (1975).

37. BERGHAUS B., US.Patent 3324027, (1967).

38. BERNHARDT W.E., (Volswagenwerk AG), General Motors Technical Center, October 1975.

39. BERTRAND C., DUSSART B. and VAN TIGGELEN P.J., 17th Symposium (International) on Combustion, Leeds, (1978).

40. BHATTACHARYYA K.K., KOK R. and BULANI W., Automotive Engineering, 78, 24 (1970).

41. BICKES R.W. Jr., NEWTON K.R., HERRMANN J.M. and BERNSTEIN R.B., The Journal of Chemical Physics, 64, 3648 (1976).

42. BIORDI J.C., LAZZARA C.P. and PAPP J.F., 14th Symposium (International) on Combustion, Pennsylvania, (1972).

43. BIORDI J.C., LAZZARA C.P. and PAPP J.F., Bureau of Mines RI 8029, (1975).

44. BLYHOLDER G., BINFORD J.S. and EYRING H., J. Phys. Chem., 62, 263 (1958).

45. BOFFA C., HEBERLEIN J. and PEENDER E., Warme-und Stoffubertragung, Bd. 4, 213 (1971).

46. BOLASNY R.E., US. Patent 4069665, January 1978.

47. BOLT J.A., SAE. SP-254, (1964).

48. BONI A.A. and PENNER R.C., Combustion Science and Technology, 15, 99 (1977).

49. BOSCH K.W. and VICKERS T.J., Spectrochim Acta, 28B, 85 (1973).

50. BOWEN I.G. and DAVIES G.P., Shell Petroleum Technical Report ICT/28, (1951).

51. BOWSER R.J., JAGGERS H.C. and WEINBERG F.J., Part I, BOWSER R.J., SANDHU S.S. and WEINBERG F.J., Part II, Combustion and Flame, 19, 135 (1972).

52. BOWSER R.J. and WEINBERG F.J., Nature, 249, 343 (1974).

53. BOWSER R.J. and WEINBERG F.J., Combustion and Flame, 18, 296 (1972).

54. BOWSER R.J. and WEINBERG F.J., Combustion and Flame, 27, 12 (1976).

55. BRADLEY D., The Institution of Electrical Engineers Colloquium, December 1977.

56. BRADLEY D. and CRITCHLEY I.L., Combustion and Flame, 22, 143 (1974).

57. BRADLEY D. and GUPTA M.L., Journal of the Institute of Fuel, p214, December 1977.

58. BRADLEY D. and IBRAHIM S.M.A., J. Phys. D:Appl. Phys., 6, 465 (1973).

59. BRADLEY D. and JESCH L.F., Combustion and Flame, 19, 237 (1972).

60. BRADLEY D. and MATHEWS K.J., Phys. Fluids, 10, 1336 (1967).

61. BRADLEY D. and SHEPPARD C.G.W., Combustion and Flame, 15, 323 (1970).

62. BROAD M.J., IEE Conference No. 141, p136, Automobile Electronics, (1976).

63. BRONFIN B.R., Symposium on Chemical Reactions in Electrical Discharges and General Papers, ACS, April 1967.

64. BROOME D. and KHAN I.M., Conference on Air Pollution Control in Transport Engines, The Institution of Mechanical Engineers, November 1971.

65. BROOME D. and WRIGHT M.J., Ricardo Consulting Engineers, DP20265, October 1975.

66. BROWALL W. and KIMURA S., General Electric Technical Information, May 1976.

67. BRUNETTI B. and LIUTI G., 2nd Simposio di Dinamica delle Reazioni Chimiche, Padova, p83, December 1975.

68. BULEWICZ E.M., EVANS D.G. and PADLEY P.J., 15th Symposium (International) on Combustion, Tokyo, (1974).

69. BURCAT A., Combustion and Flame, 28, 319 (1977).

70. BURCAT A., Combustion and Flame, 30, 327 (1977).

71. BURGESS D.D., Transcript of an Introductory Post-Graduate IC. Lecture Course, February 1967.

72. BURGETT R.R., LEPTICH J.M. and SANGWAN K.V.S., SAE. 720007.

73. BURGOYNE J.H., Proc. Roy. Soc., A175, 539 (1940).

74. BURT R., ROBERTS D.D. and WOODWORTH J.A., Conference entitled Fuel Economy and Emissions of Lean Burn Engines, The Institution of Mechanical Engineers, London, June 1979.

75. CALCOTE H.F. and FELDER W., 3rd International Symposium on Plasma Chem., Limoges, (1977).

76. CALIFORNIA STATE LEGISLATURE, Final Report, June 1979.

77. CALLENDAR H.L., Engineering, 123, (1927).

78. CAMPBELL I.M. and THRUSH B.A., Proc. Roy. Soc., A296, 201 (1967).

79. CAMPBELL I.M. and THRUSH B.A., Proc. Roy. Soc., A296, 222 (1967).

80. CAPITELLI M. and DILONARDO M., Pre print of an article submitted to Journal De Physique, paper communicated to author by E.R. Fischer, October 1978.

81. CASHIN K.D., CHINTAPALLI P.S.R.K., VANPEE M. and VIDAUD P., Combustion and Flame, 22, 337 (1974).

82. CASSELS G.R., DYER W.G. and ROLES R.T., 3rd International Symposium on Alcohol Fuels Technology, California, Vol. II, paper 3, May 1979.

83. CERKANOWICZ A.E., Air Force Office of Scientific Research, Scientific Report AFOSR-TR-74-0153, AD 774525, November 1973.

84. CERKANOWICZ A.E., STEVENS J.G. and BARTOK W., Chemical and Physical Processes in Combustion, Eastern Section of the Combustion Institute, Technical Meeting, Fall 1978.

85. CERNANSKY N.P. and NIZAMI A.A., 17th Symposium (International) on Combustion, Leeds, (1978).

86. CHESTER A.N., Proceedings of the IEEE., 61, 414 (1973).

87. CLARKE J.F., Proc. Roy. Soc., A307, 283 (1968).

88. CLEMENTS R.M. and SMY P.R., Journal of Applied Physics, 40, 4553 (1969).

89. CLEMENTS R.M. and SMY P.R., Journal of Energy, 2, 53 (1978).

90. CLEWELL D.H. and KOEHL W.J., Approaches to Automotive Emissions Control, p40, see R.W. Hurn under Bibliography.

91. CLYNE M.A.A. and STEDMAN D.H., Trans. Faraday Soc., 62, 2164 (1966).

92. CLYNE M.A.A. and THRUSH B.A., Proc. Roy. Soc., 269A, 404 (1962).

93. COCHRAN R.A. and FAY J.A., Department of Mechanical Engineering Massachusetts Institute of Technology, Fluid Mechanics Laboratory Publication No. 70-1, February 1970.

94. COLLINS D., Ricardo Consulting Engineers, DP 77/757, June 1977.

95. COLLINS D., CUTHBERTSON R.D., GAWEN R.W. and WHEELER R.W., SAE. 750904.

96. COLVER G.M. and WEINBERG F.J., Proc. Roy. Soc., A326, 375 (1972).

97. COTTON D.H., FRISWELL N.J. and JENKINS D.R., Combustion and Flame, 17, 87 (1971).

98. COX J.B., JONES A.R. and WEINBERG F.J., Proc. Roy. Soc., A325, 269 (1971).

99. CRAMAROSSA F., FERRARO G. and MOLINARI E., J. Quant. Spectrosc. Radiat. Transfer, 14, 419 (1974).

100. CREIGHTON J.R., SAE. 790249.

101. CREITZ E.C., Physics and Chemistry, 65A, 389 (1961).

102. CREITZ E.C., and LEE T.J., J. Phys. Chem., 67, 360 (1963).

103. CROWLEY J.M., Journal of Applied Physics, 48, 145 (1977).

104. CULP G., MS Thesis presented to the Faculty of the School of Engineering of the Air Force Institute of Technology Air University, August 1964.

105. CURRIE C.L. and THRUSH B.A. & S.J., Trans. Faraday Soc., 64, 390 (1968).

106. CURRIE J.H., GROSSMAN D.S. and GUMBLETON J.J., SAE. 790173.

107. CUTHBERTSON R.D., STINTON H.C. and WHEELER R.W., SAE. 790814.

108. DABORA E.K., Combustion and Flame, 24, 181 (1975).

109. DALE J.D., SMY P.R. and CLEMENTS R.M., Combustion and Flame, 31, 173 (1978).

110. DALE J.D., SMY P.R. and CLEMENTS R.M., SAE. 780329.

111. DALE J.D., SMY P.R., WAY-NEE D. and CLEMENTS R. M., Mechanical Engineering, p46, December 1976.

112. DALE J.D., SMY P.R., WAY-NEE D. and CLEMENTS R. M., Combustion and Flame, 30, 319 (1977).

113. DARRAH R., USAF. Technical Report AFAPL-TR-77-85, May 1977.

114. DEAN A.M., STEINER D.C. and WANG E.E., Project Squid, Technical Report UMO-2-PU, May 1977.

115. DIETZ P.W., General Electric Report No. 77CRD107, May 1977.

116. DIXON-LEWIS G., Combustion and Flame, 36, 1 (1979).

117. DIXON-LEWIS G. and SIMPSON R.J., 16th Symposium (International) on Combustion, Cambridge, USA., (1976).

118. DOMBROWSKI N. and WOLFSOHN D.C., Aerosol Science, 2, 405 (1971).

119. DORKO E.A., BASS D.M., CROSSLEY R.W. and SCHELLER K., Combustion and Flame, 24, 173 (1975).

120. DOWNS D., STREET J.C. and WHEELER R.W., Fuel, 32, No. 3, July 1953.

121. DOWNS D., WALSH A.D. and WHEELER R.W., Phil. Trans. Roy. Soc., Series A, No. 870, 243, 463 (1951).

122. DRYER F.L. and GLASSMAN I., 14th Symposium (International) on Combustion, Pennsylvania, (1972).

123. EBERSOLE G.D. and MANNING F.S., SAE. 720692.

124. ECKLUND E.E., US. DOE., HCP/W1737-01, May 1978.

125. EHRHARDT H., GUNTHER H. and MAY H., Private communication, Professor Ehrhardt, September 1975.

126. EKCHIAN A., HEYWOOD J.B. and RIFE J.M., SAE. 770043.

127. EMELEUS H.J., J. Chem. Soc., 228, 2948 (1926).

128. ENDO H. and GLASS G.P., 5th International Symposium on Gas Kinetics, Manchester, July 1977.

129. ENGLEMAN V.S., Symposium on Stationary Source Combustion, Atlanta, Georgia, p24, September 1975.

130. ESSENHIGH R.H., Journal of the Institute of Fuel, 34, 239 (1961).

131. EVERS L.W., FLEMING R.D. and HURN R.W., SAE. 780236.

132. FAIX L.J., SAE. 780002.

133. FEHSENFELD F.C., EVENSON K.M. and BROIDA H.P., Rev. Sci. Instr., 36, 294 (1965).

134. FENG C.C., LAM S.H. and GLASSMAN I., Combustion Science and Technology, 10, 59 (1975).

135. FENIMORE C.P., Combustion and Flame, 26, 249 (1976).

136. FENIMORE C.P., 17th Symposium (International) on Combustion, Leeds, (1978).

137. FENIMORE C.P. and JONES G.W., J. Phys. Chem., 71, 593 (1967).

138. FELLS I., FLETCHER F.J. and WILSON A., Combustion and Flame, 17, 429 (1971).

139. FERRY D.G., TEMPLE W.A. and McQUEEN E.G., 3rd International Symposium on Alcohol Fuels Technology, California, Vol. III, paper 20, May 1979.

140. FERSEN O., Editor, Autocar, 18, March 1976.

141. FEUGIER A., 2nd European Symposium on Combustion, 1, 362 (1975).

142. FINCH G.I. and SUTTON R.W., Proc. Phys. Soc., 45, 288 (1933).

143. FINDLAY F.D. and SNELLING P.R., The Journal of Chemical Physics, 54, 2750 (1971).

144. FITE W.L., Extranuclear Laboratories Research Note No. 1, January 1971.

145. FLAGAN R.C., GALANT S. and APPLETON J.P., Combustion and Flame, 22, 299 (1974).

146. FLAMM D.L., 3rd International Symposium on Plasma Chem., Limoges, (1977).

147. FORD E.H., SAE. 740152.

148. FONTIJN A., Prepared for Progress in Reaction Kinetics, 6, October 1969.

149. FOREMAN P.B., LEES A.B. and ROL P.K., Chemical Physics, 12, 213 (1976).

150. FOX M.D. and WEINBERG F.J., 13th Symposium (International) on Combustion, Utah, (1970).

151. FREEMAN G.H.C. and FREEMAN I., National Physical Laboratory Report QU 35, April 1977.

152. FREEMAN M.P., Symposium on Chemical Reactions in Electrical Discharges and General Papers, ACS., April 1967.

153. FRENCH C.C.J. and PIKE D.A., SAE. 790761.

154. FUCKS W., BARTELS K., FISCHER E. and UHLENBUSCH J., ARL. 68 0074, April 1968.

155. FULLER D.W.E. and BAKER B.O., The Radio and Electronic Engineer, 42, 364 (1972).

156. GARDNER P.J., Private Communication, June 1978.

157. GAYDON A.G. and WOLFHARD H.G., Proc. Roy. Soc., A213, 366 (1952).

158. GIBBS D.S. and SHAW I.M., Practical Electronics, March 1974.

159. GIOVANNI D.V., PAGNI P.J., SAWYER R.F. and HUGHES L., Combustion Science and Technology, 6, 107 (1972).

160. GOODGER E.M., Journal of the Institute of Fuel, p132, September 1977.

161. GRAHAM E.E., JUDD B.T. and ALEXANDER V., 3rd International Symposium on Alcohol Fuels Technology, California, Vol. III, paper 11, May 1979.

162. GRAY P. and WILLIAMS A., Chemical Reviews, 59, 239 (1959).

163. GRILLO A. and SLACK M.W., Combustion and Flame, 27, 377 (1976).

164. GRUBE W.L., General Motors Research Publication, GMR-2942, (1979).

165. GRUBE W.L. and GAY J.G., Metallurgical Transactions, A9, 1421 (1978).

166. GUILE A.E., ADAMS V.W., LORD W.T. and NAYLOR K. A., Proceedings of the IEE., 116, 145 (1969).

167. GUILE A.E. and NAYLOR K.A., Proceedings of the IEE., 115, 1349 (1968).

168. GUSSAK L.A., SAE. 750890.

169. GUSSAK L.A. and TURKISH M.C., Conference on Stratified Charge Engine, The Institution of Mechanical Engineers, London, November 1976.

170. GUSSAK L.A., KARPOV V.P. and TIKHONOV Yu.V., SAE. 790692.

171. HACK W., SCHACKE H., SCHROTER M. and WAGNER H. Gg., 17th Symposium (International) on Combustion, Leeds, (1978).

172. HAGEN D.L., M.Sc. Thesis, Graduate School of the University of Minnesota, December 1976.

173. HAGEN D.L., SAE. 770792.

174. HAMMOND G., Physics in Technology, 7, 260 (1976).

175. HAMPSON R.F.Jr., and GARVIN D., US. Department of Commerce/National Bureau of Standards, Special Publication 513, (1977).

176. HANSEN P., STRONG J., VANPEE M. and VIDAUD P., Infrared Physics, 13, 327 (1973).

177. HAQUE M.R. and VON ENGEL A., Physics Letters, 43A, 359 (1973).

178. HARDESTY D.R. and WEINBERG F.J., Proceedings of the 14th Symposium (International) on Combustion, The Combustion Institute, Pittsburgh, p907 (1973).

179. HARDESTY D.R. and WEINBERG F.J., Combustion Science and Technology, 8, 201 (1974).

180. HARDESTY D.R. and WEINBERG F.J., Combustion Science and Technology, 12, 153 (1976).

181. HARKER A.B., PAGNI P.J., NOVAKOV T. and HUGHES L., Chemosphere, 6, 339 (1975).

182. HARRISON J.W., EPA. Report 600/7-76-033, December 1976.

183. HARRISON A.J. and WEINBERG F.J., Proc. Roy. Soc., A321, 95 (1971).

184. HARRISON A.J. and WEINBERG F.J., Combustion and Flame, 22, 263 (1974).

185. HARROW G.A., MILLS W.D., THOMAS A. and FINLAY I. C., SAE. 760564.

186. HARTECK P., REEVES R.R. and MANNELLA G.G., The Journal of Chemical Physics, 29, 608 (1958).

187. HASLETT R.A., Ricardo Consulting Engineers, DP 18178, June 1974.

188. HASLETT R.A., MONAGHAN M.L. and McFADDEN J.J., SAE. 760755.

189. HASLETT R.A. and OVERINGTON M.T., Ricardo Consulting Engineers, DP 20722.

190. HAYHURST A.N. and McLEAN H.A.G., Nature, 251, 303 (1974).

191. HAYHURST A.N. and VINCE I.M., Nature, 266, 524 (1977).

192. HAYNES B.S., Fuel, 56, 199 (1977).

193. HAYNES B.S., JANDER H. and WAGNER H.Gg., 17th Symposium (International) on Combustion, Leeds, (1978).

194. HEALD M.A. and BERINGER R., Physics Reviews, 96, 645 (1954).

195. HEFFINGTON W.M., PARKS G.E., SULZMANN K.G.P. and PENNER S.S., 16th Symposium (International) on Combustion, Cambridge, USA., (1976).

196. HEINSOHN R.J., WILHELM C.F.Jr. and BECKER P.M., Combustion and Flame, 14, 341 (1970).

197. HEMPSON J.G.G., SAE. 760605.

198. HENEIN N.A., Wayne State University Technical Report NSF GI44218 and AER74-20320A01, July 1976.

199. HERRON J.T., FRANKLIN J.L. BRANDT P. and DIBELER V.H., The Journal of Chemical Physics, 30, 879 (1958).

200. HEYWOOD J.B., Prog. Energy Combust. Sci., 1, 135 (1976).

201. HEYWOOD J.B., HIGGINS J.M., WATTS P.A. and TABACZYNSKI R.J., SAE. 790291.

202. HEYWOOD J.B. and KECK J.C., Environmental Science and Technology, 7, 216 (1973).

203. HIRES S.D., TABACZYNSKI R.J. and NOVAK J.M., SAE. 780232.

204. HIL R.W., Ricardo Consulting Engineers Report DP 76/709, August 1976.

205. HILLIARD J.C. and WHEELER R.W., Combustion and Flame, 29, 15 (1977).

206. HILLIARD J.C. and WHEELER R.W., SAE. 790691.

207. HINDE P.T. and LICHTIN N.N., Symposium on Chemical Reactions in Electrical Discharges and General Papers, ACS., April 1967.

208. HIRAYAMA C. and MANIERO D.A., Symposium on Chemical Reactions in Electrical Discharges and General Papers, ACS., April 1967.

209. HOGAN J.J., Ph.D. Thesis, University of Illinois, 1964.

210. HOGER H., Dielectrics, 1, 94 (1963).

211. HOM K., OPPENHEIM A.K., TEICHMAN K. and WEINBERG F.J., Nature, 272, 341 (1978).

212. HOYAUX M.F., High Temperatures-High Pressures, 2, 17 (1970).

213. HOYERMANN K. and SIEVERT R., 17th Symposium (International) on Combustion, Leeds, (1978).

214. HUEL R.E. and HERRON J.T., Progress in Reaction Kinetics, 8, 1 (1975).

215. HUMPHREYS J.F. and LAWTON J., The Electricity Council Research Centre, Job No. 026, ECRC/M317, December 1970.

216. HUMPHREYS J.F. and LAWTON J., The Electricity Council Research Centre, ECRC/M318, (1970).

217. HURN R.W. and HUGHES K.J., Ind. Eng. Chem., 48, 1904 (1956).

218. IBARAKI T., KODERA K. and KUSUNOKI I., J. Phys. Chem., 79, 95 (1975).

219. INGHAM H.S.Jr. and FABEL A.J., Welding Journal, February 1975.

220. INTERNATIONAL PATENTS:- Specific International Patents that relate to Diesel fuel modification via peroxidic additives, Dutch P. 63850 - (1949), French P. 862974 - (1941), US. Patents (1945 to 1960), US.P 2317968, US.P 2378341, US.P 2521698, US.P 2618538, US.P 2655440, US.P 2891851, US.P 2912313, US.P 3108864.

221. ISAEV N.A. and ABRUKOV S.A., Consultants Bureau, Plenum Publishing Corp., UDC 537 566, p572 (1972).

222. ITO T. and KASHIMA T., IEEE Transactions on Industry and General Applications, IGA-6, 630, November/December 1970.

223. ITO T. and KASHIMA T., Electrical Engineering in Japan, 90, 60 (1970).

224. ITO T., KASHIMA T. and FUJIOKA T., Hitachi Review, 20, 155 (1970).

225. ITO K., YAMANE K. and FUKAZAWA S., J. Fuel Soc. of Japan, 51, 724 (1972).

226. JACKSON D.S. and SCHIFF H.I., The Journal of Chemical Physics, 23, 2333 (1955).

227. JAGODA I.J. and WEINBERG F.J., Combustion and Flame, 19, 305 (1972).

228. JAGODA I.J. and WEINBERG F.J., 3rd International Symposium on Plasma Chem., Limoges, (1977).

229. JANSSEN J.J. and CRAGGS J.D., J. Phys. B:Atom. Molec. Phys., 5, 89 (1972).

230. JAYARATNE O.W. and MASON B.J., Proc. Roy. Soc., A280, 545 (1964).

231. JET PROPULSION LABORATORY, JPL SP 43-17, Vol.1, August 1975.

232. JOHNSTON P.D., LAWTON J. and PARKER I.M., Combustion Institute European Symposium, Academic Press, London, p334 (1973).

233. JONES A.R. and SCHWAR M.J.R., High Temperatures-High Pressures, 1, 369 (1969).

234. JONES A.R. and THONG K.C., J. Phys. D:Appl. Phys., 4, 1159 (1971).

235. JONES W.E. and WINKLER C.A., Canadian J. Chem., 40, 1082 (1962).

236. JONES A.R., LLOYD S.A. and WEINBERG F.J., Proc. Roy. Soc., A360, 97 (1978).

237. JONES B.A., WEIL B.H. and GRAHAM M.H., Literature of the Combustion of Petroleum, ACS Advances in Chemistry Series No. 20 (1958).

238. JORDAN W., SAE. 790678.

239. KARIM G.A., 4th International Symposium on Combustion Processes, Poland, September 1975.

240. KARLOVITZ B., Pure and Applied Chemistry, 5, 557 (1962).

241. KAUFMAN F., Symposium on Chemical Reactions in Electrical Discharges and General Papers, ACS., April 1967.

242. KAUFMAN F., Ann. Rev. Phys. Chem., 20, 45 (1969).

243. KAUFMAN F., Adv. Chem. Series, 80, 29 (1969).

244. KEE R.J. and MILLER J.A., AIAA Journal, 16, 169 (1978).

245. KELLY A.J., Journal of Applied Physics, 49, 2621 (1978).

246. KELTNER N.R. and BICKLE L.W., The American Society of Mechanical Engineers Publication 76-HT-65.

247. KHATRI N.J. and JOHNSON J.H., SAE. 780788.

248. KHOSHNOODI M., Unpublished results, Communicated by Professor Weinberg, July 1976.

249. KILHAM J.K. and TURNER S.J., Combustion and Flame, 14, 249 (1970).

250. KIM Y.K., IWAI N., SUTO H. and TSURUGA T., Japan Automobile Research Institute Technical Report No. 41, August 1977.

251. KIM Y.K., TSURUGA T., KOBAYASHI S., YOSHIDA M., IWAI N., SUTO H. and ITO T., Japan Automobile Research Institute Technical Report No. 27, June 1976.

252. KIMURA S.G., Private Communication, March 1978.

253. KIMURA I. and IMAJO M., 16th Symposium (International) on Combustion, Cambridge, USA., (1976).

254. KIMURA I. and OGIWARA K., 15th Symposium (International) on Combustion, Tokyo, (1974).

255. KINGDON R.G. and WEINBERG F.J., Proceedings of the 16th Symposium (International) on Combustion, The Combustion Institute, Pittsburgh, p747 (1977).

256. KIRSH A.A., STECHKINA I.B. and FUCHS N.A., Aerosol Science, 6, 119 (1975).

257. KISTIAKOWSKY G.B. and VOLPI G.G., The Journal of Chemical Physics, 27, 1141 (1957).

258. KITTELSON D.B., DOLAN D.F., DIVER R.B. and AUFDERHEIDE E., SAE. 780787.

259. KONISHI M., NAKAMURA N., OONO E., BAIKA T. and SANDA S., SAE. 790389.

260. KRANZ E., Proc. IEE-Conf. on Gas Discharges, London, September 1970.

261. KRAUS B.J., GODICI P.E. and KING W.H., SAE. 780155.

262. KYDD P.H. and FOSS W.I., General Electric Report No. 63-RL-(3415C), August 1963.

263. KYDD P.H. and FOSS W.I., General Electric Report No. 64-RL-3581C, February 1964.

264. LAPWORTH K.C., Journal of Physics E:Scientific Instruments, 7, 413 (1974).

265. LAPWORTH K.C., J. Quant. Spectrosc. Radiat. Transfer., 16, 357 (1976).

266. LAPWORTH K.C. and ALLNUTT L.A., Inst. Phys. Conf. Ser. No. 26, 341 (1975).

267. LARSON A.V., AIAA Journal, 6, 1001 (1968).

268. LAVOIE G.A., HEYWOOD J.B. and KECK J.C., Fluid Mechanics Laboratory Publication No. 69-10, Massachusetts Institute of Technology, November 1969.

269. LAWTON J., Physics in Technology, 6, 190 (1975).

270. LAWTON J. and WEINBERG F.J., Proc. Roy. Soc., A277, 468 (1964).

271. LAZZARA C.P., BIORDI J.C. and PAPP J.F., Bureau of Mines RI 7766, (1973).

272. LEE K.B., THRING M.W. and BEÉR J.M., Combustion and Flame, 6, 137 (1962).

273. LEUTNER H.W., Ind. Eng. Chem., Process Design & Development, 2, 315 (1963).

274. LEUTNER H.W. and STOKES C.S., Ind. Eng. Chem., 53, 5 (1961).

275. LEVY A. and WEINBERG F.J., Combustion and Flame, 3, 229 (1959).

276. LEVY A. and WEINBERG F.J., Proceedings of the 7th Symposium (International) on Combustion, Butterworths, (1959).

277. LIFSHITZ A., SCHELLER K., BURCAT A. and SKINNER G. B., Combustion and Flame, 16, 311 (1971).

278. LLOYD A.C., DARNALL K.R., WINER A.M. and PITTS J. N., J. Phys. Chem., 80, 789 (1976).

279. LLOYD S.A. and WEINBERG F.J., Nature, 251, 47 (1974).

280. LLOYD S.A. and WEINBERG F.J., Nature, 257, 367 (1975).

281. LLOYD S.A. and WEINBERG F.J., Combustion and Flame, 27, 391 (1976).

282. LONGWELL J.P., Prog. Energy Combust. Sci., 3, 127 (1977).

283. LONGWELL J.P. and WEISS M.A., Ind. Eng. Chem., 47, 1634 (1955).

284. LOVACHEV L.A., GONTKOVSKAYA V.T. and OZERKOVSKAYA N.I., Combustion Science and Technology, 17, 143 (1977).

285. LYON R.K. and BENN D., 17th Symposium (International) on Combustion, Leeds, (1978).

286. MACCORMAC M. and TOWNSEND D.T.A., J. Chem. Soc., 238, (1938).

287. MAHONEY J.F., YAHIKU A.Y., DALEY H.L., MOORE R. D. and PEREL J., Journal of Applied Physics, 40, 5101 (1969).

288. MALTE P.C. and PRATT D.T., 15th Symposium (International) on Combustion, Tokyo, (1974).

289. MALTE P.C. and PRATT D.T., Combustion Science and Technology, 9, 221 (1974).

290. MALVERN INSTRUMENTS, Malvern, England, Particle and Droplet size Distribution Analyser Type ST. 1800.

291. MALY R. and VOGEL M., 17th Symposium (International) on Combustion, Leeds, (1978).

292. MANNELLA G.G., Chemical Reviews, 63, 1 (1963).

293. MARDANOV M.A., VELIEV K.G., Et Al., Azerb. Khim. Zh., 1, 3 (1965).

294. MATTHES W.R. and McGILL R.N., SAE. 760117.

295. MAY K.R., J. Sci. Instr., 22, 187 (1945).

296. MAY K.R., J. Sci. Instr., 27, 128 (1950).

297. MAY M.G., US. Patent 4000722, (1977).

298. MAY M.G., SAE. 790386.

299. MAY M.G., Conference entitled Fuel Economy and Emissions of Lean Burn Engines, Paper C97/79, The Institution of Mechanical Engineers, London, June 1979.

300. MAYO P.J. and WEINBERG F.J., Proc. Roy. Soc., A319, 351 (1970).

301. MERZHANOV A.G. and AVERSON A.E., Combustion and Flame, 16, 89 (1971).

302. MILKOVIC M., General Electric Report No. 77CRD087, April 1977.

303. MILLER C.O., SAE. 670093.

304. MILLER J.A. and KEE R.J., J. Phys. Chem., 81, 2534 (1977).

305. MILLINGTON B.W. and HARTLES E.R., SAE. 680590.

306. MILLS R.M., Combustion and Flame, 12, 513 (1968).

307. MIRSKY W.P., Private Communication, June 1979.

308. MONAGHAN M.L., SAE. 790038.

309. MOORE G.E. and FOSS W.I., General Electric Report No. 66-C-430, November 1966.

310. MORI T. and YAMAZAKI K., Bulletin of the JSME., 50, 600 (1970).

311. MUIR A.J., Plant Engineering, December 1972.

312. MULLER-DETHLEFS K. and WEINBERG F.J., 17th Symposium (International) on Combustion, Leeds, (1978).

313. MURPHY R.E., The Journal of Chemical Physics, 54, 4852 (1971).

314. MUZIO L.J., MALONEY K.L. and ARAND J.K., 17th Symposium (International) on Combustion, Leeds, (1978).

315. MYERS T.W., Aerospace Research Labs., Office of Aerospace Research, Wright-Patterson AFB, Ohio, R ARL 66 0184, 126P, September 1966.

316. McCLENNY W.A., The Journal of Chemical Physics, 60, 793 (1974).

317. McKAY G., Prog. Energy Combust. Sci., 3, 105 (1977).

318. McMILLAN G.R., J. Am. Chem. Soc., 83, 3018 (1961).

319. NACHMAN M., Rev. int. Htes Temp. et Refract., 10, 65 (1973).

320. NAGLE J. and STRICKLAND-CONSTABLE R.F., Proc. Fifth Carbon Conf., 1, 154 (1962).

321. NICHOLSON R.C., SAE. 780616.

322. NIGHTINGALE D.R., Ricardo Consulting Engineers, DP 16473, April 1973.

323. NOGUCHI M., TANAKA Y., TANAKA T. and TAKEUCHI Y., SAE. 790840.

324. NORMAN P. and FELLS I., The Institution of Electrical Engineers Colloquium, December 1977.

325. O'FARRELL M., Uncorrected Proof of Paper presented at the Institute of Petroleum, London, June 1948.

326. OGATA S., KAWASHIMA T., NAKAYA O. and SHINOHARA H., Journal of Chemical Engineering of Japan, 9, 6 (1976).

327. OKADA H. and KUMAGAI S., archiwum termodynamiki i spalania, 7, 109 (1976).

328. OLDERSHAW G.A., Chem. Soc. Specialist Periodical Reports, Reaction Kinetics, 2, 94 (1977).

329. OPPENHEIM A.K. and WEINBERG F.J., Astronautics and Aeronautics, 12, 22 (1974).

330. OPPENHEIM A.K., TEICHMAN K., HOM K. and STEWART H.E., SAE. 780637.

331. O'SULLIVAN D.A., Description of work of C.A. McAuliffe et al. at UMIST C & EN., 24, December 1978.

332. PADOVANI C., PALEARI C. and RENZANIGO F., Rivista Dei Combustibili, 14, 193 (1960).

333. PARK C. and APPLETON J.P., Combustion and Flame, 20, 369 (1973).

334. PARKS M.V., POLONSKI C. and TOYE R., SAE. 660747.

335. PANETH F. and HOFEDITZ W., Ber., B62, 1335 (1929).

336. PETERS B.D. and QUADER A.A., SAE. 780234.

337. PHILLIPS L.F. and SCHIFF H.I., The Journal of Chemical Physics, 37, 1233 (1962).

338. PHILLIPS L.F. and SCHIFF H.I., The Journal of Chemical Physics, 42, 3171 (1965).

339. PICKERING H.S. and LINNETT J.W., Trans. Faraday Soc., 47, 1101 (1951).

340. PIKE D.A. and WRIGHT M.J., Ricardo Consulting Engineers, DP 20795, February 1976.

341. PITTS J.N.Jr., VAN CAUWENBERGHE K.A., GROSJEAN D., SCHMID J.P., FITZ D.R., BELSER W.L.Jr., KNUDSON G.B. and HYNDS P.M., Science, 202, 515 (1978).

342. PLACE E.R. and WEINBERG F.J., Proc. Roy. Soc., A289, 192 (1965).

343. PLACE E.R. and WEINBERG F.J., Proceedings of the 11th Symposium (International) on Combustion, The Combustion Institute, Pittsburgh, p245 (1967).

344. POLYMEROPOULOS C.E. and DAS S., Combustion and Flame, 29, 123 (1977).

345. PRICHAMUTHU J.P., J. Phys. D:Appl. Phys., 7, 1056 (1974).

346. PRIOR D.S., SWITHENBANK J. and FELTON P.G., Progress in Astronautics and Aeronautics, 58, 351 (1978).

347. PUCHIN V.A., et al., USSR. Patent 214,710.

348. PUCHIN V.A., et al., USSR. Patent 236,897.

349. PUROHIT G. and HOUSEMAN J., SAE. 790427.

350. QUADER A.A., SAE. 710009.

351. QUADER A.A., SAE. 730153.

352. QUADER A.A., SAE. 760760.

353. RADO W.G., Journal of Applied Physics, 46, 2468 (1975).

354. RAMSHAW C., Journal of the Institute of Fuel, 41, 286 (1968).

355. RANDALL J.M., Ph.D. Thesis, University of Wisconsin, (1964).

356. RANDALL K.W. and POWELL J.D., SAE. 790139.

357. RAUCKIS M.J. and McLEAN W.J., Combustion Science and Technology, June 1978.

358. RAYLEIGH (Lord), Proc. Roy. Soc., 29, 71 (1879).

359. REISCHL G., JOHN W. and DEVOR W., J. Aerosol Sci., 8, 55 (1977).

360. RICARD A., BLOYET E., HOCHARD L., LEPRINCE Ph. and MAREC J., 3rd International Symposium on Plasma Chem., Limoges, (1977).

361. RICARDO H.R., The Automobile Engineer, June 1921.

362. RICARDO H.R., Institution of Petroleum Technologists, London, 150 (1924).

363. RICARDO CONSULTING ENGINEERS LTD., DP 79/542.

364. RICE F.O., JOHNSTON W.R. and EVERING B.L., J. Am. Chem. Soc., 54, 3529 (1932).

365. RIECHE A., Published by Theodor Steinkopff, Dresden and Leipzig 1931, (Issued by British Ministry of Supply 1947), Library Translation No. 156.

366. ROBBINS W.E., AUDETTE R.R. and REYNOLDS N.E. III, SAE. Quarterly Transactions, 5, 405 (1951).

367. ROTH W., GUEST P.G., VON ELBE G. and LEWIS B., The Journal of Chemical Physics, 19, 1530 (1951).

368. RUPPEL T.C., MOSSBAUER P.F. and BIENSTOCK D., Symposium on Chemical Reactions in Electrical Discharges and General Papers, ACS., April 1967.

369. SADEGHI N. and NGUYEN T.D., Le Journal De Physique - Lettres, 38, 283 (1977).

370. SAFRANY D.R., Progress in Reaction Kinetics, 6, (1971).

371. SAFRANY D.R. and JASTER W., J. Phys. Chem., 72, 518 (1968).

372. SAHETCHIAN K.A., HEISS A., DUMAS G.M.L. and BEN-AIM R.I., Combustion and Flame, 34, 153 (1979).

373. SALOOJA K.C., Journal of the Institute of Petroleum, 48, 119 (1962).

374. SALOOJA K.C., Nature, 240, 350 (1972).

375. SAWYER R.F. and GLASSMAN I., 12th Symposium (International on Combustion, (1968).

376. SAYERS J.F., The Institution of Electrical Engineers Colloquium, December 1977.

377. SAYERS J.F. and WILSON J.R., Gas Warme International, 24, 218 (1975).

378. SCHNEIDER J.M., Ph.D. Thesis, University of Illinois, 1964.

379. SCHWARZ H., Conference entitled Fuel Economy and Emissions of Lean Burn Engines, Paper C95/79, The Institution of Mechanical Engineers, London, June 1979.

380. SCOTT W.M., Land Transport Engines Conference, January 1977.

381. SEERY D.J. and BOWMAN C.T., Combustion and Flame, 14, 37 (1970).

382. SETSER D.W., STEDMAN D.H. and COXON J.A., The Journal of Chemical Physics, 53, 1004 (1970).

383. SHAW J.T., Brit. J. Anaesthesia, 40, 299 (1968).

384. SHAW T.M., General Electric Publication, August 1958.

385. SHENSTON R.S. and WILLIAMS F.W., Combustion and Flame, 21, 221 (1951).

386. SHIMOURA A., YAMAMOTO S., AKAHANE H. and HASEGAWA K., Journal of the Society of Automotive Engineers of Japan, Inc. Magazine, (Automotive Technique), 32, 1018 (1978).

387. SHIOMOTO G.H., SAWYER R.F. and KELLY B.D., SAE. 780235.

388. SHUI V.H., APPLETON J.P. and KECK J.C., Department of Mechanical Engineering, Massachusetts Institute of Technology, Fluid Mechanics Laboratory Publication No. 70-2, February 1970.

389. SHULER K.E., 6th International Astrophysical Symposium on Solid Particles in Astronomical Objects, Liege, Belgium, July 1954.

390. SHTERN V.Ya., REVSIN A.F. and SOKOLOVA E.I., International Journal of Chemical Kinetics, 5, 593 (1973).

391. SINNAMON J.F. and COLE D.E., SAE. 790438.

392. SKINNER G.B. and RUEHRWEIN R.A., J. Phys. Chem., 63, 1736 (1959).

393. SLACK M.W., Combustion and Flame, 30, 325 (1977).

394. SLOANE T.M. and RATCLIFFE J.W., General Motors Research Publication GMR-2845, PCP-83, (1978).

395. SMY P.R., Advances in Physics, 25, 517 (1976).

396. SOKOLIK A.S., Israel Program for Scientific Translations, 1963.

397. SOO S.L., Int. J. Multiphase Flow, 1, 89 (1973).

398. SOO S.L., Environmental Science and Technology, 7, 63 (1973).

399. SPEDDING P.L., Department of Chemical Engineering, University of Newcastle, Report No. 4.

400. SPENCE D. and McHALE E.T., Combustion and Flame, 24, 211 (1975).

401. SPEROS D.M., CALDWELL R.M. and SMYSER W.E., High Temperature Science, 4, (1972).

402. STAATS G.E. and McGREGOR W.K.Jr., AEDC-TR-68-171, AD 675, 552, October 1968.

403. STAVELEY L.A.K. and HINSHELWOOD C.N., Proc. Roy. Soc., A154, 335 (1936).

404. STAVELEY L.A.K. and HINSHELWOOD C.N., J. Chem. Soc., 1568 (1937).

405. STEENBECK M., Phys. Z., 38, 1099 (1937).

406. STEINER J.C. and MIRSKY W., SAE. 660346.

407. STEPHENS J.B. and MILLER C.G., JPL 13798/3070; Also discribed under "Electrostatic Ignition Fires Ultralean Fuel Mixtures", Machine Design, 49, 42 (1977).

408. STINTON H.C., Ricardo Consulting Engineers Report, DP 77/1435, December 1977.

409. STREET J.C. and THOMAS A., Fuel, 34, 4 (1955).

410. STRUTT R.J., Proc. Roy. Soc., A85, 219 (1911).

411. SUTO H., IWAI N., TSURUGA T., KIM Y.K. and HIRAO O., Proceedings: International Symposium on Alcohol Fuel Technology Methanol and Ethanol, Wolfsburg, November 1977, US. DOE Publication CONF-771175, July 1978.

412. SWATIK D.S. and HENDRICKS C.D., AIAA Journal, 6, 1596 (1968).

413. SWITHENBANK J., BEÉR J.M., TAYLOR D.S., ABBOT D. and McCREATH G.C., AIAA Paper No. 76-69, (1976).

414. TABAYASHI K. and BAUER S.H., Combustion and Flame, 34, 63 (1979).

415. TANFORD C., The Journal of Chemical Physics, 15, 433 (1947).

416. TANFORD C. and PEASE R.N., The Journal of Chemical Physics, 15, 431 (1947).

417. TANFORD C. and PEASE R.N., The Journal of Chemical Physics, 15, 861 (1947).

418. TAYLOR E.H. and HARMON D.B., Ind. Eng. Chem., 46, 1455 (1954).

419. TAYLOR G.I., Proc. Roy. Soc., A280, 383 (1964).

420. TAYLOR G.I., Proc. Roy. Soc., A313, 458 (1969).

421. THONG K.C. and WEINBERG F.J., Proc. Roy. Soc., A324 201 (1971).

422. THRING R.H., SAE. 790387.

423. THRUSH B.A., Chemistry in Britain, 287 (1966).

424. TOPHAM D.R., SMY P.R. and CLEMENTS R.M., Combustion and Flame, 25, 187 (1975).

425. TOPPS J.C.F. and TOWNEND D.T.A., Trans. Faraday Soc., 42, 345 (1946).

426. TORPEY P.M., WHITEHEAD M.J. and WRIGHT M., Conference on Air Pollution Control in Transport Engines, C124/71, The Institution of Mechanical Engineers.

427. TRAYSER D.A., CRESWICK F.A., GIESEKE J.A., HAZARD H.R., WELLER A.E. and LOCKLIN D.W., Battelle Columbus Report (CPA 22-69-9), April 1969.

428. TURKISH M.C., SAE. 741163.

429. TUTTLE J.H. and TOEPEL R.R., SAE. 790388.

430. US. DEPARTMENT OF ENERGY, Report No. HCP/W1737-01 UC-96, May 1978.

431. VARDE K.S. and LUCAS G.G., SAE. 741017.

432. VARFOLOMEEVA E.K. and ERSHOV A.V., J. Appl. Chem. USSR., 27, 595 (1954) (Engl. Translation).

433. VANPEE M. and SHIRODKAR P.P., 17th Symposium (International) on Combustion, Leeds, (1978).

434. VINCENZO FERRARO C., SAE. 780154.

435. VOMELA R.A. and WHITBY K.T., Journal of Colloid and Interface Science, 25, 568 (1967).

436. WALCOTT J., Science Writer, The Sunday Record, New Jersey, A2, March 31st 1974.

437. WALDER C.J., SAE. 730214.

438. WALKER J., An article describing the 'reverse flames' of Stuart Travis. Scientific American, p192, November 1979.

439. WANG Yi.Y., RAPPAPORT S.M., SAWYER R.F., TALCOTT R.E. and WEI E.T., Cancer Letters, 5, 39 (1978).

440. WARD M.A.V., US. Patent 3,934,566.

441. WARD M.A.V. and WU T.T., Combustion and Flame, 32, 57 (1978).

442. WATSON N. and KAMEL M., SAE. 790039.

443. WEINBERG F.J., Proc. Roy. Soc., A230, 331 (1955).

444. WEINBERG F.J., Inaugural Lecture, Imperial College, April 1968.

445. WEINBERG F.J., Nature, 233, 239 (1971).

446. WEINBERG F.J., Proc. Roy. Institution, 45, 299 (1972).

447. WEINBERG F.J., Ind. Chim. Belg., 38, 2 (1973).

448. WEINBERG F.J., Phys. Bull., 25, 56 (1974).

449. WEINBERG F.J., 2nd Simposio di Dinamica delle Reazioni Chimiche, Padova, pl5, December 1975.

450. WEINBERG F.J., Physics in Technology, 6, 95 (1975).

451. WEINBERG F.J., Proceedings of the 15th Symposium (International) on Combustion, The Combustion Institute, Plenary Lecture, Pittsburgh, (1975).

452. WEINBERG F.J., Prog. Energy Combust. Sci., 1, 17 (1975).

453. WEINBERG F.J. and WILSON J.R., Proc. Roy. Soc., A321, 41 (1971).

454. WESTBROOK C.K., Lawrence Livermore Laboratory Preprint UCRL-81507, July 1978.

455. WESTBROOK C.K., SAE. 790248.

456. WESTBROOK C.K., CREIGHTON J., LUND C. and DRYER F.L., J. Phys. Chem., 81, 2542 (1977).

457. WHEELER R.W., The Institution of Mechanical Engineers, C100/75.

458. WHEELER R.W., The Institution of Electrical Engineers Colloquium, December 1977.

459. WHEELER R.W., Ricardo Consulting Engineers, DP 78/212, March 1978.

460. WHITBY K.T., The Rev. Sci. Instr., 32, 1351 (1961).

461. WILSON R.P.Jr., FOWLE A.A., RAYMOND W.J. and McLEAN W.J., SAE. 790293.

462. WINIARSKI D.M., Annual Economic Outlook Conference, Chicago, June 1978.

463. WIDGINTON D.W., Nature, 198, 959 (1963).

464. WONG V.W., RIFE J.M. and MARTIN M.K., SAE. 780638.

465. WOOD C.D., SAE. 780341.

466. WOOD R.W., Phil. Mag., 44, 538 (1922). Also Phil. Mag., 42, 729 (1921).

467. WRIGHT M.J., Ricardo Consulting Engineers, DP 76/686, September 1976.

468. WYCZALEK F.A., FRANK D.L. and NEUMAN J.G., SAE. 750349.

469. YAGI S., FUJII I., NISHIKAWA M. and SHIRAI H., SAE. 790439.

470. YOUNG P.W. and FINCH G.I., US. Patent 3,169,914, February 1965.

471. YOUNG R.A., The Journal of Chemical Physics, 36, 2854 (1962).

472. YOUNG R.A. and ST. JOHN G.A., Symposium on Chemical Reactions in Electrical Discharges and General Papers, ACS., April 1967.

473. YOUNG R.A. and ST. JOHN G.A., Chemical Reactions in Electrical Discharges, Adv. Chem. Series 80, (1969).

474. YOUNG R.A., SHARPLESS R.L. and STRINGHAM R., The Journal of Chemical Physics, 40, 117 (1964).

475. YOUNG W.S., RODGERS W.E. and KNUTH E.L., The Rev. Sci. Instr., 40, 1346 (1969).

476. ZEL'DOVICH Y.B., Acta Phys.-Chim. URSS., 21, 577 (1946).

477. ZEL'DOVICH Y.B. and LIBROVICH V.B., Central States Meeting of the Combustion Institute, Columbus, Indiana, April 1979.

478. ZELENY J., Proc. Cambridge Philos. Soc., 18, 71 (1915).

479. ZELENY J., Physics Reviews, 10, 1 (1917).

BIBLIOGRAPHY

ADAMS H.T., "Elements of Internal Combustion Turbine Theory", Cambridge University Press, 1949.

ALLEN T., "Particle Size Measurement", Chapman & Hall, 1968.

AMDUR I. and HAMMES G.G., "Chemical Kinetics:Principles and Selected Topics", McGraw-Hill, 1966.

ASHMORE P.G., "Principles of Reaction Kinetics", Second Edition, Royal Institute of Chemistry Monographs, No. 9, 1969.

ATTWOOD S.S., "Electric and Magnetic Fields", Dover, 1967.

AYRES R.U. and McKENNA R.P., "Alternatives to the Internal Combustion Engine", The Johns Hopkins University Press, 1972.

BAULCH D.L., DRYSDALE D.D., HORNE D.G. and LLOYD A. C., "Evaluated Kinetic Data for High Temperature Reactions", CRC Press, 1973.

BEÉR J.M. and CHIGIER N.A., "Combustion Aerodynamics", Applied Science Publishers, London, 1972.

BENSON S.W., "Thermochemical Kinetics", John Wiley, 1968.

BIRD R.B., STEWART W.E. and LIGHTFOOT E.N., "Transport Phenomena", John Wiley, 1960.

BLACKMORE D.R. and THOMAS A., Editors, "Fuel Economy of the Gasoline Engine", MacMillan Press, 1977.

BRADLEY J.N., "Flame and Combustion Phenomena", Methuen, 1969.

CADOGAN J.I.G., "Principles of Free Radical Chemistry", The Chemical Society Monographs, No. 24.

CAMBEL A.B., "Plasma Physics and Magnetofluid-Mechanics", McGraw-Hill, 1963.

CANDLER C., "Practical Spectroscopy", Hilger & Watts, 1949.

CANNON C.G., Editor, "Electronics for Spectroscopists", Hilger & Watts, 1960.

CARNAHAN B., LUTHER H.A. and WILKES J.O., "Applied Numerical Methods", John Wiley, 1969.

CHEMICAL SOCIETY (The), "Conservation of Resources", Special Publication No. 27, 1976.

CHEMICAL SOCIETY (The), "Oxygen in the Metal and Gaseous Fuel Industries", Special Publication No. 32, September 1977.

COBINE J.D., "Gaseous Conductors", Dover, 1958.

CONSIDINE D.M., "Energy Technology Handbook", McGraw-Hill, 1977.

CUNDALL R.B. and GILBERT A., "Photochemistry", Nelson, 1970.

DAINTON F.S., "Chain Reactions", Second Edition, Methuen, 1966.

DIXON R.N., "Spectroscopy & Structure", Methuen, 1965.

DUNN P.D. and REAY D.A., "Heat Pipes", Pergamon Press, 1976.

EYRING L., Editor, "Advances in High Temperature Chemistry", Volume I, Academic Press, 1967.

FRANCIS W., "Fuels and Fuel Technology", Volumes I & II, Pergamon Press, 1965.

FRISTOM R.M. and WESTENBERG, A.A., "Flame Structure", McGraw-Hill, 1965.

GAYDON A.G., "Dissociation Energies and Spectra of Diatomic Molecules", Third Edition, Chapman & Hall, 1968.

GAYDON A.G., "The Spectroscopy of Flames", Second Edition, Chapman & Hall, 1974.

GAYDON A.G. and WOLFHARD, H.G., "Flames", Fourth Edition, Chapman & Hall, 1979.

GLASOE G.N. and LEBACQZ J.V., Editors, "Pulse Generators", Dover, 1965.

GOODGER E.M., "Hydrocarbon Fuels", MacMillan Press, 1975.

HAGUE D.N., "Fast Reactions", John Wiley, 1971.

HINSHELWOOD C.N., "The Kinetics of Chemical Change in Gaseous Systems", Oxford University Press, 1926.

HIRSCHFELDER J.O., CURTISS C.F. and BIRD R.B., "Molecular Theory of Gases and Liquids", John Wiley, 1964.

HUANG K., "Statistical Mechanics", John Wiley, 1963.

HURN R.W., Editor, "Approaches to Automotive Emissions Control", Am. Chem. Soc. Symp. Ser. 1, 1974.

HUSH N.A., Editor, "Reactions of Molecules at Electrodes", John Wiley, 1971.

ISENBERG C., "The Science of Soap Films and Soap Bubbles", Tieto, 1978.

JAHN R.G., "Physics of Electric Propulsion", McGraw-Hill, 1968.

JANAF, "Thermochemical Tables", Dow Chemical Company, Michigan, 1968.

KAY J.M. and NEDDERMAN R.N., "Fluid Mechanics and Heat Transfer", Third Edition, Cambridge University Press, 1974.

KEEN B.E., Editor, "Plasma Physics", The Institute of Physics, Conference Series No. 20.

KEENAN J.H. and KAYE J., "Gas Tables", John Wiley, 1948.

KOCK W.E., "Engineering Applications of Lasers and Holography", Plenum Press, 1975.

KRAUSE L., "Sensitized Fluorescence and Quenching", John Wiley, 1975.

LAIDLER K.J., "Chemical Kinetics", Second Edition, McGraw-Hill, 1965.

LAUNDER B.E. and SPALDING D.B., "Mathematical Models of Turbulence", Academic Press, 1972.

LAWTON J. and WEINBERG F.J., "Electrical Aspects of Combustion", Clarendon Press, 1969.

LEWIS B. and VON ELBE G., "Combustion Flames and Explosions of Gases", Second Edition, Academic Press, 1961.

LIVERHANT S.E., "Atomic Physics", Regents, 1966.

LLEWELLYN-JONES F., "Ionization and Breakdown in Gases", Methuen, 1966.

LORRAIN P. and CORSON D., "Electromagnetic Fields and Waves", Second Edition, Freeman, 1970.

MINKOFF G.J. and TIPPER C.F.H., "Chemistry of Combustion Reactions", Butterworths, 1962.

MONTGOMERY C.G., "Technique of Microwave Measurements", Volumes I & II, Dover, 1966.

MULCAHY M.F.R., "Gas Kinetics", Nelson, 1973.

McCRACKEN D.D., "A Guide to Fortran IV Programming", Second Edition, John Wiley, 1972.

McGLASHAN M.L., "Physicochemical Quantities and Units", Second Edition, The Royal Institute of Chemistry, 1971.

McTAGGART F.K., "Plasma Chemistry in Electrical Discharges", Elsevier, 1967.

NASH L.K., "Statistical Thermodynamics", Addison-Wesley, 1968.

OBERT E.F., "Internal Combustion Engines and Air Pollution", Harper & Row, 1973.

PATTERSON D.J. and HENEIN N.A., "Emissions from Combustion Engines and Their Control", Ann Arbor Science Publishers, 1978.

PEARSE R.W.B. and GAYDON A.G., "The Identification of Molecular Spectra", Third Edition, Chapman & Hall, 1963.

PUNGOR E., "Flame Photometry Theory", Van Nostrand Company, 1967.

REIF F., "Fundamentals of Statistical and Thermal Physics", McGraw-Hill, 1965.

RICARDO H.R. and HEMPSON J.G.G., "The High Speed Internal Combustion Engine", Blackie, 1968.

ROBINSON P.J. and HOLBROOK K.A., "Unimolecular Reactions", John Wiley, 1972.

ROGERS G.F.C. and MAYHEW Y.R., "Engineering Thermodynamics Work and Heat Transfer", Second Edition, Longman, 1967.

ROSENFELD L., "Theory of Electrons", Dover, 1965.

RUDINGER G., "Nonsteady Duct Flow", Dover, 1969.

SAE, "SAE Handbook 1979" Parts I & II, Published by Society of Automotive Engineers, 1979.

SEMENOFF N., "Chemical Kinetics and Chain Reactions", Oxford University Press, 1935.

SEMENOV N.N., "Some Problems in Chemical Kinetics and Reactivity", Pergamon Press, 1958.

SHAPIRO A.H., "The Dynamics and Thermodynamics of Compressible Fluid Flow 1 and 2", Ronald Press, 1954.

SHAPIRO A.H., "Shape and Flow", Heinemann, 1974.

SHAW D.J., "Introduction to Colloid and Surface Chemistry", Second Edition, Butterworths, 1970.

SMITH R.J., "Circuits, Devices and Systems", John Wiley, 1966.

SONNTAG R.E. and VAN WYLEN G.J., "Fundamentals of Statistical Thermodynamics", John Wiley, 1966.

SPALDING D.B., "Some Fundamentals of Combustion", Academic Press, 1955.

SPALDING D.B., "Combustion and Mass Transfer", Pergamon Press, 1979.

SPEAKMAN J.C., "The Hydrogen Bond and other Inter-Molecular Forces", The Chemical Society Monographs, No. 27, 1975.

STAMBULEANU A., "Flame and Combustion Processes in Industry", Abacus Press, 1976.

TAYLOR C.F. and TAYLOR E.S., "The Internal Combustion Engine", Second Edition, International Textbook, 1961.

TENNENT R.M., Editor, "Science Data Book", Oliver & Boyd, 1974.

THIRD SYMPOSIUM, "Third Symposium on Combustion Flame and Explosion Phenomena", Williams & Wilkins, 1949.

THRING M.W., "The Science of Flames and Furnances", John Wiley, 1952.

TROTMAN-DICKENSON A.F., "Free Radicals", Methuen, 1959.

VAN WYLEN G. and SONNTAG R.E., "Fundamentals of Classical Thermodynamics", Second Edition (SI), John Wiley, 1978.

VENUGOPALAN M., Editor, "Reactions Under Plasma Conditions", Volumes I & II, John Wiley, 1971.

VON ENGEL A., "Ionized Gases", Second Edition, Oxford University Press, 1965.

WAYNE R.P., "Photochemistry", Butterworths, 1970.

WEAST R.C., Editor, "Handbook of Chemistry and Physics", 55th Edition, CRC Press, 1973.

WEINBERG F.J., "Optics of Flames", Butterworths, 1963.

WHITE H.J., "Electrostatic Precipitation", Addison-Wesley, 1963.

WILLIAMS A., "Combustion of Sprays of Liquid Fuels", Elek Science, 1976.

WILLIAMS D.A. and JONES G., "Liquid Fuels", Pergamon Press, 1963.

WILLIAMS F.A., "Combustion Theory", Addison-Wesley, 1965.

WOLFRUM J., "Atom Reactions", Physical Chemistry An Advanced Treatise, Volume VIB/Kinetics of Gas Reactions Edited by Wilhelm Jost, Academic Press, 1975.

WYATT P.A.H., "The Molecular Basis of Entropy and Chemical Equilibrium", The Royal Institute of Chemistry Monographs, No. 19, 1971.

ZEEGERS P.J.T., "Recombination of Radicals and Related Effects in Flames", Bronder-Offset, Rotterdam, 1966.